SURFACE HYDROXYLATION OF STYRENE-BUTADIENE-STYRENE
BLOCK COPOLYMERS FOR BIOMATERIALS

by

Michael Vivian Sefton

B.A.Sc., Chem. E., University of Toronto (1971)

Submitted in Partial Fulfillment of the Requirements for the Degree of

Doctor of Science

at the

MASSACHUSETTS INSTITUTE OF TECHNOLOGY

June 1974

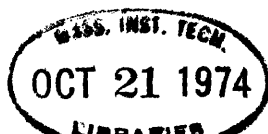Signature of the Author:

Department of Chemical Engineering

Certified by:

Edward W. Merrill, Thesis Supervisor

Accepted by:

G. C. Williams, Chairman
Departmental Committee on Graduate
Theses

SURFACE HYDROXYLATION OF STYRENE-BUTADIENE-STYRENE BLOCK COPOLYMERS FOR BIOMATERIALS

by

Michael Vivian Sefton

B.A.Sc., Chem. E., University of Toronto (1971)

ABSTRACT

This work pertains to the development of high strength elastomers potentially useful as nonthrombogenic cardiovascular prostheses. Triblock copolymers of the styrene-butadiene-styrene type have been subjected to surface hydroxylation via intermediate epoxides providing reactive sites at the surface for the subsequent coupling of heparin while retaining the unique mechanical properties of the SBS copolymers.

Curves of hydroxyl content versus the copolymer film thickness demonstrated the effect of swelling in the surface region on the product distribution and on the time dependence of the hydroxylation process. The results indicated that swelling in the surface region is modified by stress transfer to the unreacted, nonswelling core, giving rise to a lower hydroxyl content in thicker films than in thinner films due to separate effects on both the epoxidation agent and on the cleavage agents, and an exponential time dependence with the appearance of a significant induction time.

Detailed quantitative analysis of the infrared spectra of surface reacted samples indicated the presence of a thickness dependent diffusion lag between the cleavage agents and the peracid, confirming the observation of a decreased hydroxyl content in thicker films. Delamination of surface reacted samples occurred on swelling in chloroform. Through analysis of the weights of the resulting fractions, the depth of penetration and the shape of the reaction front was estimated as a function of time, temperature and the composition of the reaction bath.

The general applicability of this surface modification scheme to biomaterial development and the use of SBS triblock copolymers as potential biomaterials was also evaluated.

Thesis supervisor: Edward W. Merrill
                       Professor of Chemical Engineering

ACKNOWLEDGEMENTS

This thesis is dedicated

to

the three trees in

my forest.

TABLE OF CONTENTS

LIST OF FIGURES

LIST OF TABLES

I. SUMMARY

1. <u>INTRODUCTION</u>

In order to prepare a suitable high strength elastomeric substrate potentially useful as nonthrombogenic cardiovascular prostheses, certain triblock copolymers of the styrene-butadiene-styrene type have been subjected to surface hydroxylation. In consequence to this treatment, an elastomeric material modeling the laminate structure of the arterial wall has been developed; namely, a soft hydrophilic layer bound to a tough elastomeric substrate. The hydrophilic layer may be subsequently rendered nonthrombogenic by fixation of heparin therein.

2. <u>BACKGROUND</u>

(a) <u>SBS Triblock Copolymers as a Biomaterial</u>

The unique porperties of the styrene-butadiene-styrene triblock[1] copolymers makes them particularly useful as biomaterials. First, because of the requirements of the 'living-polymer' anionic polymerization technique by which they are synthesized they are ultrapure and contain no elutable contaminants which might render them toxic to the human system. The work of Nyilas, et al., (1970) demonstrated the strong effect that trace contaminants and defects in the microstructure have on the blood compatibility of silicones. Second, as a result of the

---

[1]   In contradistinction to random copolymers, these *block* copolymers are linear macromolecules in which, beginning at one end, there is a sequence of several hundred styrene units, followed by a sequence of several hundred butadiene units, and finally finished by another sequence of styrene units about as long as the first sequence.

thermodynamic incompatibility of the polystyrene and polybutadiene

blocks there is a phase separation in the solid phase, with the for-

mation, in a SBS triblock copolymer containing 25% polystyrene[1], of

glassy domains of polystyrene dispersed in a *continuum* of the rubbery

polybutadiene. However, because of the bonds between the two phases,

the polystyrene domains act to keep the polybutadiene entanglements

in place, in addition to acting as particles of reinforcing filler to

give the copolymer, at body temperature, the properties of high strength

elastomer (initial modulus, 650 psi; tensile strength, 3900 psi) (All-

port and Janes, 1973). Thus without any further potentially contaminating

crosslinking or strength inducing steps, the SBS copolymer containing

approximately 25% wt. polystyrene satisfies all the mechanical require-

ments of a vascular prosthesis.

The glassy domains in a 25 wt. % copolymer are cylindrical and rod-

like in shape[2] (Lewis and Price, 1971). Although they may orient them-

selves near the surface so as to extend through the surface to expose

polystyrene, the drying conditions of solvent cast films would have a

strong effect on the degree of separation of the two phases. The resulting

mixed surface which can be hydroxylated would mediate against the throm-

bogenicity of the otherwise pure, exposed polystyrene.

The polybutadiene block is generally stable to biological degrada-

---

1   The morphology is affected by a number of factors of which the
    styrene content is the most important. With higher polystyrene
    contents, the morphology could involve discrete phases of poly-
    butadiene in a polystyrene continuum.

2   Confirmed by transmission electron micrographs taken in con-
    junction with this work (section V-1.)

tion (Coscarelli, 1972) and would only be subject to oxidative degradation in the presence of ultraviolet light or ozone, neither of which are present inside the body (Hawkins, 1972).

In addition because the dimensional stability of the SBS copolymer is the result of a polystyrene phase formation which may be simply reversed by addition of a solvent for polystyrene or by raising the temperature above the polystyrene's glass transition temperature (100°C), the elastomer can be easily extruded or molded to give the required final form. This processability is an added advantage of these materials.

(b) Surface Reaction Scheme

In order to utilize one of the techniques that has been developed to prepare a nonthrombogenic surface (coupling of heparin to a polyhydroxy polymer through an acetal bridge (Merrill, et al., 1970)), reactions for producing hydroxyl groups on the surfaces of SBS triblock copolymer specimens were extensively studied in this thesis. By modifying only the surface of the triblock copolymers, their unique mechanical properties can be retained.

Hydroxylation of polybutadiene copolymers in solution is a well established procedure that has, in fact, been used on SBS and SIS copolymers to prepare biomaterials (Winkler, 1971, Bishop and O'Neill, 1969).

It is established that each double bond in the polybutadiene block is oxidized by peracetic acid to form an epoxide product which is immediately cleaved by the acetic acid in the reaction bath, in the presence of mineral acid, to form a hydroxyacetate addition product (Figure I-1). The acetate group is then replaced by a second hydroxyl group by base hydrolysis; the net result being a 1,2 glycol structure.
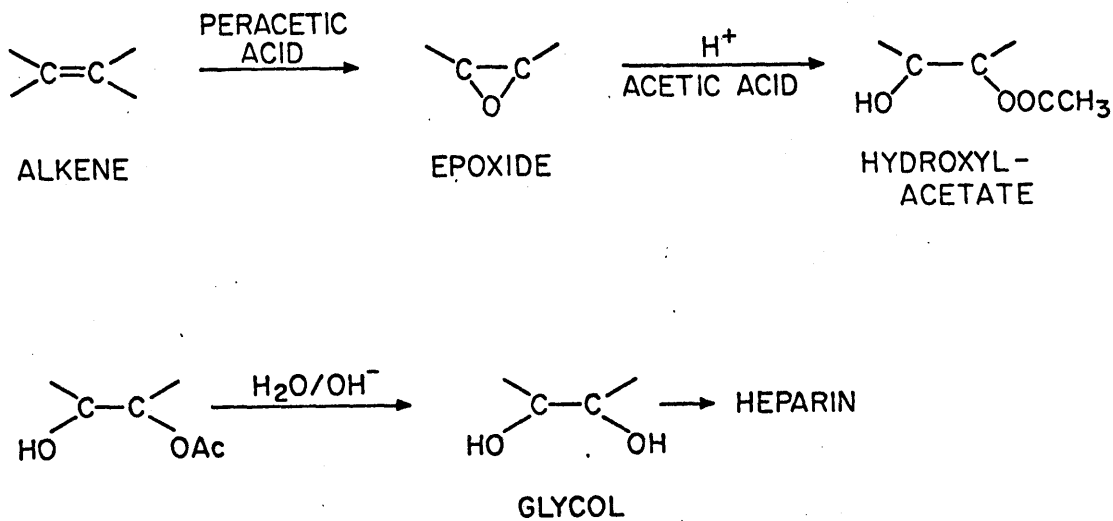
Figure I-1. Surface hydroxylation reaction scheme.
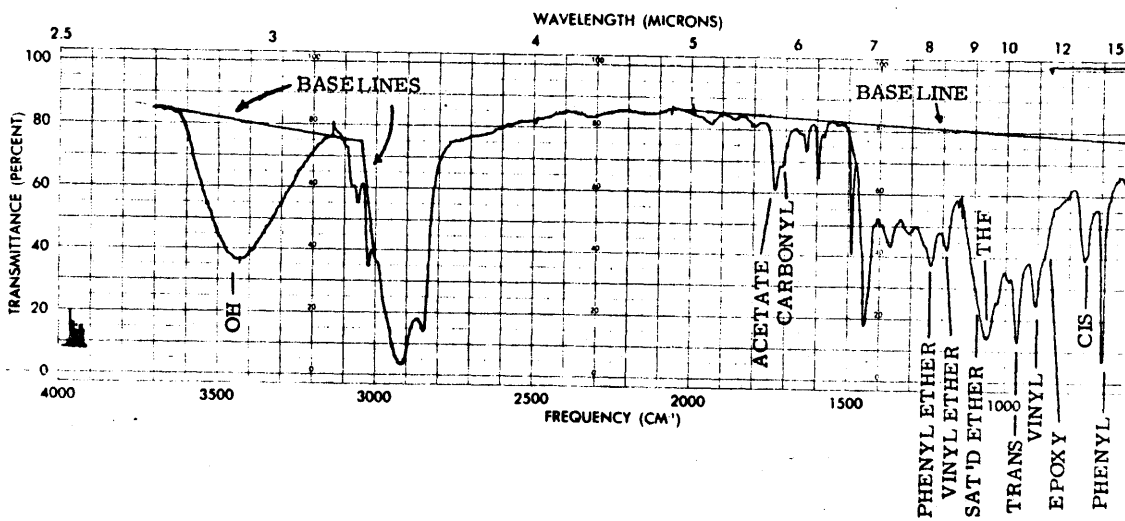
Figure I-2. Typical infrared spectrum of surface hydroxylated SBS.

In this work the SBS copolymer is in the solid phase during reaction and not in solution. Consequently side reactions take on an added importance. Similar to the rearrangements reported by Ohloff, et al., (1964) in the epoxidation of various terpenes, an intramolecular epoxide - epoxide reaction can occur to form substituted tetrahydro-furan rings internal to the polymeric chain:
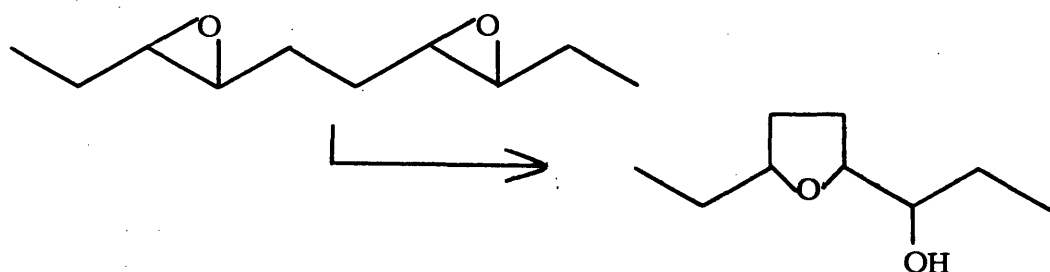
Identical rearrangements can occur intermolecularly to form cross-linking ethers in a mechanism similar to that of epoxide ring-opening polymerization. Vinyl or saturated acyclic ethers are equally possible:
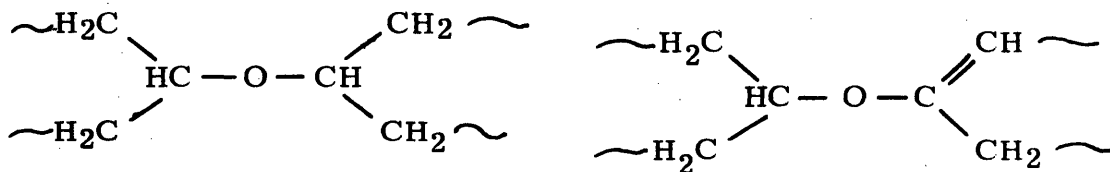
Aside from considerations of yield, intermolecular ethers resulting from epoxide - epoxide reactions are crosslinks which strongly affect the mechanical and swelling properties of the resulting material.

Another consideration common to both the solution and surface reactions is the different reactivities of the three double bond isomers

in the polybutadiene block. The cis 1,4 and trans 1,4 isomers are approximately twenty-five times as reactive as the vinyl isomer resulting from 1,2 addition during the polymerization. (The microstructure of the polybutadiene block is controllable, to a certain extent, by the choice of polymerization solvent (Allport and Janes, 1973).) However it might be supposed that due to a reduction in steric hindrance the pendant double bonds from 1,2 addition would provide a pair of alcohol groups, one group being secondary and one primary, that might be more suitable for the subsequent coupling of heparin.

In the process of hydroxylation of bulk polybutadiene (in contrast to dissolved polybutadiene), peracetic acid must diffuse through the polybutadiene phase to effect epoxidation of the polymer. The parameters governing this reaction/diffusion process are the diffusivity and solubility of the peracid in the polymer and the kinetic constant of epoxidation. After reaction has occurred the polymer is converted from a hydrophobic to a hydrophilic material and the solubility of the peracid in the polymer increases. In addition, swelling occurs simultaneously with reaction, with an increase in diffusivity and a still further increase in solubility. According to Crank (1953) this diffusivity and solubility increase on swelling is modified by the presence of an elastic network which transfers stress to the interior, unreacted nonswollen core. Since the degree of stress transfer depends on the relative size of the unreacted core and the reacted surface, the thickness of the film has a strong effect on the diffusion rate of peracetic acid.

In the reaction procedure used here, no attempt was made to isolate the epoxide groups and, in fact, epoxide cleavage was encouraged. There-

fore, the diffusion of the cleavage agents (acetic acid, water and sulphuric acid) was also important in evaluating the structure of the surface hydroxylated polymer. Their diffusion rates were subject to the same stress transfer mechanism as peracetic acid but since the solubilities of the cleavage agents (especially sulphuric acid) are less than that of peracetic acid, their diffusion rates were lower, and a lag existed between the advancing concentration profiles of peracetic acid and the cleavage agents.

3. EXPERIMENTAL

Experimental work was principally directed toward the determination of and quantitative evaluation of the content of hydroxyl and other chemical groups in films of the copolymer as a function of time, temperature, composition of the reaction bath, and film thickness. In addition, the depth of penetration of the surface hydroxylation process was estimated by comparing the weights of unreacted and reacted material in these films.

(a) Surface Hydroxylation

Films of SBS (Shell Experimental Block Copolymer TR-41-2443, (M_w = 118,000; 27.7 Wt. % polystyrene), cast from benzene solution onto mercury were suspended in a flask in a reaction medium composed of peracetic acid (FMC, 40% peracetic acid), H_2SO_4 and varying amounts of acetic acid and water, all maintained at a fixed temperature (30°-45°C). After sufficient time had elapsed the films were removed from the bath, washed free of acid and then the acetate groups were hydrolyzed in 2N KOH in a separate bath. The films were dried under light compression.

With a Perkin-Elmer model 521 grating infrared spectrometer, the spectrum between 3,800-3,000 cm^{-1} of each of the dried films was recorded. The area under the OH stretching peak centered around 3,430 cm^{-1} was calculated using the formula of Ramsay. With the absorptivity of the same peak determined from films of polyvinyl alcohol, the values of "area concentration," mathematically defined as $\int_0^b C_{OH}$ (b = film thickness, cm; C_{OH} = local concentration of hydroxyl groups, moles/cm^3) were determined using the Lambert-Beer law. (No other chemical groups present absorb in this wavelength region.) The values of $\int C_{OH}$, that is, the moles of hydroxyl groups per unit area of film, were then plotted against the film thickness.

(b) Infrared Spectroscopy

Quantitative infrared analysis was used to follow the reaction and to note the effect of various parameters (e.g. film thickness and time of reaction) on the product distribution. The Lambert-Beer law extended for a multicomponent system and written at more frequencies than absorbing components present in the sample (an over-determined system) formed the basis for the quantitative analysis scheme. Due to the complexities present in the spectra of the surface reacted samples, however, it had to be considered as a model fitting procedure. The least squares solution to the resulting set of linear equations was given by (Herschberg and Sixma, 1962):

$$<X> = (a^T a)^{-1} a^T A \qquad (III-5)$$

where   <X> = average values of area concentrations of components

present in samples ($moles/cm^2$)

A = absrobances determined from spectrum

a = absorptivities determined separately

The resulting area concentrations ($moles/cm^2$) were converted to 'true'

concentrations by dividing by the <X> value for polystyrene, thus elim-

inating any effect of the size of the sample, of which the spectrum was

recorded.

Qualitative spectral analysis, according to standard group correla-

tions (Bellamy, 1958), was also performed.

If the films were thin enough no further preparation was necessary

to obtain a suitable spectrum. For thicker films, however, it was neces-

sary to grind portions of the film at liquid nitrogen temperatures and

to disperse the ground polymer in carbon disulphide before suitable spec-

tra could be obtained.

(c.) Delamination

Allowing samples of known area of the surface reacted films to swell

in chloroform resulted in delamination and separation of the (cross-linked)

surface reacted region from the unreacted portion of the sample. Three

fractions were recovered: crosslinked gel, chloroform soluble but reacted

polymer fraction, and a chloroform soluble unreacted fraction. By compari-

son of the weights of these fractions, two estimates of the depth of pene-

tration of the reaction were obtained.

4. RESULTS AND DISCUSSION

(a) Qualitative Spectral Analysis

Qualitative analysis of the spectrum of a surface hydroxylated sample (Figure I-2) shows unequivocally the presence of phenyl groups (polystyrene), residual unsaturation (cis, trans, and vinyl double bonds), hydroxyl groups, uncleaved epoxy rings, and unhydrolysed acetate esters. In addition, there is spectral evidence in favour of the presence of carbonyl groups (from epoxide-to-carbonyl rearrangements), substituted tetrahydrofuran rings and acyclic ethers (from intramolecular and intermolecular epoxide - epoxide reactions, respectively). The ethers formed are a combination of vinyl ethers, phenyl - phenyl ethers, phenyl - alkyl ethers, and symmetric saturated ethers. (The aromatic ethers result from nonspecific reactions of polystyrene.)

There is no definite evidence in the spectrum in favour of the presence of unsaturated allylic ethers, peroxides, primary alcohols, dioxane structures, and tetrahydropyran structures, thus, further consideration was not given to these structures in the development of the spectroscopic model.

(b) Hydroxyl Content

By analysis of the curves of extent of reaction (area concentration, hydroxyl) versus film thickness (Figures I-3,8b), the various parameters governing the diffusion/reaction process were evaluated.

All the curves of hydroxyl content (area concentration) versus film thickness were found to show the same behaviour as in Figure I-3, an initial linear increase in hydroxyl content followed by a gradual decrease beyond a certain maximum value. The linear portion of the curve--AB--defines the range of films over which the peracetic acid, under the given experimental conditions, has diffused through the complete film, and all
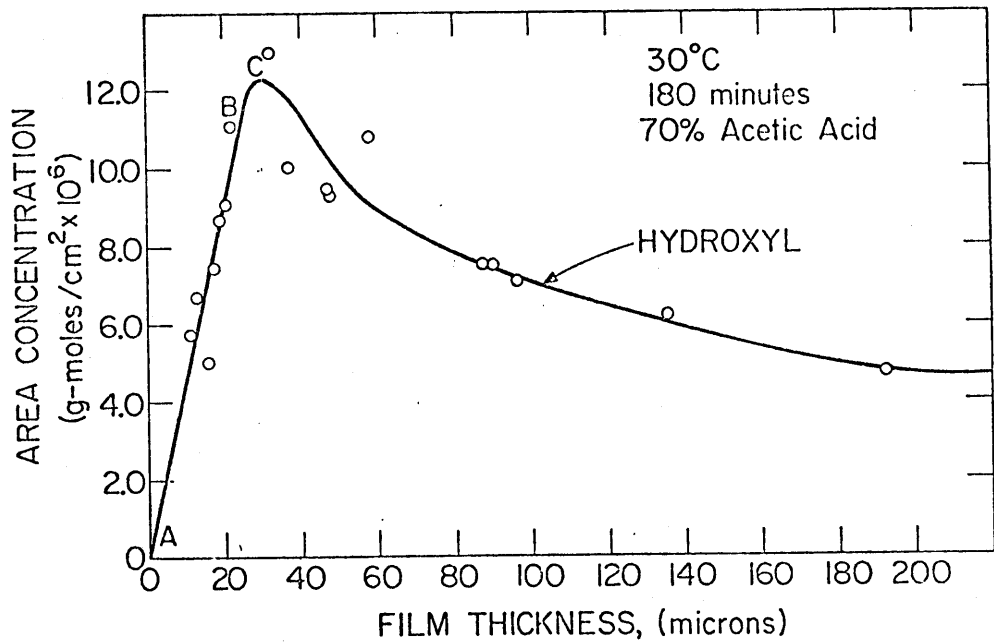
Figure I-3. Area concentration, hydroxyl versus film thickness;

30°C, 180 min., 70% acetic acid.
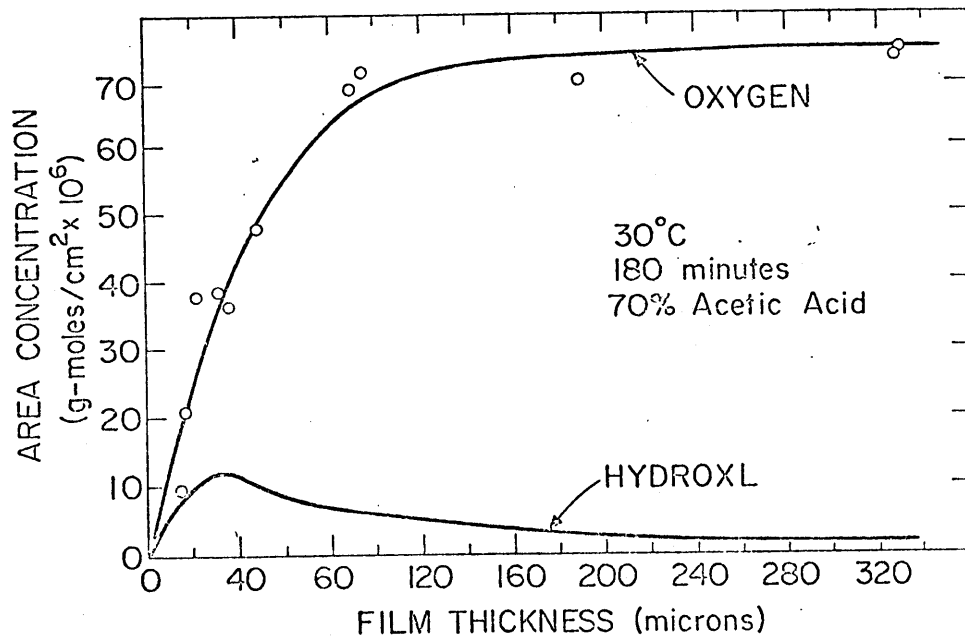
Figure I-4. Area concentration, oxygen versus film thickness

potentially reactive double bonds are presumed to have reacted. The slope of this portion is independent of time and temperature and only slightly dependent on the composition of the reaction bath. The value of the slope corresponds to a 24% conversion of the double bonds to the glycol structure in the 71% acetic acid - 23% water reaction bath. While some of the double bonds are unreactive due to steric or electronic effects (e.g. vinyl groups) many of the double bonds reacted to form intramolecular or intermolecular ethers, as confirmed by the qualitative analysis of the complete infrared spectrum.

However the maximum at C in Figure I-3 and the subsequent decrease was not expected. In a simple sorption experiment for a given set of experimental conditions, there is a particular film thickness at which the weight gain per unit area would become independent of film thickness; this film thickness being the depth of penetration of the permeant (Crank, 1956). In larger films, the polymer beyond this depth of penetration would have no effect on the amount of permeant being absorbed. To understand the anomalous behaviour in our system, the total oxygen content of some of our samples was determined (Figure I-4). To the extent that the assumption of a constant stoichiometric ratio (constant moles oxygen to moles double bond reacted) is valid, the total oxygen content reflects the number of double bonds reacted. This curve, as expected, asymptotically approaches a much higher level and at a film thickness greater than that at point C. Thus it appears that the peracetic acid diffuses in a normal manner through the films but a change in product distribution occurs in the thicker films.

According to this reasoning, by addition of oxygen to the polymer,

¢

c_{OH}

S_2 S_1

NO SWELLING

SWELLING

REACTED SURFACE | UNREACTED CORE | REACTED SURFACE

b
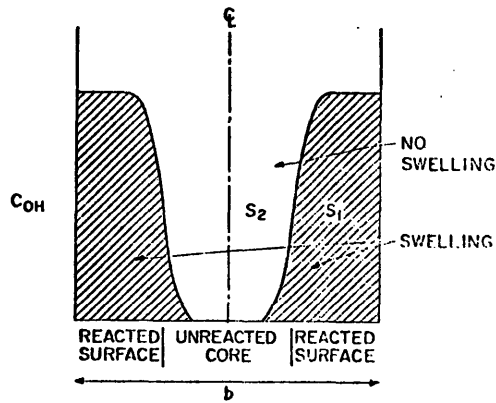
Figure I-5. Reacted film model.

the polymer is converted from a hydrophobic to a hydrophilic material; the reacted surface region of the polymer therefore, swells in the acetic acid - water reaction bath. However, this swelling behaviour is modified by the presence of the unreacted core (Figure I-5), since the swelling stresses near the surface are transferred by the elastic network to the higher modulus unreacted portion of the polymer; this stress transfer is dependent on the ratio of the size of the surface region to that of the total material. Hence, the surface region of the thinner films swells more than that of the thicker films enabling the slower diffusing epoxide cleavage agents (acetic acid, water, and sulphuric acid) to diffuse more effectively into the thinner films. (The higher diffusivity and solubility for the cleavage agents along the epoxidation reaction front reduces the limiting lag between the diffusion of per-acetic and the cleavage agents.) As a result, cleavage of the epoxy rings is more nearly complete in thinner films yielding higher hydroxyl contents in these thinner films than in the thicker ones where cleavage

is not as complete.

Quantitative analysis of spectra of the films that had been pre-
pared at 30°C for 180 minutes in 70% acetic acid show the expected
decrease in hydroxyl concentration and the expected increase in epoxide
content with increasing film thickness (Figure I-6 , the concentration
of a given species i being reported as the fraction $C_i/\Sigma_i C_i$ where
$\Sigma_i C_i$ = sum of equivalents of all oxygen containing species). It is
also apparent that there is no correlation of the ether content (acyclic
or cyclic) with film thickness, indicating that their formation is
directly proportional to the epoxide concentration and that their concen-
tration profile matches exactly the concentration profile which defines
the reaction front. The concentration profiles for the various functional
groups present are shown in Figure I-7.

This change in product distribution from a hydroxyl rich surface in
thinner films to an epoxy rich surface region in thicker films renders the
assumption made earlier with regard to a constant stoichiometric ratio in-
valid. The true value of the area concentration of reacted double bonds
then decreases with increasing thickness, due to the direct effect of the
stress transfer process on the epoxidation rate in producing a lowered
depth of penetration in thicker films.

In Figures I-8a and I-8b, the time course of the surface hydroxyla-
tion process is evident. The exponential nature of the process is evi-
dent from Figure I-8a and the observation of an apparent induction time
of approximately fifty minutes before there is any evidence of hydroxyl
groups in the infrared spectrum, is evident in Figure I-8b. The depth of
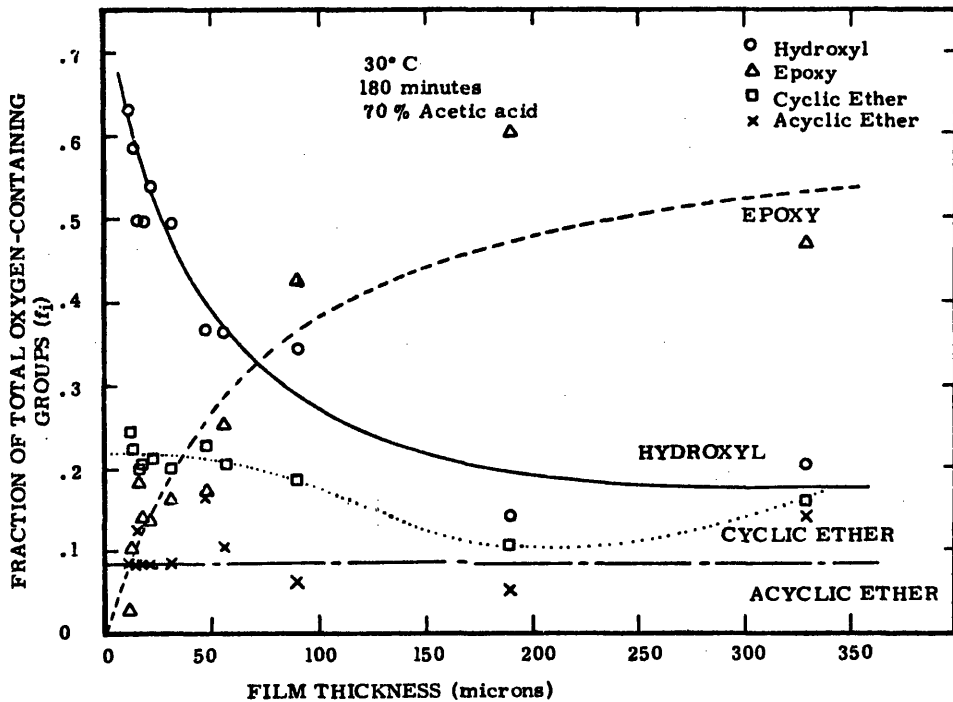
Figure I-6. Composition of surface hydroxylated films as a function of film thickness; 30°C, 180 min., 70% acetic acid
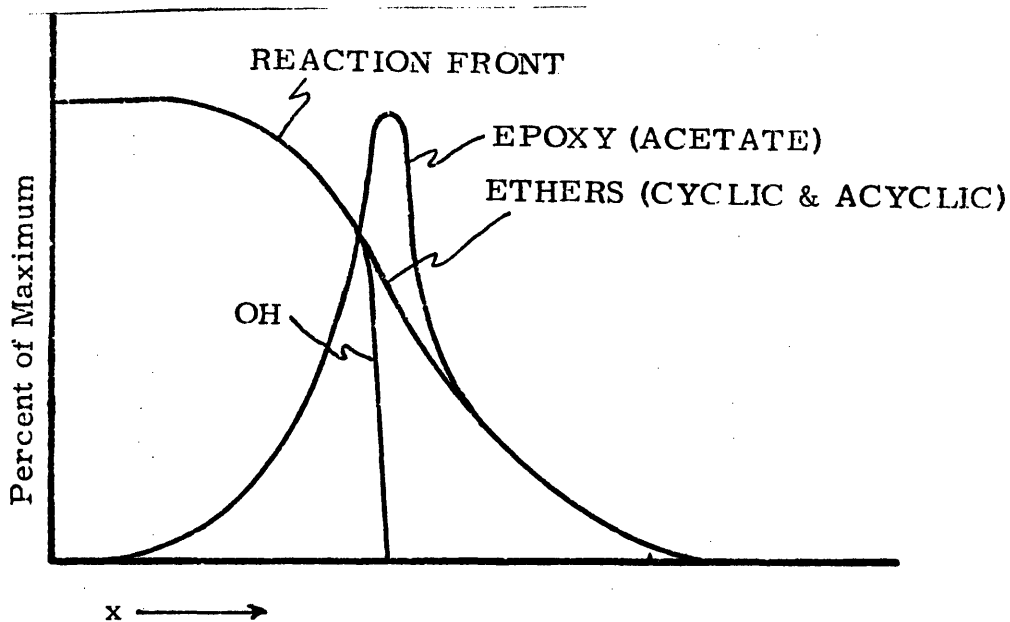
Figure I-7. Typical concentration profiles of oxygen-containing functional groups
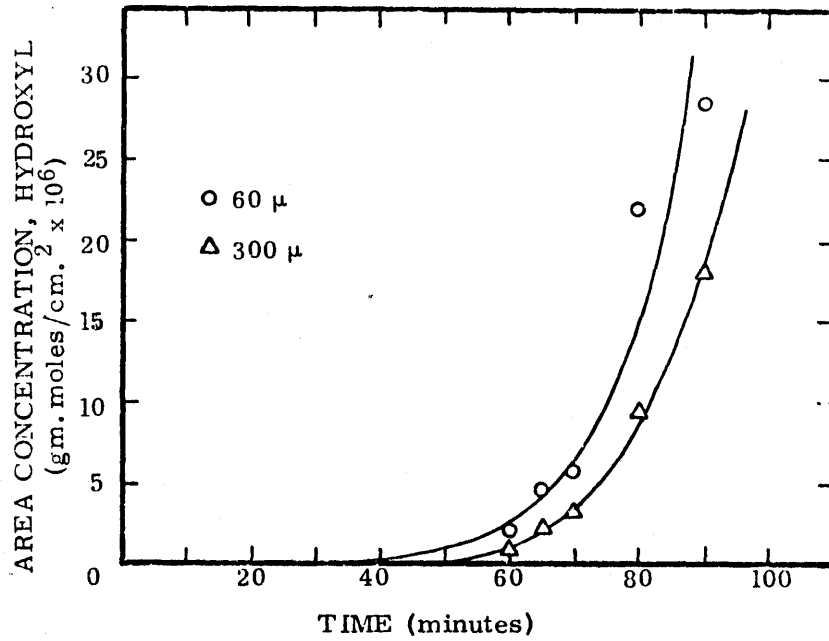
(a) Area concentration, hydroxyl versus time
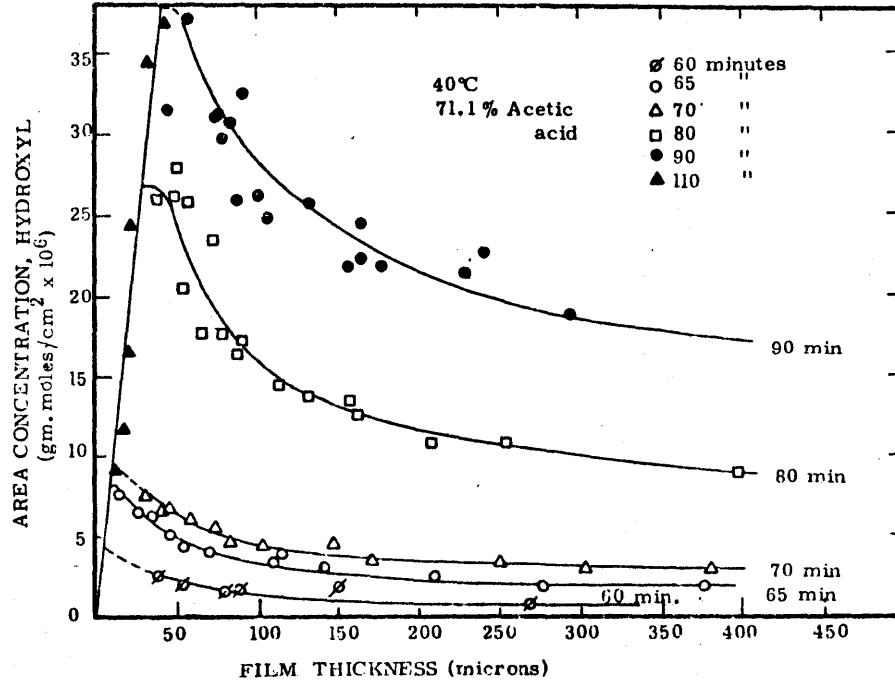
(b) Area concentration versus film thickness

Figure I-8.   Time course of surface hydroxylation; 40°C, 71% acetic acid.

penetration is, therefore, less than 0.2 - 0.3 microns (as calculated from the OH absorptivity and the minimum peak area distinguishable in the spectrum) with fifty minutes of reaction but is increased to a depth on the order of 20-25 microns, a hundred-fold increase, in just 15 minutes. This apparent induction time is directly related to the exponential nature of the process as is seen from the time intercepts at extents of reaction of 0.2 - 0.3 x 10^{-6}moles/cm^2 in extrapolated semi-log plots of A_c^{OH} (area concentration, hydroxyl groups) versus time, which for a 300 micron film were:

35.1°C	66 - 72 minutes
40°C	41 - 46 "
45.1°C	18 - 22 "

The exponential nature of the process is considered, also, to be due to swelling in the surface region. As the surface region swells the solubility of the peracetic acid in the polymer increases and the driving force for diffusion is increased commensurately. Hence the diffusion rate increases with a subsequent increase in the penetration depth and the degree of swelling at the surface due to relief of the limiting compressive stresses, which further increases the peracetic acid solubility. This 'autoacceleration' behaviour is verified by increasing the concentration of acetic acid in the reaction bath. Acetic acid, being a better swelling agent for the reacted polymer, should lower the length of the induction period since the same solubility should be attained at an earlier time. This is shown in Figure I-9, where the extent of reaction is greater after only twenty minutes in 93%
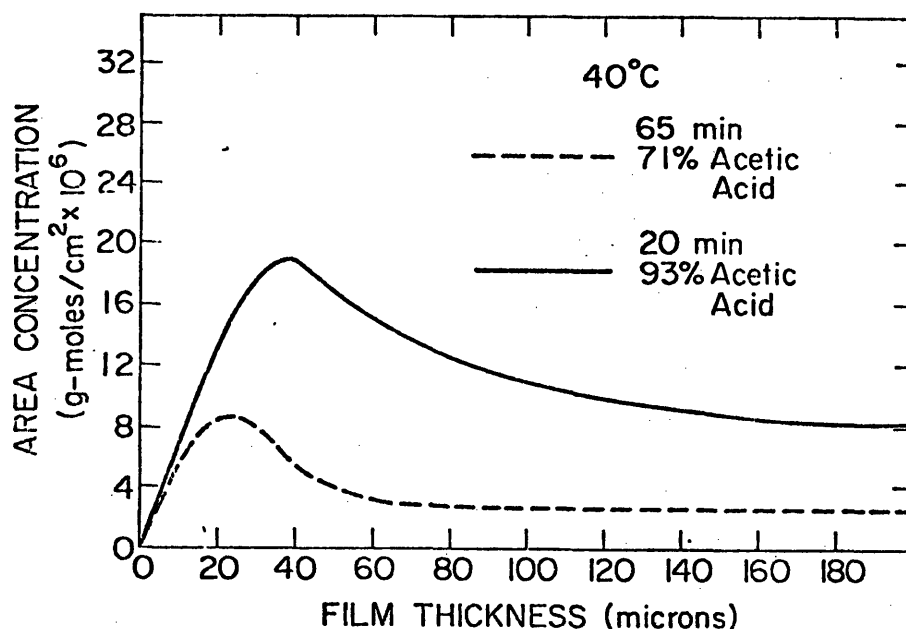
Figure I-9. Comparison of area concentration, hydroxyl
in 71% and 93% acetic acid.

acetic acid than after sixty-five minutes in 71% acetic acid.

(c) Depth of Penetration

The weights of the gel fraction from the delamination experiments
(see section I-3c) give directly an estimate of the depth of penetra-
tion, λ_x. λ_x is an underestimate of the true depth of penetration
since reacted but not crosslinked material present in the advancing
tail of the reaction front is not considered part of this depth of pene-
tration. Weights of the gel fraction (directly proportional to λ_x) as
a function of thickness for the runs conducted at 40°C in 71.1% acetic
acid are plotted in Figure I-10. The initial linear portion defines
the range of films through which peracetic acid has completely diffused
and for which all of the material has reacted and been crosslinked to
form a gel. The distribution of gel is shown in Figure I-11a. The
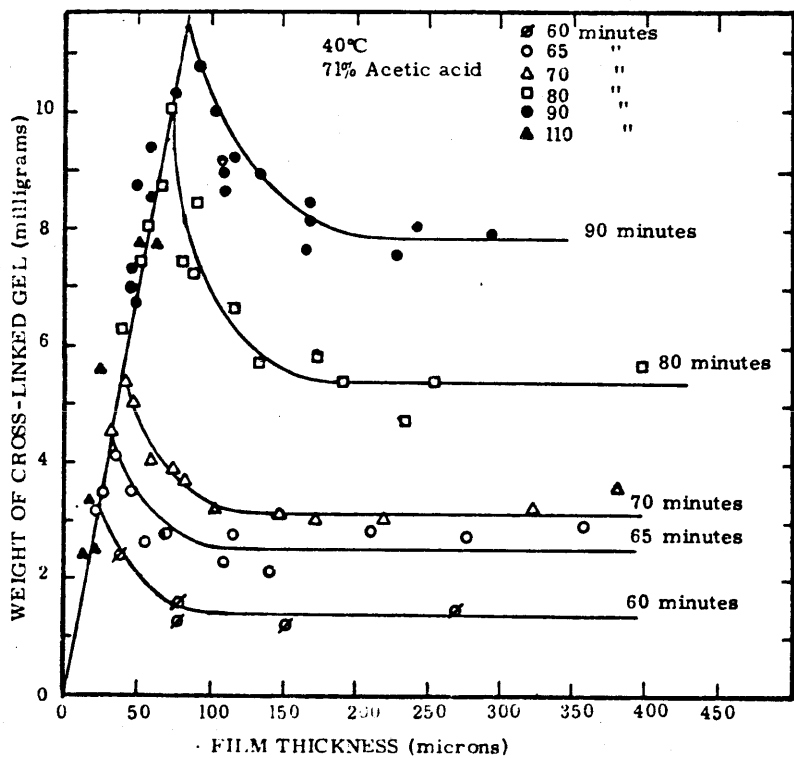
Figure I-10. Weight of crosslinked gel fraction versus
film thickness; 40°C, 71% acetic acid
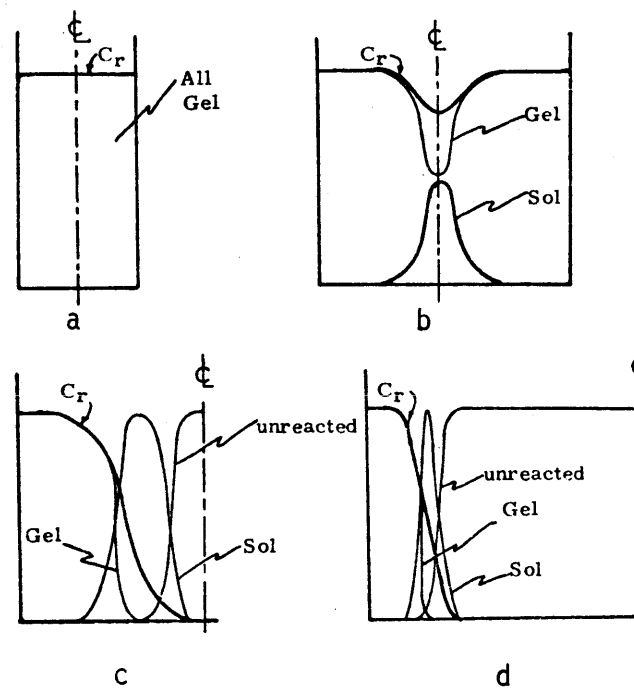
Figure I-11. Distribution of delamination
fractions; C_r = reaction front
(ordinate, fraction of total weight W/W_t,
abscissa, x; (a) - (d) increasing film thickness)

horizontal segment corresponds to the range of films for which the stress transfer mechanism is at its maximum effectiveness and thus, the diffusion rate is maximal. The depth of penetration (of fully crosslinked material) is independent of thickness and dependent only on time, temperature, and the composition of the reaction bath. The distribution of gel in the film is shown in Figure 1-11d.

The intermediate decrease between the linear and horizontal portions is attributed to the increased amount of reacted polymer being non-crosslinked material (sol) compared to the 100% crosslinked nature of the films that account for the initial portion. For thicknesses beyond the one giving rise to the maximum gel weight, the reaction front takes on the shape shown in Figure II-11b. Because of the lower concentration of epoxides in the central portion, fewer crosslinks form and the material in the center, while reacted, is not fully crosslinked. As the thickness increases, the degree of overlap of the reaction fronts decreases and the amount of chloroform soluble material (reacted sol and unreacted polymer) increases with consequent decrease in the weight fraction of gel. This increase in soluble material continues until the stage of reaction front shown in Figure I-11c is reached. From this stage on the decrease in the area under the reaction front - concentration profile causes a decrease in the amount of both crosslinked gel and reacted sol, this decrease generally arising through both a steepening of the slope of the reaction front and an actual decrease in the true depth of penetration. This continues until the stage shown in Figure I-11d, is reached which corresponds to the levelling off of the curve of weight of crosslinked material versus thickness.

The slope of a plot of $\frac{W_t - W_s}{W_t}$ versus $\frac{1}{W_t}$ (where W_t = weight of

the sample before delamination and W_s = weight of recovered, unreacted

fraction) is directly proportional to an average depth of penetration

(average over the range of film thicknesses for which W_s could be mea-

sured), λ_s. The resulting values of $2\lambda_s$ and the values of $2\lambda_x$ calculated

from the weight of the gel fraction are shown in Table I-1. Because no

account is taken of the unreacted sites in the partially reacted sol

fraction, λ_s is a slight overestimate of the true depth of penetration.

The differences between the two values of depth of penetration are

interpreted according to the model shown in Figure I-12. Three regions

can be distinguished: $x = 0$ to $x = \lambda_x$, fully reacted, fully crosslinked,

$x = \lambda_x$ to $x = \lambda_s$, partially reacted, uncrosslinked, $x = \lambda_s$ to $x = $,

fully unreacted region. For example, for films reacted for 80 minutes
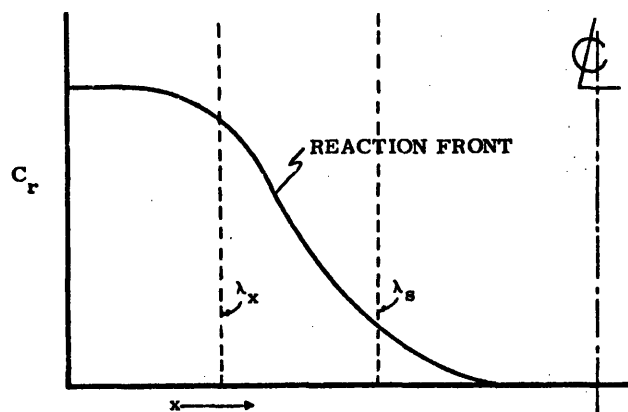
Figure I-12. Reaction front model showing location of λ_x and λ_s.

at 40°C in 71% acetic acid, the fully crosslinked portion is 15µ thick

and the partially reacted region extends for another 8.5 microns.

Table I-1

Depth of Penetration By Delamination

71% Acetic Acid

	35°			40°			45°	
t (min)	$2\lambda_x$ (μ)	$2\lambda_s$ (μ)	t (min)	$2\lambda_x$ (μ)	$2\lambda_s$ (μ)	t (min)	$2\lambda_x$ (μ)	$2\lambda_s$ (μ)
90	10.4	31.5	60	8	30.0	40	10.5	26
			65	14.5	-			
105	21.3	35	70	17.5	38	50	24	35
			80	30	47			
115	28.5	42.5	90	43	62.5	55	30	43

92.5% Acetic Acid, 40°C

t (min)	$2\lambda_x$ (μ)	$2\lambda_s$ (μ)
20	36	65
25	41	72.5
30	60	95.5

The reaction profile is thus not very steep and appears, then, to have the shape shown in Figure I-11c, for these reaction conditions.

5. CONCLUSIONS

(a) Styrene-butadiene-styrene triblock copolymers are ideally suited for potential use as biomaterials.

(b) By surface hydroxylation of SBS copolymers, materials are prepared which have hydroxyl groups near the surface but still retain the high strength elastomeric nature of the original copolymer.

(c) Surface hydroxylation is a combined reaction- and diffusion-limited process which is modified by the simultaneous swelling of the reacted surface region limited, in turn, by stress transfer to the unreacted core. As a result, the principal parameters governing the reaction/diffusion process are the film thickness, time, and the composition of the reaction bath.

(d) The extent of reaction as expressed by the area concentration of hydroxyl groups, decreases with increasing reaction due to the direct effect of stress transfer on reducing the diffusion rate of peracetic acid and to the change in product distribution secondary to the increased diffusion lag between peracetic acid and the cleavage agents (acetic acid, water, and sulphuric acid).

(e) Surface hydroxylation is an autoaccelerative process and exhibits an apparent induction time before there is any infrared evidence of hydroxyl formation.

(f) Swelling in chloroform results in delamination of the reacted films. From the weights of the recovered fractions the depth of penetration of

the reaction and the shape of the reaction front can be determined.

(g) With suitable control of time, temperature, and the composition of the reaction bath, depths of penetration on the order of 1 micron or less are attainable.

(h) Quantitative and qualitative infrared analysis is an excellent technique for determining the structure of the reacted polymer.

(i) The surface reacted scheme described here is generally applicable to any styrene-butadiene-styrene copolymer in which polybutadiene is the continuous phase and thus can be used to prepare a wide variety of biomaterials with their mechanical requirements satisfied by proper choice of the substrate copolymer.

II. INTRODUCTION

Over the past several years many implantable devices have been devised which aid the circulation of blood in diseased patients. One of the simplest of these is the vascular prosthesis, designed to act as a replacement or bypass for arteries or veins which have become occluded. While Dacron® velour is most commonly used for these protheses, the use of a velour limits the use of the prosthesis to those portions of the circulatory system (principally the larger arteries) where the blood flow rate is sufficiently fast to prevent build up of thrombin to levels sufficient to activate fibrin formation. The development of a non-thrombogenic material suitable for these protheses would significantly extend the applicability of vascular replacement surgery.

In order to prepare suitable high strength elastomeric substrates potentially useful as nonthrombogenic cardiovascular prostheses, certain triblock copolymers of the styrene-butadiene-styrene type have been subjected to surface hydroxylation. In consequence to this treatment, an elastomeric material modeling the laminate structure of the arterial wall has been developed; namely, a soft hydrophilic layer bound to a tough elastomeric substrate. The hydrophilic layer may be subsequently rendered nonthrombogenic by fixation of heparin therein.

1. BIOLOGICAL REQUIREMENTS

In addition to the mechanical requirements of performance, the biological environment and, in particular, contact with blood, imposes certain stringent requirements on any material that is to be implanted in humans. These are listed in Table II-1.

Table II-1

Biological Requirements of Blood Compatible Materials

(Bruck, 1974)

nonthrombogenicity

no toxic or allergic reactions

no effect on cellular elements of blood

no alteration of plasma proteins or cellular enzymes

no adverse immune responses

no damage to adjacent tissue

no depletion of electrolytes

noncarcinogenic

nondegradable in biological environment

sterilizable

The most difficult of these requirements to attain in practice is the first: nonthrombogenicity. For a material to be nonthrombogenic, (i.e. resistant to the formation of blood clots) the activation of factor XII and subsequent polymerization of fibrinogen to fibrin (intrinsic clotting system) must be suppressed in addition to the prevention of platelet adhesion and release of platelet factor III. The relevant details of thrombosis and the problem of evaluating nonthrombogenic surfaces has been critically reviewed by Salzman (1971).

While no material currently available satisfies all of the requirements listed in Table 1, certain materials can be used in particular devices in contact with blood due to the nature of the dynamics of flow past the material. Of relevance here is the use of Dacron® velour (E. I. DuPont de Nemours) for vascular prostheses. The use of Dacron® and other inert materials in vascular prostheses, however, is limited to those portions of the circulatory system (principally the larger arteries) where the blood flow is sufficiently fast to prevent build up of thrombin to levels sufficient to activate fibrin formation.

The purpose of this thesis was to develop a material suitable for these prostheses, that could be made actively nonthrombogenic, to extend the applicability of vascular replacement surgery.

2. HEPARINIZATION

One of the most successful schemes for the preparation of nonthrombogenic materials is the incorporation of heparin (the natural anticoagulant) into hydroxyl containing polymers such as polyvinyl alchohol (Merrill, et al., 1970, Merrill and Wong, 1970). The process uses a mixture

of glutaraldehyde and formaldehyde (with $MgCl_2$ catalysis) to couple the secondary hydroxyls of heparin to polyvinyl alchohol via an acetal bridge. The covalently linked heparin is very stable and retains most of its anti-coagulant activity.

Heparin appears to act by complexing with antithrombin (heparin co-factor (Rosenberg, 1973)) and accelerating the reaction of thrombin with antithrombin to form an inactive complex (Fitzgerald and Waugh, 1956). The action of surface incorporated heparin is discussed further by Salz-man (1971).

3. SBS COPOLYMERS AS BIOMATERIALS

The unique properties of the styrene-butadiene-styrene block copoly-mers make them particularly useful as biomaterials.

Styrene-Butadiene-Styrene (SBS) block copolymers have the molecular structure shown in Figure II-1.
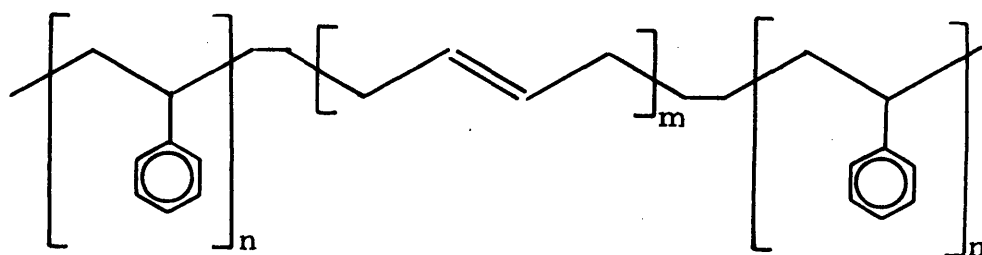
POLYSTYRENE--POLYBUTADIENE---POLYSTYRENE

Figure II-1. Molecular structure of Styrene-Butadiene-Styrene block copolymer.

Unlike a random copolymer of styrene and butadiene, a block copolymer
has an organized structure composed of two blocks of styrene units, one
at each end of a center block of butadiene units. It is prepared by
'living polymer' anionic polymerization techniques. The polymerization
and the properties of SBS block copolymers have been the subjects of
many recent reviews (Allport and Janes, 1973, Morton, 1972, Bradford and
McKeever, 1971). Therefore, only certain relevant aspects will be pre-
sented here.

(a) <u>Properties</u>

To prevent unwanted termination during anionic polymerization, close
attention must be paid to the elimination of all adventitious impurities
from the polymerizing systems. Hence the resulting triblock copolymer
is ultrapure and as such contains no elutable contaminants which might
be toxic to the human system. The work of Nyilas et al (1970) demonstra-
ted the strong effect that trace contaminants and defects in the morpho-
logical microstructure have on the blood compatibility of silicone rub-
ber. Also, by virtue of the polymerization process, SBS copolymers can
be prepared with varying total and/or block molecular weights and thus,
with varying polystyrene contents. Coupled with the ability to vary the
microstructure of the polybutadiene block, SBS copolymers can be prepared
with widely different properties. For example, a copolymer with 90%
polystyrene has a high impact strength, while the copolymer used in this
work containing 25 wt. % polystyrene is a high strength elastomer.

As a result of the thermodynamic incompatibility of the polystyrene
and polybutadiene blocks there is a phase separation in the solid phase,
with the formation, in a SBS containing 25% polystyrene, of discrete

glassy domains of polystyrene in a continuum of the rubbery polybutadiene (Figure II-2). (In figure II-2, the domains are shown as spheres; the morphology is discussed further in section III-1). However, because of the bonds between the two phases, the polystyrene domains act to keep the polybutadiene entanglements in place, in addition to acting as particles of reinforcing filler to give the copolymer, at body temperature, the properties of a high strength elastomer (initial modulus, 650 psi; tensile strength, 3900 psi) (Allport and Janes, 1973). Thus without any further potentially contaminating crosslinking or strength inducing steps, the SBS copolymer containing approximately 25% by weight polystyrene satisfies the mechanical requirements of a vascular prosthesis.

In addition, because the dimensional stability of the SBS copolymer is the result of a polystyrene phase formation which may be simply reversed by addition of a solvent for polystyrene or by raising the temperature above polystyrene's glass transition temperature (approximately 100°C), the elastomer can be easily extruded or molded to give the required final form. This processability is an added advantage of these materials.

(b) Degradation

In the use of polybutadiene based elastomers as vascular prostheses, particular attention must be paid to the effects of long term ageing (approximately 2-5 years) in the biological environment on the elastomer.

Potential ageing mechanisms (Hawkins, 1972) are degradation by enzymatic action and thermal oxidation. Due to the absence of high temperatures, ozone and ultraviolet light in the body, pure thermal degradation, ozonolysis, and oxidative photodegradation are not relevant here (but would be during the processing of these copolymers).

POLYBUTADIENE
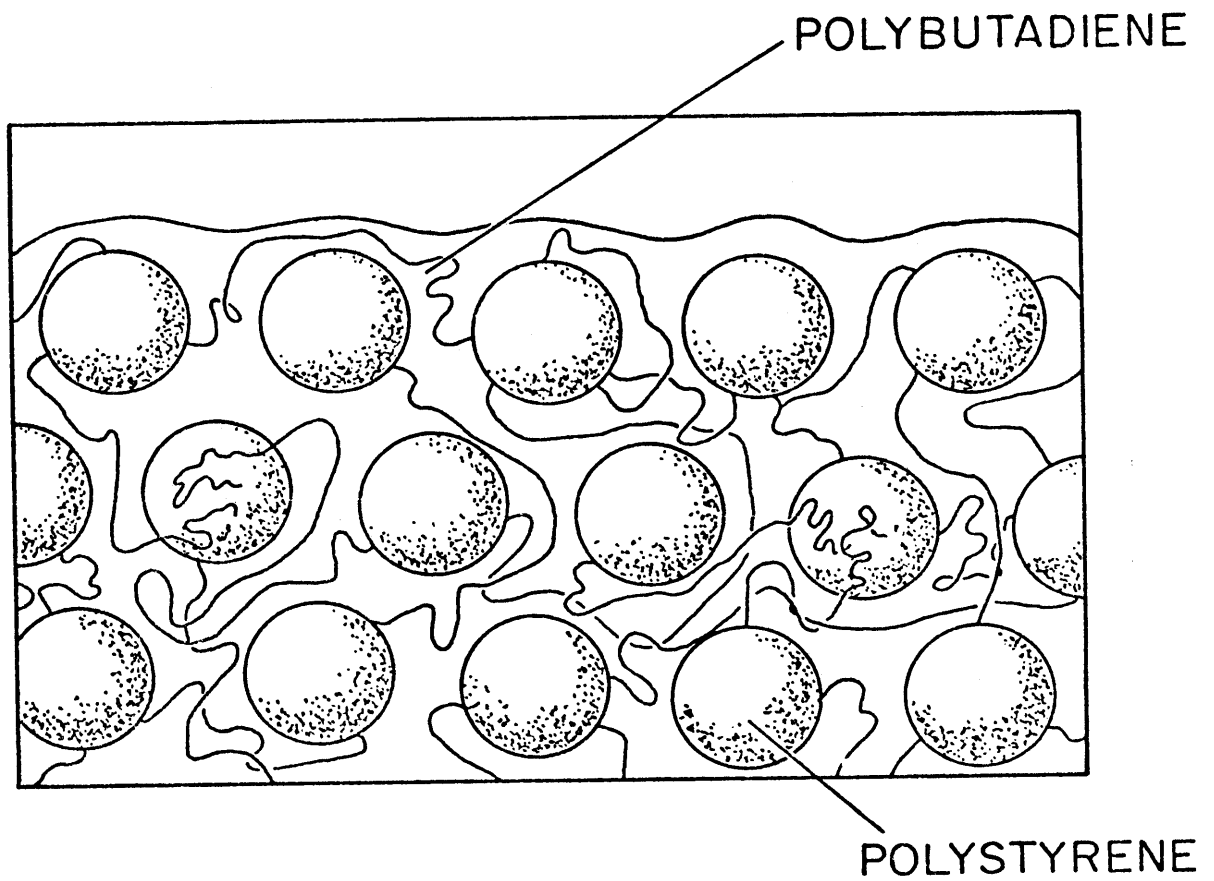
POLYSTYRENE

Figure II-2. Morphology (schematic) of a styrene-butadiene-styrene
block copolymer (approx. 25% polystyrene).

In considering enzymatic action, no a priori remarks can be made regarding the stability of SBS copolymers in the presence of the enzymes found in blood at 37°C and pH 7.4. However, from tests of elastomers using microbes not commonly found in humans it was concluded that the material susceptible to microbial attack is not the elastomer molecule itself, but rather the other material in the formulation (Cosarelli, 1972). This problem was avoided here by using these ultrapure elastomers. Nevertheless, the enzymatic stability of SBS copolymers in contact with blood must still be investigated.

Thermal autooxidation is a free radical process involving the addition of molecular oxygen at relatively low temperatures to a polymer, the net result of which, in unsaturated polymers, is chain scission and hence, de- gradation of mechanical properties (Shelton, 1972). Initiation may be by a variety of free radical generating processes, although the only possible ones here might be mechanical stress or thermal decomposition of weak bonds (e.g. peroxides in the surface hydroxylated layer). While the SBS copoly- mers used in this study needed to be stabilized with an antioxident to pre- vent thermal oxidation initiated by ultraviolet light (Keelen, 1972), it was not clear that in the absence of ultraviolet light (as in the body) and with the presence of the surface hydroxylated layer, the oxidative stability of the polybutadiene block would be critical. Like the enzymatic stability, it must be studied further.

Mediating against any potential degradation process, whether it be en- zymatic or oxidative, is the fact that polystyrene is generally unaffected by these processes. As such, the reinforcement function (stress redistribu- tion) of the polystyrene domains would remain intact and act to minimize the effect of chain scission in the polybutadiene block on the bulk

mechanical properties. In effect, the process of ageing would be pro-
longed.

4. SURFACE REACTION SCHEME

In order to utilize the established heparinization scheme of coupling
via an acetal bridge to a hydroxyl containing polymer (Merrill, et al, 1970,
Merrill and Wong, 1970) (section II-2), the surfaces of our SBS copolymers
have been hydroxylated to provide reactive sites for such a coupling pro-
cedure. By modifying only the 'surface' of the triblock copolymers, their
unique mechanical properties were retained. This concept of a surface
modified polymer for use as a blood compatible biomaterial has also been
incorporated in the microwave discharge graft copolymerization of polar
monomers onto certain polymers to prepare a surface hydrogel on a sub-
strate which gave the whole material the desired bulk properties for its
use as a vascular prosthesis (Scott, et al, 1971). The technique used
here also resulted in a surface hydrogel firmly bound to an elastomeric
substrate but, in addition, the incorporation of heparin in the hydrogel
layer is anticipated.

Hydroxylation of polybutadiene copolymers can be accomplished in a
number of ways (Meyer, 1970). The simplest and most convenient is the
reaction of polybutadiene with preformed peracetic acid to form an epoxide
product which is then cleaved to the desired 1,2-glycol structure (see Figure
III - 3). Epoxidation/hydroxylation of polybutadiene copolymers in so-
lution with preformed peracetic acid is a well-established procedure
(Dittmann and Hamann, 1971, Greenspan, 1964, Makowski,et al, 1970, Meyer,
1970, Sakaguchi, et al, 1972, Winkler, 1971) that has, in fact, been used

on SBS and SIS (I-isoprene) copolymers to prepare biomaterials (Winkler, 1971, Bishop and O'Neill, 1969). However, since the ultimate purpose was to prepare sulphonated block copolymers, the results reported therein are of limited applicability to this study.

Unlike the above cited work, the SBS copolymer was in the solid phase during reaction in this work and not in solution. As expected, diffusion limitations played an important part in the hydroxylation process. To adapt these procedures to the solid phase hydroxylation, no attempt was made to prevent the epoxide group from undergoing cleavage reactions. In fact it was encouraged by the addition of sulfuric acid catalyst and excess acetic acid and by raising the temperature (Swern, et al., 1946). The above mentioned workers (Winkler, 1971, Sakaguchi, et al., 1972, Bishop and O'Neill, 1969) used acid catalysed cleavage of the epoxide to produce the glycol; in this work base catalysed hydrolysis of the resulting ester was used. Further information on the chemistry is given in Section III-2.

Previous work on solid phase hydroxylation is virtually non-existent. While Meyer (1970) hydroxylated a SBS copolymer as a solid film and a patent exists for surface epoxidized polybutadiene to be used as a can coating (N.V. de Baataafsche Petroleum Maatschappij, 1960) no attempts were made to determine the kinetics of the process. The work of Grauer (1973) and Traut (1973) was performed in conjunction with this thesis and so their contributions to the subject will be discussed here.

5. STATEMENT OF OBJECTIVES

The purpose of this thesis, then, was to investigate the diffusion/reaction process associated with the peracetic acid hydroxylation of

styrene-butadiene-styrene copolymers in the solid phase ('surface' hy-
droxylation) and to determine the properties of the resulting material.

III   THEORETICAL

1.   SURFACE MORPHOLOGY

It is fairly well established that the morphology of a styrene-butadiene-styrene block copolymer of number average molecular weight greater than about 75,000, with about .25 - .30 weight fraction polystyrene, cast from a good solvent (e.g. benzene, toluene), consists of discrete domains of polystyrene in a polybutadiene continuum (Allport and Janes, 1973). For a SBS copolymer to be used as a biomaterial the polystyrene domains near the surface must be completely covered by the polybutadiene; exposed polystyrene would be potentially thrombogenic even after surface hydroxylation. Therefore, the morphology of an S B S copolymer near the surface must be investigated.

(a)   Domain Shape

    i)   Experimental Observations

Contrary to the opinion and observations of certain early investigators (Beecher, et al., 1969, McIntyre and Campos-Lopez, 1970), the shape of the discrete polystyrene domains in SBS copolymers, containing about 27% by weight polystyrene, is not spherical. The domain shape appears to be nearly parallel, slightly curved, cylindrical rods of polystyrene in the polybutadiene matrix (Figure V-1) for solvent cast films (using a good solvent for both components) (Douy and Gallot, 1971, Hendus, et al., 1967, Inoue, et al., 1971, Krigbaum, et al., 1973, Lewis and Price, 1971,1972, Turecek, 1972, Uchida, et al., 1972) for solvent cast films annealed at 100°C (Hoffman, et al., 1971) and for compression

molded samples (Lewis and Price, 1971)[1].

The spherical domains only appear in films of block copolymers containing 27% polystyrene cast from a poor solvent for the polystyrene block (e.g. cyclohexane) (Beecher, 1969, Inoue, et al., 1969, 1970) and in films of SBS copolymers containing less than 20% polystyrene (Soen, et al., 1972). The diameter of these rod-like domains is on the order of 300 $\overset{\circ}{A}$ (Soen, et al., 1972) (depending on the polystyrene block molecular weight and the preparation of the sample.)

A model of a random array of hard spherical particles of polystyrene in a rubbery polybutadiene continuum was proposed by Holden, et al., (1969) to explain the elastomeric behavior of a SBS copolymer with 27 % (wt.) polystyrene. Beecher, et al.'s (1969) electron micrographs of solvent cast and compression molded films of the same SBS copolymer, indicated circular patterns of polystyrene dispersed in a polybutadiene matrix. From this limited two-dimensional information, Beecher, et al. concluded that the domains were spherical (and not oblate ellipsoids or cylinders viewed end on). McIntyre and Campos-Lopez (1970) fit their x-ray scattering data with a hexagonal close packed array of spheres and so concluded that the domains were indeed spherical. Despite their insufficient consideration of other possibilities, these works were cited in later reviews (Bradford and McKeever, 1971, Morton, 1972) as confirmation of Holden's model.

The validity of Holden's model, however, is really dependent just

---

1. The polymers studied were either commercial KRATON K1101 or experimental block copolymer TR-41-1648, which is virtually identical to the copolymer TR-41-2443 used intthis thesis.

on the presence of discrete polystyrene domains. Their shape is important only in the consideration of simple models, originally developed for filled elastomers, to quantitatively predict the mechanical properties of block copolymers. The qualitative agreement of model and actual properties would be just as good for discrete cylindrical rods as it is for spheres (certain anistropic properties, in fact, would be better explained).

ii) Theoretical Models

However, the nature of the interface between the domains and the continuum is still unclear, especially with regards to the orientation of the polybutadiene chain at the domain interface and the degree of uniformity in the coverage of these rodlike polystyrene domains.

Inoue, et al., (1969; Uchida, et al., 1972) assumed the absence of any mixed region between the domains and the matrix, with the polymer chains oriented normal to the domain interface at the junction point and were able to predict reasonably well (from statistical thermodynamics) the effect to volume fraction of polystyrene and the nature of the solvent on the domain size and shape. Meier (1970) in similar calculations was also able to predict the most stable domain shape as a function of the block molecular weights in a diblock copolymer but without assuming anything regarding the orientation of the chains at the junction points. (Both theories predict that for a film of a tri-block copolymer containing 27% polystyrene, cast from a good solvent for both components, the most stable domain shape is the cylindrical rod; the oblate ellipsoid was not considered.) The more recent work of Meier (1974) and Leary and Williams (1973, 1974), has confirmed, however,

the presence of a relatively large mixed region between the domains (thickness on the order of one-third the domain radius). Regardless of the specific theory used to predict the size and shape of the domains, however, an assumption of constant densities in the domains and in the matrix (and in the intermediate region(s)) implies a unifrom coverage of polybutadiene at the polystyrene domain interface (i.e. at the interface containing the junctions between the blocks).

However, the junction interface may represent only a fraction of the surface of the polystyrene domain (see Figure III-la).

junction
points

complete coverage
of domain surface

uncovered

(a) cylindrical domain;
longitudinal section

(b) Oblate ellipsoidal
domain; longitudinal
section showing complete
coverage of whole
surface
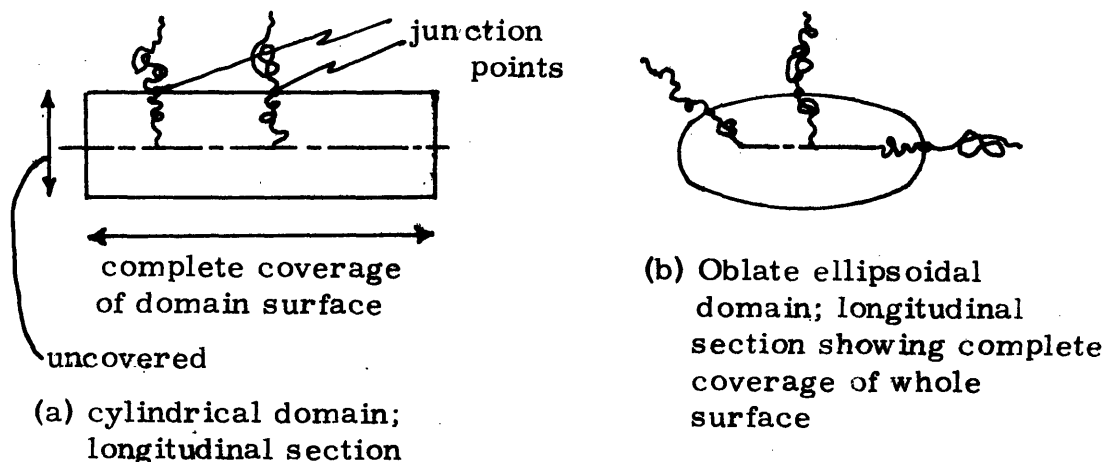
Figure III-1. Domain interface (schematic)

For a cylinder with radial alignment of block ends or junctions, the ends of the cylinder do not contain any junction points. Hence the coverage of a cylindrical domain of polystyrene by polybutadiene need not be completely uniform (e.g. vacuoles could form without disrupting the formation of domains). An oblate ellipsoid (see Figure III-1b) on the other hand, would have junctions distributed throughout the domain surface and hence would be completely covered by polybutadiene.

(b) Surface Tensions

To a certain extent, the relative surface (or interfacial) tensions of polystyrene and polybutadiene control the nature of the surface in a styrene-butadiene-styrene block copolymer. Interfacial tensions of polymers have generally not been measured but they may be estimated in a number of ways (Van Krevelen, 1972). Independent of the estimation procedure the surface (air/polymer interface) tension of polystyrene is greated than the surface tension of polybutadiene (approximate values: γ = 42 dynes/cm for polystyrene, γ = 32 dynes/cm for polybutadiene). On the other hand, the interfacial tension of polystyrene at the mercury/polymer interface (as is formed in the solvent cast films prepared in section III-2), is lower than that for polybutadiene, according to the equation of Fowkes (Van Krevelen, 1972). (Approximate values: $\gamma_{PST/Hg}$ = 15.3 dynes/cm, $\gamma_{PB/Hg}$ = 16.2 dynes/cm.) The difference in tensions is obviously much less.

If the hypothesis of a critical micelle concentration at which phase separation occurs in solution, to form the domains apparent in solvent cast films, is correct (Uchida, 1972), then the relevant interfacial tensions are those of a benzene solution of the polymers. (The interfacial tensions of the melt are virtually identical to those of the amorphous polymer as described above). Using a simple linear relationship (Adamson, 1967) and assuming the absence of any adsorption phenomena, the (air) surface tension of a polystyrene solution is still greater than that of a polybutadiene solution at the same concentration ($\gamma_{PST/Hg} < \gamma_{PB/Hg}$ would also be true.) Assuming further, that for a SBS copolymer dissolved in a good solvent, the degree of solvation of both the polystyrene and poly-

butadiene blocks are equal, then the following remarks concerning the relationship between the surfaces of SBS copolymers and the interfacial tensions of polystyrene and polybutadiene are equally applicable, whether the copolymer film has been prepared by casting as a solution in a good solvent, or from the melt.

(c) Surface Morphology

It is apparent from the above discussion that for a given triblock sample and sample history, there exists only one thermodynamically stable domain shape, size and interfacial mixed region. In order to change this morphology to a slightly different one there must be a decrease in free energy resulting from some other source. Therefore the morphology near an interface would change only in the direction that would result in that component, that has the lower interfacial tension, being closer to the surface. Thus polybutadiene would be the thermodynamically more favorable component at the air interface (of a film of SBS copolymer cast on mercury) and polystyrene would be the more favorable component at the mercury interface. Considering the very small differences in interfacial tension involved (especially for the mercury interface) and considering the very little effect that the polystyrene/polybutadiene interfacial free energy has in the theories of domain formation (Meier, 1969, 1970, Leary and Williams, 1973, 1974), it is extremely doubtful that these interfacial tension differences would result in a change in the shape of the domain. (In fact the electron micrographs of stained thin films that were cast from a good solvent directly onto EM grids or onto mercury (Lewis and Price, 1972), show the 'surface' morphology and not the bulk morphology because of the extreme thinness of the films: ~500 Å)

The only conceivable effect would be in the orientation of the domains. Thus for a SBS copolymer containing 27% polystyrene, the cylindrical domains would orient themselves parallel to the air surface so that the polybutadiene cover along the length of these domains would be exposed and the polystyrene domains themselves would be buried in the interior. (The morphology near the air interface is shown in Figure II-2.) On the other hand, the cylindrical domains would orient themselves normal to the mercury surface so that the uncovered polystyrene ends would be exposed and the free energy would be minimized. After surface hydroxylation it is then expected that the blood compatibility of the mercury side of the interface would be different from that of the air side of the interface. If the domains were oblate ellipsoids, on the other hand, there would be no difference due to the absence of an uncovered polystyrene interface.

Two other phenomena, however, interfere with this strict thermodynamic (equilibrium) morphology. First of all, the solvent cast films dry from the center out so that it is conceivable that the orientation of the cylindrical domains near the surface would be 'locked in' before the effect of the surface would become apparent. Thus the orientation and the resulting surface composition would reflect the interior morphology and be similarly randomized. Secondly, all the above arguments have considered the equilibrium morphology exclusively. Should the film be dried relatively quickly, a nonequilibrium morphology results as the glass transition of polystyrene is passed (Lewis and Price, 1971, Hoffman, et al., 1971). While the effects on the mechanical properties might be disastrous, the resulting randomization of surface composition might be beneficial with

regard to the ultimate blood compatibility. After surface hydroxylation, a mixed interface would be uniformly hydroxylated while an interface composed of discrete domains would result in definite regions of potentially thrombogenic sites.

(d) Effect of Processing

Although it is of little specific relevance to this thesis, the theoretical predictions of Leary and Williams (1973, 1974) are extremely important to the definition of melt processing conditions for SBS copolymers (especially for biomaterials). Figure III-2 shows the separation temperatures T_s and free energy of domain formation (from a random mixture) at 100°C (the nominal glass transition of polystyrene) as a function of the microstructural parameter β for the various domain shapes, for two block copolymers containing 27 wt. % polystyrene: K1101, the commercial Kraton® rubber of total molecular weight 100,000 and for the experimental block copolymer TR-41-1648 of total molecular weight, 112,000 (virtually identical to TR-41-2443). T_s is the temperature at which phase separation takes place, in the absence of solvent, to form domains from a random mixture of the component blocks. The microstructural parameter β defines the size of the intermediate mixed region between the domains.

The predicted behavior of K1101 is described for illustrative purposes. Figure III-2a indicates that cooling of a melt leads to phase separation first at 590°K when the lamellar (P) microstructure forms with β = 0.4, together with spherical domains of polybutadiene (IS) with β = 0.1 (nearly equal to T_s). Subsequent cooling would make other structures possible as their T_s line was passed, but these would not form unless their ΔG were lower than that for the P and IS structures. For example,
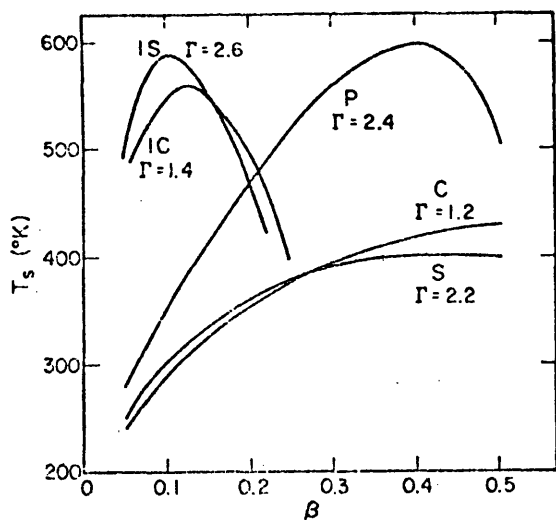
(a) K1101
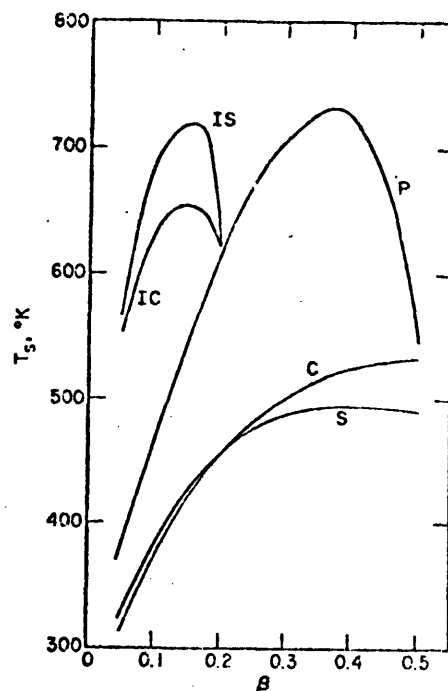
(c) SBS 1648
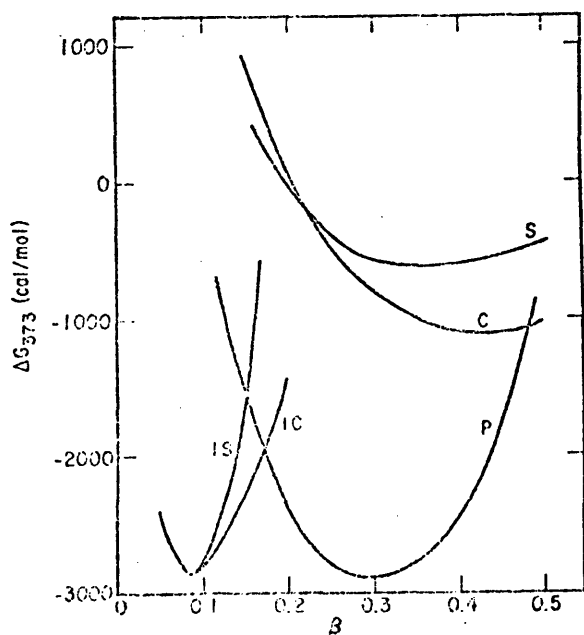
(b) K1101
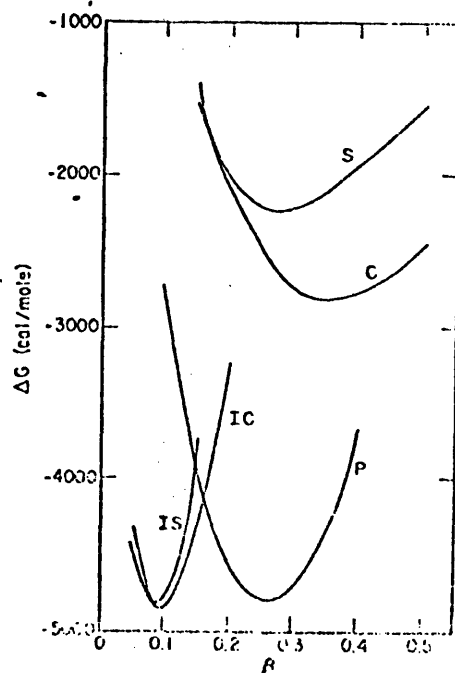
(d) SBS 1648

Figure III-2. Separation temperatures (T_S) and free energies of forma-
tion at 373°K (G); S spheres of polystyrene, C cylinders,
P planar, IC inverted cylinders, IS inverted spheres.
(Leary and Williams, 1974).

Figure II-2b shows that at 373°K the P and IS structures are nearly equally favored, far more so than polystyrene spheres and cylinders. A similar process occurs in the equilibrium melt cooling of TR-41-1648 but the transitions occur at much higher temperatures (despite the only slightly higher total molecular weight). Regardless of the sample, by melt cooling from a sufficiently high temperature, to temperatures less than 373°K where the polystyrene chains are immobile (glassy state) the morphology in the resulting piece would not be one of discrete polystyrene domains but rather a combination of lamellae and inverted spheres or cylinders.

On the other hand if a film is prepared by solvent casting from a good solvent at room temperature, the domain structure for both samples would be discrete domains of polystyrene (cylindrical rods). If the samples were then annealed at 400°K the sample of K1101 would have passed through the T_s for cylinders of polystyrene, the polystyrene domains would 'melt' out, and a combination of IS, IC and P doamins form due to their thermodynamic favourability. However, for the sample of TR-41-1648, the T_s for polystyrene cylinders would not have been passed and so the more favourable IS, IC and P domains could not form. The maximum annealing temperature for TR-41-1648, then, is approximately 475°K, should discrete polystyrene domains be desired.

The observation of Keller, et al. (1970) of a cylindrical morphology in extruded plugs of SBS with the cylinders oriented parallel to the extrusion direction should also be noted.

2. REACTION SCHEME

To effect the surface hydroxylation of styrene-butadiene-styrene block copolymers, the reaction between preformed peracetic acid and the residual unsaturation of the polybutadiene block was used (Figure III-3). Peracetic acid reacted with the double bonds in polybutadiene to form an epoxide product (Chemical Abstracts name: oxirane) which was not isolated but cleaved by the acetic acid present in the reaction bath to form the hydroxyacetate addition product. This acetate was hydrolysed in base to form the desired 1,2 glycol. (The glycol could then be used in the heparin coupling scheme.) As noted in section II-4, the precautions (strict limitations on temperature, reaction time and peracetic acid, acetic acid and sulphuric acid concentrations) described in many of the reviews on epoxidations (Swern, 1949, 1953, 1971, Rosowsky, 1964), necessary for epoxide isolation, were disregarded. Because of the absence of olefinic unsaturation, polystyrene is considered unreactive to epoxidation.

(a) Epoxidation: Mechanism and Kinetics

The kinetics and stereochemistry of epoxidation suggest the presence of a highly ordered non-ionic transition state in this reaction between the electrophilic peracid and the nucleophilic double bond. Following Swern (1971), two transition states are possible. In Figure III-4a the original 'molecular' mechanism proposed by Bartlett (1950) is shown, in which oxygen transfer occurs by a concerted intramolecular process via a spiro transition state. Alternatively, a possible mechanism involving 1,3 dipolar addition to the double bond as the rate determining step (rds) is shown in Figure III-4b.
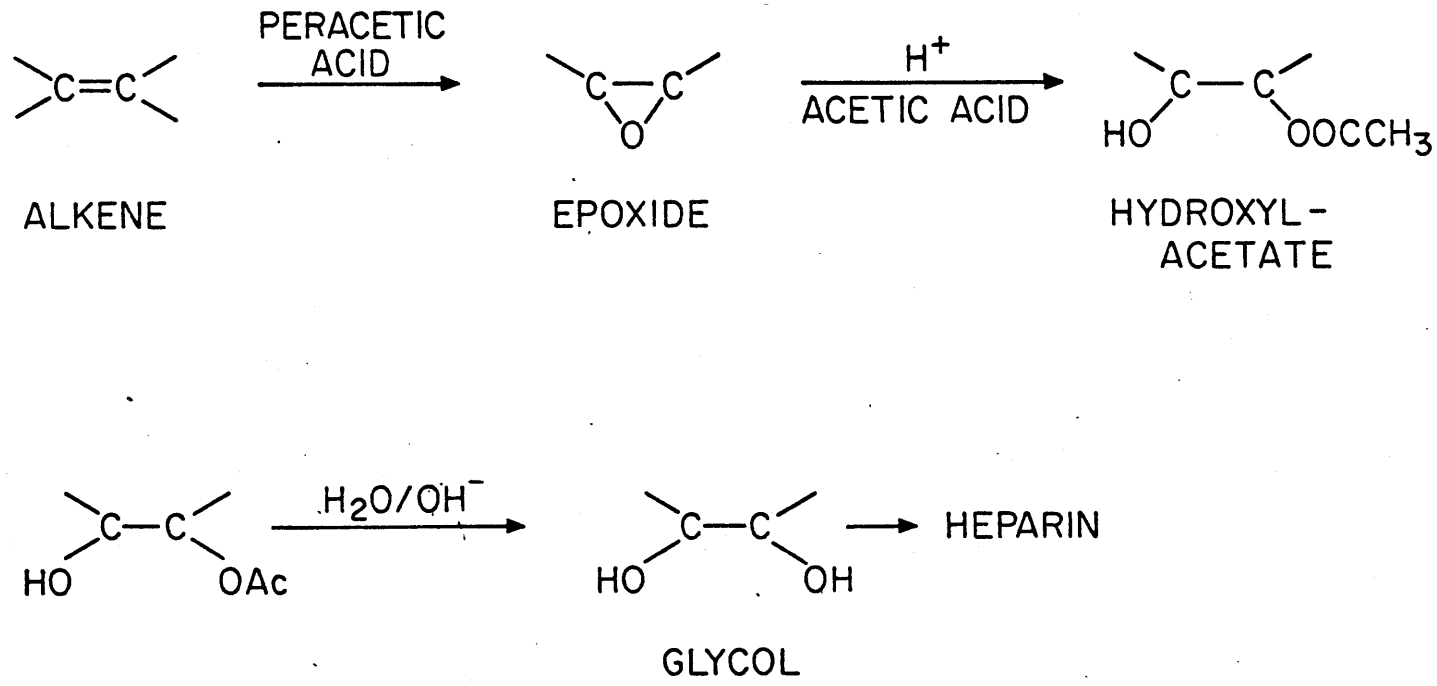
Figure III-3. Surface hydroxylation reaction scheme.

Figure III-4. Mechanisms of epoxidation (Swern, 1961)
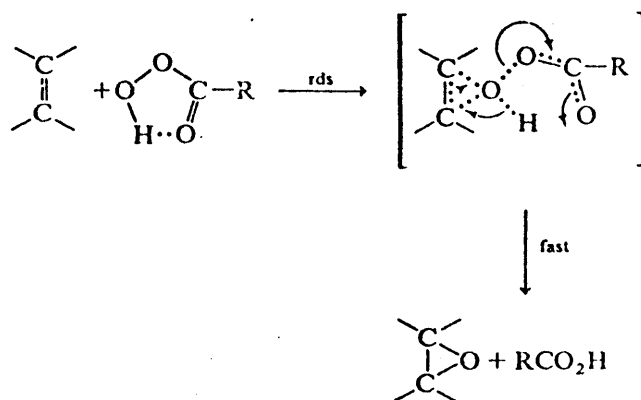
(a) Bartlett (1950)
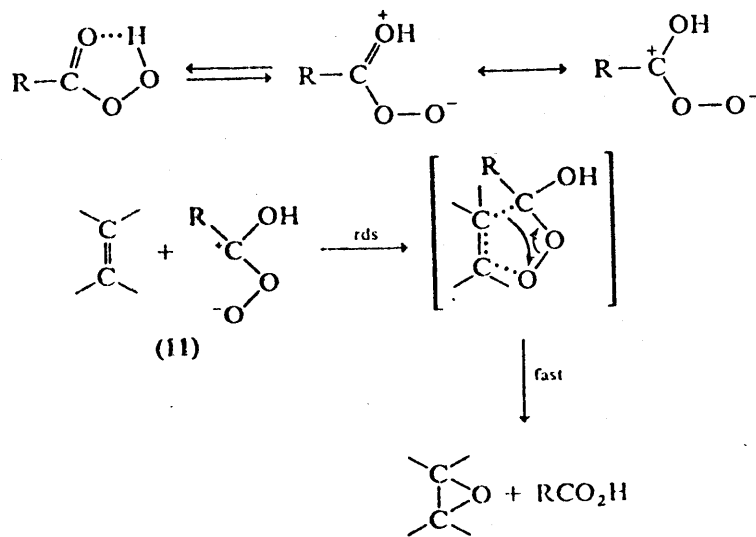
(b) 1,3 dipolar addition

Epoxidation is a second order chemical reaction, first order in olefin and first order in peracid. The specific value for the kinetic constant at a given temperature depends on the structure of the olefin, the structure of the peracid and to a lesser extent on the solvent. Because epoxidation is an electrophilic addition to the double bond (nucleophile), electron donating substituents on the double bond enhance the reaction rate and electron withdrawing groups diminish it (in the absence of steric or resonance stabilization effects)(Swern, 1947): the converse applies with respect to the effect of substituents in the peracid. Since peracetic acid was used exclusively in this thesis, the effect of substituents on the peracid will not be considered further. Vinyl units in polybutadiene have only one alkyl electron-donating substituent whereas the cis or trans isomers from 1,4 polymerization have two alkyl substitutents. Therefore, the cis or trans double bonds, internal to the polymeric chain, are twenty-five times as reactive in epoxidation as the vinylic unsaturation, external to the main chain, (Swern, 1947). (This is important in considering steric hindrance during the heparin coupling reaction; hydroxylated vinyl groups should be more reactive here than the more hindered hydroxylated cis or trans isomers.) In addition it has been reported (Swern, 1947) that cis double bonds are 1.5 times as reactive as trans double bonds. While the difference between the reactivity of internal and external double bonds in the epoxidation of polybutadiene is generally apparent (Makowski, et al., 1970, Dittman and Hamann, 1971), the difference between cis and trans isomers is generally not apparent. (The presence of a third alkyl substituent on the double bonds in polyisoprene makes polyisoprene even more reactive to

epoxidation than polybutadiene.)

The presence of electron withdrawing polar groups, such as alkoxy, aryloxy, epoxy, corbonyl or ester groups on the carbon α to the double bond, results in a decreased rate of epoxidation. (The conjugative electron releasing effect of ether substituents is not efficiently transferred through the intervening carbon atom.) The anomalous effect of a hydroxyl substituent on the carbon α to the double bond in increasing the rate of epoxidation in allyl alcohols is explained by assuming the presence of specific hydrogen bonding between the hydroxyl group and the incoming peracid which tends to activate the peracid (Swern, 1971). However, the presence of these polar substituents in the reacted polybutadiene chain would have no effect on the reactivity of the double bond in the neighboring repeat unit due to the damping out of these inductive effects by the three intervening carbon atoms.

On the other hand, the double bond in vinyl ether structures is extremely reactive towards epoxidation because of the conjugative electron releasing effect of the lone pairs on the ether oxygen. Although the epoxide would not be recoverable because of the extreme lability of this epoxide to hydrolysis, the hydroxy acetate addition product should be (Swern, 1971). However, this reactivity is counterbalanced by steric factors; as a crosslink, the ether oxygen is between two tertiary carbon atoms which limit the approach of a molecule of peracetic acid (Figure III-9), and thus reduce the overall rate of reaction. Similar arguments would probably apply to a double bond substituted with a tetrahydrofuran ring.

Chlorinated solvents and benzene generally provide the highest epoxidation rates; ethers and other more basic solvents provide the lowest,

although the difference is modest. The interpretation given is that the more basic solvents hydrogen bond with the peracid. These hydrogen bonds must be ruptured in order to achieve the required transition state between olefin and peracid. Acetic acid as a solvent is intermediate: a relative rate decrease on the order of 30% - 50% for a relatively reactive olefin (less of an effect for less reactive double bonds)(Swern, 1971).

Configuration is generally retained on epoxidation (Rosowsky, 1964). Epoxidation of a cis-olefin yields a cis-epoxide and similarly a trans-olefin yields a trans-epoxide. Exceptions occur in the epoxidation of allylic alcohols (cis directing effect of hydrogen bonded complex between hydroxyl and peracid) or when steric or field effects predominate (substituted cyclohexenes and other alicyclic compounds) (Swern, 1971).

The Arrhenius activation energy for epoxidation was calculated by Meyer (1970) to be 12 kcal/mole.

(b) Epoxide Cleavage

Epoxides are very susceptible to attack by nucleophilic reagents because of the considerable release of strain energy on cleavage of the three membered ring. Both water and acetic acid are suitable nucleophiles. The acid catalysed cleavage relevant here, proceeds by way of the protonated oxide

$$\underset{HC\text{———}CH}{\overset{\displaystyle H}{\overset{\displaystyle \underset{O}{\diagup \diagdown}{}^{+}}{}}} \quad .$$
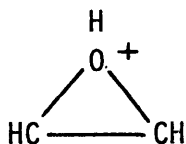
While there is still some question with regards to the molecularity of the reaction, the stereochemical evidence is in favour of a bimolecular (modified A2) mechanism in which the transition state has a great deal of

carbonium ion character (Buchanan and Sable, 1972) (Figure III-5). The transition state is characterized as borderline S_N2 or as one in which bond breaking is more important (i.e. more nearly complete in the transition state) than bond formation (Rosowsky, 1964). As in epoxidation, electron-donating substituents (R_1, R_2) on the epoxide accelerate the reaction by stabilizing the intermediate 'carbonium' ion.

Epoxides are also cleaved under alkaline conditions. However, the lower reactivity of the nonprotonated epoxide must be compensated for by using more basic reagents such as alkoxide ions or ammonia. In the absence of these reagents, base catalysed cleavage does not occur and so will not be considered further.

Unless water is the nucleophile, cleavage of assymetric epoxides demonstrates regioselectivity (preference for the formaiton of one or the other positional isomer) depending on the nature of the substituents attached to the epoxide ring. For example, with acetic acid as the nucleophile, mixtures of isomeric 1,2 diol monoesters are obtained on cleavage of the epoxide. Referring to Figure III-5, if R_1 is a weakly electron releasing group such as alkyl and R_2 is a hydrogen atom (terminal epoxide), a considerable proportion of the 'abnormal' isomer A is formed. The alkyl group is able to stabilize the developing carbonium ion at a vicinal carbon atom as in (a) but will have little effect on the more distant carbon atom (b). This tends to counteract the steric preference for nucleophilic attack at the primary carbon atom (Buchanan and Sable, 1972). Therefore, in terminal epoxides (e.g. epoxides of vinyl double bonds in polybutadiene) cleavage by acetic acid results in a significant proportion of primary alcohols (with acetate esters on the C-2 atom) in addition to the normal
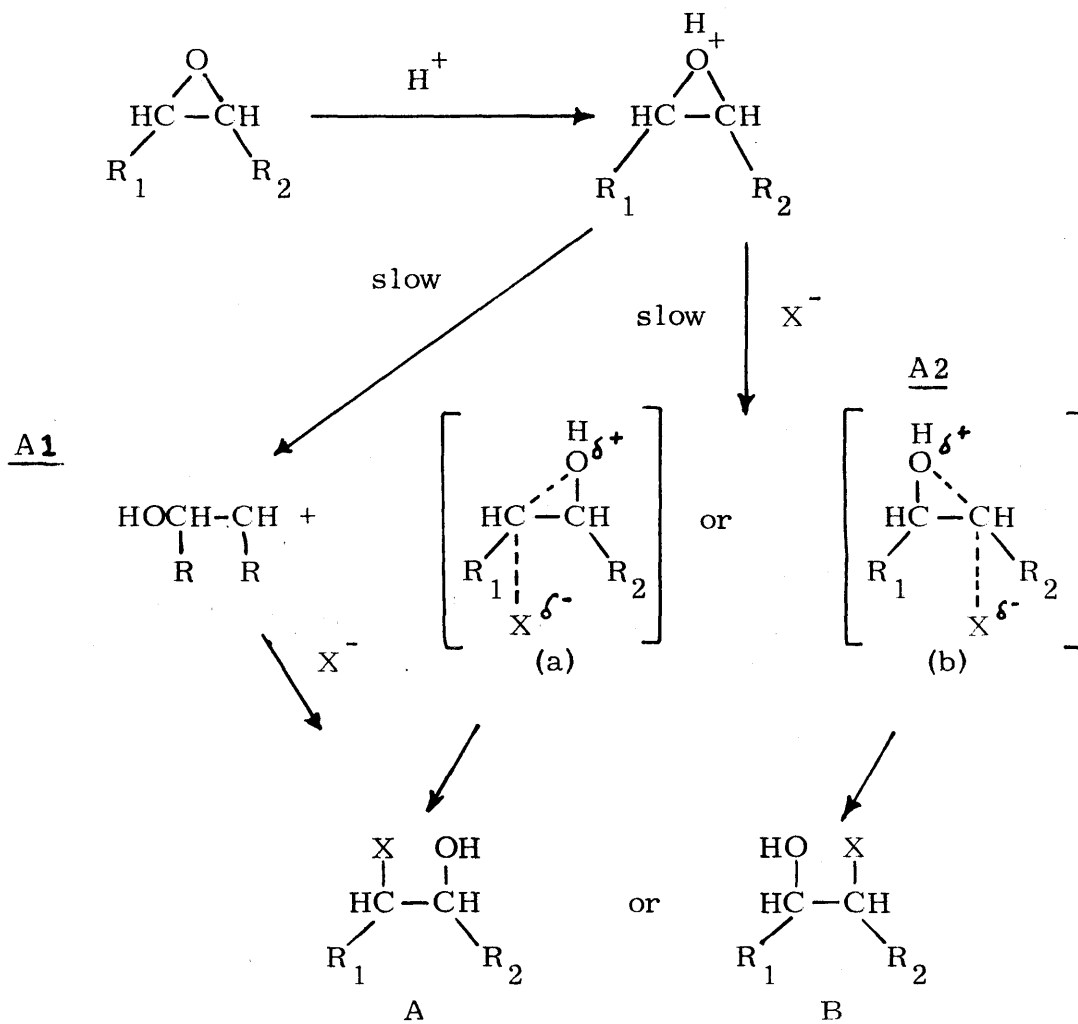
Figure III-5. A1 and A2 mechanisms of epoxide cleavage
(Buchanan and Sable, 1972)

secondary alcohol product.

Acid catalyzed cleavage involves Walden inversion of configuration, typical of an S_N2 displacement and thus results in trans addition. Because of equally likely back side attacks in cis or trans epoxides (from olefins like 2-butene or polybutadiene), the trans epoxide results in a meso diol structure while the cis epoxide results in a mixture of erythro and threo enantiomers (Figure III-6). The regioselectivity of assymmetric epoxides would, of course, affect this stereospecificity.

Acid catalysed cleavage is generally a much faster reaction than epoxidation as is exemplified by the already discussed difficulty in isolating epoxides unless certain precautions are taken. For example, the kinetic constant for epoxidation of propylene oxide is 7×10^{-5} litres/mole·sec. at 25°C (Swern, 1947) while at 0°C the kinetic constant for epoxide hydrolysis is $3.50 \times 10^{-3} sec^{-1}$. (Pritchard and Long, 1956).

(c) Acetate Hydrolysis

Hydrolysis of the monoester of the 1,2 diol formed by acetic acid cleavage of the epoxide can be effected with either basic or acidic catalysis. Both are biomolecular processes involving an addition-elimination mechanism, with addition of either hydroxide ion directly onto the ester in basic hydrolysis or water onto the already protonated ester in acidic hydrolysis. Acyl oxygen fission occurs to give the acid (acid salt) and alcohol. Base hydrolysis is generally irreversible while acidic hydrolysis is not . However, in the presence of an excess of water, acid hydrolysis can also be considered to go to completion. Further details of the mechanism are available in a recent review (Euranto, 1969).

The only additional point that requires mention is the observed
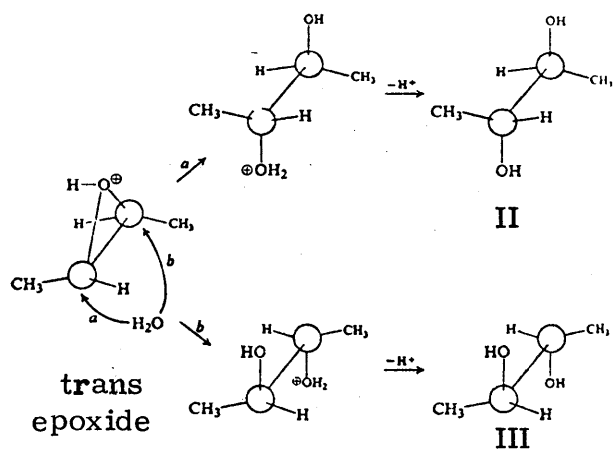
II and III are same as

meso
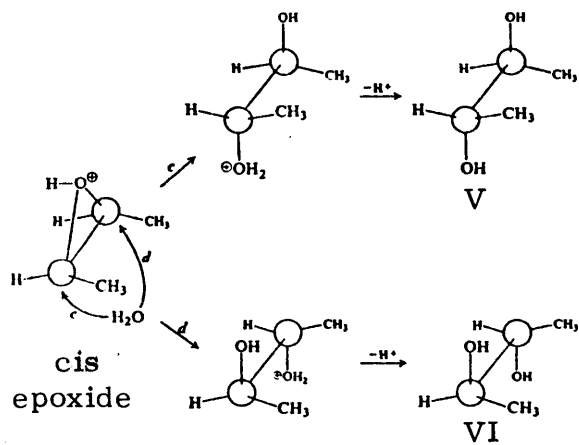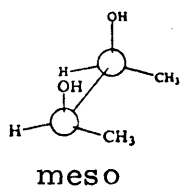
V and VI are enantiomers

Figure III-6. Stereospecificity of epoxide cleavage
(Morrison and Boyd, 1966)

neighboring group participation of hydroxyl groups in the alkaline

hydrolysis of the ester bond. Internal solvation of the transition

state for attack of OH^- at the ester carbonyl group is postulated to

account for the more than expected increase in rate of alkaline hydroly-

sis of 2-hydroxy cyclopentyl acetates (Bruice and Fife, 1962).

(d) Epoxide Rearrangements

The tendency of ethylene oxides to undergo isomerization to car-

bonyl compounds, thermally or by acid catalysis, is well established

(Rosowsky, 1964). Hydride ion shift rather than migration of alkyl

groups appears to be responsible, resulting in the formation of a ketone

from cis 2,3-epoxy butane, for example.

Epoxide-to-ketone rearrangement is relatively slow at normal epoxi-

dation temperatures (40°C) with H_2SO_4 catalysis and thus, its effect is

generally not very significant. Nevertheless, this isomerization reaction

has been noted by Greenspan (1964) as a potential side reaction in the

epoxidation of polybutadienes. With more highly alkyl substituted epoxides

(more stable carbonium ions), the rearrangement is much less specific and

results in the formation of a number of other products (in smaller propor-

tions): unsaturated alcohol, aldehyde, dioxane and a shifted epoxide

(Swern, 1971).

More important for the epoxidation of polybutadiene is the potential

rearrangement of epoxide to form substituted tetrahydrofuran rings. For

example, epoxidation of linalool and alcohols related to it does not yield

epoxides, but rather hydroxy-tetrahydrofurans and hydroxy-tetrahydropyrans

by intramolecular reaction of the appropriately placed hydroxy group with

the epoxy ring (Figure III-7a) (Felix, et al., 1963, Klein, et al., 1964,
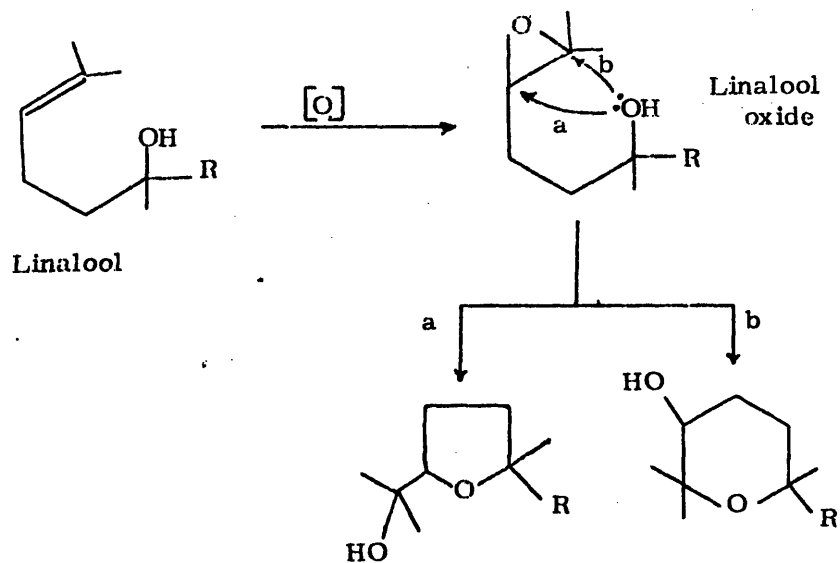
(a) Rearrangement of Linalool oxide (R: $CH-CH_2$, Swern (1971))
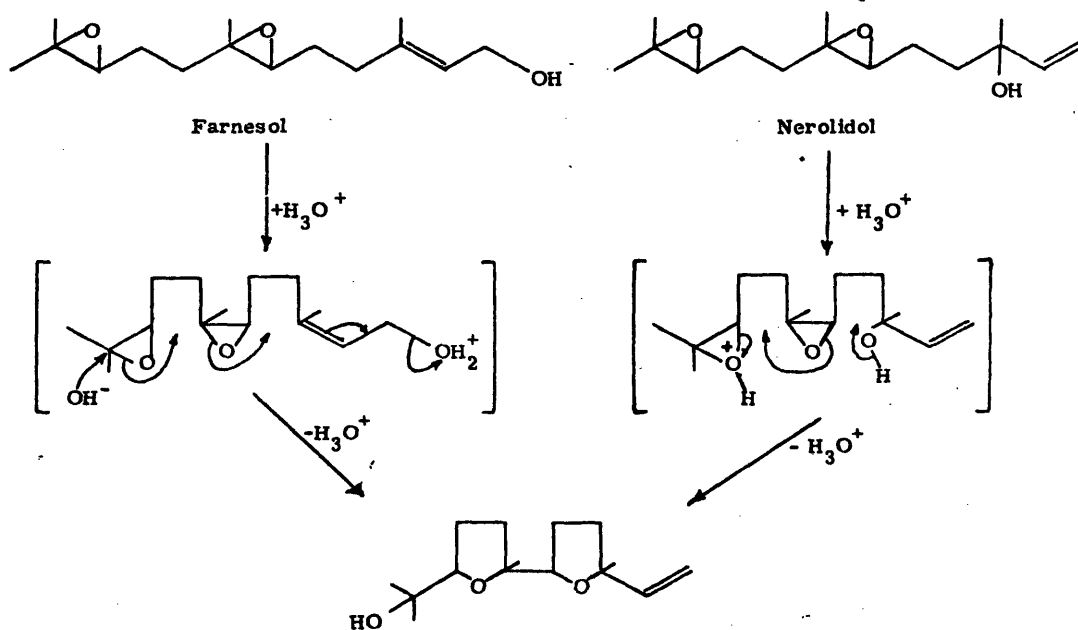
(b) Rearrangement to 'Nerolidol oxide' (Ohloff, 1964).

Figure III-7. Cyclization rearrangements of epoxides.

Mousseron-Canet, et al., 1961, 1966, Mousseron-Canet and Levallois, 1965, Ohloff, et al., 1964). Additional examples drawn from the carbohydrate field can be found in the review of Buchanan and Sable (1972).

Because the epoxide ring can be introduced from either side of the double bond, pairs of isomeric tetrahydropyrans and tetrahydrofurans are formed (i.e. four products). The tetrahydrofuran alcohols are the principal products in the 'spontaneous' rearrangement of epoxidized dimethyl heptenol, while the tetrahydropyran alcohol isomers are more favourably produced in the acid catalysed cyclization, due to the increased tendency for epoxide ring scission at the tertiary carbon atom under acidic concitions (Mousseron-Canet, et al., 1966).

Of particular interest to this thesis are the cyclization-rearrangements reported by Ohloff, et al., (1964), and shown in Figure III-7b. The epoxides were prepared by peracetic acid epoxidation of the related terpenes (farnesol, nerolidol). The resulting mixture of stererisomers (termed Nerolidoloxide by Ohloff) were produced in greater than 90% yield with other compounds in much smaller amounts (tetrahydropyran structures?).

While these ether formations involved isoprenoid derivatives (terpenes) exclusively, a similar rearrangement has been noted in the anionic polymerization of 1,2 - 5,6 diepoxyhexane (terminal epoxides) to form tetrahydrofuran structures (not tetrahydropyran rings) in the polymeric chain   [-CH$_2$ -⟨ ⟩-CH$_2$-O-], as determined by NMR (Bauer, 1967). Therefore, there is no a priori reason why similar reactions do not occur in the epoxidation of polybutadienes, where the absence of tertiary carbon atoms in the epoxide ring would result in the preparation of tetrahydrofuran products in larger proportion than tetrahydropyran rings, as in the 'spon-

taneous' rearrangement described above.

This reaction has already been considered by Dittmann and Hamann (1972) to account for the low value of the degree of epoxidation, determined by HBr titration, of polybutadiene epoxides. Because both epoxidation and the subsequent cyclization are random processes, statistical calculations are necessary to determine the true effect of cyclization. In a homopolymer, for example, 13.5% of the repeat units should fail to cyclize owing to isolation between already reacted pairs of units (Flory, 1953a). By performing similar calculations, Dittman and Hamann (1972) were able to account for the sometimes major discrepancy between chemical and physical epoxide numbers.

However, there is still some uncertainty in the nature of the groups prepared by cyclization of the epoxide. Firstly, tetrahydropyran (or larger) ring structures may be the end product of these cyclizations. The NMR work of Bauer (1967), the absence of tertiary carbon atoms in the epoxides and the general stability of five membered rings makes the formation of six (or higher) membered rings unlikely, in the rearrangement of epoxidized polybutadiene. Secondly, the rearrangements described by Ohloff, et al., (1964) did not involve a net increase in the number of moles of oxygen whereas those considered by Dittman and Hamann (1972) incorporated a molecule of water in the rearranged product. It is also conceivable that a mole of water could be released in a dehydration reaction during cyclization. The possible structures are shown in Figure III-8a. Both cis and trans isomers of each of these structures would be expected. Finally, the statistical process of cyclization in polymers suggests the presence, in the chain, of short sequences of tetrahydrofuran rings terminated by the

$R = OH, H$

$R_1 = R_2 = CH \sim$
$\qquad\qquad\quad OH$

$R_1 = CH_2 \sim$, $R_2 = CH \sim$
$\qquad\qquad\qquad\qquad OH$

$R_1 = CH_2 \sim$, $R_2 = CH=CH-CH_2 \sim$

$R_1 = CH \sim$, $CH_2 \sim$
$\qquad\quad OH$
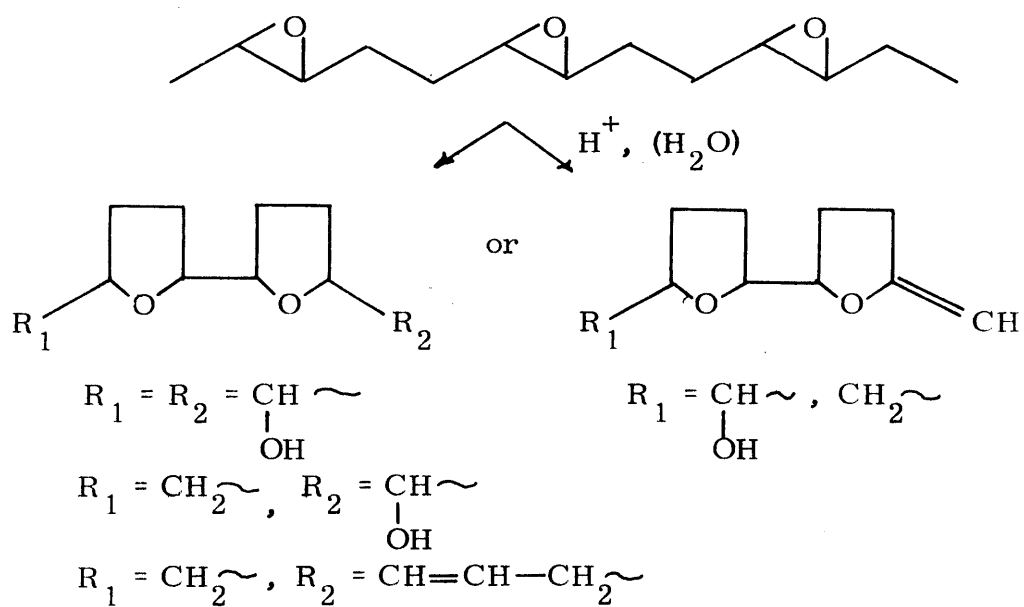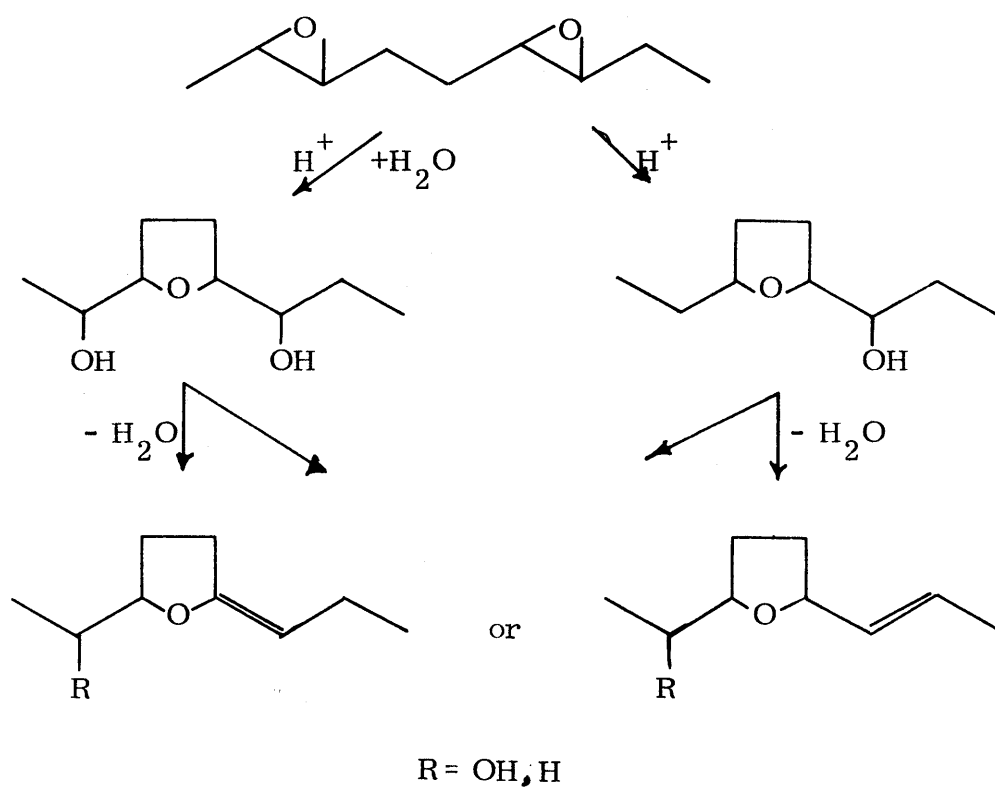
Figure III-8. Possible products of intramolecular cyclization of epoxides.

same substituents shown in Figure III-8a. A tetrahydrofuran diad is shown in Figure III8b. The implications of these various structures on the interpretation of the IR spectra of hydroxylated SBS copolymers is discussed in section IV-4c.

It is also possible that a very similar rearrangement would take place intermolecularly. The intermolecular process would involve simultaneous cleavage of two epoxides on two separate chains in a mechanism similar to the intramolecular one (Figure III-8). As a result, ether bonds would form to join the two chains (cross-link) with formation of hydroxyl groups or unsaturation in the chain α to the ether (Figure III-9). In addition, dimerization could take place to form an intermolecular dioxane structure.

This intermolecular rearrangement is, in some respects, similar to the well known cationic polymerization of epoxides catalysed by Lewis acids (Ishii and Sakai, 1969) or by acetic acid (Lebedev and Gus'kov, 1963). A second epoxide ring acts as a nucleophile to open an epoxide ring which has been sensitized to cleavage by the Lewis acid (or acetic acid), in a mechanism similar to the modified A2 nucleophilic cleavage of a protonated epoxide (section III-2c). The end result of this polymerization, in polybutadiene epoxides, would also be intermolecular ethers, identical to those shown in Figure III-9, since termination of the growing species would readily occur in the presence of water (more reactive nucleophile) or in the solid phase with the limited availability of other epoxide groups.

Another type of epoxide rearrangement is 'epoxide migration' under alkaline conditions (Buchanan and Sable, 1972). Since it appears that this rearrangement involves a hydroxyl group on the carbon α to the epoxide,
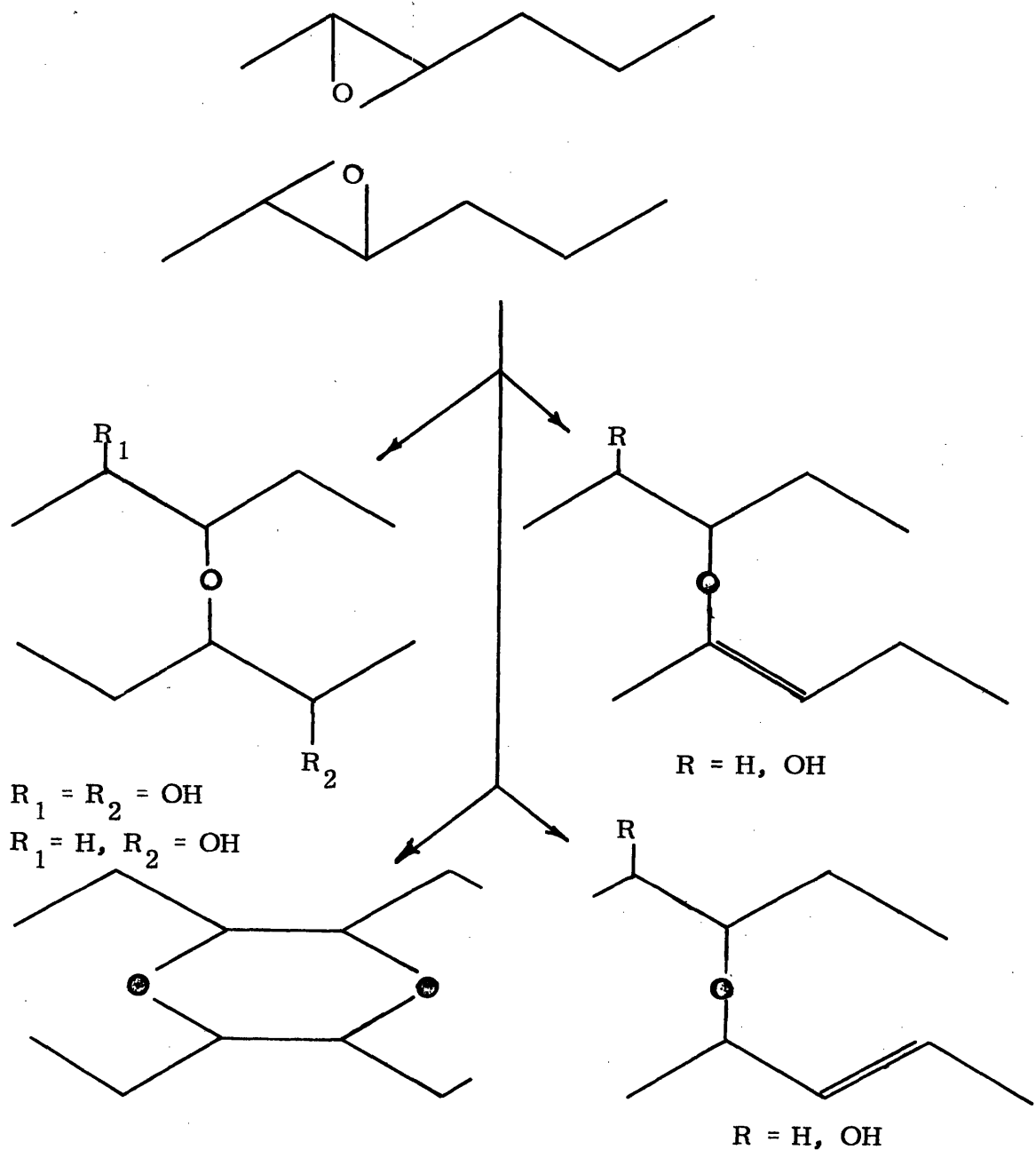
Figure III-9. Intermolecular acyclic ethers by epoxide rearrangement

(a structure not normally present in polybutadiene epoxides), it will not be discussed further.

(e) Additional Side Reactions

Cis/trans isomerization of alkenes is also a well known reaction that may take place under a number of conditions: thermally, acid catalysed (e.g. phosphoric acid) or base catalysed (NaOH with mild heating). (It is generally recognized that for many of the modes of exchange the trans isomer is the more thermodynamically favourable one (Mackenzie, 1964).) While there has been no report of true cis/trans isomerization taking place during epoxide reactions, highly substituted epoxides may rearrange under some circumstances to form unsaturated alcohols as discussed above (Swern, 1971). This, nevertheless, should be considered a conceivable side reaction in polybutadiene epoxidation, which might take place either directly from double bond isomer to isomer or through dehydration of a (protonated) epoxide.

A number of other side reactions may occur in the preparation of surface hydroxylated SBS block copolymers. Among these may be free radical oxidation with the formation of peroxides, lactonization from carbonyl-epoxide reactions, oxetane formation, acyclic ether rearrangements, acetal formation, or direct nucleophilic attack of hydroxide ions onto the double bonds, etc. Except for free radical oxidation, all the other possibilities are highly unlikely or insignificant considering the polymer structure and the conditions of the hydroxylation reaction. In the absence of information to the contrary, these reactions are not considered further. Free radical oxidation and the formation of peroxides, however, is a conceivable process and the question of the presence of peroxides in surface reacted

SBS copolymers will be discussed further in section V-2a.

3.   INFRARED SPECTROSCOPY

The use of infrared spectroscopy for qualitative and quantitative analysis in organic chemistry, and especially for polymers, is well established (Henniker, 1967). Infrared vibrational spectra occur when the absorption of radiant energy produces changes in the energy of molecular vibration; namely, a transition between two of the discrete energy levels of the molecule. While the number of normal modes of vibration of a particular molecule depends on the structure of that molecule, the frequency of each vibration (i.e. the frequency of light required to cause a transition) for a certain chemical bond depends mainly on the masses of the atoms joined by the bond and the valence force between them and only to a very small extent by the molecular environment. This is the theoretical justification for the empirical interpretation of IR spectra based on group frequency correlations (Bellamy, 1958). The validity of group frequency correlations and the comparisons with spectra of model compounds were the basis of the qualitative analysis of the spectra of hydroxylated SBS copolymers (see section IV-4 and Appendix 1).

The quantitative application of absorption spectrometry depends on the use of the simple Lambert-Beer law:

$$A = \log_{10}\left(\frac{T_0}{T}\right) = abc \qquad (III-1)$$

where A = absorbance

T_0 = (apparent) intensity of incident radiation

T = (apparent) intensity of transmitted radiation

a = absorptivity (extinction coefficient)$(cm^2/mole)$

c = concentration of absorbing material in sample $(moles/cm^3)$

b = path length of radiation within sample (cm)

According to the nomenclature of Ramsay (1952), T_0, T and a are apparent quantities due to the use of finite slit widths and a is an extinction coefficient rather than absorptivity (both terms are used interchangeably here). Because corrections were not made for reflection losses and base line procedures were used in both sample and calibration spectra, T and T_0 were equated with the transmittance at the peak and the transmittance at the base line, respectively.

The absorptivity of a peak in an infrared spectra defines the intensity of absorption of radiation at that frequency. The intensity of a vibration depends on the polar nature of valence bonds and, in fact, can be considered to be the rate of change of dipole moment along the vibration axis. While a more sophisticated unit of absorption is obtained when the spectral width of the peak is taken into consideration, the interfering absorptions of neighboring peaks makes the use of this integrated absorption intensity impractical. Only for the OH stretching peak near 3450 cm^{-1} was this practical (and, in fact, necessary; see section IV-4d(ii)) (Ramsay, 1952):

$$a' = \frac{1}{bc} \int log_{10}\left(\frac{T_0}{T}\right) d\nu$$

$$= \frac{\pi}{2} \cdot \frac{1}{bc} \cdot log_{10}\left(\frac{T_0}{T}\right) \nu_{max} \cdot \Delta\nu_{1/2} \qquad \text{(III-2)}$$

where a' = (apparent) integrated absorption intensity (cm/mole)

ν = frequency (wavenumber) (cm^{-1})

ν_{max} = frequency of peak maximum

$\Delta\nu_{1/2}$ = half-absorbance peak width

Despite the difference in units, this integrated absorption intensity was consistently used along with the extinction coefficients defined solely by the peak heights. Obviously the larger the absorptivity, the better the precision of the quantitative analysis.

The Lambert-Beer law is extended to a multicomponent system (at a single frequency ν) by simply adding on additional terms, one for each component present in the mixture:

$$A^{\nu} = a_1^{\nu}bc_1 + a_2^{\nu}bc_2 + a_3^{\nu}bc_3 + \cdots + a_n^{\nu}bc_n = b \sum_{i=1}^{m} a_i^{\nu}c_i \quad (III-3)$$

where m is the number of components present. This equation is set up at m frequencies characteristic of the components in the sample and the resulting set of m equations in m unknowns is solved (if the absorptivities and path length are known) to determine the values of the m concentrations. The frequencies chosen for the analysis are those at which just one of the components absorbs strongly with only minor interfering absorptions of the other components; i.e., that set of frequencies which maximizes the absolute value of the determinant of the absorptivity coefficients of the m linear equations.

In order to improve the precision of the multicomponent analytical scheme, an over determined system of equations is used and a least squares solution determined by standard techniques (Clifford, 1973). Herschberg

and Sixma (1962) and Bauman (1959) have discussed the applicability of over-determined systems in absorption spectroscopy.

Using matrix notation, the set of n linear equations in m unknowns corresponding to the Lambert-Beer law written at n frequencies for m components (n > m) is:

$$\underset{\sim}{A} = \underset{\sim}{a} b \underset{\sim}{C} \qquad (III-4)$$

where $\underset{\sim}{A}$ = vector of absorbances; length, n

      $\underset{\sim}{a}$ = matrix of absorptivities; dimension, n · m

      b = path length

      $\underset{\sim}{C}$ = vector of concentrations; length, m

      n = number of frequencies in over-determined system (n > m)

      m = number of components in sample

Defining $X_i = bc_i$, X_i is the area concentration of component i in the sample (moles/cm^2), equation III-4 is rewritten:

$$\underset{\sim}{A} = \underset{\sim\sim}{aX} \qquad (III-4')$$

where X is the vector of area concentrations.

The least squares solution to Equation III-4' is obtained by minimizing the sum of squared residuals. The resulting average values for the X_i, <X> in vector notation, are defined by:

$$\underset{\sim}{<X>} = (\underset{\sim}{a}^T\underset{\sim}{a})^{-1}\underset{\sim}{a}^T\underset{\sim}{A} \qquad (III-5)$$

(T denotes transpose; -1 denotes inverse.) The residuals which were minimized to obtain Equation III-5 are defined by:

$$r^{\nu} = A^{\nu} - \sum_{i=1}^{n} a_i <X_i>$$

(III-6)

or

$$\underset{\sim}{r} = \underset{\sim}{A} - \underset{\sim}{a}<\underset{\sim}{X}>$$

(III-6')

in vector notation.

That this is a plausible approach may be illustrated by application of a theorem of Jacobi: the least squares solution $<\underset{\sim}{X}>$ equals the one obtained by taking a weighted mean of the solutions of all combinations of m equations that can be selected from the n rows of $(\underset{\sim}{A}, \underset{\sim}{a})$, weights being allotted proportionally to the square of the determinant of the coefficients of each combination; that is, proportionally to the relia-bility of each solution by the criterion mentioned before (Herschberg and Sixma, 1962).

Herschberg and Sixam (1962) have pointed out that the validity of the least squares solution (Equation III-5) assumes an independently known a. However, they also demonstrated that the more formally correct solution (since coefficients of $\underset{\sim}{a}$ are subject to the same measurement errors) is not significantly different from this least squares solution.

The $<X_i>$ values were converted in this thesis into true "concentrations' (independent of spectrum sample size) using polystyrene (phenyl group) as an internal standard:

$$F_i = \frac{<X_i> N}{X_{phenyl}}$$

(III-7)

where F_i is the number of moles of component i per 100 moles of unsatura-
tion present in the original sample before reaction, and N is the ratio
of moles of phenyl groups to 100 moles of unsaturation in the copolymer
(here, N = 19.89).

The standard error of the estimate σ can be easily calculated to be:

$$\sigma = \frac{1}{n-m}\sqrt{\sum_{j=1}^{n} r_j^2} = \sqrt{\frac{\underline{r}^T\underline{r}}{n-m}} \tag{III-8}$$

The standard error of estimate is then utilized to calculate E_i, the stan-
dard deviation of each value of the area concentration $<X_i>$, due solely
to the regression:

$$\underline{E}' = \sigma\sqrt{(\underline{a}^T\underline{a})^{-1}} \tag{III-9}$$

in matrix notation (Clifford, 1973). The error calculations are discussed
fully in Appendix 1-C.

Because of the complexities of the spectra which were analysed in
this thesis, the scheme developed here must be considered to be a model
fitting procedure rather than a strict analytical method. The complexities
generally are the result of uncertainties in the spectral assignments and
due to the unavailability of proper model compounds for the calibration
of the quantitative analysis procedure. This is discussed further in the
experimental section (IV-4d(ii)), while the errors inherent in the use of
the Lambert-Beer law and other aspects of the procedure are discussed in
section V-6.

4. DIFFUSION AND RELATED PHENOMENA

The problem central to the hydroxylation of SBS copolymers in the solid phase is one of diffusion with simultaneous chemical reaction of peracetic acid through the solid copolymer. While a number of solutions already exist to various forms of this problem (Crank, 1956, Danckwerts, 1970) the particular problem relevant to this thesis is complicated by the simultaneous occurrence of swelling in the polymer, which in turn is dependent on the actual size of the polymer piece (e.g., film thickness).

A few other investigators have considered diffusional effects in second order chemical reactions on (or in) polymers: Hermans (1947) studied the reaction between thiosulphate ions and iodine immobilized in gelatin while Kemp and Paul (1947) analysed gas sorption in polymer membranes which contain adsorptive fillers. Odian and Kruse (1969) studied diffusion effects in radiation induced graft polymerization but since saturation of the reactive sites in the polymer does not occur, their mathematical solutions are not applicable here. (Rogers, et al., (1968) used these diffusion effects to prepare assymmetric membranes.) Goddard, et al., (1970) considered a reversible second order reaction, near equilibrium in their analysis of facilitated transport in membranes. In addition, the work of Reese and Ewing (1950), Katz, et al., (1950), Zimmerman (1960) and Barker (1962) are related.

(a) Diffusion Equations

The diffusion problem relevant to this thesis can be described as follows: unidirectional diffusion of peracetic acid through a film of SBS copolymer of finite thickness (and effectively infinite area), containing 25 vol. % polystyrene in isolated impermeable domains, with simultaneous

irreversible chemical reaction of the peracetic acid and the polymer

(polybutadiene block only). Water, acetic acid and sulphuric acid are

also diffusing into the polymer causing various epoxide cleavage and

rearrangement reactions (see Figure III-10 for a description of the

coordinate system).
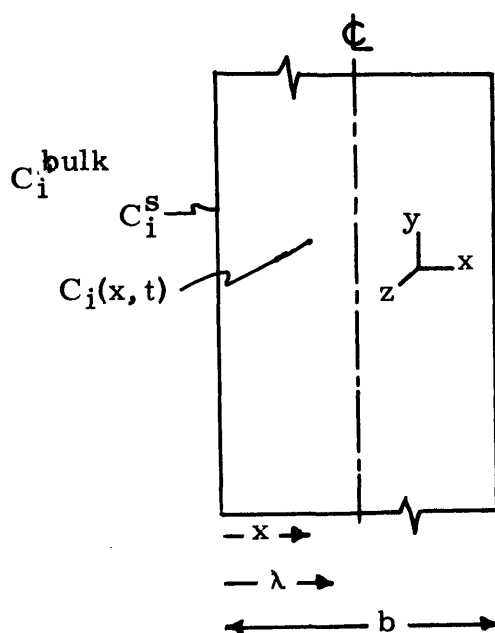
Figure III-10. Coordinate system for diffusion equations.

The occurence of reaction near the surface of the polymer film

necessitates the use of a modified equation for diffusion in one dimen-

sion. The activity coefficient approach of Petropolous and Roussis

(1967 a, b, 1968, 1969 a, b, c, d) is preferred to an alternative

irreversible thermodynamic approach (Frisch, et al., 1969; Wang, et al.,

1969), set up to account for time dependent anomalies in diffusion

through glassy polymers. (Unfortunately Petropolous and Roussis evaluated the problem of a distance dependent solubility in terms of time-lag quantities only, which are of no value here.)

Instead of writing the standard equation for diffusion in one dimension in terms of concentration of the penetrant (Equation 8.6 of Crank, 1956), Petropolous and Roussis used the thermodynamic diffusivity and a solubility coefficient and by starting from the diffusion equation with chemical potential of penetrant as the driving force, obtained a modified equation. This equation is rewritten for our system:

$$\frac{\partial}{\partial t}\left(S_i(a_i,x,t) \cdot a_i(x,t)\right) = \frac{\partial}{\partial x}\left(P_i^T(a_i,x,t)\frac{\partial a_i(x,t)}{\partial x}\right) - R_i \quad \text{(III-10)}$$

where $a_i(x,t)$ = activity of penetrant i in polymer

$S_i(a_i,x,t)$ = quasi-thermodynamic solubility of penetrant i in polymer

$\qquad\qquad$ = c_i/a_i

$c_i(x,t)$ = concentration of penetrant i

$P_i^T(a_i,x,t)$ = thermodynamic permeability of i in polymer

$\qquad\qquad$ = $D_i^T S_i$

$D_i^T(a_i,x,t)$ = thermodynamic diffusivity of i in polymer

R_i = rate of disappearance of penetrant i due to reaction

x = coordinate in diffusion direction

t = time

The boundary conditions are:

$$t = 0, \quad \text{all } x, \quad a_i = 0,$$

$$\text{all } t, \quad x = 0 \quad a_i = a_i^S = C_i^S / S(a_i^S, 0, t) \qquad \text{(III-11)}$$

$$\text{all } t, \quad x = \frac{b}{2} \quad \frac{\partial a_i}{\partial x} = 0$$

where a_i^S = activity of penetrant i at the surface of the polymer

= activity of component i in the bulk fluid, if no re-

sistance to mass transfer in bulk fluid

C_i^S = surface concentration of penetrant i

The diffusion of peracetic acid (C_p), acetic acid (C_a) and water (C_w) are all described by Equation III-10 but with different expression for R_i:

$$R_p = \left(\frac{\partial C_p}{\partial t} \right)_{\text{epoxidation}} = k_p C_p C_u \qquad \text{(III-12a)}$$

$$R_a = \left(\frac{\partial C_a}{\partial t} \right)_{\text{cleavage}} = k_a C_a C_e - k_p C_p C_u \qquad \text{(III-12b)}$$

$$R_w = \left(\frac{\partial C_w}{\partial t} \right)_{\text{cleavage}} = k_w C_w C_e \qquad \text{(III-12c)}$$

The relevant boundary conditions are:

$$t = 0, \quad \text{all } x, \quad C_u = C_u^0,$$

$$C_p = C_a = C_e = C_w = 0$$

Equation III-12a defines the rate of disappearance of peracetic acid due to epoxidation R_p in terms of the kinetic constant for epoxidation, k_p, and the concentrations of peracid, C_p, and double bonds, C_u. Equation III-12b defines the rate of disappearance of acetic acid, R_a, due to

cleavage of the epoxide (first term on right hand side) less the rate

of appearance from the epoxidation step (second term) (k_a = the kinetic

constant of acetic acid cleavage, C_a = the concentration of acetic acid,

and C_e = concentration of epoxide groups). Similarly, Equation III-12c

defines the rate of disappearance of water, R_w, due to cleavage of the

epoxide in terms of k_w, the kinetic constant for hydrolysis of the epox-

ide and C_w, the concentration of water in the polymer. The concentrations

of each penetrant are related to the activities through S_i.

The proper form for each of the defining equations for R_i should

be a sum of terms reflecting the fact that some of the functional groups

on the polymer react at different rates (e.g. epoxidation of cis, trans

and vinyl double bonds). This is unnecessary in practice, if the differ-

ences between the rates are negligible (e.g. $k_{p-cis} \simeq k_{p-trans}$) or if

some of the groups can be considered unreactive (e.g. $k_{p-vinyl} \simeq 0$).

C (e.g., C_u) is then redefined as the concentration of reactive groups.

In addition, no account has been taken of the various side reactions

(rearrangements) that can take place (section III-2d). These generally

do not involve diffusing species but do, however, reduce the number of

moles of epoxide that can react with species that are diffusing (lowered

C_e in Equations III-12). It is implicitly assumed in Equations III-12

that the concentration of sulphuric acid in the polymer is beyond the

threshold level required for it to act as a catalyst in the acid catalysed

cleavage reactions. The presence of pH (or concentration of sulphuric

acid) dependence in any of the relevant rates of reaction would neces-

sitate the presence of a fourth equation of the form of III-10 for pro-

ton (sulphuric acid) diffusion with additional terms required if there

were electrostatic forces involved in the diffusion process.

The solubility $S_i(a_i,x,t)$ reflects the degree of interaction (mixing) attainable at equilibrium between the polymer at x and penetrant i, at time t. The more compatible the penetrant and the polymer, the larger is the value of S. Since the polymer reacts and thus changes its chemical structure, its compatibility with the penetrant, as reflected in S_i, changes with reaction, which in turn, changes the diffusion process. Since the penetrants of relevance are polar and the polymer is converted from a hydrophobic rubber to a hydrophilic material, S_i generally increases on epoxidation for all penetrants. However, the cleavage of the epoxide to hydroxy-acetate groups or 1,2 diols would conceivably change S_i in different directions for the different penetrants. S_i would then be a complex function of the composition of the polymer.

S_i is an equilibrium quantity relating the concentration of penetrant i (related to the volume fraction) in the polymer to the chemical potential of component i in the polymer. It would then be of the form of the Flory-Huggins equation but extended to a multicomponent system (three low molecular weight components and each of the different polymeric functional groups possible) with a suitable correction for the elastic component of the free energy, (considering the presence of entanglements, discrete domains and stress transfer--see below) (Flory, 1953 b). While certain valid simplifications can be made (e.g., defining a single average polymer composition), an algebraic expression for S_i in terms of more fundamental variables (χ factors), is not available. It should be noted that, since the pair interaction parameters for the penetrants are negligible, the dependence of S_i on a_j, the activities of the other penetrants, can be ignored in practice

(except, of course, for volumetric considerations).

Since the relationship between activity and concentration (or volume fraction) has a contribution from the elastic free energy, it is affected by any stress transfer processes which acts to reduce the elastic free energy. Swelling occurs near the surface of the reacted polymer which, if isotropic, would be governed by the equations described by Flory (1953 b). However, the presence of a non-swelling core in the elastic network causes a reduction in the level of stress that is causing swelling to occur and hence, a reduction in the amount of swelling and the penetrant uptake. In addition anisotropies would probably be introduced: swelling being unrestrained in the x direction but highly restrained in the yz plane (the plane of the film). This stress transfer process, which is dependent on the size of the non-swelling core (or the thickness of the film), and leads to a reduction in surface swelling has been observed in the diffusion of various organic liquids through natural rubber (Southern and Thomas, 1965), the sorption of water by keratin (Feughelman, 1959) and the diffusion of methylene chloride in polystyrene of various thicknesses (Park, 1953).

Crank (1953) developed a model with which he was able to explain Park's (1953) observations of thickness dependent diffusion (more penetrant in thinner films than in thicker films). While Crank interpreted, what he termed 'strain-dependent diffusion', purely in terms of an effect on the diffusivity, (by ignoring changes in surface concentration) his model for stress trnasfer is equally applicable to effects on solubility as well as diffusivity. Crank expected that the inner non-swollen part of the sheet would exert a compressive force on the outer swelling region,
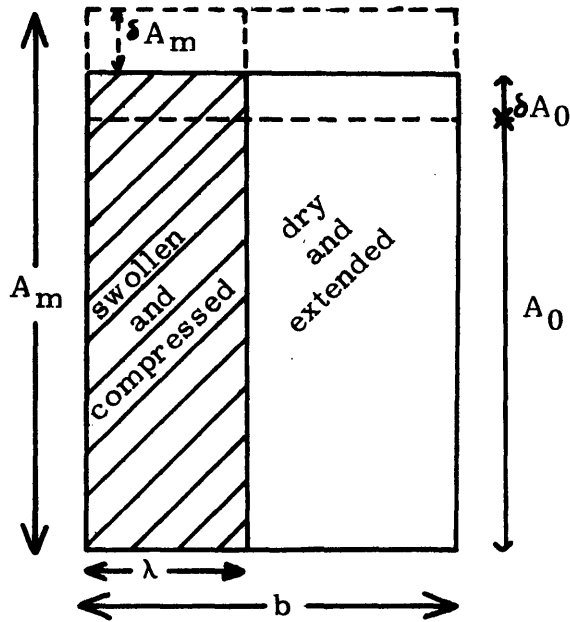
Figure III-11: Model for strain-dependent diffusion (Crank, 1953).

causing swelling to be mainly along the direction of diffusion. At the same time, the swollen regions would exert on the unattacked region forces which tend to extend it and to increase the area of the sheet. As diffusion proceeds into the sheet, the thickness of the unattacked region decreases and the sheet increases in area as the compressive forces are relieved (in addition to the swelling occurring continuously in the x direction) (Figure III-11). By assuming that the area is constant throughout its thickness (rectangular section), using Crank's model, we can derive:

$$A = A_m \left(\frac{1 + {}^{E_0}/E_m \ (\frac{b}{2\lambda} - 1)}{1 + {}^{E_0}/E_m \ (\frac{b}{2\lambda} - 1)\frac{A_m}{A_0}} \right) \tag{III-13}$$

where A = area of sheet during diffusion process

A_m = area of sheet in the absence of stress and at equilibrium with penetrant

A_0 = initial area of dry sheet

b = thickness of sheet

λ = depth of penetration of swelling agent(s)

$\approx$ depth of penetration of reaction

E_0, E_m = Young's moduli of unswollen and swollen zones, respectively

A_m/A_0 is the increase in area in a stress-free sheet, isotropically swollen at equilibrium, and so is equal to $(V_m/V_0)^{2/3}$, where V_m, V_0 are the volumes of swollen and unswollen polymer, respectively. Thus A_m/A_0 reflects the nature of the thermodynamic interaction between penetrant(s) and polymer. To demonstrate the effect of penetrant polymer compatibility on stress modified swelling, Figure III-12 shows curves of A/A_m versus $\frac{b}{2\lambda}$, with A_m/A_0 as a parameter. The time dependence of this process is implicit in the time dependence of the depth of penetration, λ; for Crank the time dependence arose from simple diffusion, while in this work it arises from the simultaneous processes of diffusion and chemical reaction.

Crank used this version of Equation III-13 to derive expressions relating the strain-dependent diffusivity to the stress-free diffusivity. He assumed that a compressive force decreases the diffusion coefficient below that for an unstressed material and vice versa for an extensive force, or in mathematical terms:
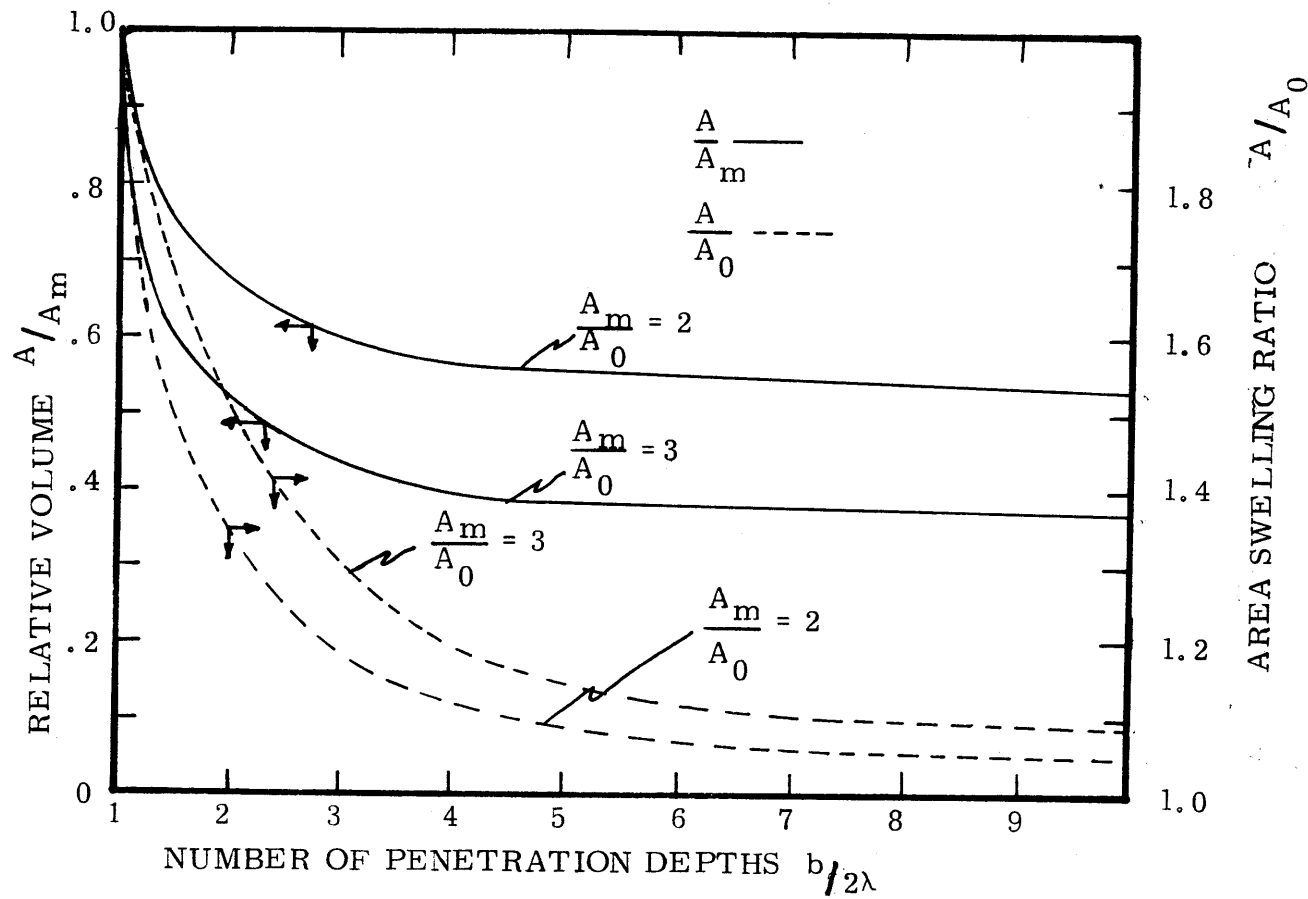
Figure III-12. Effect of compatibility (A_m/A_0) on the effectiveness of stress transfer according to Equation III-13.

$$D_i^1 = D_i^m \left(1 - \mu_m \frac{\delta A_m}{A_m}\right)$$

(III-13)

$$D_i^2 = D_i^0 \left(1 + \mu_0 \frac{\delta A_0}{A_0}\right)$$

where D_i^1, D_i^2 = diffusivities in swollen and unswollen regions, respectively, when the area = A

D_i^m, D_i^0 = diffusivity in swollen region and unswollen regions, respectively, in the absence of stress

δA_m = A_m - A = mean compression in swollen region

δA_0 = A_0 - A = mean extension in unswollen region

μ_m, μ_0 = coefficients relating the effect of compression or extension, respectively, on the relevant stress free coefficients.

In a elastomer with relatively high diffusivities, μ_m, μ_0 would probably be quite small, and the effect of strain on diffusivity would be small. However the volume effect implicit in D^m and D^0 would be significant even in an elastomer and must be considered. This effect is identical to the concentration dependence of diffusivities due to swelling or plasticization, observed in the diffusion of 'good' solvents through polymers, e.g., water in polyvinyl alcohol (Crank and Park, 1969).

Similar equations can also be written to express a strain dependence of solubility:

$$S_i^1 = S_i^m \left(1 - \gamma_m \frac{\gamma A_m}{A_m}\right)$$

(III-14)

$$S_i^2 = S_i^0 \left(1 + \gamma_0 \frac{\gamma A_m}{A_m}\right)$$

where S_i^1, S_i^2 = solubilities of penetrant i in swollen and un-

swollen regions, respectively when the area is A

S_i^m, S_i^0 = solubilities in swollen and unswollen regions,

respectively, in the absence of stress

γ_m, γ_0 = coefficients relating the effect of compression

or extension, respectively, on the relevant stress-

free solubilities

Unlike the diffusivities, the effect of strain on solubility in an elastomer could conceivably be quite significant.

It should be noted that in Equation III-11, S_i and D_i^T are expressed as functions of activity, time, and location. the effect of strain dependence necessitates the inclusion of another variable; namely, the film thickness, b. Hence $S_i = S_i$ (a_i, x, t, b) and D_i^T (a_i, x, t, b). Simplifications can be made, of course, to reduce the number of variables that need to be considered.

The presence of impermeable discrete domains in an SBS copolymer necessitates the use of a correction to a diffusivity that is measured in a polybutadiene, in the absence of impermeable heterogeneities. This correction arises from the increased diffusion path (increased tortuosity) and would be on the order of .58 (D_{SBS} = .58 D_{PB}) in an SBS copolymer containing 25% by volume spherical or parallel cylindrical polystyrene domains in a cubic lattice oriented normal to the diffusion direction (Barrer, 1968). For a lattice of rods oriented parallel to the diffusion direction, the correction would be on the order of .45. Thus, it is apparent that the correction would be significant if diffusivities were used that had been measured in a homogeneous material, but these correc-

tions are not that sensitive to small changes in morphology. There-
fore, for samples of a single SBS copolymer prepared under nearly
identical conditions, slight variations in those conditions would have
but a minimal effect on the diffusion process and hence only a minimal
effect on the surface hydroxylation process. (Obviously, the application
of diffusion measurements from one SBS copolymer to a second with dif-
ferent morphology, would be subject to a significant correction.)

In addition, the strict solution of Equation III-11 requires con-
sideration of a moving boundary, since swelling in the x direction would
increase the thickness of the film throughout the diffusion process.

By solving Equation III-11 using R_i, defined in III-12a with the
proper relations for D_i and S_i, the concentration profile of reacted double
bonds (which is equal to the number of epoxide groups added without cleavage
or rearrangement) can be determined. Analyses of just these concentration
profiles, as a function of time would yield the true time course of epoxi-
dation (polymer reaction). However, if informaiton is needed on the pro-
duct distribution during surface reaction, all three equations of the
form of III-11 (using R_i's of Equation III-12) must be solved simultaneously.

(b) Related Solutions

Because of the complexities of the system, no attempt was made, in
this thesis, to solve the equations developed in the last section. Never-
theless, solutions to certain limiting cases have been considered by others
in the literature, and those relevant to the problem of chemical reaction
on polymers are discussed here.

In these related situations, in which diffusion with simultaneous
chemical reactions are treated, D and S are generally considered constant

and the governing equation is Equation 8.6 of Crank (1956). Then in
our nomenclature if both the diffusivity and solubility are constant,
Equation III-11 with Equation III-12a reduces to:

$$\frac{\partial C_p}{\partial t} = D_p \frac{\partial^2 C_p}{\partial x^2} - k_e C_p C_u \qquad \text{(III-15)}$$

with boundary conditions:

$$X = 0, \text{ all } t, \quad C_p = C_p^s = S' C_b$$

$$\text{any } x, \quad t = 0, \quad C_p = 0, \quad C_u = C_u^0 \qquad \text{(III-16)}$$

$$x = \frac{b}{2}, \quad \text{any } t, \quad \frac{\partial C_p}{\partial x} = 0$$

where S' is a Henry's law solubility coefficient (partition coefficient).

Unfortunately the various exact numerical solutions to this equation
as discussed by Danckwerts (1970) were presented in terms of enhanced
mass transfer coefficients, rather than as concentration profiles which
would be of interest here. Lebedev (1965), for a semi-infinite cylinder
and Petropoulos and Roussis (1969 d) for a semi-infinite slab, also solved
Equation III-15 by numerical methods for reaction of a mobile penetrant
with an immobile polymer. Unfortunately, both groups were concerned with
interpreting the observed dimensionless effective time scale of the pro-
cess in terms of the dimensionless reaction and uptake halftimes, in or-
der to determine from permeation measurements, the true rate limiting
process and the order of the chemical reaction. Their published results
are thus of little value.

Lebedev, however, did include plots of the mean concentration (aver-

age over cylinder cross section) of the polymer reactive sites

C_u/C_u^0 , as a function of a dimensionless time $\tau = \frac{Dt}{R^2}$ (R =

cylinder radius). He showed that independent of the dimensionless

ratio between diffusivity and the kinetic constant $(\alpha = \frac{kC_p^s C^2}{D}$),

and independent of the ratio between initial concentration of reac-

tive sites on the polymer and the surface concentration of reacting

permeant $(\beta = \frac{C_u^0}{C_p^s}$) , the decrease of C_u/C_u^0 with τ can be satis-

factorily described by an exponential function. In other words, in-

dependent of whether the reaction/diffusion process is subject to reac-

tion or diffusion control, the increase with time of the total number

of functional groups formed by reaction, in a cylinder of a given

radius, can be described by an exponential process. Therefore, from

just the observation of an exponential increase in extent of reaction

with time, it is impossible to recognize the rate determining process.

It seems likely that this observation is valid, regardless of the geome-

try of the system, or the presence of stress transfer processes which

modify the diffusion rate, or more generally, whether the diffusivity

is a constant or not. For example, in a kinetic limited permeation,

variations in D are irrelevant and thus, the ultimate behaviour would

still appear exponential.

Hermans (1947) noted that in the diffusion of thiosulphate ions

through gels containing immobilised iodine, a sharp boundary line separ-

ates the thiosulphate from the rest of the gel which proceeds to move

further into the gel with time. Similar sharp boundaries have been

noted in the decoloration of irradiated polymers in contact with oxy-

gen (oxygen is a free radical scavenger) (Zimmerman, 1960, Barker, 1962).

In order to account for his observations, Hermans considered diffusion into a semi-infinite slab coupled with a very rapid chemical reaction that consumed the penetrant but had a limited capacity for it. Because of this very rapid chemical reaction, the concentration gradient of diffusing species is very sharp (the larger the kinetic constant, the steeper the gradient) and C_u is practically zero in all points which have been reacted by the diffusing molecules. Hermans assumed that at any point x, all sites have reacted, or none. The permeant, therefore, only exists in the region where all sites have reacted. Figure III-13
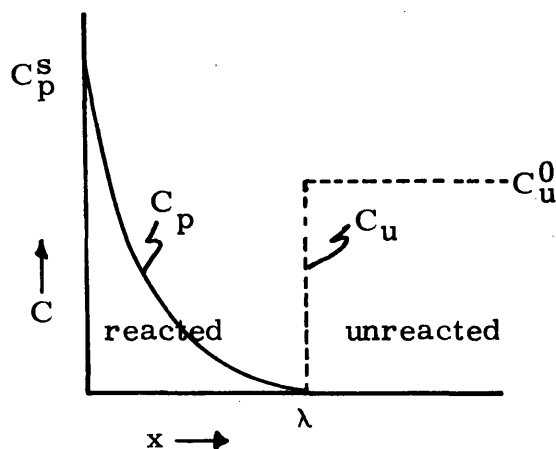
Figure III-13. Hermans' (1947) model of diffusion with simultaneous chemical reaction.

gives a diagrammatic representation of the concentration profiles. Then, in advance of the diffusion front, $x > \lambda$, $C_u = C_u^0$, whereas behind the front, $x < \lambda$, $C_u = 0$ and $C_p(x) > 0$. For this simplified limiting case $\frac{\lambda}{\sqrt{t}}$ is a constant or, in other words, the diffusion front

moves at a rate in proportion to $\sqrt{t}$. The proportionality constant depends on the value of the boundary conditions and the diffusion and kinetic constants. It is expected that in the real case, where the reaction rate is comparable with the diffusion rate, the diffusion boundary becomes more curved but still moves, to a reasonable approximation, at a rate proportional to the square root of time.

Barker (1962) and Zimmerman (1960) developed expressions similar to those of Hermans for the oxygen decoloration problem but with additional assumptions. Kemp and Paul (1974) solved a similar problem in their study of gas sorption in membranes containing adsorptive fillers.

Similarly in the diffusion through a polymer (without reaction) of a penetrant which causes local swelling of the polymer, a relatively sharp border has been observed between the swollen and unswollen regions (Hartley, 1949). After a certain concentration of penetrant C* is reacted, the network starts to swell with the final swollen concentration C_α being attained in a relatively short time. The diffusivity in the un-swollen sample increases by some orders of magnitude in the swollen region. As a consequence, the concentration is nearly constant, C_α in the swollen section, behind the advancing front, drops to C* in a rather narrow transition region and shows a diffusion type dependence in time and space in front of this layer. The larger the diffusivity in this swollen region, the steeper is the moving boundary. Crank (1956) has calculated that this boundary should move at a rate proportional to $\sqrt{t}$, confirming the observation of Hartley (1949). However, Peterlin (1965) has recently reported the observation of a boundary moving at constant

velocity (i.e. proportional to t), in the swelling of crosslinked polystyrene. Perhaps, similar to Hartley's (1949) observation of a boundary moving with constant velocity in certain oriented samples (diffusion parallel to molecules) and considering the form of Crank's model for strain dependent diffusion (1953) (see last section), the presence of a boundary moving at a rate not proportional to $\sqrt{t}$ can be considered evidence of other mechanisms affecting the diffusion process.

In addition, other limiting cases have been considered. Reese and Eyring (1950) and Katz, et al., (1950) neglected the reaction rate term (kC_pC_u) in Equation III-15, by assuming that the number of reactive sites on the polymer were much less than the number of diffusing molecules. This solution is identical to the instantaneous reaction solution that is used to model the dyeing of textiles by reactive dyes (Peters, 1968). With an instantaneous reaction in the polymer, the diffusion equation reduces to the simple one-dimensional expression of Fick's second law for which the error-function solution is well known (Crank, 1956).

IV. EXPERIMENTAL

Experimental work was principally directed toward the determination of and quantitative evaluation of the content of hydroxyl and other chemical groups in films of the copolymer as a function of time, temperature, composition of the reaction bath, and film thickness. In addition the depth of penetration of the surface hydroxylation process was estimated by comparing the weights of unreacted and reacted material in these films. Additional experiments were also performed for specific characterization purposes.

1. MATERIALS

All experiments were performed using experimental styrene-butadiene-styrene block copolymer TR-41-2443 which contains 27.7% by weight polystyrene and was graciously supplied by Dr. T.L. Keelen of the Shell Chemical Company, Torrance, California. The properties of the copolymer (as determined by Shell) are described in Table IV-1.

The copolymer as supplied contains 0.2% antioxidant which was removed (unless otherwise noted) by fractional precipitation in methanol (Keelen, 1972).

Preformed 40% peracetic acid (FMC Corp., Inorganic Chemicals Division, Buffalo, New York) was used in all hydroxylations. Its composition is listed in Table IV-2.

Reagent grade solvents were used exclusively.

2. SURFACE HYDROXYLATION PROCEDURE

Films of SBS (Shell Experiemntal Block Copolymer TR-41-2443, see

Table IV-1

Characterization of SBS TR-41-2443

(Keelen, 1972)

Block Molecular Weights

16,000 - 85,000 - 17,000

Composition

Polystyrene 27.7 wt. % (25.1 vol. %)

Triblock   100 %

Polybutadiene Microstructure

cis 1,4   40%

trans 1,4   49%

1,2   11%

Table IV-2

40% Peracetic Acid, Composition, wt. %

(FMC)

Peracetic Acid	41.3%
Hydrogen Peroxide	5.1%
Acetic Acid	39.3%
Sulfuric Acid	1.0%
Water (free)	13.3%
Total Active Oxygen	11.05%

Table IV-1), solvent cast on mercury, were suspended in a flask in a

reaction medium composed of peracetic acid (FMC, 40% peracetic acid),

1% H_2SO_4 and varying amounts of acetic acid and water, all maintained at

a fixed temperature (30°-45°C). After sufficient time had elapsed the

films were removed from the bath, washed free of acid and then, the ace-

tate groups were hydrolyzed in approximately 2N KOH in a separate bath.

the films were dried between microfiber glass disks under the pressure of

binder clips and then in vacuum. Additional details to those presented

in the following sections can be found in the theses of Grauer (1973) and

Traut (1973).

(a) Film Preparation

The films were cast from benzene solution onto previously cleaned

mercury within polyethylene retaining rings (.090" thick, 2.25" OD, 1.75"

ID). The films were allowed to dry overnight by evaporation within a par-

tial benzene atmosphere created by the simultaneous evaporation of beakers

of benzene placed alongside the drying films. The mercury and the beakers

of benzene were all placed inside a partly closed container inside of a

fumehood with a very low draft. This care was taken to obtain uniform

films and to minimize the kinetic (polystyrene mobility) limitation to

obtaining films with the fully developed thermodynamic morphology (dis-

crete polystyrene domains in polybutadiene continuum) (Hoffman, et al.,

1971, Lewis and Price, 1971, 1972). Films varying in thickness were pre-

pared by varying the concentration and volume of benzene solution used.

Contrary to the observations of Krigbaum, et al. (1973), Bénard cells

(anisotropies due to convection currents set up during evaporative drying

of films) were never observed in the cast films.

The thickness of the films was determined by a differential focusing technique. Using a 'Microstar' optical microscope (American Optical Co., Buffalo, New York), at 450x magnification, each side of the film was focused on in turn and the difference between the two positions of the lens was noted on the calibrated scale. The true thickness is obtained by multiplying by the index of refraction (1.533) of the pure SBS copolymer. The accuracy of this procedure is usually ±5%, although occasional films were found (see section V-5) which deviated further.

(b) Peracid Reaction

The apparatus for the peracid reaction is shown in Figure IV-1. A 1500 ml. 4-necked reaction flask, fitted with a stirrer, condenser, thermometer and dropping funnel was used. The temperature was maintained constant by a heated water bath.

The 6 copolymer films attached to the teflon frame were separated from the direct action of the stirrer by a 1.75" OD polyethylene tube which acted as a baffle to prevent the lateral force of the stirrer from breaking the films. The motion of the fluid past the films was then in a plane parallel to the films rather than normal to them. The stirrer assembly had still to be checked before each run to insure that maximum agitation was attained.

The reaction medium, save for the peracetic acid, was made up prior to use. For each run 540 ml of this acetic acid/water (and 1% sulfuric acid) solution was added to the reaction flask and brought up to temperature. Peracetic acid (approximately 60 ml) was added slowly and brought up to temperature again before the teflon frame with attached films were palced in the reaction bath.
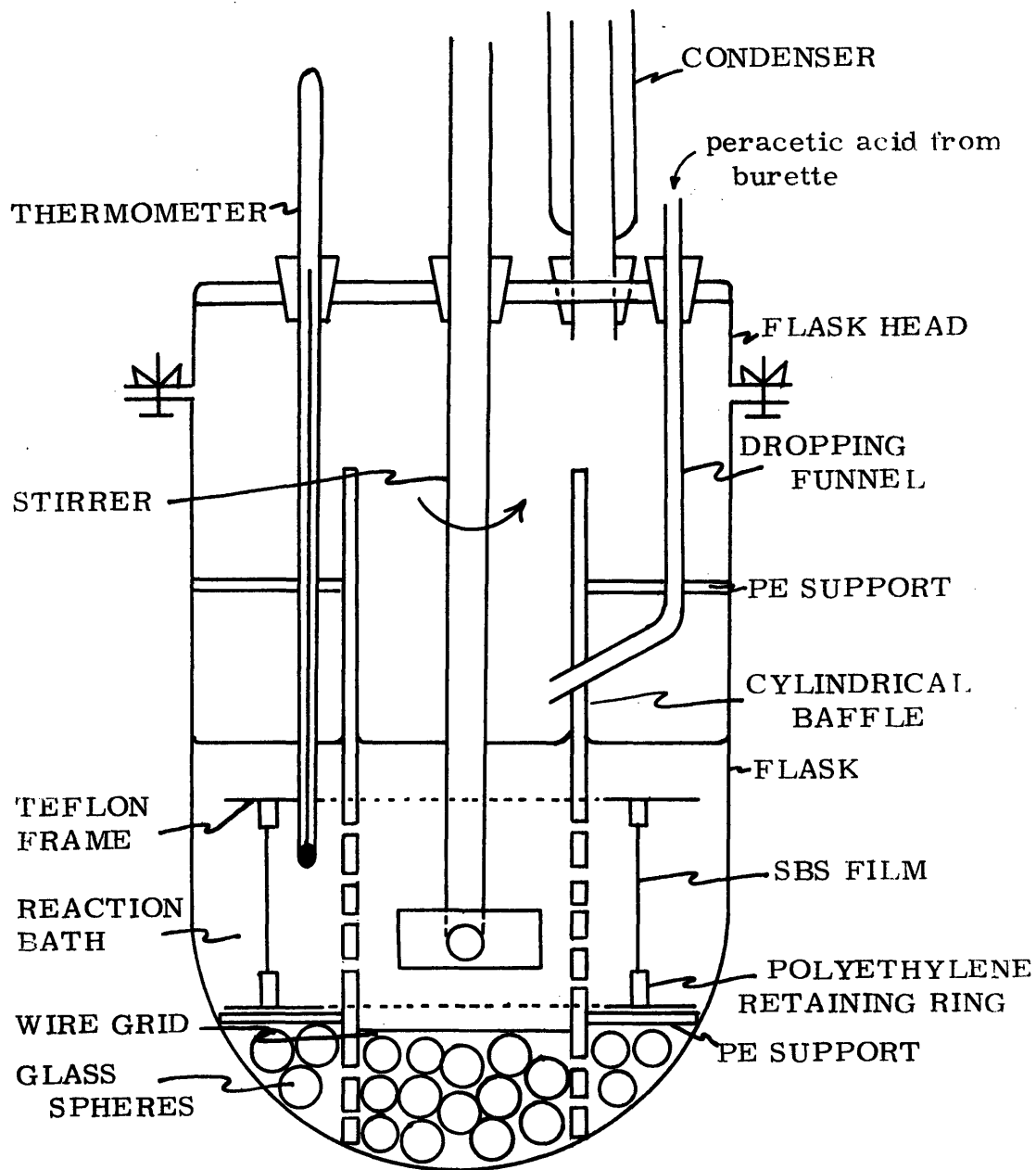
Figure IV-1. Apparatus for surface hydroxylation (peracid reaction).

In addition to the controls on temperature ($\pm 0.1°C$) and time used by Traut (1973), it was found necessary to determine the stirrer speed periodically during the reaction and the concentration of peracetic acid (as total active oxygen) before and after each reaction. The stirrer speed was determined using a stroboscope (Strobotac, General Radio Company, Concord, Mass.) and was held between the limits of 1350-1500 rpm. Higher stirring rates resulted in no increase in reaction extent demonstrating the absence of any mass transfer resistance from the bulk fluid to the film surface.

The peracetic acid (and hydrogen peroxide) concentration was determined using the procedure of Greenspan and MacKellar (1948). Three ml samples of the reaction medium were removed from the flask just prior to the beginning of the reaction and just before the end of reaction. The concentration of active oxygen was held between the limits of 1.23-1.25 gm/100 ml. The decrease in concentration of active oxygen (peracid) was less than 1% during the reaction and so the assumption of constant bulk concentration of peracetic acid was valid.

Because of the time required to reassemble the stirring assembly and the reaction flask at the beginning of the reaction and disassemble it at the end, the time of vigorous stirring (no resistance to mass transfer in bulk fluid) cannot be controlled better than ± 3 minutes. Because of the autoaccelerative nature of the process (see section V-4a) the reproducibility of the reaction extents in the more highly reacted films will be more strongly affected than in the less reacted samples (section V-4b).

Table IV-3 lists the conditions under which surface hydroxylations have been performed in this thesis and in the thesis of D.L. Traut (1973).

Table IV-3

Surface Hydroxylation Reaction Conditions

Temperature	Time (min)	Reaction Bath Composition (wt. %)[a]		
		Acetic Acid	H_2O	Active Oxygen Species[b]
30°C	180	70.2	23.7	5.1*
40°C	60	"	"	" *
	70	"	"	" *
	90	"	"	" *
35°C	90	71.1	22.8	5.1
	105	"	"	"
	115	"	"	"
40°C	60	"	"	"
	65	"	"	"
	70	"	"	"
	80	"	"	"
	90	"	"	"
45°C	40	"	"	"
	50	"	"	"
	55	"	"	"
40°C	20	92.5	1.4	5.1
	25	"	"	"
	30	"	"	"

*Traut (1973); all others this thesis

Note: (a) sum of reaction bath compositions is 99%; the remaining 1% is H_2SO_4.

(b) weight % active oxygen spesies refers to the components of the reaction bath that carry the active oxygen (i.e. per-acetic acid and hydrogen peroxide).

(c) Sample Workup

After removal from the peracetic acid reaction bath the films were washed thoroughly in cold water to stop the reaction and remove any adherent acid. The presence of peracetic acid inside the film after this washing step would also affect the measured extent of reaction (see section V-4b). The films were then allowed to sit in distilled water for 24 hours before being placed in approximately 2N KOH for 24 hours to effect the hydrolysis of the acetate groups.

In order to improve this hydrolysis step it was found necessary to conduct this hydrolysis at slightly different conditions than those used by Traut (1973): i.e., 40°-45°C, approximately 1.8 N KOH in 10% aqueous dioxane, agitated in a shaker bath (Warner Chilcott Water bath Shaker, Model 2156). These modified conditions eliminated the apparent diffusion limitation in this hydrolysis step (see section V-4b).

After hydrolysis the sample was washed thoroughly in cold water and then allowed to sit in 10% aqueous dioxane at 40°-45°C with agitation for 24 hours to remove all traces of KOH. The effectiveness of this removal was tested by qualitative emission spectroscopic analysis of some of our samples for residual potassium (see section IV-5e). The samples were then dried between microfiber glass disks under the pressure of binder clips and then in vacuum.

(d) Hydroxyl Analysis

The dried films were placed in the sample beam of a Perkin Elmer model 521 grating infrared spectrometer (Perkin Elmer, Norwalk, Conn.) and the spectrum between 3800 - 3000 cm^{-1} was recorded. The area under the OH stretching peak centered around 3,430 cm^{-1} was calculated using

the formula of Ramsay (1952), equation III-2. With the absorptivity

of the same peak determined from films of polyvinyl alchohol, the values

of $\int_0^b C_{OH}$ (b = film thickness, cm; C_{OH} = local concentration of hydroxyl

groups, gm moles/cm^3) were determined using the Lambert - Beer law

(no other chemical groups present absorb in this wavelength region).

the values of $\int C_{OH}$ -- moles of hydroxyl groups per unit area of film

(area concentration) were then plotted against the film thickness b

(see section V-4). The infrared spectroscopic technique is discussed

further in section III-4.

3. <u>DELAMINATION</u>

In attempting to dissolve the samples of surface hydroxylated mater-

ial, it was discovered that a side reaction of the hydroxylation process

was a crosslinking reaction. The knowledge of this side reaction was

used in a separate experiment to determine the depth of penetration of

the reaction process.

Using a 1/2" arch punch, 1.345 cm^2 circular pieces were stamped out

of the center of each of the samples that had been surface hydroxylated by

the procedure of the last section. These circular samples were weighed to

the nearest microgram using a Sartorius microbalance #1800 (Brinkmaan

Instruments, Westbury, New York). They were then placed in approximately

5 ml of chloroform for 3 - 4 days to reach equilibrium.

Chloroform is a good solvent for unreacted SBS copolymers and a

good swelling agent for the crosslinked, hydroxylated part of the copoly-

mer films. Chloroform then acts to delaminate the surface hydroxylated

film by dissolving the interior unreacted portion leaving the reacted

portion as a swollen gel. The gel was removed from the chloroform and
was washed with chloroform to remove any adhering soluble polymer.
The chloroform solution of polymer was precipitated in methanol (5 vol-
umes to 1) and the precipitated polymer was removed from the chloroform/
methanol supernatant (the recovery of a known amount of SBS in chloro-
form was > 98%). Both fractions were dried in vacuum and then weighed
using the microbalance.

For many of the samples, the remaining chloroform/methanol super-
natant was translucent indicating the presence of a third fraction which
did not settle out. This was recovered by evaporating the liquid to
about one-tenth the original volume and then precipitating in iso-octane.
This precipitate was also dried and weighed using the microbalance. For
a number of samples no chloroform soluble fractions were recovered at all.

4.   IR SPECTROSCOPIC CHARACTERIZATION

Infrared spectroscopy was used in two places in this thesis. As
noted in section IV-2, the area under the OH stretching peak at 3,430 cm^{-1}
was used to determine the moles of hydroxyl groups/cm^2 in the films after
reaction. IR spectroscopy was also used to characterize the chemical
structure of these surface reacted films and to test various hypotheses
concerning the reaction/diffusion process (see section V-6).

(a) Sample Preparation

The OH content (moles/cm^2) was determined directly without any fur-
ther sample preparation by placing the reacted film in the sample beam
of the IR spectrophotometer.

For those films thinner than 25 microns the complete spectrum could

also be obtained without further preparation. However, the thicker films absorbed too strongly in the rest of the spectral region for this procedure to be suitable. Portions of the thicker films were ground at 77°K to a fine powder in a Wig-L-Bug amalgamator (Crescent Dental Mfg. Company, Chicago, Illinois) inverted over a bath of liquid nitrogen. The powder was then dispersed in carbon disulphide. The unreacted polymer went into solution leaving the reacted polymer as suspended particles.

The first spectra taken were of films of these dispersed particles cast onto NaCl windows. A reference beam attenuator was necessary to get a reasonable spectrum because of the scattering of the sample beam by the translucent film which was really composed of discrete particles. This procedure was only used for the samples of copolymer surface hydroxylated at 30°C for 180 minutes (Figure V-28). For the other samples a 0.5 mm sealed liquid cell was filled with the carbon disulphide suspension of polymer and the spectrum recorded as if it were a liquid solution. Much better spectra were obtained by this method.

The baselines used are shown in Figure V-3.

(b) Instrument Parameters

A Perkin Elmer model 521 grating infrared spectrophotometer (Perkin Elmer, Norwalk, Conn.) was used for all spectra. The spectra were run at room temperature with the instrument in the normal operating mode: slits programmed for constant energy, attenuator - 3 sec. full scale, scanning at 3.3 cm^{-1}/sec and gain set at 4.2. These settings resulted in an accuracy (reproducibility) of ±0.5% transmittance with a suitable degree of resolution. Because of problems with the scan clutch, an in-

ternal standard with known absorption maxima had to be used to deter-

mine the frequencies of absorption in our samples. Polystyrene served

this purpose in our case.

(c) Qualitative Analysis

The spectra were analysed both quantitatively and qualitatively.

the qualitative analysis was accomplished by comparing the spectrum of

surface hydroxylated polymer with the spectra of model compounds, either

polymeric or of low molecular weight. (Binder, 1943, Felix, et al., 1963,

Krima, et al., 1956, Liang and Krimm, 1958, Ohloff, et al., 1964, Sadtler,

Stokr and Schneider, 1963). Detailed group frequency correlation tables

(Szymanski, 1964, 1967, Bellamy, 1958, Bomstein, 1958) were used when

available. In certain cases the results of the quantitative analysis

were used to support the exclusion of certain otherwise possible struc-

tures. The details of the assignments and how they were made are de-

scribed in Appendix I.

As noted in section III-2, there are uncertainties with regard to

the nature of the substituents on the ether groups (cyclic and/or acyclic

ethers) present in the reacted polymer. These difficulties arise from

the uncertainty in the true mechanism of ether formation and from the

statistical uncertainty peculiar to polymer reactions (section III-2d).

As a result, a broad peak, made up of smaller absorptions due to each

individual structure, appeared in the IR spectra, in the region character-

istic of that structural type. The composite peak was much broader than

any of the absorption peaks due to similar structures in the model com-

pounds, the spectra having been recorded on neat specimens (thus elimina-

ting any interfering effect of hydrogen bonding differences). This was

particularly true of the substituted tetrahydrofuran peak near 1067 cm^{-1}.
(The possible absorption frequencies of these other structures are shown
in Figure Al-1; the similarities of these structures to those shown in
Figure III-7 should be noted). This peak broadening was of more impor-
tance to the quantitative analysis than to the qualitative analysis of
the spectra.

(d) <u>Quantitative Analysis</u>

    (i) System of Equations

    As noted already in the theoretical section (section III-3), the
complexities of the system required that the results of the analysis be
considered as parameters of the spectroscopic model which best fit the
spectrum of the sample, rather than as a true composition analysis. The
form of this model was the Lambert-Beer law written for a multicomponent
system at each frequency of interest. ($A^{\nu} = \sum_{i=1}^{n} a_i^{\nu} bc_i$, Equation III-3).
For improved accuracy an over-determined system of equations was used
with the Lambert-Beer law written at more frequencies than there were
components.

    From the qualitative analysis of the reacted copolymer, the pre-
sence of 12 distinct components were detected and 22 absorptions of
analytical value were discovered. For the spectra obtained on samples
in the absence of CS_2 all 22 absorptions could be used. However, the
spectra of the remaining samples were obtained in CS_2 suspensions so
that four of these 22 absorptions (1657, 1637, 1602 and 1493 cm^{-1})
were completely masked by solvent absorptions. Therefore the system of
equations used for analysis was either 22 or 18 equations in 12 unknowns
depending on the sample. This system of equations was solved according

to the procedure of section III-3 using an IBM 1130 computer. As
noted in that section, the results of the computation were the values
of the sample area concentration $<X_i> = bc_i$, gm moles/cm^2 (b = sam-
ple absorption path length; c_i = average concentration of component in
sample). Because the path length or the total sample volume was general-
ly unknown, the $<X_i>$ values were divided by the $<X>$ value for the phenyl
groups which, with the assumption that the phenyl absorptions are unaf-
fected by reaction, and after multiplication by the number of moles of
unsaturation per mole of phenyl group, gave the relative concentrations
of each of the components in the units of moles of that functional group
per mole of unsaturation in the original unreacted copolymer (Equation
III-7). In addition the total number of oxygen-containing functional
groups and the fractions of the total for each functional group were
easily computed. The computer program was also set up to perform the
error propagation calculations outlined in Appendix 1 to give an esti-
mate of the error in each of the above 'concentrations'.

(ii) Calibration

The main reason that this analysis had to be considered as a model
fitting procedure was the absence of perfectly suitable calibration com-
pounds for the determination of the absorptivities (a_i^{ν}). Instead of
polymeric compounds containing the functional group of interest in an
environment comparable to that found in the surface hydroxylated sample,
low molecular weight compounds had to be used on occasion, containing
the functional group in a slightly different intra-molecular environ-
ment. Even where polymeric calibration compounds were available, be-
cause of the properties of the polymer the spectra for some of them had
to be run in solution (solvents: CS_2 and $CHBr_3$) rather than as films;

therefore, there were differences in the intermolecular environments (state) between sample and calibration compounds. The calibration compounds are listed in Table IV -4.

An additional reason that this scheme must be considered a model fitting procedure is that the broadness of the ether peaks (see section IV-4c) made it difficult to compute the background interferences due to ether absorptions at neighboring frequencies. The net result would be a high estimate of the absorbance at these neighboring peaks, attributed in error to the component(s) that absorb strongly at that frequency. There would also be uncertainty in the true value of the number of ether groups giving rise to the broadened peak.

Since each polybutadiene used for calibration contained some of the other types of double bonds the procedure of Silas, et al. (1959) and their assumption of 100% unsaturation was used to get the true absorptivities for each of the three double bond types. A similar procedure was used in determining the hydroxyl absorptivities from the polyvinyl alchohol-polyvinyl acetate copolymer films (the copolymer was used to avoid interferences from the crystalline environment present in a film of polyvinyl alchohol homopolymer).

The asumption of Szymanski (1967) in dividing the absorption of each assymetric ether into two components one from each half of the ether linkage, was extended here to the quantitative analysis scheme. Each half of the ether linkage was assumed to give rise to a separate absorption peak with its own extinction coefficient (absorptivity). The spectra were then analysed on the basis of moles of carbon-oxygen bonds, independent of the nature of the substituents on the second carbon of the

Table IV-4
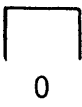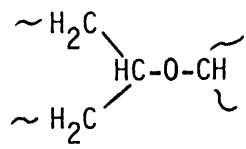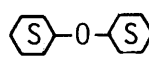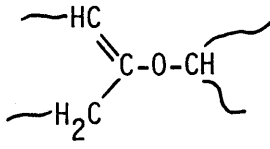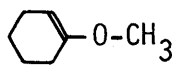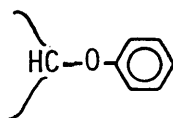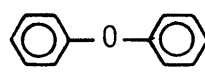
Calibration of IR Quantitative Analysis

functional group	sample molecular environment [a]	calibration compound	calibration molec. environ.	state [b]
phenyl	$\sim CH_2\text{-}CH\text{-}CH_2 \sim$ (phenyl)	polystyrene	identical	solution*
cis alkene	$\sim H_2C$ —CH=CH— $CH_2 \sim$	cis 1,4 polybutadiene	"	"*
trans alkene	$\sim H_2C$ —CH=CH— $CH_2 \sim$	trans 1,4 polybutadiene	"	"
vinyl alkene	$\sim CH_2\text{-}CH \sim$ / CH / CH₂	1,2 polybutadiene	"	"*
hydroxyl	$\sim CH_2\text{-}CH\text{-}CH\text{-}CH_2 \sim$ OH OH	polyvinyl alcohol/co- polyvinyl acetate	$\sim CH_2\text{-}CH\text{-}CH_2\text{-}CH \sim$ OH OH	film
acetate	$\sim CH_2\text{-}CH\text{-}CH\text{-}CH_2 \sim$ OH OAc	polyvinyl acetate	$\sim CH_2\text{-}CH \sim$ OAc	film
carbonyl	$CH_2\text{-}CH\text{-}CH_2$ ‖ O	literature value used (methyl-n hexyl ketone)		
epoxy	$CH_2\text{-}CH\text{-}CH\text{-}CH_2$ \O/	2,3 epoxy butane	$CH_3\text{=}CH\text{-}CH\text{-}CH_3$ \O/	solution

[continued]

* some of the absorptivities were determined in solid filsm by comparison with known absorptivities.

Table IV-4

[continued]

functional group	sample molecular environment[a]	calibration compound	calibration molec. environ.	state[b]
5 membered cyclic ether	O	tetrahydro-furan		solution
saturated acyclic ether	$\sim H_2C$ $\sim H_2C$ $HC-O-CH$	dicyclohexyl ether	⬡-O-⬡	"
vinyl ether	—HC —H_2C C-O-CH	1 methoxy-cyclohexene	⬡-O-CH$_3$	"
phenyl ether	HC-O-◯	diphenyl ether	◯-O-◯	"

---

a   this is the assumed molecular environment (see Discussion V-2)

b   solvents: carbon disulphide 3800 - 2900 cm^{-1}
                                    2000 - 1700 cm^{-1}
                                    1350 - 625 cm^{-1}
                 bromoform   1700 - 1350 cm^{-1}

c   see the body for description of the ether structures.

ether linkage. For example assymmetric vinyl ethers were assumed to be made up of two parts; the saturated part ($-O-CH\overset{CH_2\sim}{\underset{CH_2\sim}{}}$) with absorbance maximum at 1090 cm^{-1} and the unsaturated part ($-O-C\overset{CH\sim}{\underset{CH_2\sim}{}}$) with absorbance maximum at 1210 cm^{-1}. On the other hand, symmetric ethers give rise to a single peak, the absorptivity of which is halved to get the absorptivity per mole of C-O bonds. For example, acyclic saturated ethers ($\overset{\sim CH_2}{\underset{\sim CH_2}{}}CH-O-CH\overset{CH_2\sim}{\underset{CH_2\sim}{}}$) have a single absorbance maximum at 1090 cm^{-1}. The absorptivity of the saturated part of the vinyl ether is assumed to be the same as the halved absorptivity of this symmetric acyclic saturated ether. Hence, only three acyclic ether structures ($\overset{\diagdown}{\diagup}$C-O struc-tures) and only three sets of absorptivities are needed to characterize fully the six possible acyclic ether structures.

As noted in section IV-2 the area under the OH stretching peak centered at 3430 cm^{-1} was used to define the absorbance at 3430 cm^{-1}. On the assumption (Bellamy, 1958) that the absorbance at each wavenumber in this peak reflects a certain number of hydroxyl groups with a certain hydrogen bond strength, the maximum absorbance merely reflects that hydrogen bond which is most numerous. Therefore, shifts in the maximum peak indicate only changes in the distribution of hydrogen bonding. Hence the area under the peak should reflect the number of hydroxyls present irrespective of the type of hydrogen bonds present or the location of the peak. Thus the area of the OH peak in the hydroxylated SBS samples could be compared to the area of the OH peak in polyvinyl alcohol - polyvinyl acetate copolymer films which was centered at 3340 cm^{-1}--a 90 cm^{-1} shift.

Because only a small amount of carbonyl (less than 1%) was present in

our spectra, a literature value of the absorptivity at 1710 cm^{-1} was

used (Cross and Rolfe, 1951) of a suitable model compound (methyl-n

hexyl ketone). The errors, so involved, were assumed to be of little

consequence.

Further details of the calibration are given in Appendix I.

5.   ADDITIONAL CHARACTERIZATIONS

(a)   Unreacted SBS Copolymer

    i)   density

The density of unreacted SBS copolymer (TR-41-2443) was determined

by weight measurement in air and in methanol.

    ii)   IR and NMR

To confirm the Shell composition analysis of the SBS copolymer

(Table IV-1) the infrared analysis scheme presented in section IV-4 was

used on solvent cast films of the copolymer, and the proton NMR analysis

method of Mochel (1967) was used on carbon tetrachloride solutions of the

copolymer.

(b)   Electron Microscopy

Films of the SBS copolymer were prepared for electron microscopy

by casting a 12% benzene solution of the copolymer onto glass. The

films were then annealed under vacuum at 120°C for 1 hour to fully develop

the thermodynamically favorable morphology. The antioxidant was not re-

moved from the polymer prior to preparation of the films.

Carbon replicas of the films were prepared according to standard

techniques (Barr, 1973, ASTM, 1973) and examined up to magnifications of

75,000x[1].

In addition thin slices of the films were cut and stained for 144 hours in osmium tetroxide solution before being embedded in epoxy resin[2] (Bradford, 1974). Even though difficulties were encountered in sectioning, a few good sections 600 $\overset{o}{A}$ in thickness were obtained using an LKB Ultrotome III (LKB Instruments, Rockville, Maryland). The area near the surface of the films was examined up to magnifications of 160,000 x in order to determine the morphology at the surface of the copolymer films.

(c) Epoxidation Kinetics

The kinetics of the epoxidation reaction in solution was determined at 40°C in the presence of two amounts of acetic acid: 17 wt. % and 34 wt. %. To a solution of copolymer in chloroform in a 4-neck round bottom flask, maintained at 40°C by a heated waterbath, with attached stirrer, condenser, thermometer and dropping funnel, the desired amount of acetic acid and 12N H_2SO_4 (1% by weight of aqueous phase) was added. Sufficient peracetic acid to give an active oxygen/double bond mole ratio of 1.1 was added to start the reaction. At appropriate intervals samples of the reaction mixture were removed and analysed for peracetic acid and hydrogen peroxide content according to the method of Greenspan and MacKellar (1948). Difficulty was encountered because of the two phase nature of these samples. From the total active oxygen content,

1. The collaboration of Prof. Vander Sande of the M.I.T. Center for Materials Science and Engineering and Captain D. Barr of the U.S. Army Materials and Mechanics Reasearch Center, Watertown, Mass., is gratefully acknowledged

2. The collaboration of Dr. E.B. Bradford, DIG Physical Research, Dow Chemical Company, Midland, Michigan is gratefully acknowledged

the extent of reaction could be calculated and the solution phase kinetic constants for the epoxidation of SBS was determined (section IV-2b).

Conditions used were:

Volume Fraction Acetic Acid	.22	.43
Initial Concentration (moles/liter):		
active oxygen	.159	.119
double bond	.149	.108

(d) Oxygen Analysis

For the films, surface hydroxylated at 30°C for 180 minutes in 70% acetic acid, total oxygen content of the films was determined by an inert gas fusion procedure (Central Analytical Facility, Center for Materials Science, M.I.T.). By determination of the weight per unit area of these films, the oxygen contents in weight % were converted to the units of moles of oxygen/cm^2.

(e) Emission Spectra

Qualitative emission spectra (Central Analytical Facility, Center for Materials Science, M.I.T.) were used to determine the presence of potassium and other inorganic contaminants in two of the surface hydroxylated films.

(f) Ageing

Pieces of surface hydroxylated polymer (40°C, 70 minutes, 71% HAc) along with pieces of unreacted polymer (1/2" by 1/2" by .021" thick) were set aside to age for five months in various environments. The conditions

Table IV-5

Conditions for Ageing of SBS (reacted and unreacted samples)

1) dry, in vacuum, wrapped in aluminum foil (dark)

2) 70% relative humidity, in air, wrapped in aluminum foil (dark)

3) 70% relative humidity, in air, under normal room lighting

4) in sterile solution, open to atmosphere, under normal
room lighting

5) in sterile solution, open to atmosphere, wrapped in
aluminum foil (dark)

6) in sterile solution, closed to atmosphere, wrapped in
aluminum foil (dark)

Composition of sterile solution:

pH 7.4

0.9 gm % NaCl

10 ml/100 ml NaH_2PO_4-NaOH buffer

5 ml/ 100 ml formalin

used are listed in Table IV-5.

(g) Water Absorption

The swelling in water of some of the surface hydroxylated films was determined using the 1.345 cm^2 pieces of polymer prepared for delamination (section IV-3). Before being placed in chloroform, these already weighed samples were allowed to swell to equilibrium in distilled water. They were then weighed on a Sartorius analytical balance #2600 (Brinkman Instruments, Westbury, New York) to determine the amount of water absorbed. After redrying, the samples were placed in chloroform for delamination (section IV-3).

(h) Biological Tests

Films of SBS copolymer (.025" and .021" thick), surface reacted at 40°C for approximately 20 minutes in 93% acetic acid (along with unreacted films as controls) were evaluated for blood compatibility by a whole blood clotting time test (Merrill, 1974). Tubes were formed by placing folded-over triangular pieces of the film, between two pieces of silicone rubber, in the jaws of 2" binder clips.

A few grams of SBS TR-41-2443 after precipitation in methanol to remove the antioxidant were incubated in the presence of cleaned soil microorganisms. The solid copolymer was the only source of carbon. The samples were incubated for several weeks before they were examined for evidence of growth of the microorganisms.

(i) 'Hydroxylation' of Polystyrene

The assumption of polystyrene inertness of peracetic acid reaction was tested by allowing polystyrene to react under conditions similar to the solution and surface reactions of the SBS copolymer.

i) <u>Solution</u>

The same apparatus as that described in section IV-5c was used.
To a mixture of 500 gm of 1% polystyrene (Dow Chemical Co., Midland,
Michigan) in chloroform, 100 ml acetic acid and 2 ml $12NH_2SO_4$, 9.2 ml
40% peracetic acid was added slowly. After 127 minutes at 40°C, the
polymer was precipitated in methanol and then redissolved in chloro-
form. The portion of precipitate which did not dissolve in chloro-
form was removed and dried in vacuum. The soluble portion was re-
precipitated in methanol and vacuum dried. An infrared spectrum of a
film of the soluble material was recorded.

ii) <u>Solid Phase</u>

A thin film of polystyrene, the infrared spectrum of which had
been previously recorded, was placed in a typical surface hydroxyla-
tion reaction bath for 90 minutes (40°C, 71% acetic acid, 1.25 wt. % ac-
tive oxygen). After washing thoroughly in distilled water and drying
in vacuum, its infrared spectrum was recorded.

(j) <u>Miscellaneous</u>

^{13}C NMR and laser Raman spectra of the reacted copolymer were also
obtained. These are reported in Appendix 2 along with notes on the
dyeing of the surface reacted films with toluidine blue, contact angle
measurements on the original copolymer, and the solution phase reaction
between peracetic acid and SBS copolymer.

V. RESULTS AND DISCUSSION

1. SURFACE MORPHOLOGY

Figure V-1 is a transmission electron micrograph of a sample of
SBS copolymer, showing the region near the air interface of the sol-
vent cast film. The surface appears fairly smooth, despite the dif-
ficulty encountered in sectioning the films. The morphology of the
copolymer away from the surface is readily seen to correspond with
that observed by others in similar block copolymers (section III-1a):
namely, strings and circular islands of polystyrene-rich regions in a
stained polybutadiene-rich matrix. The circular patterns are presum-
ably the cylindrical domains viewed in cross-section. From the micro-
graph the diameter of the domains is approximately 100 Å.

It is also apparent that this morphological structure extends up
until the surface. However, at the surface, the fairly regular matrix
structure is replaced by a thin region (~150 Å thick) of almost uni-
form clarity, broken by only an occasional streak of stained material.
This surface region is even clearer than the interior of the polystyrene
domains. Therefore, it is believed that this thin region is an arti-
fact caused by the embedding process and, in fact, represents the epoxy
which has diffused into the surface of the polymer and has disturbed the
true surface morphology. Hence, this TEM micrograph is inconclusive
with respect to the composition of the surface.

Figure V-2a,b,c are carbon replica micrographs of the air surface
of two different samples of SBS copolymer. Figure V-2a and b shows two
different areas of the same sample at slightly different magnifications
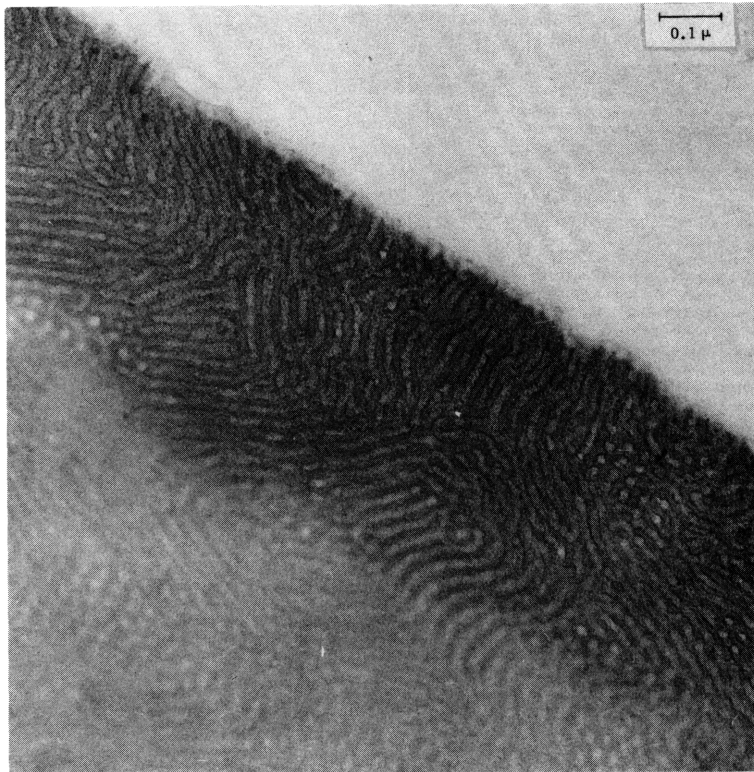
Figure V-1. Transmission electron micrograph of SBS TR-41-2443, showing the region near the air interface of the film solvent cast from a benzene solution. (Dr. E.B. Bradford, Dow Chemical Co.)
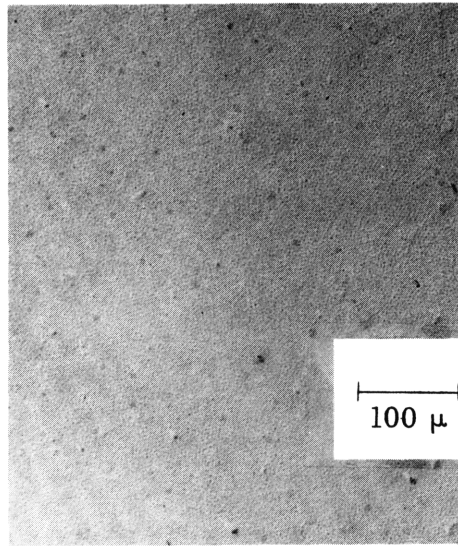
(a)
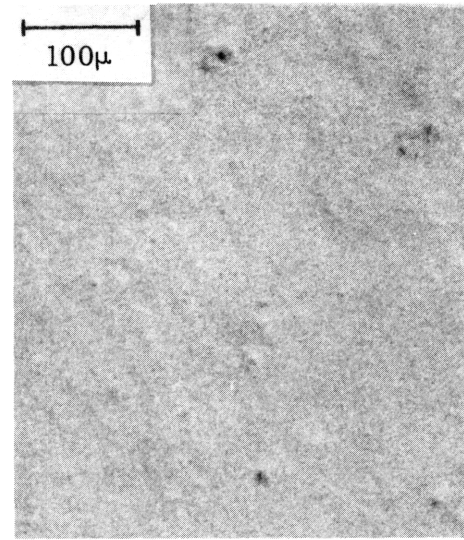
(b)
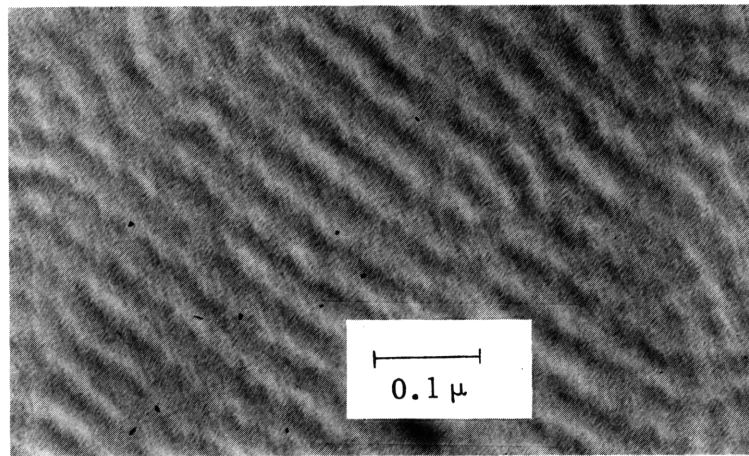
(c)

Figure V-2. Carbon replica micrographs of the air surface of SBS TR-41-2443 ((a), (b), Capt. D. Barr, U.S. Army Materials and Mechanics Research Center; (c), Prof. J. Vander Sande, M.I.T. Center for Materials Science and Engineering).

while Figure V-2c is of a different sample at much higher magnification. Both samples were prepared under identical conditions. In Figure V-2a, the surface has a fine grainy appearance, which is magnified in Figure V-2c and appears to have a regular almost spherical structure (diameter $\simeq$ 200 Å). This grainy surface, however, is not apparent in the micrograph of V-2b, even though it is but a different area of the same sample shown in V-2a. The reason for this difference is not clear at all, but is presumably related to differences in drying rate experienced by different areas of the film during the casting process. This only emphasizes the great difficulty often encountered in preparing samples of uniform surface and demonstrates a probable reason for the variability of much of the blood compatibility data already presented in the literature (Bruck, 1974).

Nevertheless, considering the frequency of observation of this grainy surface structure, it is assumed that this is a good example of the surface morphology that can be expected in solvent cast films. Unfortunately, an unequivocal explanation for this structure is made impossible by the absence of surface composition information. These grains or roughness in the surface could be exposed polystyrene domains, that are extending out through the surface. This, while not definitely excluded, is considered unlikely because: 1) the contact angle of water on SBS described in Appendix A2-E is much different than that on polystyrene (it is not very similar to that of polybutadiene either, but there may be other reasons for this); 2) the surface tension of polybutadiene is greater than that of polystyrene and so, within certain limitations discussed in section III-1c, the cylindrical domains

should orient themselves parallel to the air surface rather than normal to it, to minimize the amount of polystyrene exposed at the air surface and 3) the diameter of the domains seen in the carbon replicas is approximately twice the diameter of the domains seen in the TEM micrographs (200 Å versus 100 Å). Alternatively, these bumps could result from polystyrene domains near the surface, but not exposed, forcing up the polybutadiene cover surrounding these domains to give the surface the rough grainy appearance. While this hypothesis is consistent with the existing experimental observations there is, unfortunately, no independent confirmatory evidence available.

Although the actual nature of the surface morphology is still indeterminate, this latter hypothesis is considered to be a valid estimate of the true situation. Hence it is concluded that the air surface of SBS copolymers, containing 27% (wt.) polystyrene, is rich in polybutadiene and thus, the scheme developed here to eventually prepare blood compatible biomaterials is a feasible procedure.

2. CHEMISTRY OF SURFACE HYDROXYLATION

(a) Qualitative Spectral Analysis

The infrared spectrum of a film of SBS copolymer which had been surface hydroxylated for 65 minutes, at 40°C, in a reaction bath containing 71% acetic acid is shown in Figure V-3. The assignments of the peaks in the region between 4000 - 625 cm^{-1} are given in Table A1-1 in Appendix 1. (The baselines used for the quantitative analysis are also shown in this spectrum.)

From qualitative analysis of this spectrum and others, there is
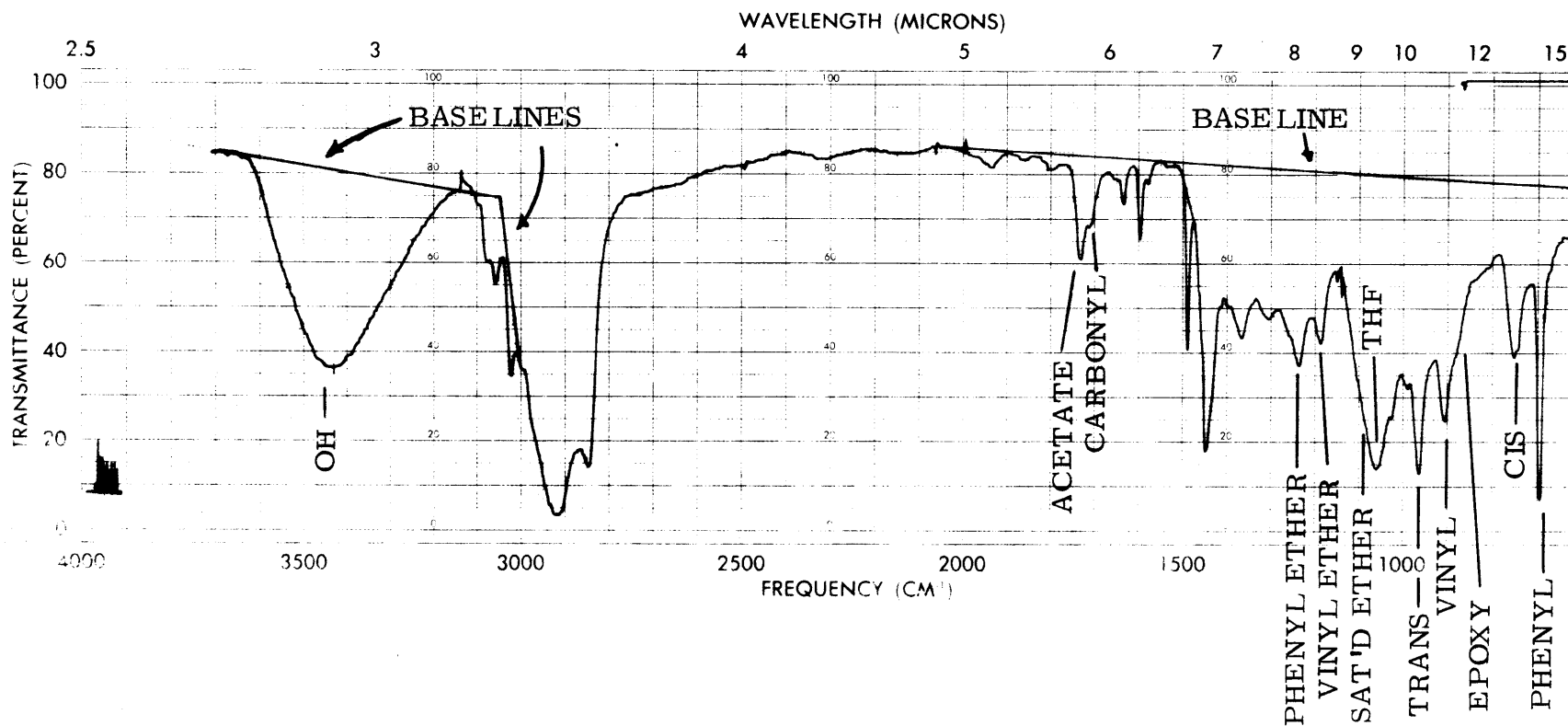
Figure V-3. Infrared spectrum of surface hydroxylated styrene-butadiene-styrene
block copolymer TR-41-2443 (40°C, 65 minutes, 71.1% acetic acid)

evidence for the presence in the sample, of phenyl groups (polystyrene), unsaturation (unreacted polybutadiene), hydroxyl groups, uncleaved epoxide groups, and unhydrolysed acetate esters. In addition, there are a number of functional groups apparent which can arise through the variety of side reactions discussed earlier in section III-2d,e: carbonyl, substituted tetrahydrofuran rings, saturated acyclic ethers, acyclic vinyl ethers and phenyl ethers.

The reason for the presence of acetate and epoxide groups after the base hydrolysis is interpreted in terms of a diffusion limitation during the cleavage and hydrolysis reaction steps. These limitations are discussed further in section V-6.

The carbonyl groups are presumed to arise from an epoxide-to-carbonyl rearrangement, catalysed by acid. (Even after improved acetate hydrolysis, the peak at 1710 cm^{-1} still appears in the spectrum). The non-aromatic ethers (both cyclic and acyclic) are considered to arise from the epoxide rearrangements, reported by Ohloff (1964) and discussed earlier (section IV-2d). Because of the multiplicity of structures possible from such rearrangements (Figure III-7,8), each of which has a fairly distinctive infrared absorption maximum (Figure IV-2), broad peaks are found in the spectrum at frequencies characteristic of the group (see especially the broad peak at 1067 cm^{-1} which has been assigned to the tetrahydrofuram ring).

It is, however, much more difficult to account for the presence of aromatic ethers. In order to test the assumption of polystyrene unreactivity in epoxidation, polystyrene homopolymer was reacted in solution, and as a solid film, under conditions similar to those used for

the SBS copolymers (section IV-5i). The film of polystyrene showed

no evidence of reaction, owing to a diffusion limitation, making per-

acetic acid unable to react with the polymer beyond a few Angstroms

(the true surface). The polystyrene in solution, however, definitely

had reacted: the spectrum after reaction of still soluble polymer

showed evidence of phenyl - phenyl (ν = 1240 cm^{-1}) ethers and a very

small amount of phenyl - alkyl ethers (ν = 1090 cm^{-1}). In addition, a

minute amount of cross-linked gel was found, presumably formed by the

action of these phenyl ethers as crosslinks. Thus it appears that poly-

styrene can react with peracetic acid, although in a very non-specific

manner. On the assumption that there is no adventitious olefinic unsat-

uration in homopolymer polystyrene, these ethers could conceivably form

via an oxygen mediated free radical reaction which couples two phenyl

groups together or couples a phenyl group to a backbone carbon atom

despite the steric hindrances involved in this latter crosslinking

reaction. If there were olefinic unsaturation in polystyrene, the

ethers could conceivably result from electrophilic substitution of a

protonated epoxide directly onto the ring. Either (or both) of these

mechanisms can account for the formation of aromatic ethers in surface

hydroxylated SBS. The diffusion limitation noted in the reaction of a

polystyrene film would not be relevant here because of the relatively

significant mixed region between polystyrene domains and polybutadiene

matrix (section III-1b; Meyer, 1974, Leary and Williams, 1973, 1974).

The presence of unsaturated acyclic ethers (other than vinyl ethers)

could not be distinguished from the spectrum. The allylic part of the

ether in model compounds, like 3-methoxy cyclohexene-1, absorbs in the

same location as the saturated part with nearly identical absorptivity. Apparently the double bond in the allylic ether does not withdraw enough electrons from the carbon-oxygen bond to significantly affect the absorption of infrared radiation by the ether linkage (as occurs in vinyl ethers). Similarly 1,4 dioxane rings and tetrahydropyran structures could not be differentiated from the tetrahydrofuran structures as both types of cyclic ether absorb in the same region. However, spectra of substituted dioxane structures (e.g. 2,6 dimethyl - 1,4 dioxane) show a complex of peaks in the 1160 - 1090 cm^{-1} region and a very sharp peak near 880 cm^{-1}. The absence of these other peaks here, makes it extremely doubtful that there is a significant amount of dioxane structure present in the sample.

The question of the presence of peroxide groups in the sample is not clear. Peroxides arise by a variety of free radical processes and have C-O absorptions identical to acyclic ethers and an O-O absorption near 880 cm^{-1}, in the same location as the major epoxy absorptions. By comparison of the ratio of epoxy absorbances at 882 cm^{-1} and 807 cm^{-1} (corrected for known interfering absorptions) to the ratio of absorptivities at these two peaks, a decision should be able to be made regarding the presence or absence of peroxide groups. In many of the spectra, calculation of this ratio indicates the presence of unaccounted for absorbance at 882 cm^{-1}. This could be attributed to peroxide absorption if it were not for some complicating factors: 1) this discrepancy in the absorption at 882 cm^{-1} is only apparent in some but not all of the spectra, indicating peroxide is not uniformly present in the samples, 2) generally, in the spectra where this discrepancy is noted, the absorb-

ance at 807 cm^{-1} is very small and, as such, changes in the location of the baseline (which, as is noted in section V-6a, is drawn fairly arbitrarily) would have a drastic effect on this absorbance, 3) while the inclusion of the peroxide absorbance in the quantitative scheme eliminated the residual absorbance at 882 cm^{-1} and yields a smaller sum of the squared residuals, the reduction in the number of degrees of freedom in the analytical scheme dominates. The net result is a larger standard error of the estimate, indicating a poorer fit of the model when peroxides are included. Finally, 4) in some of these spectra, an additional peak is apparent at 820 cm^{-1}; the shift may reflect small sample-to-sample differences in structure. This 820 cm^{-1} may be the true epoxide peak (with absorptivity that of the 807 cm^{-1} peak in 2,3 epoxybutane) and thus, the comparison should be made between the absorptivities at 882 cm^{-1} and 807 cm^{-1} and the absorbances in the sample at 882 and 820 cm^{-1} (not 807 cm^{-1}). Either the change in baseline or the change in absorption frequency can fully account for the residual absorbance at 882 cm^{-1}, and so, it is unclear whether there are peroxides present or not. Because the distinction was not important to this thesis, and because of the lack of unequivocal evidence in favour of the presence of peroxides, the carbon-oxygen peaks in the 1240 - 1090 cm^{-1} region were assigned exclusively to acyclic ethers rather than to acyclic peroxides. The presence of peroxides, however, cannot be unequivocally excluded either.

A hypothesis concerning the formation of primary alcohols in the surface hydroxylation as terminal groups after chain scission was tested by similar arguments. Primary hydroxyl groups can be distinguished from secondary alcohols by the shift of the C-O peak from 1090 cm^{-1} in secon-

dary hydroxyls to near 1050 cm^{-1} for primary groups. This absorption

is unfortunately masked by the tetrahydrofuran absorption near 1067 cm^{-1},

and since the absorptivity of OH groups near 3430 cm^{-1} is nearly iden-

tical for both primary and secondary groups, primary alcohols cannot

be distinguished at all in the spectrum. Although the quantitative

data fit very well in this region without assuming the presence of pri-

mary hydroxyl groups absorbing near 1050 cm^{-1}, this cannot be considered

conclusive with regards to their exclusion in a chemical (spectroscopic)

model of the reacted polymer. Quantitatively, it is not important,

since primary and secondary hydroxyls have nearly the same absorptivity

at 3450 cm^{-1}, but qualitatively it is, in considereig whether chain scis-

sion occurs at all.

In the absence of information to the contrary, the presence of tetra-

hydropyran and dioxane ring structures, peroxides and primary alcohols

were considered to be absent in developing the quantitative spectroscopic

model of the reacted polymer (section III-3 and IV-4d). These difficul-

ties in making a definitive qualitative analysis contributed to the de-

cision to consider the quantitative analysis scheme a model fitting pro-

cedure rather than as a true analytical method.

Additional remarks concerning the structure of the hydroxylated

polymer are made in section V-6.

In the spectrum shown in Figure V-3, hydrogen bonding is apparent

in the width of the OH stretching peak at 3430 cm^{-1}. The half-intensity

width of the peaks in the spectra of surface hydroxylated SBS were in

the range of 200-280 cm^{-1} (no correlation of peak height and peak width

was apparent), but in the calibration spectra of a copolymer of poly-

vinyl alcohol and polyvinyl acetate the width was approximately 290
$\pm$ 10 cm^{-1} (maximum at 3340 cm^{-1}, however). Using Bellamy's (1958) as-
sumption that the absorbance at each wave number in the OH stretching
peak reflects a certain number of hydroxyl groups with a certain hydro-
gen bond strength and that the maximum absorbance merely represents
that hydrogen bond which is most numerous, the differences in calibra-
tion and SBS OH peaks can be related to differences in the degree of
hydrogen bonding only. Thus, while the copolymer of vinyl alcohol
and vinyl acetate has a slightly broader distribution of hydrogen
bonds than hydroxylated SBS, the most numerous hydrogen bond is stronger
in the copolymer that the one corresponding to the peak maximum in SBS.
This is interpreted to indicate the presence of a greater quantity of
weaker hydrogen bonds in the SBS. This is expected when the variety of
structures (ethers) that can be bonded with the OH peak to form relatively
weak hydrogen bonds is considered. (In the calibration sample, only
acetate groups are present to form hydrogen bonds weaker than the strong
hydroxyl-hydroxyl hydrogen bonds).

Presumably the sample-to-sample differences in the width of the OH
peak in the hydroxylated SBS samples are the result of a combination of
sampte-to-sample differences in chemical structure (see section V-6) and
sample-to-sample differences in the approach to equilibrium of hydrogen
bond formation (kinetic limitations in hydrogen bond formation). These
differences in the approach to equilibrium could probably be eliminated
by annealing at a suitable temperature to allow the hydrogen bond struc-
ture, with minimum free energy, to form without kinetic restriction.
However, no such time dependent effect was noticed in the degree of hydro-

gen bonding in films of the copolymer of polyvinyl alcohol and polyvinyl acetate.

Hydrogen bonding of the ether peaks was not particularly significant. The widths of the ether peaks of the calibration compounds in solution (CS_2) were generally 1 - 2 cm^{-1} smaller than the widths as neat specimens. The ether peaks in the samples of hydroxylated polymer were much wider, however, and this is attributed to the multiplicity of structures present rather than to the specific effect of hydrogen bonding (section IV-4c). (Some of these ethers are probably hydrogen bonded to hydroxyl groups which may increase the width of the ether peaks more than in the pure neat specimens but this hypothesis cannot be tested.)

Comparison, however, of the width of the trans double bond peak at 967 cm^{-1} in crystalline trans polybutadiene homopolymer, and unreacted and reacted SBS copolymer, indicated that these double bonds, in films of the block copolymer, were in a high state of interaction. The half-intensity widths were:

	$\Delta\nu_{1/2}$ ($\nu = 967$ cm^{-1})
trans 1,4 polybutadiene (film - crystalline)	25 cm^{-1}
" " " (CS$_2$ solution)	13
SBS TR-41-2443	25
SBS TR-41-2443 (reacted)	20

The trans double bond peak in polybutadiene is obviously wider when the polymer is in the ordered state rather than in solution. The crystalline state enables the double bonds to interact with each other efficiently

and results in a broadened peak. The width of the same peak in the SBS samples is interpreted to indicate the presence of similar kinds of order (interaction) among the polybutadiene blocks. This order may not be as regular as that found in a crystallite, but is sufficiently regular to cause the peak broadening observed. The reduced width in the reacted SBS sample merely reflects the greater concentration of non-trans double bonds with which the double bonds are not able to interact.

(b) <u>Solution Phase Kinetics</u>

In order to test the effect of acetic acid on the kinetics of epoxidation, the concentration of active oxygen during a solution phase epoxidation was monitored during the reaction (section IV-5c). For a single order chemical reaction,

$$A + B \xrightarrow{\quad k_1 \quad} C$$
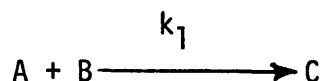
a plot of $\ln \frac{(A)(B)^\circ}{(B)(A)^\circ}$ versus time, should yield a straight line with slope equal to $[(A)^\circ - (B)^\circ]k_1$, where $(A)^\circ$, $(B)^\circ$ are the initial concentrations of A and B, respectively, and k_1 is the second order kinetic constant of the reaction (Daniels and Alberty, 1966).

Since epoxidation is known to be a second order chemical reaction (section III-2a), deviations in a plot of $\ln \frac{C_0 C_u^\circ}{C_u C_0^\circ}$ versus time (C_0, C_u = concentrations of active oxygen and double bonds respectively at time t; C_0°, C_u° = initial concentrations) would indicate the presence of either unaccounted for peracetic acid consuming reactions or the presence of double bonds which react at different rates. Because of the known presence of both internal and external (vinyl) double bonds in polybutadiene,

curavature is expected in these plots.

The results of runs performed in two volume fractions of acetic acid (.22, .43) with most of the remaining reaction bath being chloroform are presented in Figure V-4. Higher concentrations of acetic acid could not be tested because of precipitation of the polymer. $C_u(t)$ was computed from the stoichiometry of the reaction knowing C_p^o, C_u^o and $C_p(t)$. The conversion of double bonds is also reported as an ordinate on the right hand side of Figure V-4.

Figure V-4 shows that the expected non-linear curves were obtained for the epoxidation of polybutadiene. As the internal (more reactive) double bonds are reacted, leaving the less reactive vinyl double bonds, the effective kinetic constant (proportional to the slope) decreases. In order to calculate better estimates of the kinetic constants (rather than the effective one calculated using $(C_0^o - C_u^o)$, where C_u^o is the initial concentration of double bonds present, regardless of reactivity), it is assumed that 88% of the double bonds react with the kinetic constant calculated from the slope at time zero, while the remaining 12% react at a rate corresponding to the slope at 88% conversion (88% is the average of the two available values for % internal (cis/trans) double bonds: Shell (Table IV-1), 89%, this thesis (section V-6), 87%). Thus the kinetic constant at 0% conversion is: $k_0 = slope_{0\%}/(C_0^o - .88C_u^o)$ and the kinetic constant at 88% conversion, $k_{88} = slope_{88\%}/(C_0^o - .12C_u^o)$. These are estimates of the true kinetic constants for epoxidation of cis/trans double bonds and vinyl double bonds respectively, since the ordinate of $\ln \dfrac{C_0 C_u^o}{C_u C_0^o}$ in the curves of Figure V-4 must be modified in a complex (unknown) way to be able to get the true values of the kinetic constants. The kinetic
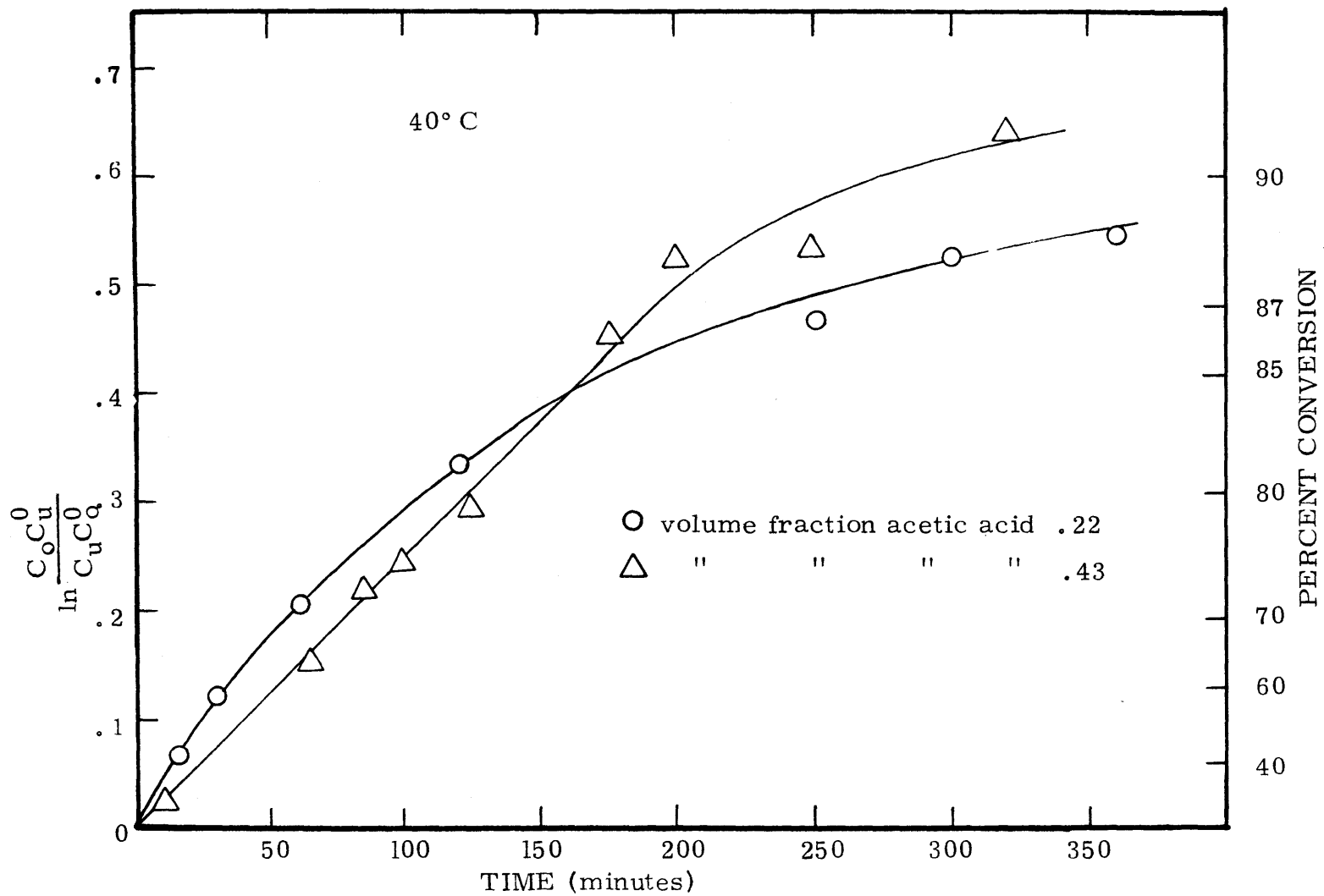
Figure V-4. Kinetics of epoxidation with peracetic acid in solution with varying amounts of acetic acid; 40°C.

constants (liters/mole-min) determined from the slopes were:

volume fraction acetic acid	k at 0% conversion	k at 88% conversion	$\dfrac{k_0}{k_{88}}$
.22	.170	.0055	31
.43	.108	.0058	19

Considering the difficulty in measureing the concentration of active oxygen at high extents of reaction (low concentrations of active oxygen), the ratio of the rates of reaction at high and low conversions (approximately equal to the ratio of reactivities of internal to external double bonds) is in good agreement with the literature value; i.e., 19 or 31 relative to 25 (section III-2a).

The slope of the curves at each point is proportional to the effective kinetic constant at that time. This effective kinetic constant is a complex function of the individual kinetic constants for 1,4 double bonds and 1,2 double bonds, and the relative amounts of each type of double bond. Changes in the slope of the curve, then, with time, reflect changes in the relative amounts of the reacting components. Thus, in the reaction curve for .22 volume fraction acetic acid, as the reaction proceeds the ratio of internal/external double bonds decreases continuously, as indicated by the monotonic decrease of the effective kinetic constant from the value of the kinetic constant of the reaction of internal (trans/cis) double bonds until that of the external (vinyl) double bonds. In the presence of a larger amount of acetic acid (volume fraction .43) the effective kinetic constant initially is lower (~35% lower) than that in

22 volume % acetic acid, but it decreases more slowly in the early stages
(less curvature), with the reaction curve intersecting the other one
near 85% conversion and then decreasing further to a 'final' value, al-
most identical with the one observed in the smaller amount of acetic
acid.

As was discussed in section III-2a, acetic acid decreases the rate
of olefin epoxidation by about 30 - 50% for a reactive olefin and less so
for nonreactive olefins. This is confirmed by these experiments: doub-
ling the amount of acetic acid (with commensurate decrease in chloroform
content) decreases the initial reactivity which is contributed to mainly
by the more reactive trans/cis double bonds. The reactivity of the
vinyl double bonds is also reduced but to a lesser extent. Hence, as the
vinyl double bonds contribute increasingly to the reaction rate, this
lesser effect of acetic acid on the vinyl double bonds appears as a slower
decrease in the effective kinetic constant. This continues until 85 - 90%
conversion, at which point the acetic acid can only affect the reactivity
of the remaining vinyl double bonds, an effect which cannot be determined
by this procedure, and the kinetic constants at 88% conversion appear
identical (within experimental error).

The kinetic constant for epoxidation of internal double bonds deter-
mined here is in reasonable agreement with that given by Meyer (1970)
($k \sim .3$ litres/mole·min), considering the difference in solvent system
(22 volume % acetic acid versus 4-5% acetic acid) and the fact that the
value determined here is an estimate of the true constant.

3. MODEL CONCENTRATION PROFILES

From the results to be described in the following three sections, a
model of the concentration profiles in surface reacted styrene-butadiene-
styrene block copolymers has been developed. The full model is presented
in this section to aid in the understanding of the contributions of each
of the experiments to the development of this picture of the diffusion/
reaction process in SBS copolymers.

The time history of the concentration profiles in a single film is
shown in Figure V-5 and the concentration profiles after a certain time
period in films of varying thickness is shown in Figure V-6. In both of
these figures, the concentration of reacted unsaturation $(1 - c_u/c_u^0)$ is
plotted versus the distance into the film. These profiles then show the
time course and qualitative shape of the reaction front--the front which
separates reacted, swelling material from unreacted, nonswellable material.

Initially the material is completely unreacted (Figure V-5a). After
the region near the surface has reacted the concentration profile of
reacted polymer appears as in Figure V-5b: very sharp boundary between
the swelling, reacted material and the unreacted material. The reaction
front has a slope inversely proportional to the effective diffusion/reac-
tion rate (Hartley, 1949, Hermans, 1947), which, in the initial stages of
the process, is relatively low because of the efficient transfer of swel-
ling stresses to the much larger unreacted core. The solubility and dif-
fusivity of peracetic acid are relatively low at this stage and thus dif-
fusion is slow. The sigmoidal shape of the curve is the direct result of
the limited number of reactive sites in the polymer. As reaction proceeds
further, the compression forces in the swelling reacted region behind the
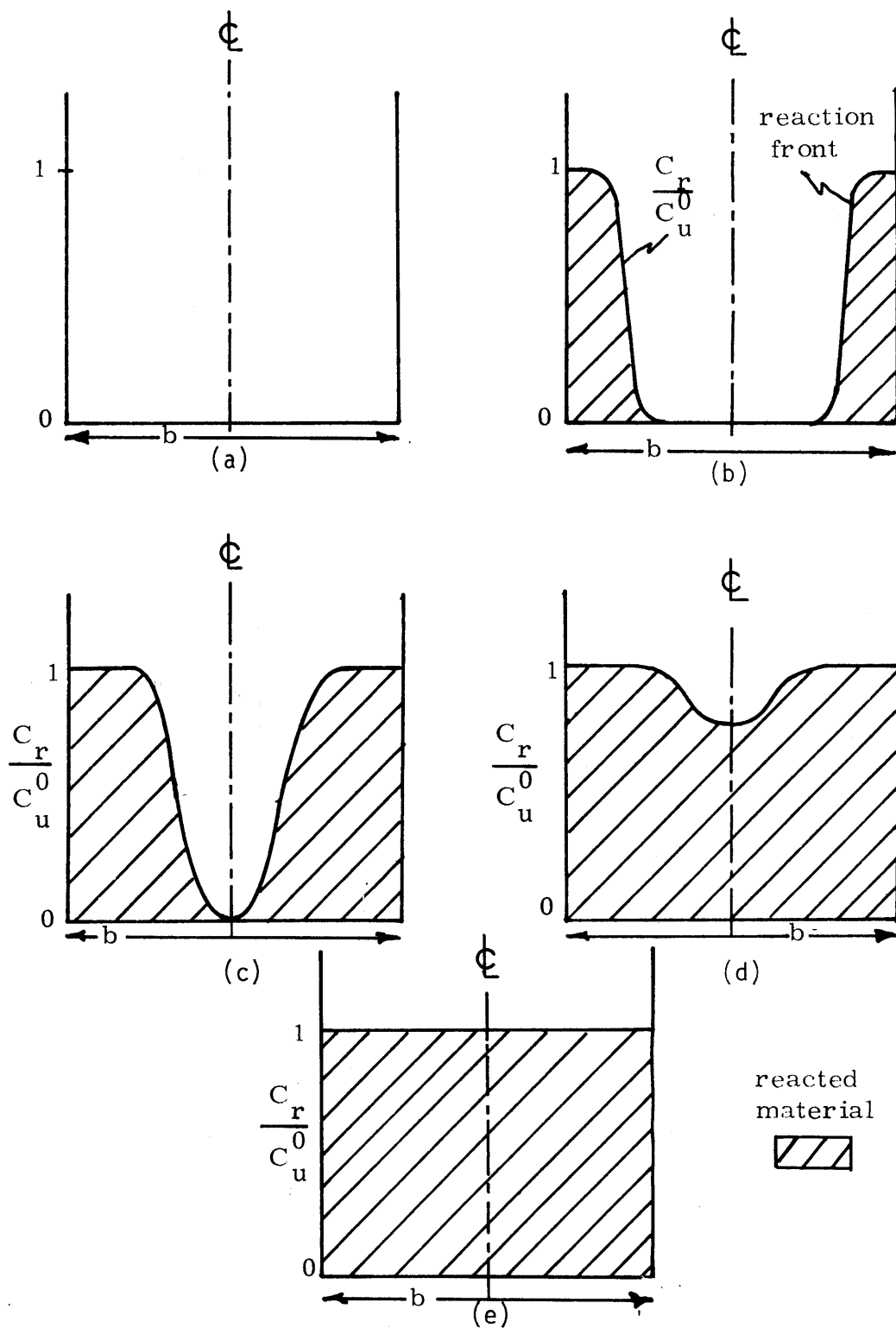
Figure V-5. Reaction fronts (model) for surface hydroxylation for various times of reaction (constant film thickness); (a) to (e), increasing time (C_r/C_u^0 = fractional conversion of double bonds).

front are relieved (the interior core is decreasing in size), the diffusion rate is increasing and the slope of the reaction front decreases (Figure V-5c). Eventually the two reaction fronts, proceeding from each side of the film, meet and overlap to get the near Fickian profile as in Figure V-5d. The stress transfer mechanisms are almost ineffective because of the partial reaction (partial swelling) in the central region. A delay in the diffusion of the swelling agent (slower diffusion rate than the coupled reaction - diffusion of peracetic acid) would make the transfer of stress effective despite the presence of reacted double bonds throughout the material. Finally, when all the double bonds have reacted, peracetic acid is able to diffuse completely through the material and the material can be considered to be a membrane, with a horizontal concentration profile. (A deviation in profile would result as the slower reacting vinyl double bonds react. This is not a strong effect and is ignored in Figures V-5 and V-6; C_u^0 should be redefined then to be the initial concentration of reactive double bonds).

Since, for a given film thickness, there is a time at which the reaction front has a definite shape, at a given time there should be a film, with certain thickness, in which the reaction front has the identical shape. Thus there is a correspondence between film thickness and time; this is shown in Figure V-6. It should be noticed that the depth of penetration decreases with increasing thickness at constant time. Because the overall diffusion rate is less in thicker films, due to stress transfer, the depth of penetration of the reaction front is less in the thicker films (d) than in the thinner films (c). Beyond a certain thickness (d), however, changes in the thickness do not have a strong effect
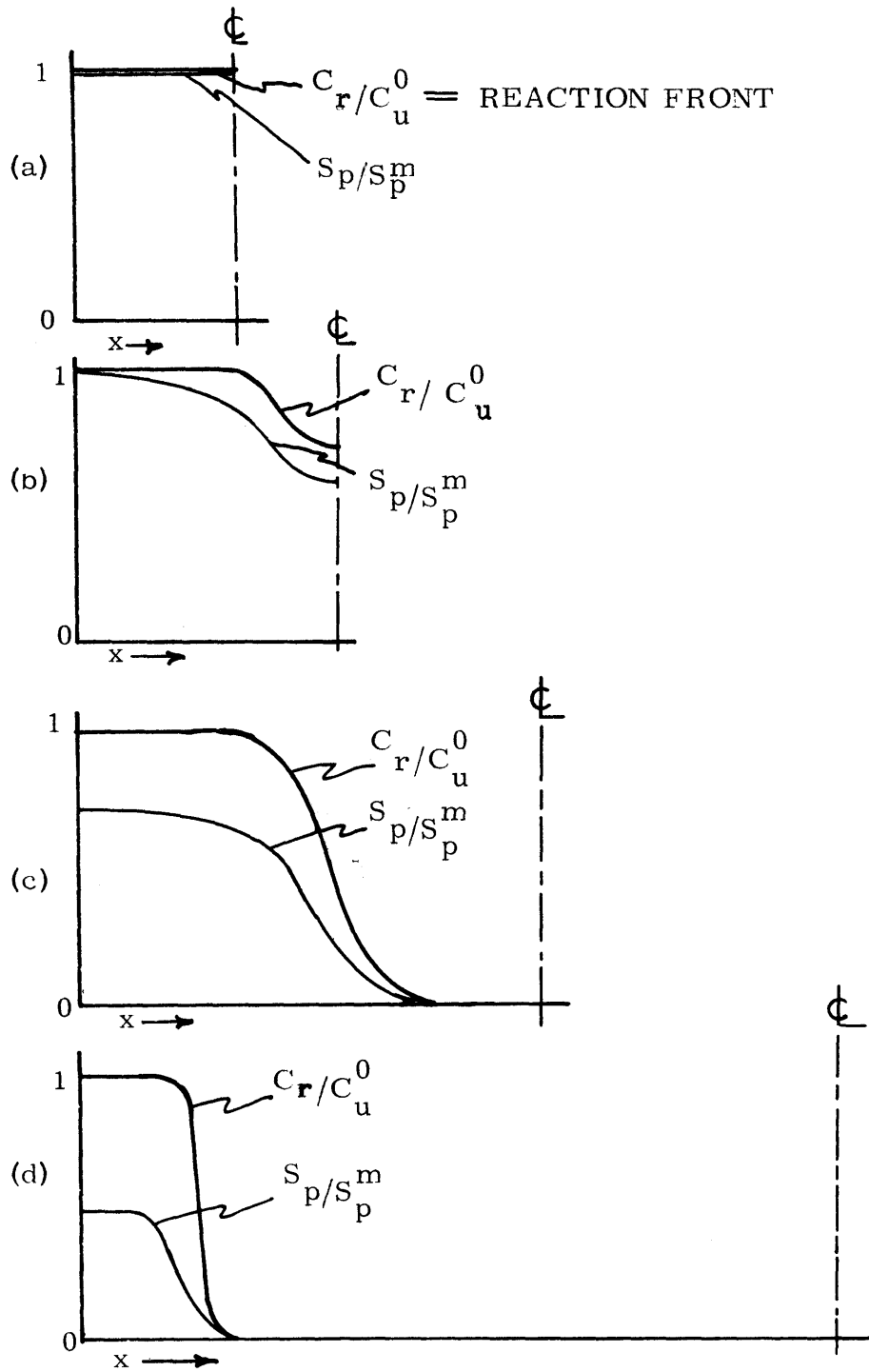
Figure V-6. Reaction fronts (model) for surface hydroxylation for various film thicknesses (constant time); (a) to (d) increasing film thickness (C_r/C_u^0 = fractional conversion of double bonds, S_p/S_p^m = reduced solubility).

on the degree of stress transfer and the depth of penetration and the shape of the reaction front are nearly constant with increasing thickness. While the actual magnitude of the effect depends on the polymer penetrant system, it is drawn in an exagerrated form in Figure V-6. From the figures, it is obvious the total moles of reacted material (i.e. area under the concentration profile curves - area concentration) decreases with increasing thickness in the range of thicknesses from (c) to (d).

The reduced solubility of peracetic acid S_p/S_p^m , where $S_p = C_p/a_p$ and S_p^m is the solubility of peracid in the fully swollen, stress-free, hydroxylated copolymer, is also shown in Figure V-6. The solubility increases with reaction and with swelling. Since swelling depends on the diffusion of acetic acid and water and is modified by stress transfer to the interior, the solubility will not necessarily follow exactly the curve of the reaction front. On the assumption of a slower moving swelling front, the solubility curve is shown to be behind the reaction front, but have a similar shape near the advancing tail (low concentration) of the front. Near the surface, however, due to the transfer of swelling stress to the interior, the solubility in the fully swollen zone (fully swollen in the presence of a compressive force) is less than that in the absence of stress. (Because of this assumption, the swelling agents (cleavage agents) concentration profiles match these solubility profiles.) The thicker the film, the greater the efficiency of stress transfer and the lower the value for S_p/S_p^m near the surface ((d) versus (c)). The diffusivity shows a nearly identical behaviour. In actual fact, the section will not be rectangular (the area of the film in Crank's

(1953) strain dependent diffusion model will not be constant; section III-4) and the solubility near the surface will show a slight curvature--convex towards the zero line.

In Figure V-7, the distribution of reacted-gel, reacted-sol and unreacted material, as found in the chloroform delamination experiments (section V-5) is shown. In the interior of the film, 100% of the polymer is soluble, unreacted material while near the surface, 100% of the material is cross-linked and forms a gel in chloroform. Intermediate between these two is the reacted, but still chloroform-soluble, material (fewer crosslinks/chain). Closer to the surface most of the reacted material forms a gel, but near the advancing tail of the reaction front, the epoxide group concentration is too low for crosslinking to be significant. The reacted material in this region does not form a gel in chloroform but also does not precipitate out in methanol and is separable from the fully unreacted fraction.

The concentration gradient, as interpreted from the IR data of section V-6, of each component in the surface hydroxylated SBS copolymer is shown in Figure V-8. Tetrahydrofuran ring structures, intermolecular ethers and carbonyls do not depend on the presence of a cleavage agent for their formation; they depend solely on the formation of epoxides via the action of diffusing peracetic acid on the polymer. Thus the profile of these groups matches the shape of the reaction front. The unreacted double bonds profile, obviously, has a form complementary to the reaction front. The formation of hydroxyls, however, depends on the presence of other molecules which also have to diffuse through the polymer and as assumed here, permeate more slowly than the peracetic acid. Hence, the
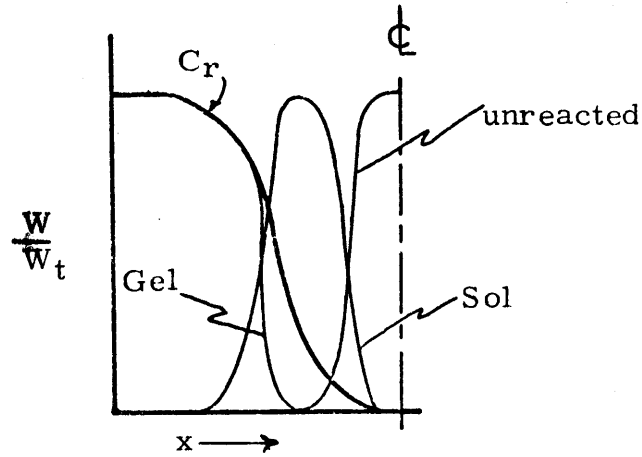
Figure V-7.   Distribution of delamination fractions in a typical film
              (C_r = reaction front).
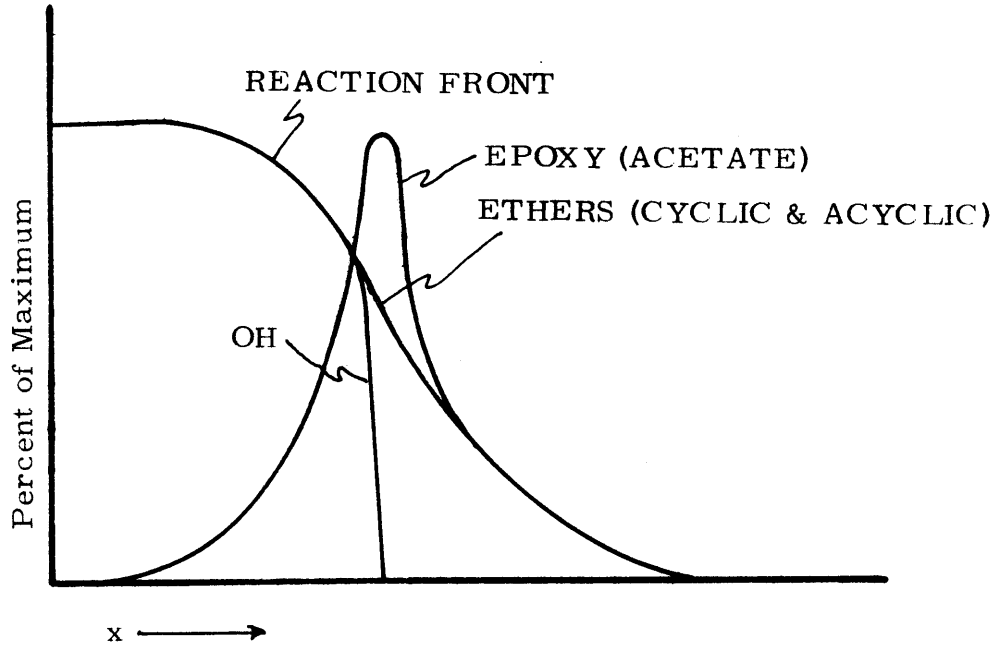
Figure V-8.   Typical concentration profiles of oxygen-containing
              functional groups.

hydroxyl concentration profile is a little steeper than the reaction front and is shifted to a position behind the front because of the additional diffusion limitation. The epoxy concentration profile reflects the competition between epoxidation and epoxide cleavage. Thus, near the advancing tail of the reaction front (deeper into the film), the epoxy concentration matches the front since the cleavage reagents do not penetrate this far. Near the surface, however, epoxide cleavage reduces the concentration of epoxy groups. As the concentration of these cleavage (swelling) agents decrease due to diffusional effects, the number of epoxide groups left uncleaved increases and then passes through a maximum as the epoxidation reaction front is met. A similar curve is expected for the profile of acetate groups, after base hydrolysis, although the absolute number of these groups should be less because of the attempt to allow the acetate hydrolysis to go to completion.

4. HYDROXYL CONTENT

(a) Interpretation of Results

The principal effort of the thesis was the evaluation of curves of

the extent of reaction, in terms of moles of hydroxyl groups per unit

area (area concentration), versus the film thickness before reaction

(Figures V-9, 12, 13, 14, 15). Through analysis of these curves the
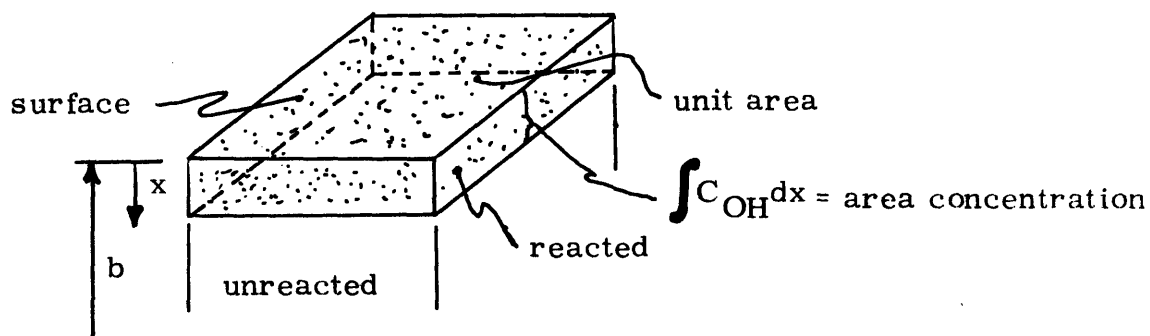
major parameters governing the diffusion/reaction process were investi-

gated. The *area concentration* is the area under the concentration pro-

file in the film and, for the hydroxyl group, is equal to $\int_0^b C_{OH}dx$, where

C_{OH} is the local concentration (at x) of hydroxyl groups in the film.

(a basic assumption is one-dimension uniform advance of the reaction

zone, well supported by evidence presented elsewhere-in contrast to

glassy, semicrystalline polymers which undergo crazing.) The experi-

mental procedure is discussed in section IV-2.

All the curves of hydroxyl content (area concentration) versus film

thickness were found to show the same behaviour as in Figure V-9: an

initial linear increase in hydroxyl content followed by a gradual decrease

Figure V-9. Area concentration, hydroxyl versus film thickness; 30°C, 180 min, 70% acetic acid. (thickness measured prior to reaction)

beyond a certain maximum value. The linear portion of the curve--AB--
defines the range of films over which the peracetic acid, under the given
experimental conditions, has diffused through the complete film, and
all potentially reactive double bonds are presumed to have reacted.

According to Traut (1973), the slope of this linear portion was
virtually independent of time and temperature (within experimental error).
The value of the average slope (using the data from all of the reaction
conditions used by Traut in his thesis) corresponds to a 24% conversion
of the double bonds to the glycol structure (two hydroxyls/double bond)
in the 70% acetic acid - 24% water bath. This low yield is the result
of side reactions: while some of the double bonds are unreactive due to
steric or electronic effects (e.g. vinyl groups) many of the double bonds
reacted to form intramolecular or intermolecular ethers (it will be re-
called that these become crosslinking points, converting the hydrophilic
reacted butadiene part of the triblock copolymer to a true three dimen-
sional network), as confirmed by the qualitative (section V-2a) and
quantitative (section V-6) analysis of the complete infrared spectrum.

Detailed examination of the data of Traut (1973) confirmed the
time independence but the conversion increased from a low of 17% at 30°C
to a high of 26% at 45°C. However, considering the difficulty in deter-
mining the slope, the differences in conversion are not particularly
significant. In 71% acetic acid at 40°C, the slope corresponds to a
slightly higher conversion: 28 - 34% depending on how the initial line
is drawn. These differences (if significant) result from the small
effect of temperature or solvent composition on swelling in these fully
reacted material. While a more complete explanation of these effects

are given in section V-6, the relationship is summarized here: with
increasing temperature or acetic acid content in the reaction bath
the equilibrium degree of swelling of the reacted polymer in the
reaction medium is larger (acetic acid is a better 'solvent' for the
reacted polymer than water). This increase in equilibrium swelling
affects the approach to equilibrium so that, at a given time, the
degree of swelling under these 'stronger' conditions is higher than
at lower temperatures, or with less acetic acid. With this higher
degree of swelling throughout the reaction process, crosslinking is
rendered less favourable (from volume considerations alone), and a
higher degree of hydroxylation is obtained, even though at the end of
the process, peracetic acid permeates completely through the film under
both sets of conditions. The results described in section V-6 show
changes in the number of crosslinks of a similar order. Since the
hydroxyl area concentrations of thicker films yield more information on
the reaction/diffusion process than thinner films, the experiments de-
scribed here were performed mainly on thicker films.

The maximum at C in Figure V-9 and the subsequent decrease was not
initially expected. In a simple sorption experiment for a given set of
experimental conditions, there is a particular film thickness at which
the weight gain per unit area would become independent of film thickness;
this film thickness being the depth of penetration of the permeant (Crank,
1956). In larger films, the polymer beyond this depth of penetration
would have no effect on the amount of permeant being absorbed. To under-
stand the anomalous behaviour in our system, the total oxygen content
(moles/cm^2) of some of our samples was determined (Figure V-10). To the
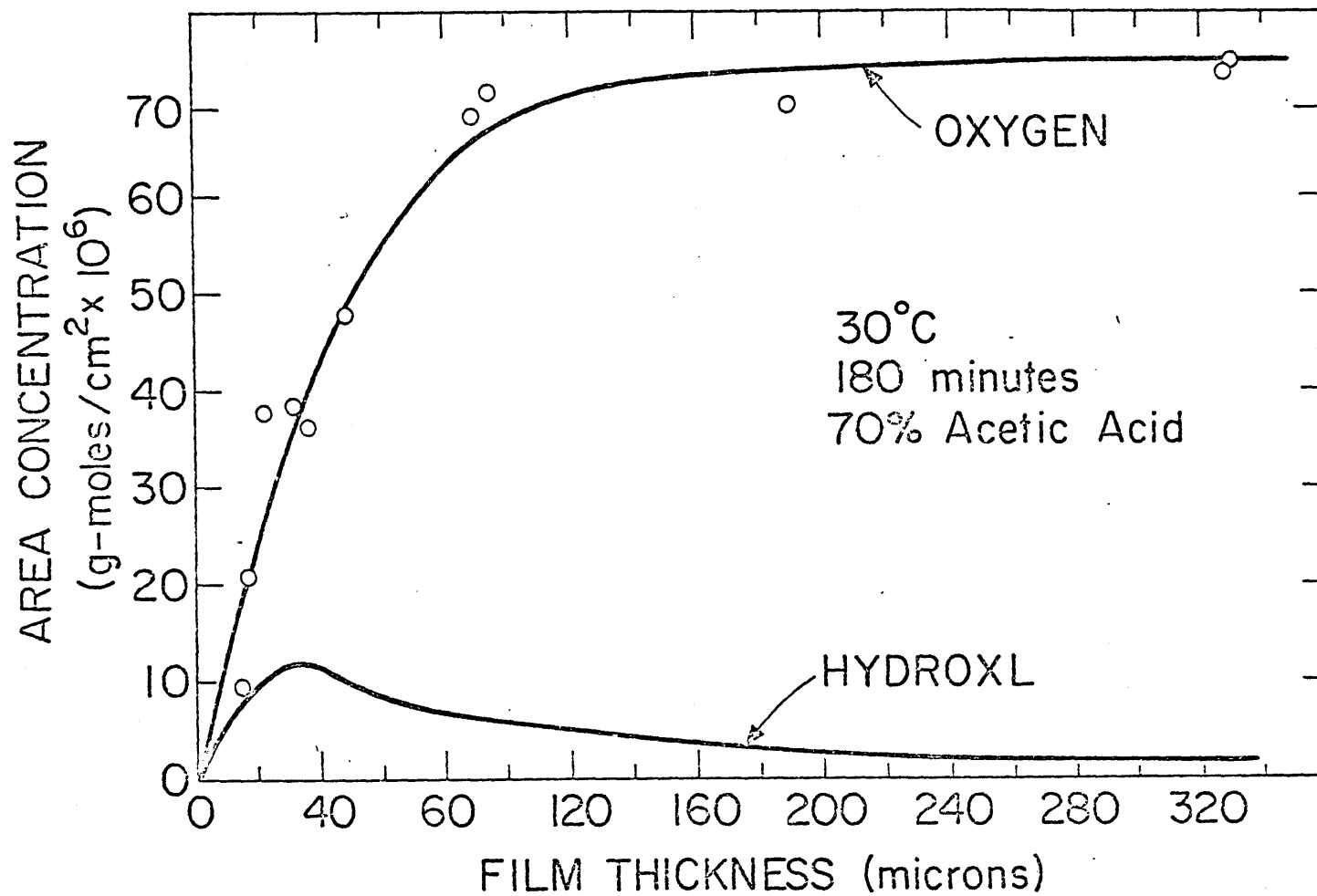
Figure V-10. Area concentration, oxygen versus film thickness; 30°C, 180 min, 70% acetic acid (with A_c^{OH} for comparison).

extent that the assumption of a constant stoichiometric ratio (constant moles oxygen to moles double bond reacted) is valid, the total oxygen content reflects the number of double bonds reacted. This curve, as expected, asymptotically approaches a much higher level and at a film thickness greater than that at point C. Thus it appears that the peracetic acid diffuses in a normal manner through the films but a change in product distribution occurs in the thicker films; i.e., a larger fraction in thinner films than in thicker ones of oxygen containing functional groups as hydroxyls and a commeasurately larger fraction in thicker films as some other oxygen containing group. From the results to be discussed in section V-6 (see Figures V-27, 28) this other species is the uncleaved epoxy ring, $-C\overset{\displaystyle O}{\diagup\!\!\diagdown}C-$ (In addition, these same results render the assumption made above of a constant stoichiometric ratio incorrect and the true values of moles of reacted material would show a decrease with increasing thickness attributable to the effect of the stress transfer process on the overall epoxidation rate.)

According to this reasoning, by addition of oxygen to the polymer, the polymer is converted from a hydrophobic to a hydrophilic material; the reacted surface region of the polymer therefore, swells in the acetic acid-water reaction bath. However, this swelling behaviour is modified by the presence of the unreacted core (Figures V-5, V-11), since the swelling stresses near the surface are transferred by the elastic network to the higher modulus unreacted portion of the polymer; the degree of stress transfer is dependent on the ratio of the size of the surface region to that of the total material (as in Crank's model for strain-dependent diffusion (1953), section III-4a). Hence, the surface
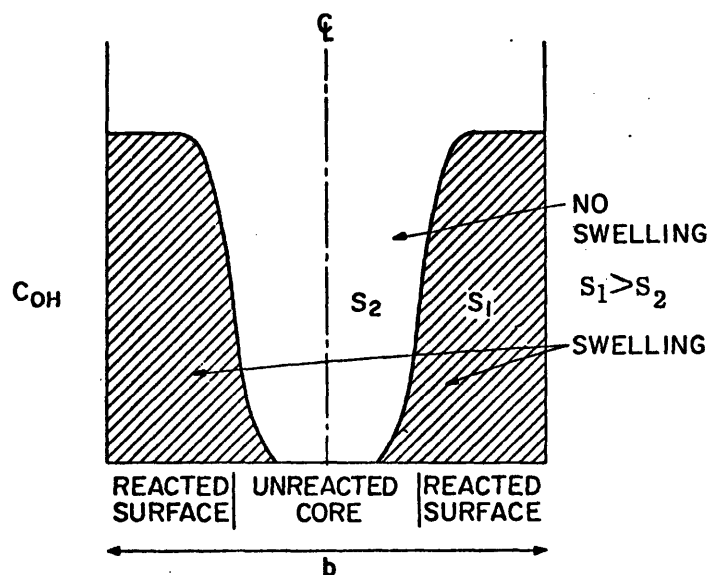
Figure V-11. Reacted film model.

region of the thinner films swells more than that of the thicker films, enabling the epoxide cleavage agents (acetic acid, water, and sulphuric acid) to diffuse more effectively into the thinner films (higher D, S along the epoxidation reaction front, see last section). As a result, cleavage of the epoxy rings is more nearly complete in thinner films, yielding higher hydroxyl contents in these thinner films than in the thicker ones, where cleavage is not as complete. The quantitative confirmation of this is reported in section V-6.

Curves of area concentration versus film thickness of a similar shape were obtained for a number of other conditions (Figures V-12, 13, 14, 15). Figures V-12, 13, 14 show the results for reactions carried out at 35.1°C, 40°C, and 45.1°C, respectively in a reaction bath containing 71% acetic acid and 23% water (note the differences in the ordinate scale). Figure V-15 shows the observed area concentration/film thickness for surface hydroxylations at 40°C, but in 92.5% acetic acid and 1.4% water. The initial line in Figure V-14 represents the best fit
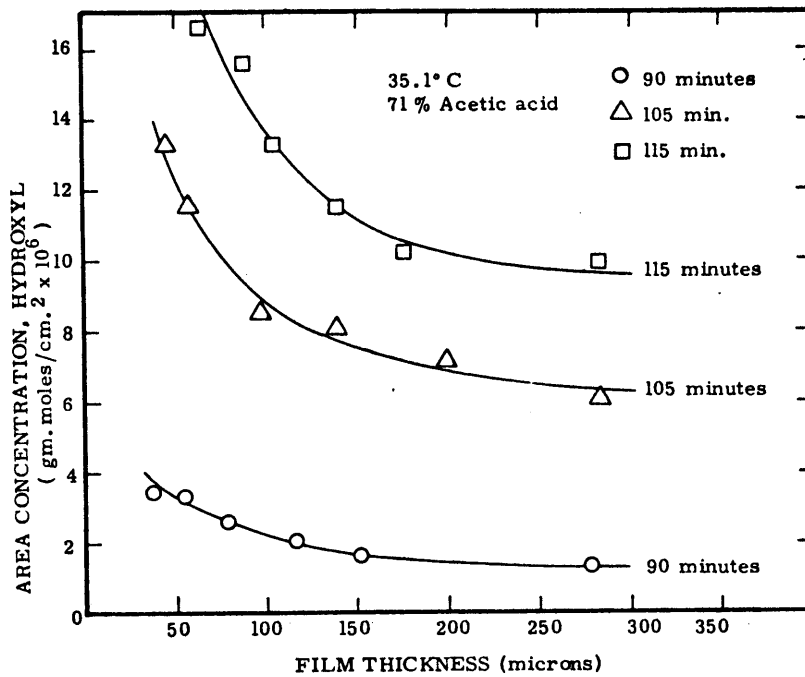
Figure V-12. Area concentration, hydroxyl versus film thickness prior to reaction; 35.1°C, 71% acetic acid.

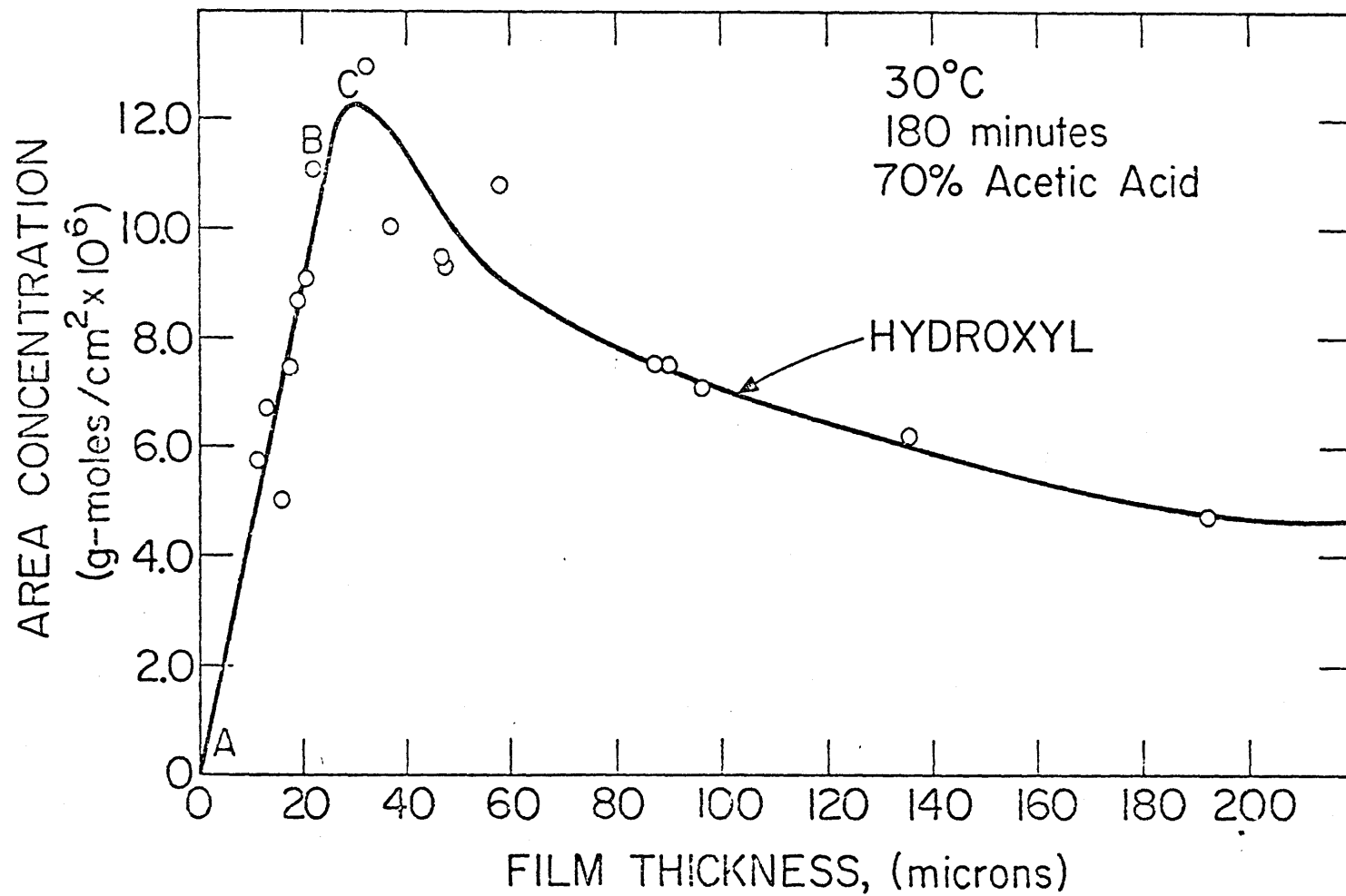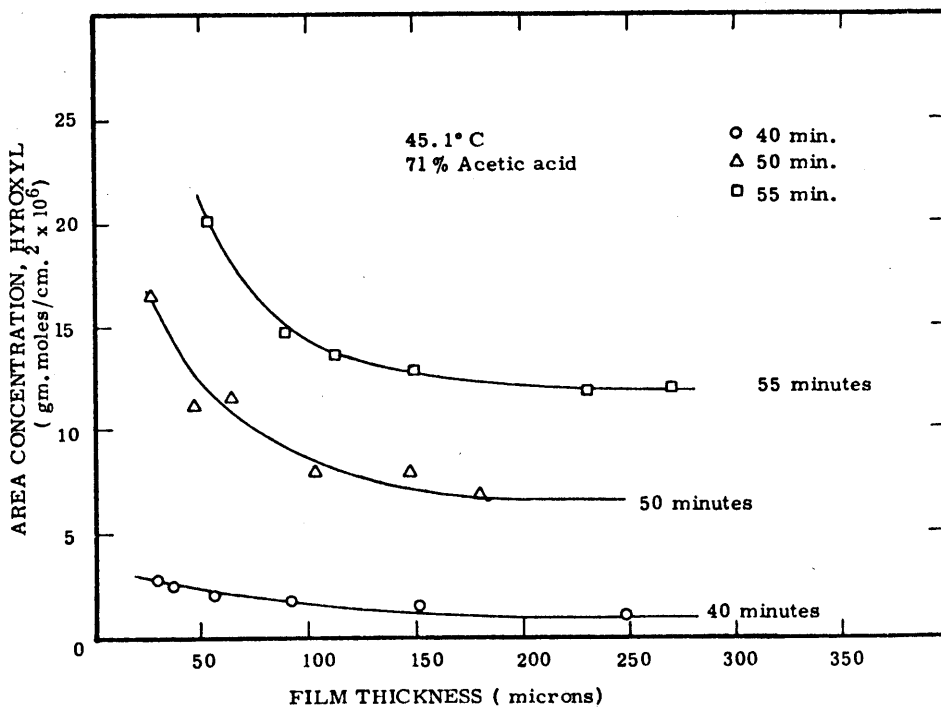Figure V-13. Area concentration, hydroxyl versus film thickness prior to reaction, 45.1°C, 71% acetic acid.
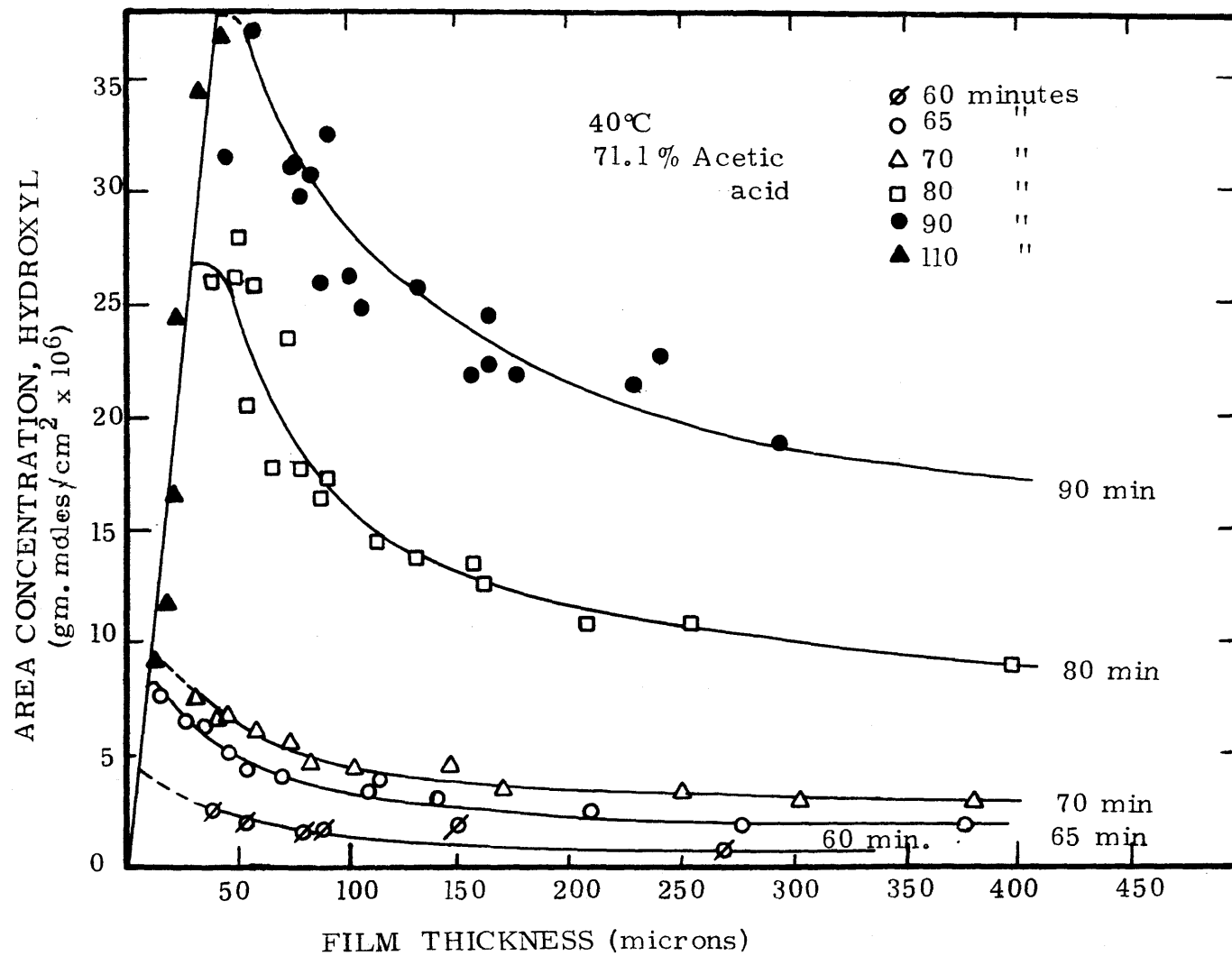
Figure V-14. Area concentration, hydroxyl versus film thickness; 40°C, 71% acetic acid.

(thickness measured prior to reaction)
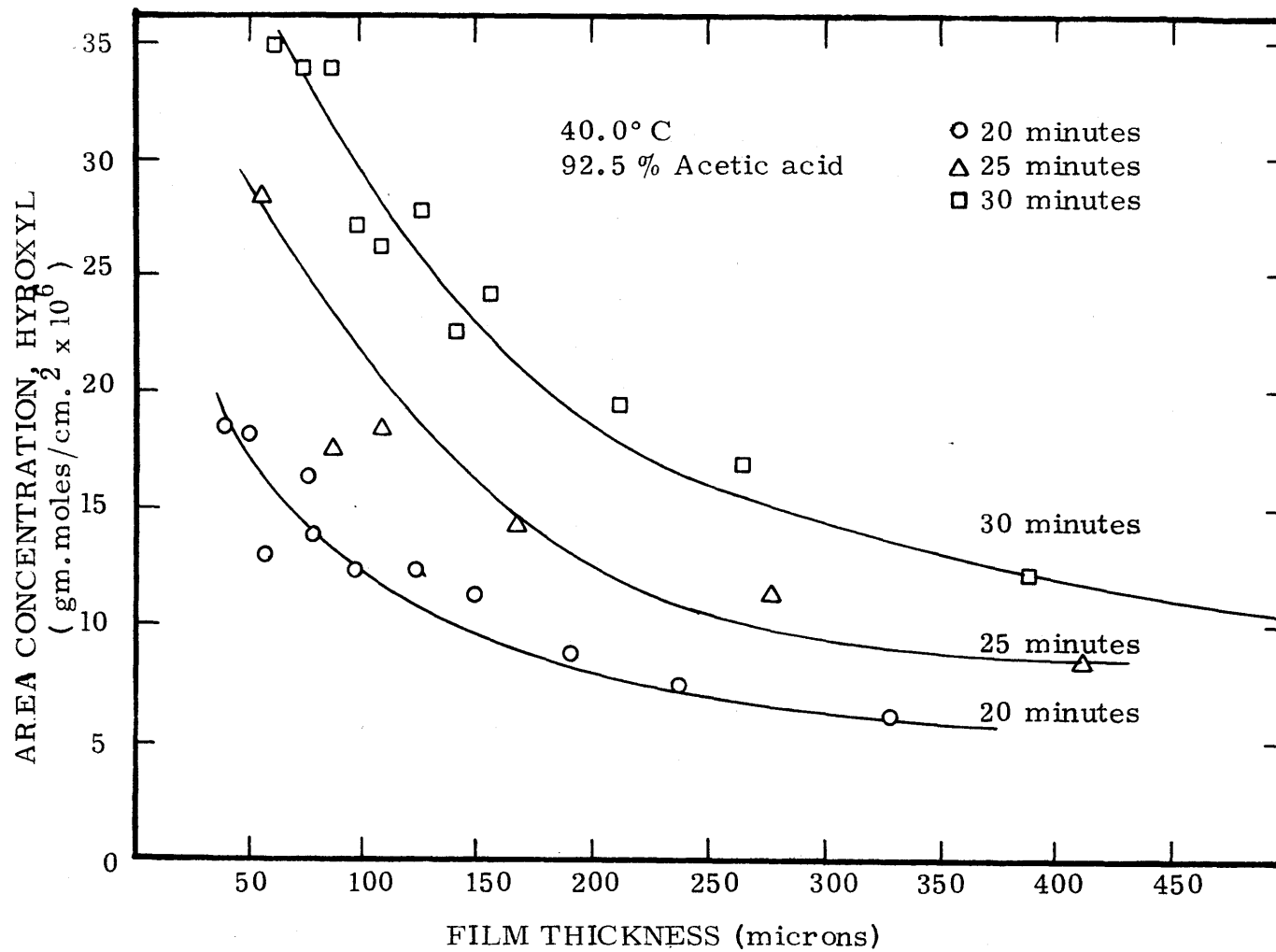
Figure V-15. Area concentration, hydroxyl versus film thickness prior to reaction; 40°C, 92.5% acetic acid.

to the values of area concentration for fully reacted films reacted for 110 minutes at 40°C, 71% acetic acid in a separate run to determine solely the position of this line. The slope of this line was discussed earlier.

In all of these cases, log - log plots of concentration versus film thickness yielded straight lines, the slopes of which are presented in Table V-1:

Table V-1: Slopes of log - log plots of A_c^{OH} versus film thickness, b

| 71% acetic acid | | | | 92.5% acetic acid |
35.1°C	40°C	45°C		40°C
90 min -.509	60 min -.419	40 min -.388		20 min -.492
	65 " -.476			
105 " -.397	70 " -.381	50 " -.422		25 " -.549
	80 " -.522			
115 " -.382	90 " -.357	55 " -.308		30 " -.571
AVERAGE -.429	-.431	-.379		-.537

Thus, the area concentration of hydroxyl groups A_c^{OH}, beyond a certain maximum value, can be empirically related to film thickness through a relationship of the form:

$$A_c^{OH} = K_1(t)b^{K_2} \qquad\qquad (V-1)$$

K_1 is a measure of the time course of the reaction and is further discussed below.

From the values of the slopes (K_2) tabulated in Table V-1, it is apparent that there is no correlation between K_2 and time at a given temperature, and that for reactions in 71% acetic acid, there is no correlation between the average value of K_2 and the temperature. However there is a definite increase in the absolute value of K_2 in going from reactions in 71% acetic acid to 92.5% acetic acid. The value of K_2 is interpreted as a measure of the transfer of stress from the swelling surface to the unreacted core. A larger absolute value for K_2 (as for the 92.5% acetic case) is interpreted to mean that the stress transfer mechanism reaches its maximum effectiveness at a larger b; i.e., it ceases to further affect the solubility or diffusivity at a larger thickness, than if the absolute value of K_2 were lower. Then K_2 should depend on the swelling ratio.

The absence of correlation between K_2 and time or temperature, demonstrates the small effect that these parameters have on the swelling process and on the stress transfer mechanism, while the addition of acetic acid, a better solvent for the reacted polymer, has a strong effect on the effectiveness of the stress transfer mechanism. This is consistant with the force balance equation of Crank's (1953) model for strain dependent diffusion, Equation III-13, through which, as is shown in Figure III-12, an increase in swelling ratio (A_m/A_0) causes the compressed area of the swelling zone to become its smallest at a larger value of $\frac{b}{2\lambda}$; i.e., at a larger thickness. Hence, an increase in swelling ratio, results in the stress transfer mechanism reaching its maximum effectiveness in a thicker film. Since time does not affect the equilibrium stress-free swelling ratio, A_m/A_0, and the temperature coefficient of swelling is

small, it is not surprising that there is no correlation between these parameters and K_2. Similarly, the increase in the absolute value of K_2 observed in 92.5% acetic acid is consistant with the increase in the swelling ratio extending the range before maximum effectiveness of the stress transfer mechanism occurs.

In Figure V-16a, the time course of surface hydroxylation is shown more clearly by plotting area concentration of hydroxyl groups versus time, for a number of film thicknesses for reactions at 40°C, and 71% acetic acid. The exponential nature of the process is more apparent in this figure than in Figure V-14. In fact, semi-log plots of A_c^{OH} versus time, at constant thicknesses, for all reaction conditions yield straight lines (Figure V-16b). The slopes of these lines can be considered effective kinetic constants, being measures of the rate of the reaction. These slopes are related to $K_1(t)$ of Equation V-1, and are termed here the effective kinetic constant K_1' ($K_1' = e^{K_1 t}$). The values are tabulated below in Table V-2:

Table V-2: Slopes of $\ln A_c^{OH}$ versus time, $(min)^{-1}$

b	71.1% acetic acid			92.5% acetic acid
	35.1°C	40°C	45.1°C	40°C
60μ	.0714	.0891	.1461	.0918
300μ	.0818	.0948	.1513	.0762
AVERAGE:	.0766	.0920	.1487	.0840

Plots of area concentration versus time did not yield straight lines. To the extent that the area concentration of 300 micron films is linearly
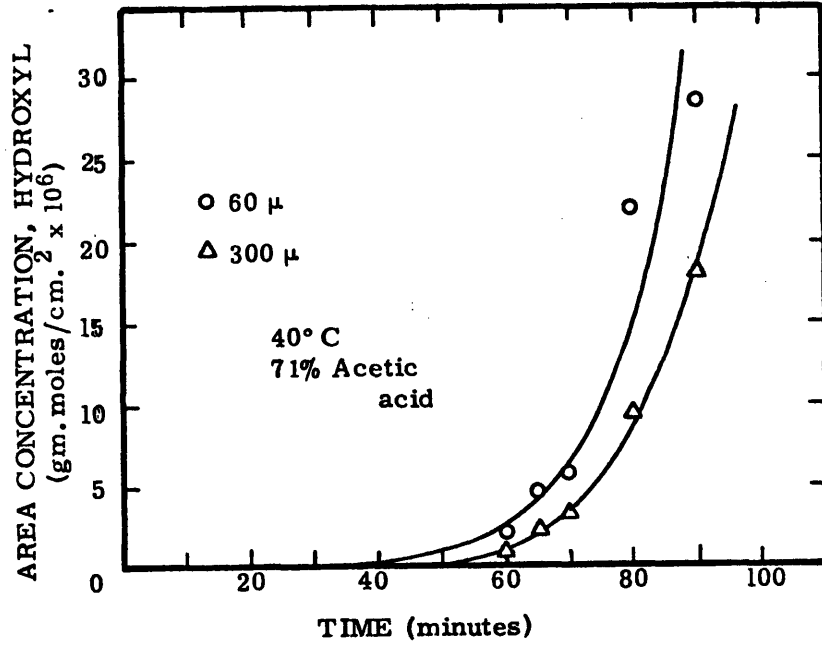
(a) Area concentration, hydroxyl versus time
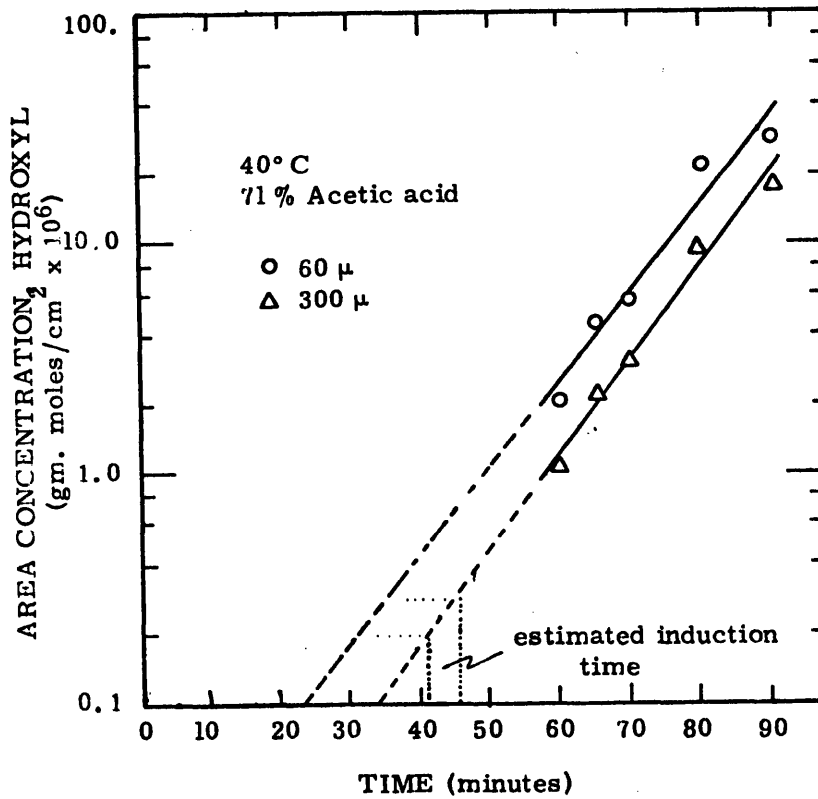
(b) Semi-log plot of A_c^{OH} vs time.

Figure V-16. Time course of surface hydroxylation.

proportional to the depth of penetration, these curves would yield straight lines if the process were controlled by simple swelling and/or by a second order reaction as was found by Hartley (1949) or Hermans (1947) for such processes (see section III-4b).

Since the deviations between K_1' for 60 microns and 300 microns merely represent the difference in values of K_2 (slopes of log A_c^{OH} versus log b) for the various times (60 microns and 300 microns were the ends of the log - log plots) and since there was no observed correlation between K_2 and time, these differences in K_1' are considered random errors, and hence, only the average of the two K_1' is considered significant. An Arrhenius plot of ln K_1' versus 1/T, yielded a straight line (within experimental error) with slope corresponding to an Arrhenius activation energy of 13 kcal/mole. For comparison the activation energy of the epoxidation reaction in solution is 12 kcal/mole (Meyer, 1970). The good agreement between the two values of activation energy is interpreted to show that the major effect of temperature is on the kinetic constants governing epoxidation (and cleavage) with but a very small effect on diffusion (and swelling). This is consistent with the earlier discussion in regards to the minimal temperature dependence of swelling as reflected in the absence of a correlation of K_2 with temperature.

The exponential nature of the reaction process also aids in explaining the apparent induction time observed by Traut (1973) and, most effectively, observed here in the reaction at 40°C, in the 71% acetic acid. A reaction conducted under these conditions with thicker films for only 50 minutes showed virtually no sign of reaction in the infrared spectrum, but some 15 minutes later displayed significant evidence of the formation

of hydroxyl groups (Figure V-14). Since the minimum OH absorbance distinguishable in the spectrum at 3430 cm^{-1} is equivalent to an extent of reaction of 0.2 - 0.3 moles hydroxyl/cm^2 or, in other terms, a depth of penetration of approximately 0.2 to 0.3 microns, the depth of penetration at 50 minutes is on the order of 0.2 - 0.3 microns, but increases to a depth on the order of 20-25 microns, a hundred-fold increase, in just 15 minutes. This apparent induction time is directly related to the exponential nature of the process as is seen from the time intercepts at extents of reaction of 0.2 - 0.3 moles/cm^2, in the extrapolated semilog plots of A_c^{OH} versus time (Figure V-16b). These values for the predicted induction time (71% acetic acid only) for a film 300 microns thick are:

35.1°C	66 - 72 minutes
40 °C	41 - 46 "
45.1 °C	18 - 22 "

Although the observed induction time for reactions at 40°C is a little higher than the range predicted from the extent of reaction at longer times, the agreement is still quite good.

The semi-log plot for the runs in 92.5% acetic acid extrapolated back to give a negative time. Combined with the lower value for K_1' in the higher acetic acid content reactions than in 71% acetic acid at 40°C, it is assumed that the slope (the value of K_1') of the semi-log plot is in error due to the imprecision in determining the true time of reaction for a reaction of only twenty minutes duration. This is discussed further in the second part of this section.

Although Lebedev (1965) has suggested that an exponential increase in extent of reaction with time cannot be used, by itself, to differentiate between reaction and diffusion control in reactions in polymers, all the available evidence suggests (section V-4, 5, 6) that this exponential process (and the consequent induction time) is the direct result of stress transfer modified swelling, occurring simultaneously with reaction. As the surface region swells, the solubility of the peracetic acid in the polymer increases and the driving force for diffusion is increased commensurately. Hence, the diffusion rate increases with a subsequent increase in the penetration depth and the degree of swelling near the surface (due to relief of part of the compressive stress which limits swelling) which further increases the peracetic acid solubility, diffusion rate and depth of penetration, etc.

This is verified in part by comparison of the extents of reaction in 71% acetic acid and 92.5% acetic acid. Acetic acid, being a better swelling agent for the reacted polymer, should lower the length of the induction time, since the same solubility should be attained at an earlier time. While the actual induction time for the reactions in 92.5% acetic acid is unavailable, Figure V-17 confirmed the expected behaviour: the extent of reaction is greater after only twenty minutes in 92.5% acetic acid than after sixty-five minutes in 71% acetic acid. (The comparison may be between a reaction time of 25 minutes if correction is made for the apparent error in the twenty minute run (section V-4b); this does not affect the conclusion.
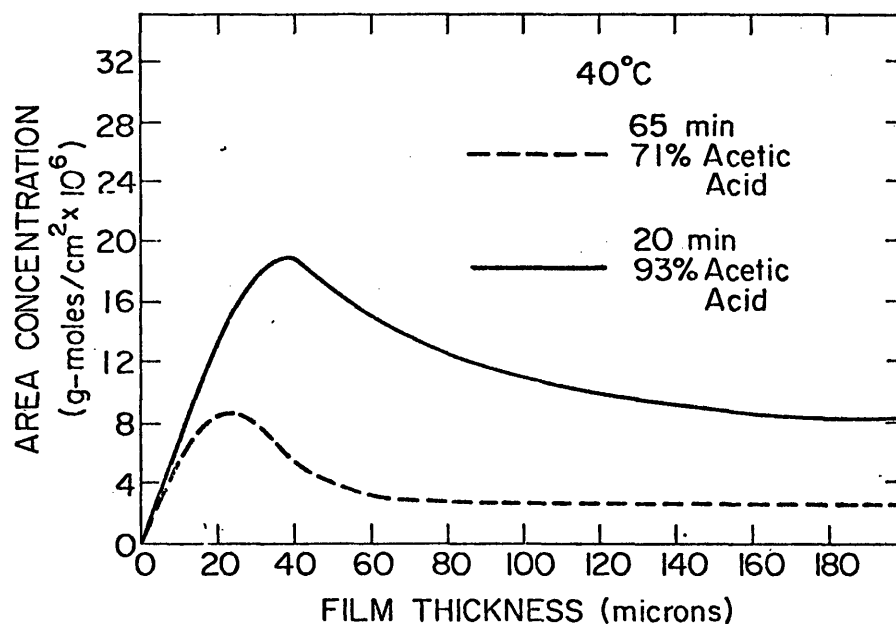
Figure V-17.   Comparison of area concentration, hydroxyl in
71% and 93% acetic acid.

Hydroxylation is the result of two processes, epoxidation and cleavage, both of which are affected, although in different ways, by the occurence of swelling in the surface region and by the modification of this swelling by transfer of stress to the interior unreacted core. Therefore the simple parameters used to interpret the area concentration thickness/time data are, in fact, complex variables of the relevant diffusivities, solubilities and kinetic constants. In order to gain a better understanding of these processes and in order to determine the actual depth of penetration, the delamination experiments and quantitative spectroscopic measurements to be discussed in sections V-5 and V-6 were performed.

A similar autoaccelerative behaviour is noted in the data of Burgess (1953) for the photo-oxidation of polyethylene (Figure V-18a) and the

data of Winslow, et al., (1969) for the weathering of polyethylene
(Figure V-18b). Burgess's observation of an exponential increase
of hydroxyl groups with time and of an apparent induction time in a
polymer/penetrant system in which the penetrant (oxygen) reacts with
the polymer and converts it from a hydrophobic to a hydrophilic mater-
ial has obvious parallels to the surface hydroxylation of SBS copolymer.
The determination of Winslow et al., (1969), of the anomalous effect
of film thickness on the photodegradation of polyethylene (an increase
in film thickness resulting in a decrease in reaction) is identical
to our observation of the effect of film thickness on hydroxylation.
Instead of Winslow's (1969) postulate of different reaction mechanisms
near the surface and in the bulk for photo-oxidation of polyethylene,
the effect of diffusion and swelling (by ambient water vapor) near the
surface can account for both Winslow's and Burgess's data. The com-
bined reaction/diffusion process as modified by stress transfer would
be nearly identical to that used here to explain very similar results.

(b) Reproducibility

It is obvious from Figure V-14 (or from the other figures) that the
scatter of points about the best fitting curve is much greater in the
curve defining the extent of reaction at 90 minutes than at 70 minutes.
This scatter is the result of a run-to-tun variation which becomes evi-
dent at a sufficiently high extent of reaction. Since a run-to-run dis-
tinction in the data was not made in Figures V-14, the area concentra-
tions of most of the films reacted at 40°C, for 90 minutes in 71% acetic
acid are replotted in Figure V-19 to show these variations. From Fig-
ure V-19 it is obvious that the curve of each run has a form similar
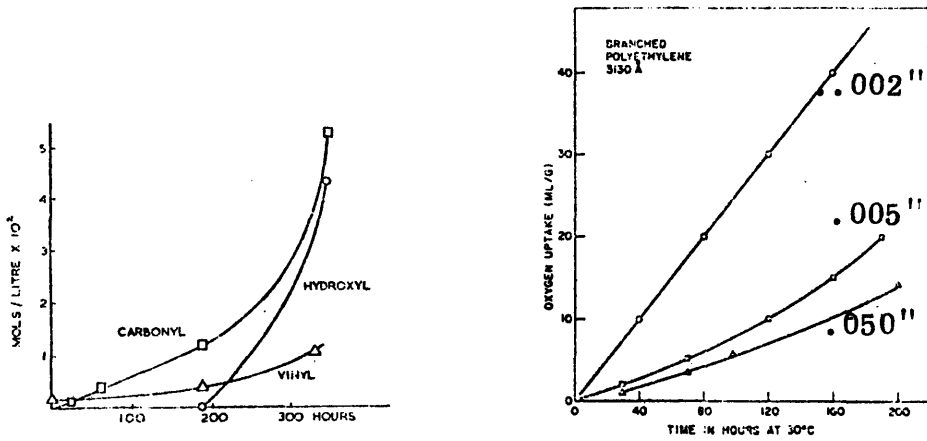
(a) Increase of products of
    oxidation with time
    (Burgess, 1953)

(b) Effect of film thickness
    (Winslow, et al., 1969)

Figure V-18. Photooxidation of polyethylene
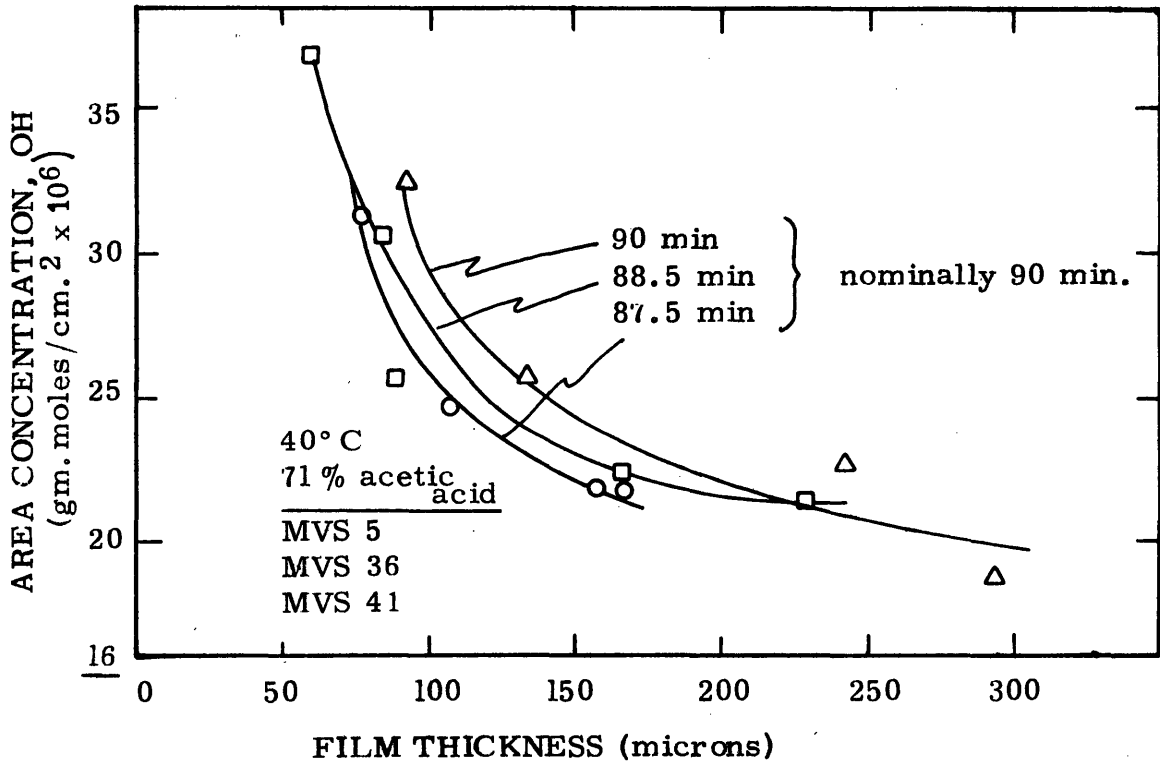
Figure V-19. Run-to-run variation in area concentration, hydroxyl;
              40°C, 90 min, 71% acetic acid

              (Note: only portion of ordinate scale shown)

to the composite curve of Figure V-14, but shifted slightly along a vertical axis. (The slight variations in shape reflect the presence of other errors--see below.) These vertical shifts are shifts in the time scale and using the semi-log plot of area concentration versus time, a 'true' reaction time can be estimated for each run. These are noted on Figure V-19 and are in the range of 90 ±3 minutes. (In fact, the predicted times are all lower than the measured time.)

This run-to-run variation is caused by the already noted (section IV-2x) difficulty in controlling the time of vigourous stirring (no resistance to mass transfer in bulk fluid) to better than ±3 minutes. This is approximately the time required to reassemble the stirring assembly and the reaction flask at the begining of the experiment and to disassemble it at the end. For the reactions at lower extents of reaction, this error is not important, but because of the 'auto-accelerative' (exponential) nature of the reaction/diffusion process, at higher extents of reaction this inaccuracy in the true time of reaction becomes more important and causes a greater scatter of results. The correspondence of this estimated error in controlling the time and the time-shifts between runs for 90 minutes reaction confirms this interpretation.

Additional sample-to-sample variations in the data occur primarily because of the inaccuracies in the optical measurements of film thickness (±5 microns generally). In the high thickness region, these deviations are not important because of the very low curvature of the plots at high thickness. The sharp curvature in the thinner film region gives this ±5% error more weight in producing observable sample-to-sample deviations. The error in measuring the absorbance is only ±1%; the error in the absorp-

tivity is not significant as long as the absorptivity is not a function
of the absorbance concentration (see section V-6). The uncertainty in
a constant absorptivity only changes the value of the ordinate; the
relative values are unaffected.

A phenomenon relevant to the ageing of these materials was also
observed in curves of area concentration versus film thickness. The
spectrum between 3800 - 3000 cm^{-1} was recorded a second time for a
number of samples two to three months after the first spectrum was re-
corded. In many of these (generally the thinner films, with the higher
extents of reaction), the measured area concentration of hydroxyl groups
had increased over the two to three months period. This increase oc-
curred in films stored in the dark, both in vacuum and in air. The pos-
sible sources of this error are: 1) variations within the sample,
2) ageing of the sample or 3) reaggregation of hydrogen bonds. The
first is unlikely because these random variations within the sample would
appear in all of the plots of area concentration versus time as a random
scatter of the data. This was not observed. Ageing of the sample, which
results in an increase in the true moles of hydroxyl is, however, quite
unlikely. The possible known mechanisms could be cleavage of residual
epoxy rings or the hydrolysis of remaining acetate. The possibility of a
specific reaction with potassium hydroxide was rendered unlikely by the
qualitative evaluation of the emission spectra showing the absence of po-
tassium in the samples which demonstrated this increase in hydroxyl con-
tent. The absence of potassium hydroxide also makes the occurrence of
a base catalysed reaction unlikely. Since the samples which displayed
this increase in hydroxyl content were subject to hydrolysis using the

conditions of Traut (1973), which were found to result in incomplete hydrolysis of the ester, it is believed that the increase in hydroxyl content is the result of a slow uncatalysed hydrolysis of the ester which had been hydrolysed before the first spectra were run. The water of hydrolysis would be the ambient water vapour in the case of the films stored in the air or be unreleased water in the case of the films stored in vacuum. Epoxy cleavage by the same water is conceivable, but the un-catalysed epoxy cleavage would be even slower than uncatalysed ester hydrolysis. The possibility of free radical oxidative reactions is dis-cussed further in section V-7, although these cannot account for the in-crease in hydroxyl content observed in the films stored in the dark in vacuum.

The possibility of a slow reaggregation of the hydrogen bonds between already existing hydroxyl groups resulting in a sharper OH stretching bond with a slightly different average absorptivity (as discussed in section V-2a) would also account for the observed increase in hydroxyl con-tent.

5. DELAMINATION

The discovery of a crosslinking reaction occurring concurrently with hydroxylation, made it feasible to delaminate samples of reacted SBS copolymer by swelling in chloroform.

gel → ... chloroform solution of reacted sol and unreacted fractions
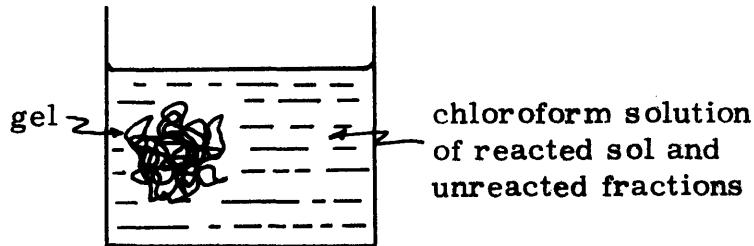
Three fractions were recovered: crosslinked gel (insoluble in chloroform), unreacted polymer (soluble in chloroform, insoluble in methanol) and reacted sol (soluble in chloroform and chloroform/methanol mixtures). Only a crude fractional precipitation was used to separate the chloroform soluble fractions. Little control was made of the volume of methanol added to precipitate the chloroform soluble polymer and therefore the composition limit defining the (solubility) difference between the two fractions was not sharp. There is thus a significant amount of scatter in the sizes of these two fractions. (In hindsight, this could have been executed more carefully; the conclusions would not be much affected.) The sizes of all of the fractions was determined by weighing to the nearest microgram.

Infrared spectra were recorded of two composite samples, one containing the gel fractions and one of the sol fractions, from four individual films. These spectra showed the difference in the

average composition of these fractions. Qualitative inspection of
the spectra showed the expected composition: the gel fraction had
a higher proportion of ether crosslinks than the sol fraction,
which, in turn, had a higher proportion of unreacted double bonds
than the gel fraction. Quantitative results according to the scheme
described in sections III-3 and IV-4 are:

	Gel Fraction*	Sol Fraction*
hydroxyl	73 %	20
epoxy	11	7
tetrahydrofuran	14	3
acyclic ether	20	4

*results reported as a percentage of unsaturation originally
present in polymer; sum is not necessarily 100%.

As part of the delamination procedure the total weights before
delamination of the reacted films were determined. The weights for
an area of 1.345 cm^2 (the area of the arch punch used to stamp out
the films) are plotted in Figure V-20, as a function of the thickness
of the films prior to reaction.. Most of the weights lie on a single curve.
The slope of the curve at any thickness corresponds to an overall
density of the film. For thin films, through which the peracetic
has diffused completely and 'all' double bonds have reacted (cor-
responding to the linear AB portion of Figure V-9), the overall
density (from slope at b = 0) is the true density of the fully reacted,
crosslinked surface region (or gel fraction), and is equal to 1.19 gm/cm^3.
For films of intermediate thickness, the overall density (from the
slope of the curve shown in Figure V-20) is equal to the sum of the
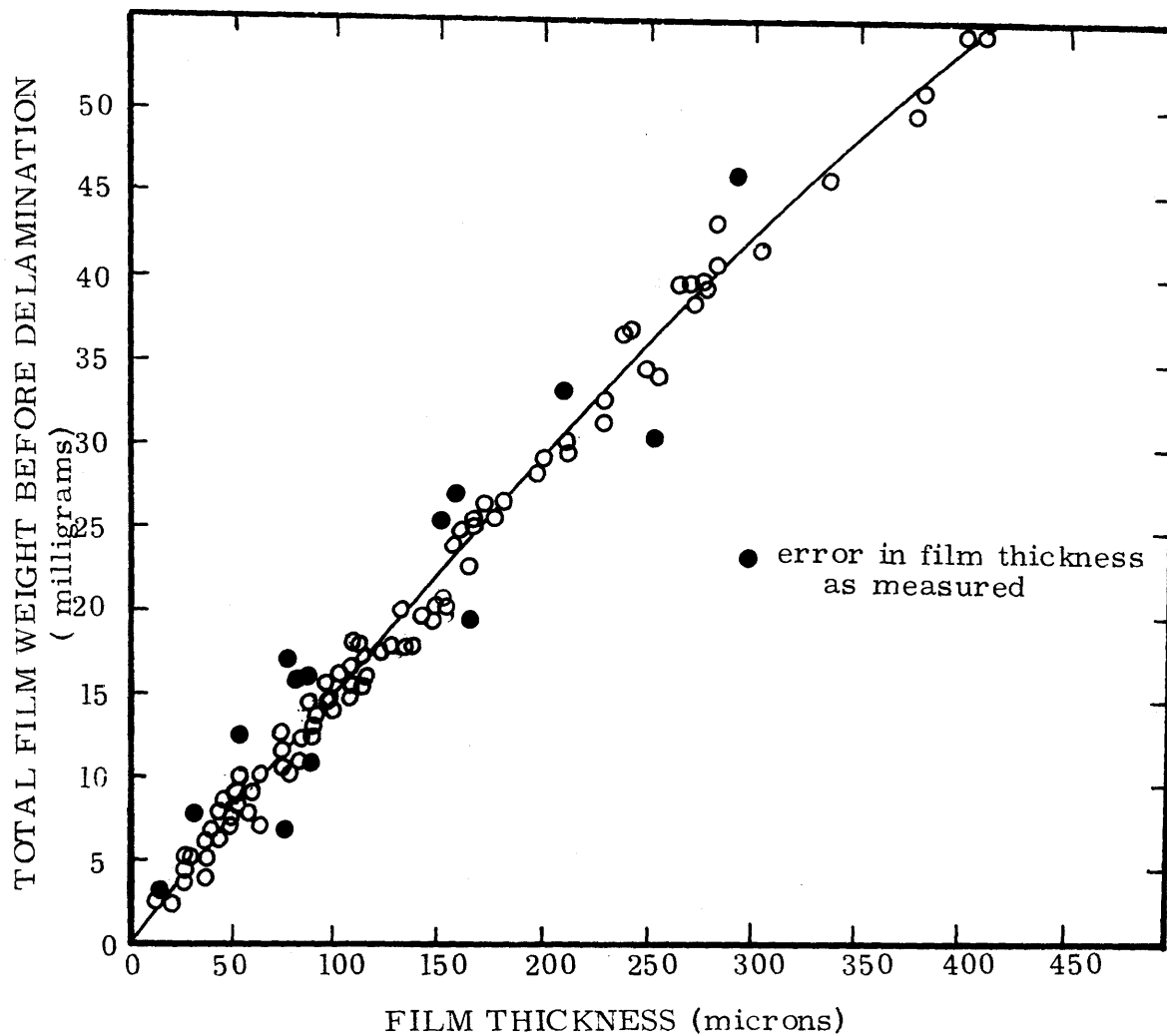
Figure V-20. Total weight of delamination samples (prior to delamination); area = 1.345 cm^2

products of the true densities and the volume fractions of material with those densities. At very high thicknesses, the overall density ($\rho \approx .95$) is almost identical to the density of pure, unreacted SBS TR-41-2443 ($\rho_{SBS} = .943$) measured by standard buoyancy techniques. Considering the larger proportion of unreacted material in thicker films, this agreement between the two densities is expected. The curvature in the plot shown in Figure V-20, then indicates the changes in the relative volume fractions of reacted (denser) material and unreacted (lower density) polymer.

Although deviations in the curve are expected because of the different proportions of reacted and unreacted material in samples of the same thickness prepared under different reaction conditions (different depths of penetration), this curve is considered to be a calibration curve for the optical microscope determination of film thickness (section IV-2a). The error in points which deviate significantly from the curve were attributed to errors made in the microscope thickness measurement. These deviations had little effect on the area concentration-thickness curves but did affect the delamination results. Therefore, a corrected value of thickness was used to improve the appearance of the delamination results. (In no case did this correction affect the conclusions deduced from these results.) This correction, when interpreted in terms of the thickness measurement, corresponded to discarding one or two of the individual thickness measurements which had been averaged to get the thickness reported here. The thicknesses which were considered to deviate significantly are indicated by solid circles on Figure V-20.

The weights of the gel fraction as a function of thickness are presented in Figures V-21 and V-22a, b, c. There are three portions to each curve: initial linear increase, smooth decrease from a maximum value (usually estimated by extrapolation) and a horizontal portion beyond a sufficiently large film thickness. The initial linear portion defines the range of films through which peracetic acid has completely diffused and for which all of the material has reacted and been crosslinked to form a gel. The slope of this portion is identical to the slope of the initial portion of Figure V-20 since 99% of the material is recovered as gel (the remaining 1% was not recovered by the fractional precipitation in methanol, either). The distribution of gel is shown in Figure V-23a.

The horizontal segment corresponds to the range of films for which the stress transfer mechanism is at its maximum effectiveness. The depth of penetration (of fully crosslinked material) is independent of thickness since the diffusion rate becomes independent of thickness when the transfer of stress is maximal, and dependent only on time, temperature and the composition of the reaction bath. The reaction front then has the shape shown in Figure V-6d, independent of the thickness. Therefore, the proportion of reacted material which is fully crosslinked (gel) and the proportion of material reacted but not crosslinked (sol) are constant and there is a direct proportionality between depth of penetration and weight of crosslinked gel. The distribution of gel is shown in Figure V-23d.
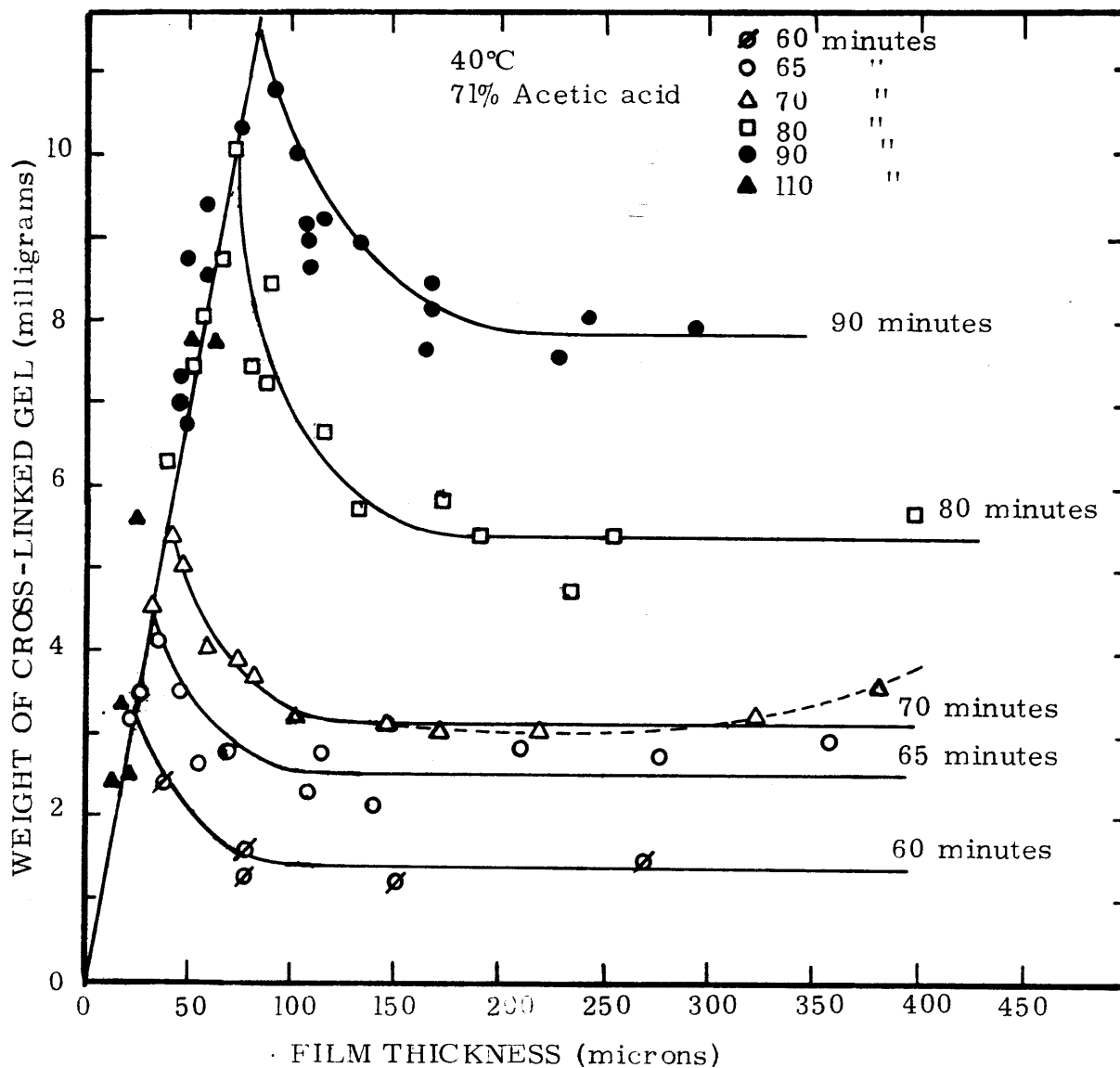
Figure V-21. Weight of crosslinked gel fraction versus film thickness; 40°C, 71% acetic acid (A = 1.345 cm^2; thickness measured prior to reaction)
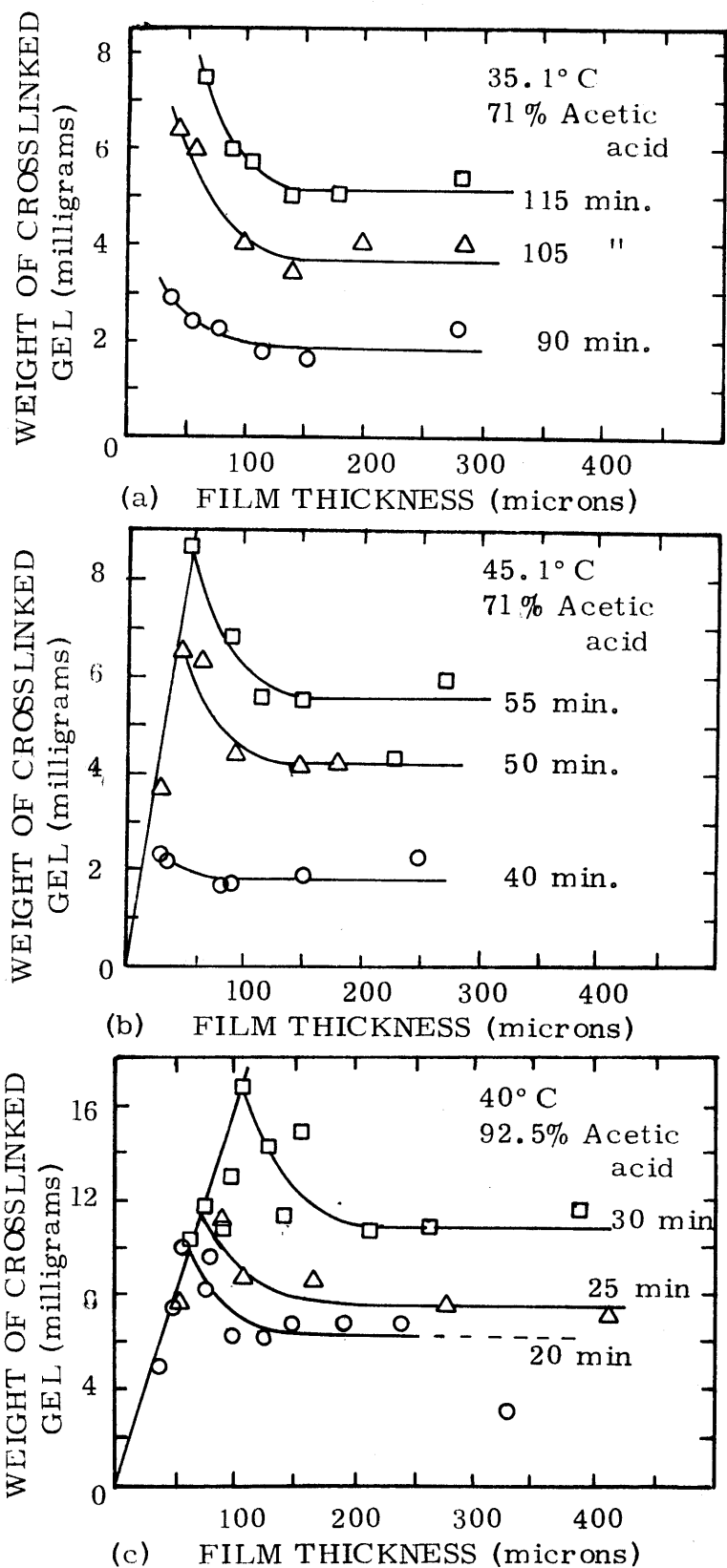
Figure V-22.   Weight of crosslinked gel versus film thickness prior to
reaction; (a) 35.1°C, 71% acetic acid, (b) 45.1°C, 71% acetic
acid (c) 40°C, 92.5% acetic acid.
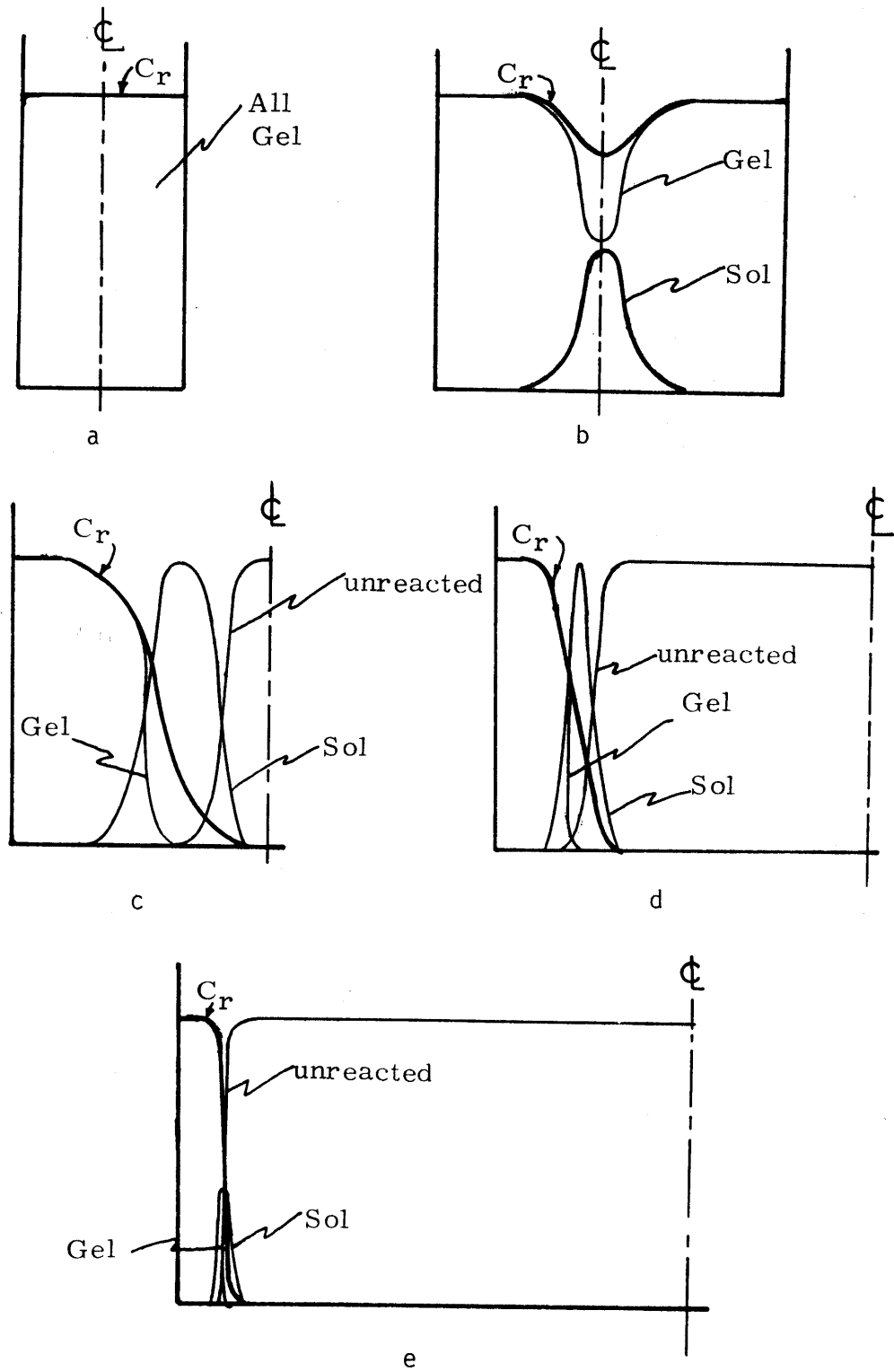
Figure V-23. Distribution of delamination fractions; C_r = reaction front (ordinate, fraction of total weight W/W_t, abscissa, x; (a) - (e), increasing film thickness)

Dividing the weight of gel corresponding to the ordinate of

these horizontal lines by the density of fully reacted material

(1.19 gm/cm^3) and by the area of the sample delaminated (1.345 cm^2)

yields values for the depth of penetration of fully reacted, cross-

linked material (2λ_X - the 2 arises from the fact that permeation

occurs from both sides of the film.) This is an estimate of the

true depth of penetration of the reaction, which is defined as

the depth at which a rectangular distribution of reaction would

have a total moles of reacted material identical to the total number

of moles under the true sigmoidal concentration profile (reaction

front). Obviously the weight of crosslinked gel, corresponding to

this depth of penetration estimate, does not take into consideration

the presence of reacted but not crosslinked material. Thus, the

depth of penetrations calculated from the weights of the gel

fractions are underestimates of the true values.

In all of these plots, it is possible to draw a curve (convex

to abscissa) rather than a straight line through the gel weights

at high thickness. (See dashed curve for 70 minutes reaction in

Figure V-21) Although the accuracy of these measurements does

not warrant this curvature being drawn, an observation of an increase

in the weight of the gel portion with an increase in thickness, in

this thickness range, is consistent with the effects of increased

thickness on swelling, the rate of diffusion and the shape of

the reaction front. This increase would be interpreted to reflect

the approach of the estimated depth of penetration to the true value

with increasing film thickness; the advancing tail of the reaction

front becomes smaller, the slope of the reaction front becomes steeper and the proportion of reacted polymer, which is fully crosslinked, is increased, while the true depth of penetration remains constant. (Compare V-23d and V-23e) Therefore, the depth of penetration estimated from the weight of gel increases with film thickness and approaches the limit of the true value, as defined earlier.

The intermediate decrease between the linear and horizontal portions is attributed to the increased amount of reacted polymer being non-crosslinked reacted material (sol), compared to the 100% crosslinked nature of the films that account for the initial portions. For thicknesses beyond the one giving rise to the maximum gel weight, the reaction front takes on the shape shown in Figure V-6c. From this stage, on the decrease in the area under the reaction front concentration profile causes a decrease in the amount of cross-linked gel and reacted sol, this decrease arising through both a steepening of the slope of the reaction front and an actual decrease in the penetration of the front. This continues until the stage shown in Figure V-6d is reached. This corresponds to the levelling off of the curve of weight of crosslinked material versus thickness. The range of films with decreasing gel weight for a reaction con-ducted for 80 minutes, at $40^{\circ}C$, in 71.1% acetic acid (70 - 180 μ) agrees well with the range of maximum decrease of area concentration with film thickness for the same runs (50-170μ, Figure V-14). The distributions of gel are shown in Figure V-23b and c.

Figure V-24 confirms this interpretation. It is a plot of the weight of recovered sol fraction for two of the reaction conditions (90 minutes, 71% acetic acid and 30 minutes in 92.5% acetic acid, both at 40°C). The plots for other runs show a similar behaviour although the fit to the curve is not as good. The initial increase corresponds to the lessened overlap of the two reaction fronts and the exchange of fully reacted and crosslinked material for polymer that is reacted but not crosslinked. The decrease beyond the maximum corresponds to the steepening of the reaction front that is occurring concurrently with the decrease in the depth of penetration as between the stages of reaction shown in Figure V-6c and V-6d. This decreasing portion also corresponds to the range where unreacted chloroform soluble material is recovered and so, the decrease can be considered to be the consequence of an increase in the amount of unreacted material due to a change in shape (and size) of the reaction concentration profile. The scatter in this curve is caused by the absence of control of volume of precipitant in the fractional precipitation step used to separate the soluble reacted material from the soluble unreacted material. The slower decrease in 92.5% acetic acid is attributable to the larger thickness at which the stress transfer mechanism reaches maximum effectiveness.

As film thickness is increased, it is expected that changes in the shape or size of the reaction concentration profile would have little effect on the weight of unreacted polymer recovered, due to the fact that, for thick films, this fraction predominates and it is difficult to observe small shanges in large numbers. However a relationship has been derived which relates the weight of unreacted
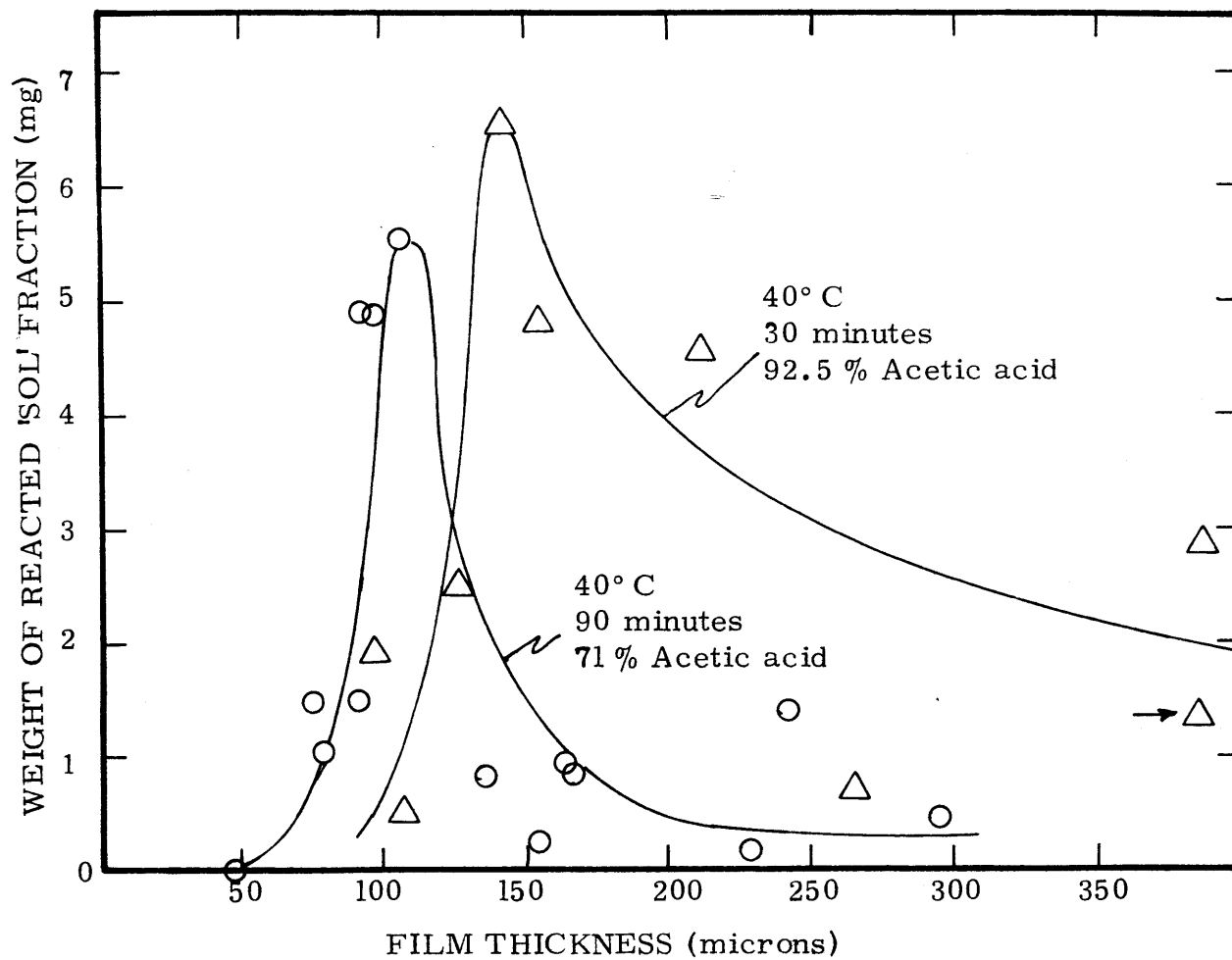
Figure V-24. Weight of recovered, reacted sol fraction versus film thickness prior to reaction.

polymer and the total weight of the delaminated sample (measured before delamination) to another estimate of the depth of penetration (λ_s). The relationship is derived in Appendix 3:

$$\frac{W_t - W_s}{W_t} = \frac{2\lambda_s \, A\rho_r}{W_t} \qquad\qquad (V-2)$$

where W_t = weight of A cm^2 of sample before delamination

W_s = weight of unreacted portion of sample

λ_s = depth of penetration calculated using weight of unreacted material

A = area of sample = 1.345 cm^2

ρ_r = density of reacted layer near surface

$\approx$ density of fully crosslinked material, ρ_x

= 1.19 gm/cm^3

The only assumption behind this relationship is that the density of the reacted material is equal to that of the fully crosslinked material (i.e. the sample can be split into just two volume fractions of two different densities). This assumption is better in thicker films where the amount of non-crosslinked but reacted material is small. To the extent that this assumption is correct and within the limits of accuracy resulting from the absence of proper control during the fractional precipitation procedure, a plot of $\frac{W_t - W_s}{W_t}$ (fraction of material that is unreacted) versus $\frac{1}{W_t}$ (inverse of weight of sample which, in turn, is inversely proportional to the film thickness after reaction) should yield a straight line for each

set of reaction conditions. For every set of conditions but one

(65 minutes, 40°C, 71%HA$_c$) a straight line was obtained and an

average depth of penetration 2λ$_s$ was calculated. Figure V-25

shows a typical plot.
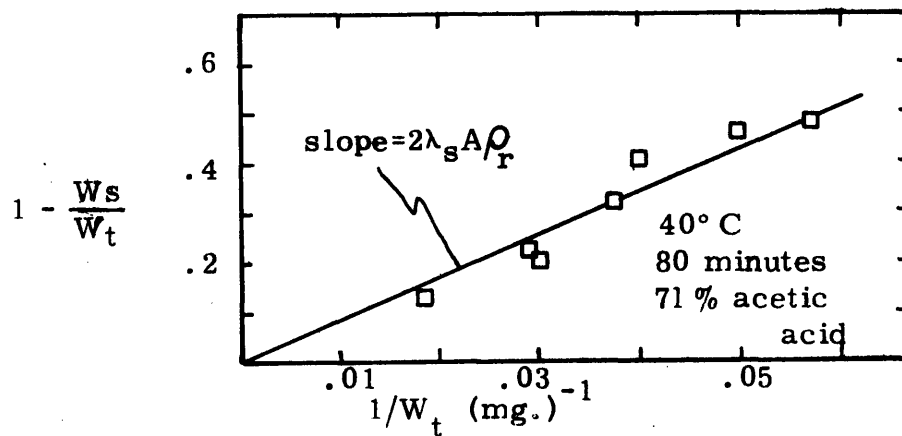
Figure V-25. Determination of λ$_s$.

The results are reported in Table V-3, along with the values for 2λ$_x$

calculated from the weight of the gel fraction. Because no account

is taken of the unreacted sites in the partially reacted sol fraction,

this depth of penetration is an overestimate of the true depth of

penetration. This estimate, however, is closer to the true values

than 2λ$_x$, since the number of unreacted sites unaccounted for is

much less than the weight of the sol fraction, of which the unreacted

sites are but a portion.

The differences between the two values of depth of penetration

are interpreted according to the model shown in Figure V-26.

Table   V-3

Depth of Penetration By Delamination

71%   Acetic Acid

	35°			40°			45°	
t (min)	$2\lambda_x$ (μ)	$2\lambda_s$ (μ)	t (min)	$2\lambda_x$ (μ)	$2\lambda_s$ (μ)	t (min)	$2\lambda_x$ (μ)	$2\lambda_s$ (μ)
90	10.4	31.5	60	8	30.0	40	10.5	26
			65	14.5	-			
105	21.3	35	70	17.5	38	50	24	35
			80	30	47			
115	28.5	42.5	90	43	62.5	55	30	43

92.5% Acetic Acid,   40°C

t (min)	$2\lambda_x$ (μ)	$2\lambda_s$ (μ)
20	36	65
25	41	72.5
30	60	95.5

Figure V-26. Reaction front model showing location of λ_x λ_s; C_r = concentration of reacted double bonds

Three regions can be distinguished: x = 0 to x = λ_x, fully reacted, fully crosslinked, x = λ_x to x = λ_s, partially reacted, uncrosslinked x = λ_s to x = ₵, fully unreacted region. For example, for films reacted for 80 minutes at 40°C in 71% acetic acid, the fully cross-linked portion is 15μ thick and the partially reacted region extends for another 8.5 microns. The reaction profile is then not very steep and appears to have the shape shown in Figure V-6c.

The depths of penetration λ_x, λ_s are based on the thickness of the polymer after reaction, not the thickness before reaction which is used as the abscissa in the plots of area concentration. They define, then, the position and shape of the reaction front in the final reacted state. A depth of penetration was also calculated from the weights of the soluble fractions, which corresponds to a

fraction of the starting polymer that is to be reacted. It is then

a depth of penetration λ_s' based on the initial thickness of the

films (see Appendix 3, Equation A3-6). For the reaction at 40°C,

80 minutes, 71% acetic acid, this depth of penetration is 27 microns,

to be compared with a λ_s of 23.5 microns, based on the final thickness

of the sample. This approximately 15% difference in depth of penetra-

tion compares well with the 20% increase in densities between the

fully unreacted and the fully reacted material.

Semi-log plots of depth of penetration, $2\lambda_s$, versus time yield

straight lines, the slopes of which are reported in Table V-4.

Semi-log plots of $2\lambda_x$, however, yield more complex curves as in

Figure V-27a for reactions at 40°C in 71% acetic acid. However,

a plot of depth of penetration versus the square root of time

(Figure V-27b)gives rise to straight lines for $2\lambda_x$ but not for

$2\lambda_s$. (See Table V-4 for slopes; there is no available explanation

for the decrease in slope at 45°C other than experimental imprecision.)

This observation is interpreted to reflect the presence of two almost

independent mechanisms governing the time dependence of λ_s and λ_x.

The depth of penetration for crosslinked material moves at a rate

proportional to the square root of time, similar to the rate of pene-

tration of the moving boundary in the swelling experiments of Hartley

(1949) and in the second order reaction controlled diffusion system

studied by Hermans (1947). Thus, the depth of penetration λ_x is

assumed to be identical to the depth of the moving boundary separating

swollen (or reacted) material from unswollen (or unreacted) material.

The movement of this boundary (the reaction front)is then governed by

Table V-4

Rates of Propagation of Reaction Front

71.1% acetic acid

	$2\lambda_x$ (a)	$2\lambda_s$ (b)
35.1°	14.2	.0120
40°	20.2	.0242
45.1°	17.8	.0338

(a) from $2\lambda_x$ versus $t^{1/2}$ plot

(b) from ln $2\lambda_s$ versus t plot
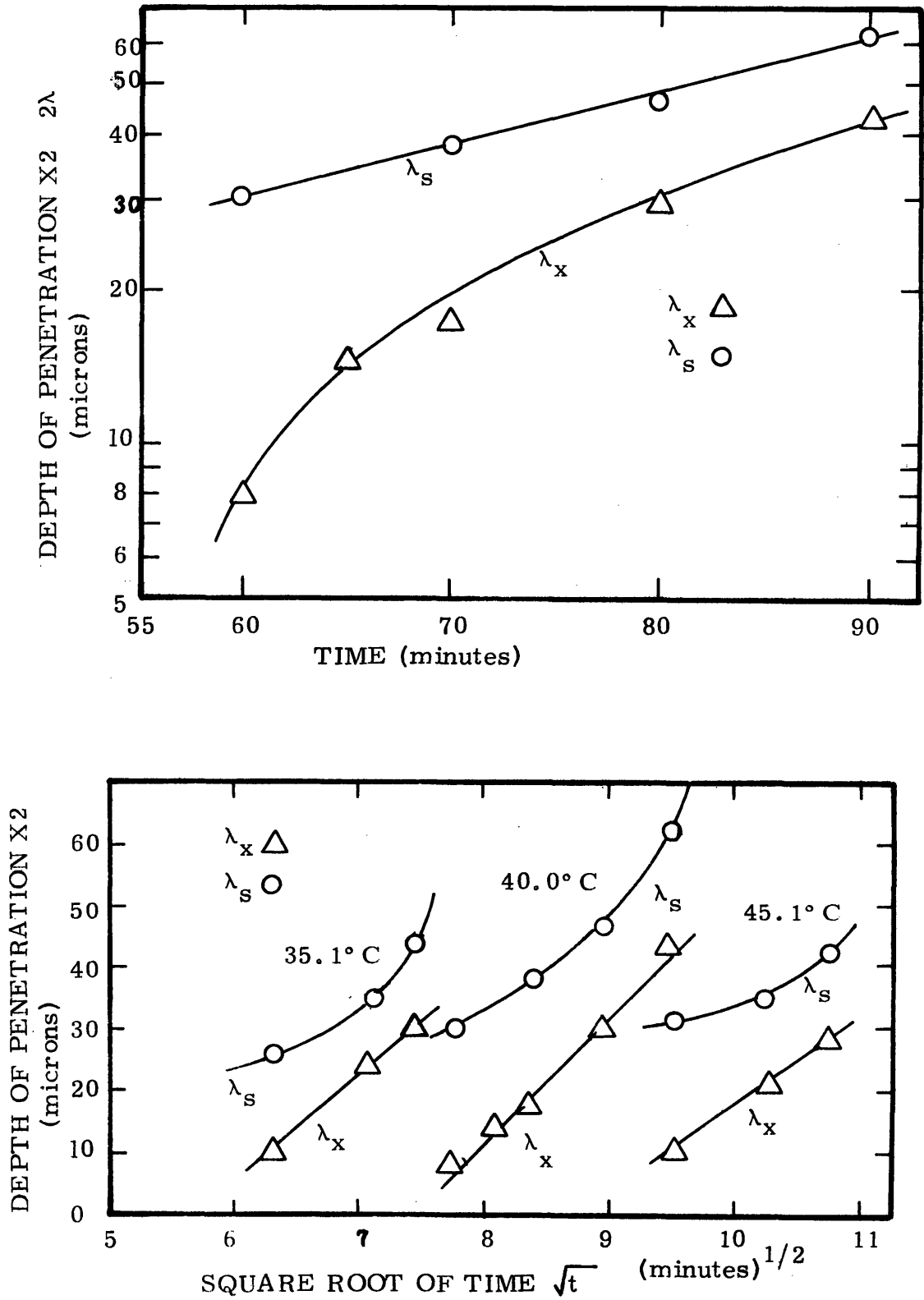
Figure V-27. Rate of movement of the depths of penetration

similar processes to those studied by Hartley and Hermans: simple swelling or simple reaction controlled diffusion. The depth of penetration λ_s based on the weight of the unreacted sample, however, moves at a rate proportional to e^t similar to the rate of increase of hydroxyl content (area concentration, hydroxyls) with time. This increase in λ_s with time is considered to indicate the dominant influence of stress transfer processes in changing the shape of the advancing tail of the reaction front (steepening the reaction front) identical to those governing the degree of hydroxylation.

The range ($\lambda_s - \lambda_x$) is the size of the advancing tail which does not significantly change with increasing time in the time periods observed. It is apparent, however, from the shapes of the curves in Figure V-27b that λ_s increases faster than λ_x at longer times. This indicates that the shape of the reaction front broadens out faster than it moves into the polymer; i.e., the front gets less steep faster, than it actually penetrates into the polymer. This is reasonable considering the shape of the front depends not only on the penetration into the polymer, but also, on the relief of the compressive stresses limiting swelling. The increase in λ_s is then thought of to be composed of two parts: one part directly proportional to the increase in penetration of reactants into the polymer (λ_x) and a second part resulting from relief of stress secondary to the increase in penetration.

Extrapolation of the λ_x versus t curves also indicates the presence of a fairly significant induction time in concordance with the observations in section V-4. However, an Arrhenius plot of the slopes of the ln $2\lambda_s$ versus time plots (a rate coefficient) versus $\frac{1}{T}$ yields a

straight line but with a much larger slope (corresponding to an activation energy of 19,000 k cal/mole) than expected (activation energy of epoxidation 12 k cal/mole). This is interpreted to indicate the presence of processes other than epoxidation which have a significant influence on the shape (and size) of the reaction front (and which have a significant temperature coefficient).

6.   QUANTITATIVE IR MODEL

(a)   Oxygen-containing Functional Groups

The results of the quantitative infrared modeling scheme are shown

in Figures V-28, 29, 31, 32, as plots of f_i versus film thickness. (f_i

is the fraction of oxygen-containing functional groups that are of one

type: hydroxyl, epoxy, acyclic ether, or tetrahydrofuran, mathematically

defined as $C_i/\Sigma C_i$.) The ethers are reported as the complete ether struc-

ture; the values from the model for half ethers were divided by two to

get the f_i values. The values for carbonyl or acetate were very small

($f_i < .01$) and, in many cases, negative (an anomaly attributable directly

to the model). Because the error associated with these fractions of car-

bonyl or acetate were generally larger than the values themselves, no

attempt was made to define a correlation for these fractions on thickness,

and the values are not even reported in these figures. The f_i values

are all calculated from F_i values reported on the basis of 100 moles of

unsaturation in original polymers (section III-3).

The errors, attributable to the regression or resulting from the

uncertainty in the absorptivity matrix as calculated by the procedure

outline in Appendix 1c, are not shown as error bars in these figures

but are listed in Table V-5, for the case of the reaction at 30°C, 180

minutes, 70% acetic acid. The conclusions derived from this data are

all made in consideration of the limitations of the data as expressed

by their associated errors. The errors (determinate and indeterminate)

are discussed further in part b.

Figure V-28 and V-29 show the behaviour alluded to in section V-4;

namely, a change in product distribution with increasing thickness.

Table V-5.

Fractions of Oxygen Containing Functional Groups (f_i) With

Associated Errors; Surface Hydroxylation at 30°C,

for 180 Minutes, 70% Acetic Acid.

film thickness (microns)	hydroxyl	epoxy	tetrahy- drofuran	ether	carbonyl	acetate
11.6	.63±.23	.03±.09	.24±.10	.08±.04	.01±.05	0 ± .04
16.2	.49±.17	.18±.14	.20±.09	.12±.05	.01±.09	0 ± .07
22.4	.54±.19	.14±.09	.21±.08	.09±.04	.02±.05	.01± .04
31.3	.50±.17	.17±.10	.20±.08	.08±.04	.02±.06	.03± .05
47.5	.37±.13	.18±.14	.23±.09	.17±.07	.04±.08	.02± .07
57.3	.36±.13	.26±.18	.21±.09	.11±.06	.04±.09	.02± .07
90.0	.34±.15	.43±.30	.18±.11	.06±.07	.01±.12	.01± .09
191	.14±.05	.60±.30	.11±.08	.05±.05	.07±.11	.03± .09
330	.20±.08	.47±.26	.16±.09	.14±.07	.02±.10	.01± .08
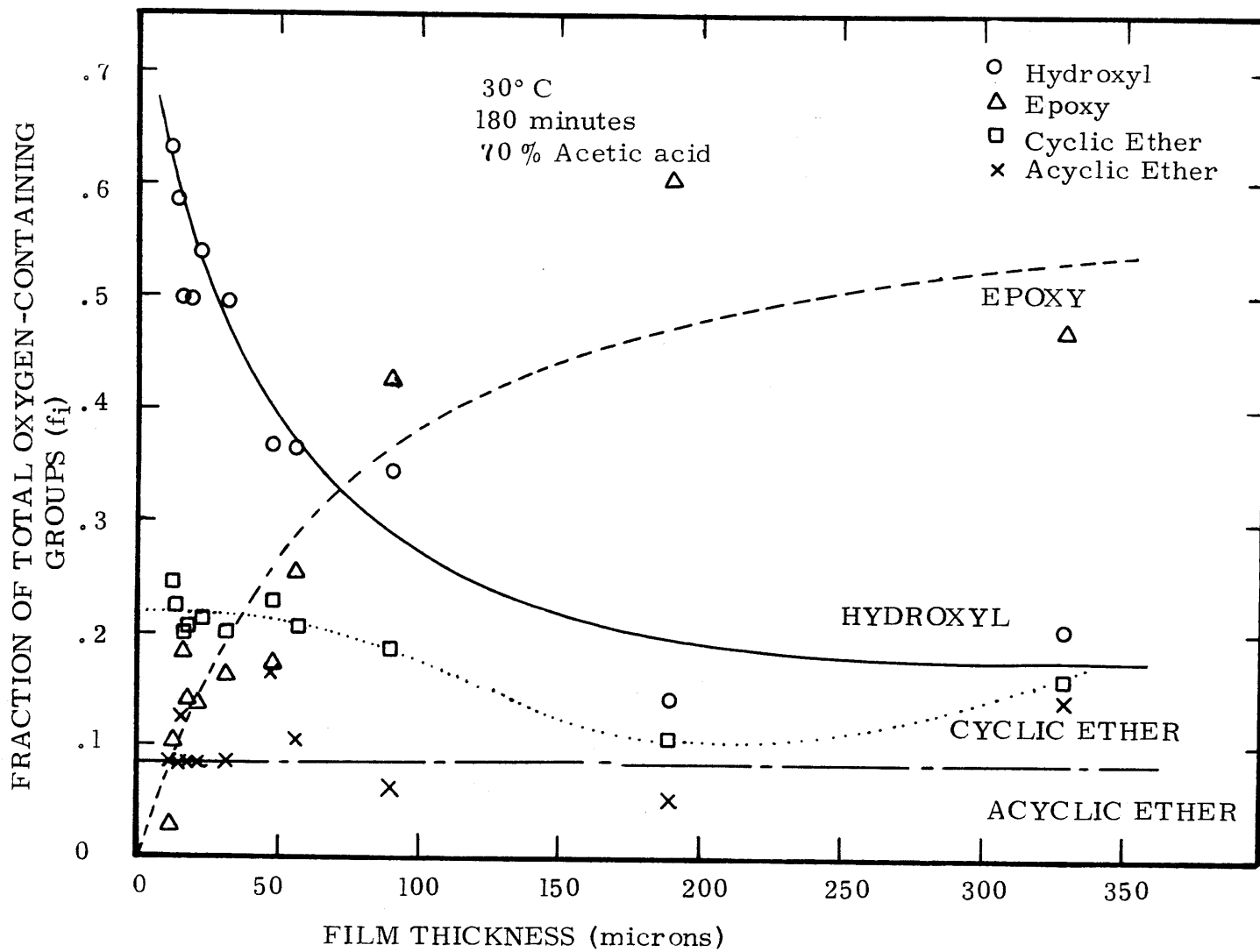
Figure V-28. Composition of surface hydroxylated films; 30°C, 180 min, 70% acetic acid. (thickness measured prior to reaction)
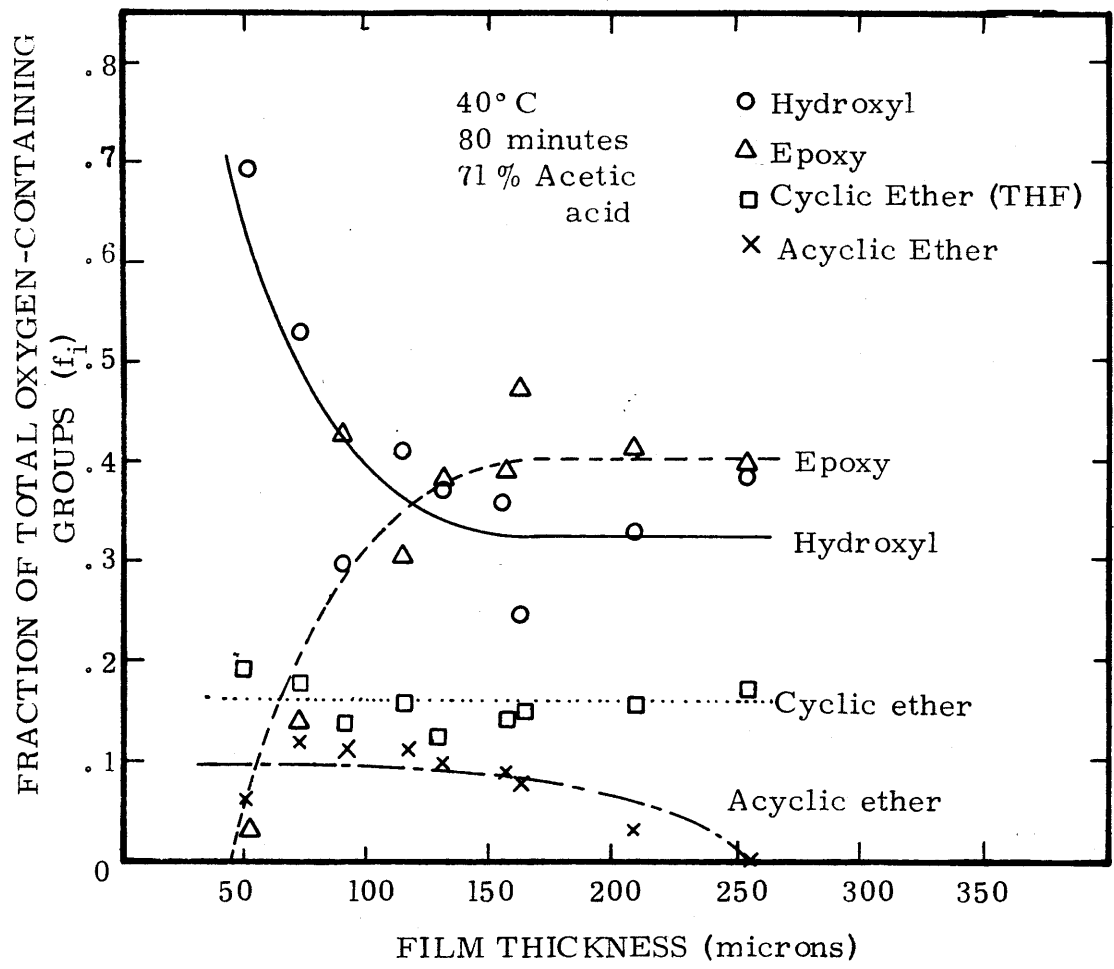
Figure V-29. Composition of surface hydroxylated films; 40°C, 80 min, 71% acetic acid. (thickness measured prior to reaction)

While there is no apparent correlation (within experimental error) of the ether fractions (acyclic or cyclic), there is a definite decrease in the moles of hydroxyl and a definite increase in the moles of epoxy left uncleaved with increasing thickness.

The competitive reactions involved in this change of product distribution, which results in the discrepancy between the area concentration of hydroxyl groups and the area concentration of oxygen (Figure V-10), are then, epoxide formation and epoxide cleavage. This occurs despite the fact that cleavage is generally faster (larger kinetic constant) than epoxidation (section III-2b). The competition arises because the two different permeating species required for hydroxyl formation, permeate at different rates. If it is assumed that the cleavage agents (acetic acid or water) diffuse through the polymer slower than the peracid, at any point in time, the peracetic acid concentration profile (the reaction front) will be ahead of the cleavage agents reaction profile and there will always be a portion of the reaction front (the advancing tail), in which the concentration of acetic acid or water is effectively zero and cleavage of the already formed epoxy rings in this portion cannot occur. As the thickness of the film is increased, the shape of the reaction front changes to make the reaction front steeper and to reduce the swelling at the surface (stress transfer). This has a more drastic effect on the already more slowly diffusing cleavage agents by making the limiting value of solubility occur earlier in the film (the limiting or cut-off solubility is the one at which the corresponding diffusion rate is so low that in the time scale considered diffusion stops and the concentration gradient is zero). As a result the propor-

tion of uncleaved epoxide is increased (with a commensurate decrease of the amount of hydroxyl groups) giving rise to the curves shown in Figures V-28 and 29.

While the slower diffusion rate of water in the polymer is directly attributable to its lower solubility in the reacted portion of the polymer, the slower diffusion rate of acetic acid is not as easy to explain. Comparing the molecular size and polarity of acetic acid and peracetic acids nearly identical diffusivity and solubility and hence, nearly identical diffusion rates are expected. The competition between epoxide cleavage and formation is also difficult to reconcile with the fact that one molecule of acetic acid is formed at the site of epoxidation from peracetic acid for each double bond epoxidized, regardless of any diffusional limitations. It thus appears that the limiting step is actually the diffusion of sulphuric acid through the polymer. Since a protonated epoxide is required for cleavage, any limitation on the availability of protons would result in a reduced rate of epoxide cleavage independent of the concentration of acetic acid or water. Although it is difficult to comment exactly on the diffusion of sulphuric acid or protons through the reacted swollen polymer, it is obvious that if sulphuric acid or protons diffuse in association with water, then the diffusion rate of water is the only one of importance with regard to the availability of cleavage agents and the slower, diffusion-controlled cleavage rate is well accounted for. In all probability, an assumption of association with water is not necessary as the diffusion rate of sulphuric acid or protons would presumably be slower than that of peracetic acid independent of the state of association of the acid

(or protons).

This change in product distribution from hydroxyl or glycol for-
mation (2 moles oxygen per mole of double bond reacted) to epoxy ring
retention (1 mole oxygen per mole of double bond) with increasing
thickness renders the assumption made in the last section with regard
to a constant stoichiometric ratio of oxygen to reacted double bond
invalid. As a result the area concentration of oxygen (Figure V-10)
does not reflect the true area concentration of reacted double bonds,
which actually decreases with increasing thickness.

A similar diffusion limited competition occurs in the potassium
hydroxide hydrolysis of the acetate esters, for which the diffusing
species is the hydroxide ion (or water). Considering a polymer which
had been prepared at 40°C, for example, in the presence of a large amount
of acetic acid, and in which there are acetate groups uniformly through-
out the reacted portion, hydrolysis in aqueous base at room temperature
would be limited by the diffusion of the base (or water) into the less
swollen polymer. The limiting solubility of base (or water) in the
reacted polymer at room temperature in the presence of only water occurs
earlier in the polymer (at a smaller C) than the position of the reaction
front (see Figure V-30).
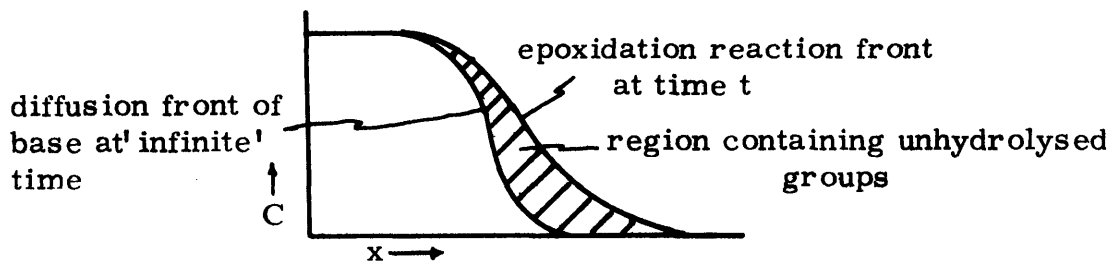
Figure V-30. Diffusion limitation in ester hydrolysis.

There is thus a number of acetate groups that lie beyond the diffusion front of base, that will not be subject to hydrolysis even after an experiment has been taken to 'completion'. The discovery of this diffusion limitation in acetate hydrolysis made it necessary to modify the conditions used by Traut (1973) to effect the hydrolysis: i.e., higher temperatures (40°C) were used and a swelling agent (dioxane) was added to the hydrolysis medium (section IV-2c).

The absence of a thickness dependence of tetrahydrofuran ring structure formation was expected considering that it is an intra-molecular process involving only already formed epoxide groups.
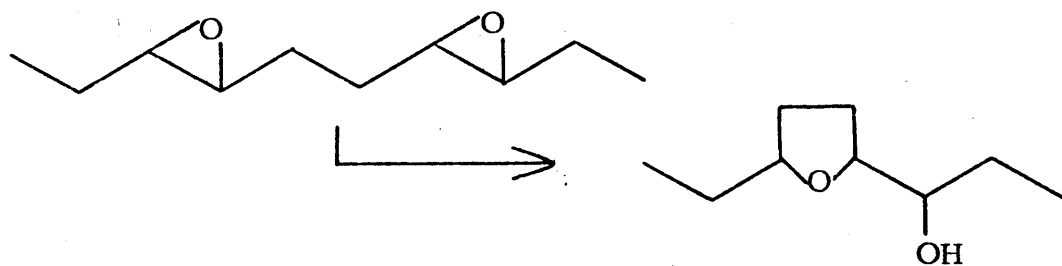
The only dependence on thickness would be through any dependence of epoxide fromation on thickness, a dependence which can not be determined using the values of F_i. A similar absence of thickness dependence of the formation of intermolecular ethers results from the absence of any secondary diffusing molecule being required for their formation. The direct effect of volume fraction of polymer on an intermolecular cross-linking process, expressed by the square of a concentration ([1]/volume, squared), is not important because of the low concentration of polymer

(epoxide groups) even in the unswollen state ($\sim$. 01 moles/cm^3).

In Figure V-31 and Figure V-32 the change in product distribution described above is not apparent. Because of the first data point, the plots of Figure V-31 are equivocal concerning a decrease in the hydroxyl fraction with increasing thickness and an increase in epoxide fraction. The plots of Figure V-32, however, show without a doubt the independence (within experimental error) of hydroxyl and epoxy fractions with increasing thickness. It appears that for these two runs, at least, which are at reaction conditions giving rise to high extents of reaction, the product distribution is independent of thickness and there is no diffusion lag between peracetic acid/epoxidation and acetic acid (or water, H_2SO_4)/cleavage which was apparent in the reactions conducted at 30°C, 180 minutes or 40°C, 80 minutes. The absence of a difference in diffusion rates is expected considering the large degree of swelling consequent to the relatively high extents of reaction encountered under the conditions used (90 minutes, 40°C, 71% acetic acid and 30 minutes, 40°C, 93% acetic acid). With these large swelling ratios, the slightly lower diffusion rate for the cleavage agents, relative to peracetic acid, would have no effect on cleavage as the limiting or cut-öff solubility would be effectively identical with the limiting solubility for peractic acid diffusion.

In the absence of a change in product distribution for these runs an explanation is still needed for the decrease in the moles of hydroxyl groups (area concentration) with increasing thickness observed for these reaction conditions. It is presumed that this decrease is the result of stress transfer mechanisms reducing the depth of penetration with increasing thickness (as in the difference between the reaction fronts shown in
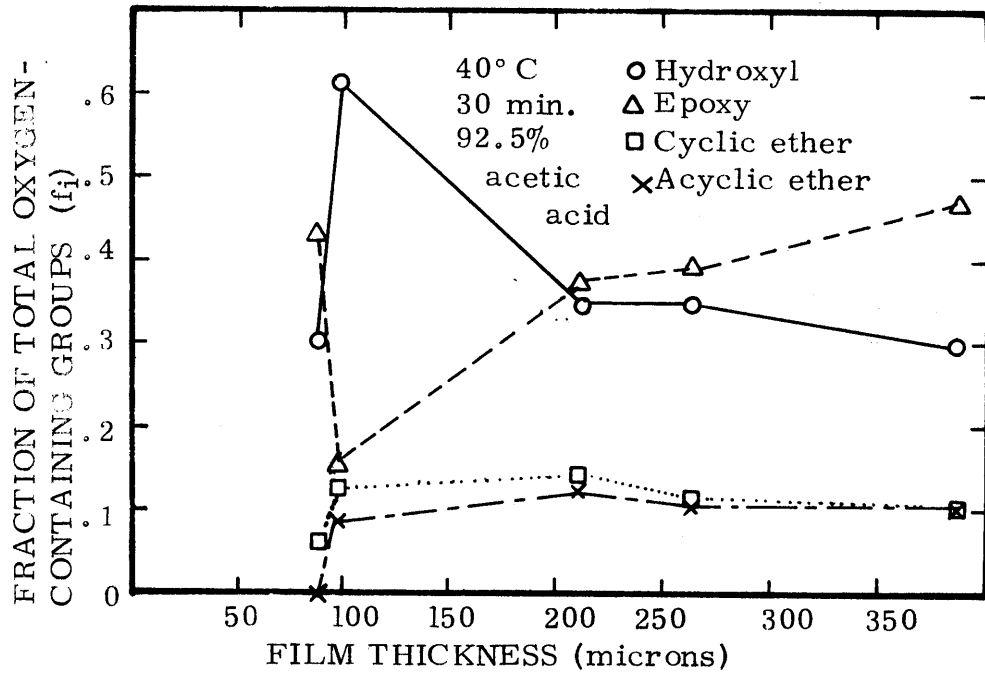
Figure V-31. Composition of reacted films, 40°C, 30 min, 92.5% acetic acid.
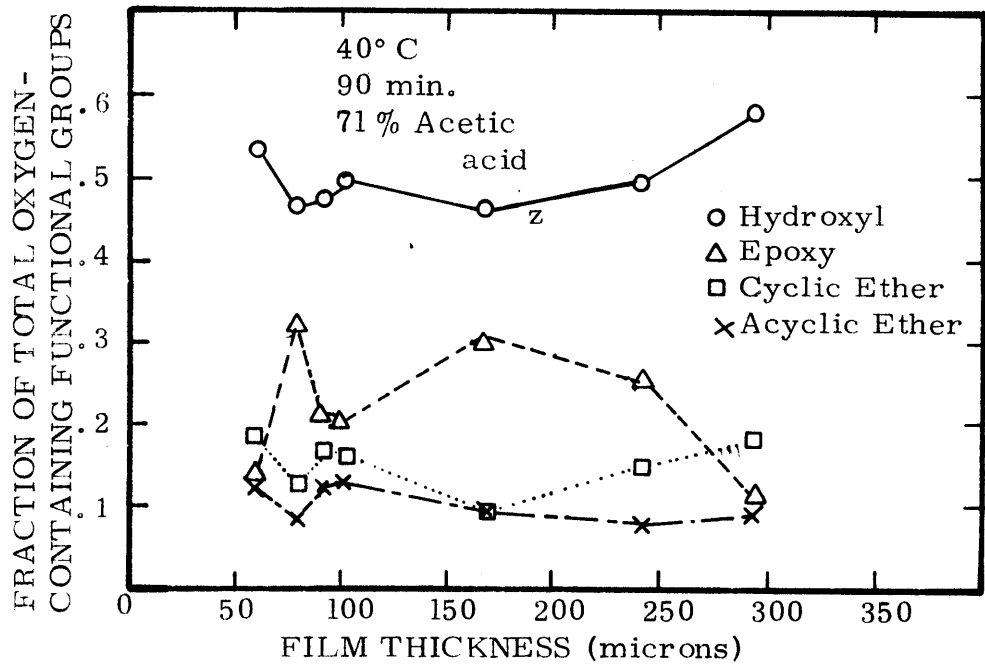
Figure V-32. Composition of reacted films, 40°C, 90 min, 71% acetic acid.

Figure V-6c and V-6d). The decrease in hydroxyl content with increasing thickness is then, the result of a reduced degree of epoxidation in thicker films, due to a reduced diffusion rate in these films.

Unfortunately, the infrared data discussed here cannot be used to give experimental verification of this hypothesis. (Delamination gives indirect confirmation, section V-5.) For a test of this hypothesis, the total number of moles of oxygen-containing functional groups must be accurately known. However, because of the grinding/suspension procedure used to prepare samples for infrared analysis (section IV-4a), a separation of the sample was effected into two fractions: a CS_2 soluble, unreacted polymer fraction and CS_2 insoluble, reacted polymer fraction. In transferring the suspension to the solution cell used to contain the sample while the spectrum is being recorded, a sample-to-sample variation results in the relative amounts of each fraction transferred. Ideally, the ratio of fractions transferred should be the ratio that they appear in the sample but since this cannot be controlled, a larger part is lost of one fraction than the other during the filling of the solution cell. For example, loss of part of the CS_2 soluble fraction would result in a low value of the moles of oxygen-containing functional groups and a loss of the CS_2 insoluble fraction would result in a relatively high value for the moles of oxygen-containing groups. Opposite considerations apply to the moles of double bonds remaining (section V-6b).

This error is not applicable to those films which are thin enough for good spectra to be recorded without resorting to these grinding/ suspension techniques. Unfortunately no information concerning the effect of thickness on the diffusion process can be obtained from these thin films. However, the moles of oxygen per square centimeter of the films

reacted at 30°C for 180 minutes were computed and the values compared with those obtained by oxygen analysis. The agreement is quite good: .013 moles/cm^3 by IR and .011 moles/cm^3 by oxygen analysis, in fully reacted films.

As described in section V-2, there are three types of acyclic ethers present in samples of surface hydroxylated styrene-butadiene-styrene block copolymers: saturated, vinyl and phenyl ethers. Because the ethers are measured as half ethers ($-$C-O structures), the other half of the ether structure is unknown. More detailed examination of the relative amounts of each ether type yielded only a little more information with regard to their structure. Generally, the number of moles of vinyl ethers (per 100 moles of original unsaturation) is equal (approximately) to the moles of phenyl ethers (both half ether struc-tures) present in the sample. Also, the fraction of the total number of ethers that are either vinyl eithers or phenyl ethers does not correlate with film thickness and thus, within experimental error, it is considered independent of film thickness.

The total moles of vinyl and phenyl half ether structures was, in most cases, less than the moles of saturated structures indicating the feasible presence of assymmetric ethers (i.e., vinyl - saturated alkyl ethers and phenyl - saturated alkyl ethers). Phenyl-phenyl ethers are also possible with only the vinyl ethers present as assymmetric ethers. In addition, the equal concentrations of vinyl and phenyl ethers suggests the exclusive occurrence of assymmetric ethers of the form of vinyl - phenyl ethers, although this possibility is unlikely chemically and spectroscopically.

Even though there are, then, three cases for the determination of the proportions of each type of ether structure, the proportions of each ether structure are independent of film thickness, for all three. The three cases are:

1) All phenyl ethers are phenyl-phenyl ether structures, with only vinyl ethers as assymmetric ethers.

2) All phenyl and vinyl ethers are assymmetrically linked to saturated ethers.

3) All phenyl and vinyl ethers are phenyl-vinyl ethers and all saturated ethers are symmetric.

The fraction of each type of ether structure for each case, are listed in Table V-6. The real situation in samples of hydroxylated SBS copolymers is probably a combination of cases 1 and 2 with a negligible contribution of phenyl-vinyl assymmetric ethers.

Further information with regards to the nature of the substituents on the tetrahydrofuran rings formed by epoxide rearrangement (Figure III-8) is not obtainable from the quantitative spectral information due to the absence of any correlation of the number of hydroxyls and the number of cyclic ether structures found in the samples analysed.

Table V-6

Ether Structures; Fraction of Total Number of Ethers

		40°C, 80 min 71.1% HAc	40°C 90 min 71.1% HAc	40°C 30 min 93% HAc	30°C 180 min 70% HAc
Half [a] ethers					
	vinyl	.44	.46	.48	.32
	phenyl	.44	.46	.48	.32
Full ethers					
Case 1					
vinyl/sat'd		.44	.46	.48	.32
phenyl/phenyl		.22	.23	.24	.16
sat'd/sat'd		.34	.31	.28	.52
Case 2					
vinyl/sat'd		.44	.46	.48	.32
phenyl/sat'd		.44	.46	.48	.32
sat'd/sat'd		.12	.08	.04	.36
Case 3					
vinyl/phenyl		.44	.46	.48	.32
sat'd/sat'd		.56	.54	.52	.68

a   thickness independent values; directly from infrared modelling
    scheme

(b) Residual Unsaturation

Application of this quantitative infrared model to films of SBS TR-41-2443 prior to reaction, results in a microstructural composition slightly different than that obtained by Shell (Table IV-1). The micro-structure determined here is:

trans   47%

cis   40%

vinyl   13%

Using these values, plots of N_i/N_i^0 (where N_i = moles of double bond isomer i remaining in sample after reaction and N_i^0 = moles of double bond isomer i in sample prior to reaction) versus film thickness were made. The values of N_i/N_i^0, fractional conversion of double bonds are calculated from the values for F_i (equation III-7), the moles of double bond isomer per 100 moles original unsaturation. Because absolute (and not relative) values of the number of double bonds are used, the values of N_i/N_i^0 are subject to the same error in transferring the two-phase sample to the solution cell for spectrum recording, that was discussed earlier in connection with the use of the total number of moles of oxygen-containing functional groups. Although these plots are then subject to a lot of scatter, since in most (thicker) films the volume fraction of the unreacted portion is the greater one, these errors in transferring the sample have a small effect on the numbers of moles of double bonds found in the spectrum and scatter is not severe.

A typical plot is shown in Figure V-33 for the films reacted at 30°C for 180 minutes, in 70% acetic acid. As expected the moles of each double bond isomer increase uniformly up until a certain point, after which they increase much more slowly. An exception is the cis
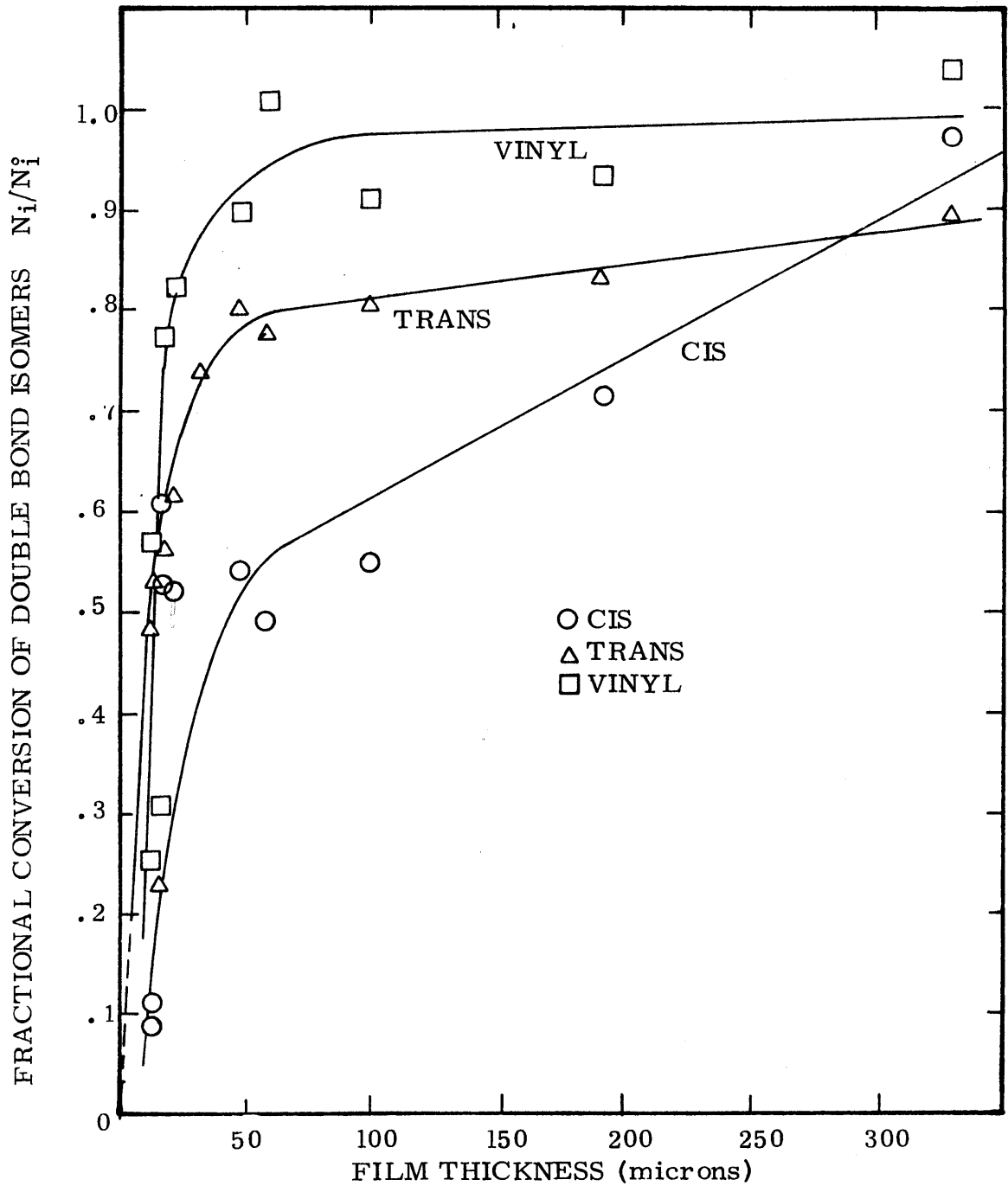
Figure V-33.   Fractional conversion of double bonds versus film thickness
prior to; 30°C, 180 minutes, 70% acetic acid.

double bond which still increases quite rapidly after the sharp break in the curve near 30 - 50 microns. This is attributed in part to the higher reactivity of cis double bonds, but in larger part to the great difficulty in determining accurately the concentration of cis double bonds (the % error in the F_{cis} value is approximately 80%). In some samples, the value for the concentration of vinyl double bonds was greater than that initially present. This is wholly accounted for by the errors in the regression and is not considered to represent a true (net) production of vinyl double bonds. As a result, some of the N_i/N_i^0 values for vinyl groups are greater than unity.

The break in the curve near 30 - 50 microns reflects the depth of penetration of the reaction in accordance with the value that is estimated from the plot of area concentration of hydroxyls versus film thickness (Figure V-9). The subsequent increase after the break demonstrates the relative reactivities of the three double bond types:

$$\frac{\Delta\left(N_i/N_i^0\right)}{\Delta b} = \frac{1}{N_i^0} \cdot \frac{\Delta N_i}{\Delta b} \tag{V-3}$$

where $\dfrac{\Delta\left(N_i/N_i^0\right)}{\Delta b}$ is the slope of the line at large thicknesses.

Comparing slopes of the curves of two different double bond isomers:

$$\frac{(slope)_i}{(slope)_k} = \frac{N_k^0 \Delta N_i}{N_i^0 \Delta N_k} \simeq \frac{k_i}{k_k} \tag{V-4}$$

where $\dfrac{k_i}{k_k}$ is the ratio of the kinetic constants of epoxidation of isomer i and isomer k, respectively; $\dfrac{\partial N_i}{\partial t} \simeq k_i N_i^0 N$ peracid.

From the slopes of the curves, it is apparent that $k_{cis} > k_{trans} > k_{vinyl}$.
The actual values of the relative rates are impossible to determine
accurately because of the uncertainties in the concentrations of each
of the double bond types (especially cis double bonds).

Although it is difficult to compare the concentrations of vinyl
ethers and trans double bonds because of the errors in handling the
two-phase ground sample, from such comparisons, it is quite apparent
that there is no correlation between the concentrations of trans double
bonds and vinyl ethers (and between trans double bonds and all acyclic
ethers) even in the spectra of thin films for which no sample grinding
was required. ($F_{trans} \sim 20$, $F_{vinyl\ ethers} \sim 3$). The anomalous appear-
ance of a large amount of trans double bonds remaining in thin films
which are apparently completely reacted (show no change in further
reaction, (Traut, 1973), is then, not accounted for by the formation of
unsaturated ethers with an unreactive trans double bond as part of the
structure. The large amount of trans double bonds in thin films, is
apparent from the fractional values plotted in Figure V-33; both vinyl
and cis double bonds have values near zero in thin films. It thus appears
that the high values for trans results from interfering absorptions at
$967\ cm^{-1}$ particularly that of the broad tetrahydrofuran peak at $1067\ cm^{-1}$
in the infrared spectrum. The resulting values for trans would then be
high due to the presence of unaccounted for absorption from interfering
groups (see section IV-4d(ii)). The interference would be less in thicker
films where the proportion of oxygen containing groups is much less.
Alternative explanations based on the isomerization of cis double bonds to
form trans double bonds, which are unreactive due to the presence of
neighboring electron withdrawing groups is also possible although this

cannot be checked using the data obtained here.

(c) Errors and Assumptions

The assumptions or errors, indeterminate and determinate, involved in infrared quantitative analysis are summarized here. The prime assumption in quantitative analysis by absorption spectroscopy is that the Lamber-Beer law is valid; i.e., there is a linear relationship between concentration and absorbance. Although deviations from the Lambert-Beer law are reflected in curvature of the absorbance versus concentration calibration curves and so, are accounted for in part by choosing the best straight line through the data and the evaluation of the standard deviation of the absorptivity, there is an indeterminate aspect to the direct comparison of the spectra of calibration compounds with the to be analysed sample. This results from variations in the spectrometer conditions: the presence of a finite slit width, stray light and nonhomogeneities in the medium which would result in scattering and variations in reflection losses produce unaccountable differences in the spectra. It is also assumed that the radiation is monochromatic and unpolarized, so that changes in the orientation of the sample have no effect on the spectra obtained. All of the indeterminate errors resulting from these sources are small, however.

More major limitations are encountered when direct comparisons of the sample and calibration compounds are made. These arise from the assumption that the functional group is in an environment in the calibration sample equivalent to the environment found in the sample to be analysed, itself. This refers to both the state of the calibration sample and its intramolecular environment (see section Iv-4d).

A necessary prerequisite for this is the absence of any physical/ chemical interactions in the sample to be analysed. The errors resulting from failure of these assumptions are indeterminate, but, as is discussed in section IV-4d, are important. The indeterminate errors that result if not all of the components present in the reacted polymer sample are taken into consideration in the infrared model are similarly significant.

The determinate errors arising from the uncertainty in the values of absorptivity used and from the least squares solution to the over-determined system of equations are discussed further in Appendix 1C. Generally, the error resulting from the uncertainties in the absorptivities accounted for 70% of the final error in the concentrations ($< X_i >$ values), calculated from the infrared spectra.

7. AGEING

The appearance of films of reacted and unreacted SBS TR-41-2443 that had been set aside for five months in the various environments described in Table IV-5 are described in Table V-7. From the results it is quite obvious that the major degradative mechanism in SBS copolymers, reacted or unreacted is oxidative photo-degradation: samples in the dark showed no change after five months independent of the presence or absence of oxygen. When not stored in the dark, both reacted and unreacted films showed evidence of ageing: 1) the unreacted SBS, after ageing in the dry state, had a brittle surface that cracked on flexing, indicating the presence of a less flexible, probably oxygenated surface with the interior unreacted core maintaining its original flexibility and 2) both reacted and unreacted SBS copolymer showed signs of yellowing, presumably attributable to the ageing of the polystyrene portion, which is known to yellow in contact with air (Hawkins, 1972). The absence of any change in the unreacted SBS stored wet, in light and air is the result of the surface plasticizing effect of water and the color-hiding effect of the white swollen film (see section V-8a), making it impossible to distinguish the above noted signs of ageing.

In addition, there was no evidence of erosion of the surfaces of the surface reacted films when in contact with a sterile, aqueous solution of saline at pH 7.4. The absence of any ageing or erosion effects in films stored in the dark even in the presence of oxygen demonstrates the absence of a limitation to the potential use of SBS copolymers as biomaterials, resulting from changes in the film properties while implanted in the body, over a five month period.

Table V-7

Appearance of SBS After Ageing for 5 Months

Environment (see Table IV-5)	Unreacted SBS	Reacted SBS
dry, light, air	brittle surface, slight yellowing	same as unreacted
dry, dark, air	no change	no change
dry, dark, vacuum	no change	no change
wet, light, air	no change	slight yellowing at edge
wet, dark, open to atmosphere	no change	no change
wet, dark, closed to atmosphere	no change	no change

8. PROPERTIES OF SURFACE HYDROXYLATED FILMS

(a) General Appearance

Films which were truly surface hydroxylated (i.e., retained an interior, unreacted core) were opaque (white) when swollen in water. The opacity was attributed to clustering of water at the reaction front, or interface between unreacted and reacted polymer. The water which was able to penetrate the reacted portion of the polymer, was unable to diffuse beyond the reaction front because of solubility limitations. At its solubility limit, the water clustered together, with the partially wetted polymer also clustering to form, in effect, a 'precipitate', which as nonhomogeneties in composition act as scattering centers to make the film appear white.

In the swollen state the surface hydroxylated materials are very flexible with (estimated) mechanical properties approaching those of the original unreacted SBS. When dry, however, ther surface of the unreacted polymer is brittle and surface cracks appear if the material is flexed. The brittle surface is the direct consequence of having oxygenated material at the surface which has a higher glass transition than the material in the interior continuum (polybutadiene). When swollen with water, water acts as a plasticizer to reduce the glass transition of the surface material and so make the surface as flexible (if not more so) than the bulk.

The actual water uptake of the films is very difficult to measure because of the small film samples available and because of the difficulty in removing all adhering water when the weight of the swollen polymer is measured. Nevertheless, it is consistently observed that films that

are reacted completely, absorb about 25% of their weight in water so
that in the final state, the water content is about 20% of the total,
an amount that is not enough to cause any real disruption of the material
or to significantly affect its strength. While in thicker films, that
are only partly reacted, the water uptake is definitely less, the
direct evaluation of the effect of film thickness on swelling in the
surface region was impossible because of the difficulties in obtaining
reproducible swelling ratios.

(b) Biological Tests

The results of whole blood clotting time tests, in terms relative
to the WBCT time for unsiliconized glass, are:

	$\dfrac{\text{WBCT - sample}}{\text{WBCT - unsilicon.glass}}$
reacted SBS, air surface	1.5
reacted SBS, mercury surface	1.5 - 2.2
unreacted SBS, air surface	1.9 (3.4, Merrill 1974)
unreacted SBS, mecury surface	1.7

Despite the definite crudeness of the WBCT and the variability in the
data obtained, it is obvious that surface hydroxylation, by itself,
does nöt produce a polymer inactive with regards to the intrinsic
clotting system. This test is also not sufficiently sensitive to
changes in morphology to distinguish between the air and mercury
surfaces of films cast on mercury (see section III-1).

Incubation of a few grams of SBS   TR-41-2443 with soil micro-
organisms failed to result in any significant growth of the microbes.
Although this is not conclusive with regards to the biological stability

of SBS copolymers it is an encouraging observation, and confirms the remarks made in the Introduction (section II-3b) concerning the potential stability of SBS in a biological environment.

There is also no evidence suggesting that epoxy groups (or the other ether structures) in the polymer are potentially harmful in the biolgical environment or that these groups would react further when implanted.

VI CONCLUSIONS

1. Styrene-butadiene-styrene triblock copolymers have a number
of properties which make them ideally suited for potential use
as biomaterials: ultrapurity, high strength, flexibility,
processability, and sufficient resistance to ageing. Their
thrombogenicity can be modified by surface hydroxylation with
subsequent coupling of heparin therein.

2. Solid phase (surface) hydroxylation of SBS copolymers is a
feasible procedure and results in materials which have hydroxyl
groups near the surface but still retain the elastomeric mechanical
properties of the original triblock copolymer.

3. The most important parameters governing the surface hydroxyla-
tion of SBS copolymers are the thickness of the film, time, and
the composition of the reaction bath (especially with regard
to the concentration of acetic acid). The effect of temperature
is chiefly limited to its effect on the kinetic constant.

4. Surface hydroxylation is a combined reaction- and diffusion-
limited process which is modified by the simultaneous swelling
of the reacted surface region. The swelling is, in turn, controlled
by a stress transfer mechanism which acts to transfer swelling
stresses from the surface to the unreacted core of the films.
The net effect of the resulting compressive stress in
the surface layer is a reduction in the solubility and diffusivity
and hence, diffusion rate, for each permeating species, relative
to their values in a stress-free, fully swollen sample.

5. Because of these stress transfer processes and the critical dependence of the diffusion rate on the solubility, the extent of reaction as expressed by the area concentration of hydroxyl groups decreases with increasing thickness. Two processes are responsible:

(a) The transfer of stress, through its influence on the solubility of peracetic acid, increases the steepness and decreases the size of the reaction front (the boundary delineating reacted from unreacted material); the reduced amount of hydroxyl groups follows directly from the smaller depth of penetration.

(b) The lower solubility (and diffusivity) of the cleavage agents acetic acid, water, and sulphuric acid (protons), results in a lag between the advancing diffusion fronts (concentration profiles) for epoxide groups and for the cleavage agents; the epoxide groups beyond the diffusion front for these agents are not cleaved. Since this lag increases with increasing thickness (via the stress transfer mechanism),the number of epoxy groups in thicker films is greater than in thinner films and the number of hydroxyl groups is then less in thinner films.

6. Surface hydroxylation is an autoaccelerative process, the area concentration of hydroxyl groups increasing exponentially with time, in consequence to the relief of part of the compressive stress in the surface region increasing the solubility of the permeants in this region; with the increased solubility, the

diffusion rate is increased, with the depth of penetration increasing to relieve the stress still further.

7. A significant induction time is observed in all of the surface hydroxylations before there is any infrared evidence of hydroxyl formation (i.e., the depth of penetration is less than 0.2 microns). This is directly related to the exponential nature of surface hydroxylation.

8. Swelling in chloroform results in delamination of the surface reacted material with the formation of three fractions: crosslinked gel, reacted sol, and unreacted chloroform soluble material. From the relative weights of these fractions, the depth of penetration of the reaction and the shape of the reaction front are measured.

9. Although the depths of penetrations encountered in this thesis were on the order of 10 micons or larger, suitable control of time, temperature, and the composition of the reaction bath would enable depths of penetration of the order of 1 micron or less to be attained.

10. Quantitative infrared spectroscopic analysis is an excellent technique for determining the structure of surface reacted SBS. Not only does it reveal the time course of the reaction and the thickness dependence of epoxide formation and epoxide cleavage, it gives detailed structural information with regard to the types of rearrangements possible during the epoxidation/hydroxylation of SBS copolymers. The presence of a multiplicity of substituted tetrahydrofuran groups, acyclic ether crosslinks (vinyl, phenyl, and saturated ethers), and carbonyl groups is indicated unequivocally.

11. The surface reaction scheme described herein is generally
applicable to any styrene-butadiene-styrene triblock copolymer.
Because SBS copolymers can be prepared with a wide variety of
properties, there is a high probability that a SBS copolymer can
be found which would satisfy the mechanical requirements for any
given biomaterial use. To make this material nonthrombogenic,
the surface hydroxylation scheme developed here can be used to
provide reactive sites for whatever heparinization treatment is used
and as such, by a suitable combination of a triblock substrate,
surface modification and heparinization treatment any set of
biomaterial requirements can be satisfied.

VII RECOMMENDATIONS

1. To determine the surface morphology and the composition of
the surfaces of styrene-butadiene-styrene block copolymers,
(i.e. which is major component at surface), an autoradiography
technique should be developed using either a specific adsorbent,
a specific reactant, or a specially prepared triblock copolymer
to distinguish between the two phases of the copolymer.

2. In order to investigate the separate influences of epoxidation
and epoxide cleavage on the properties of the final polymer, attempts
should be made to limit epoxide cleavage during the reaction
with peracid (no sulphuric acid and less acetic acid present and
lower temperatures used). Cleavage can then be conducted in a
highly swollen polymer, in a separate bath in the absence of peracetic
acid, to effect a complete conversion to the glycol structure.
The depth of penetration would then be wholly determined by the
conditions of the first step. A surface hydroxylation resulting
in a higher yield of hydroxyl groups may also develop and so, from
a practical point of view, this process would be more desirable in
preparing biomaterials.

3. Other peracids (e.g. monoperphthalic acid) should be inves-
tigated to determine the effect of the peracid structure on the
properties of the resulting surface hydroxylated copolymer.
(Monoperphthalic acid is known to cause fewer side reactions,
especially chain scission, in epoxidation (Pinazzi, et al., 1973)

4. Fundamental information regarding the diffusivity and solubility in similar polymer-penetrant systems should be obtained by direct sorption measurements (rather than through their effect by reaction on the polymer).

5. The resistance of these materials to mechanical flexural fatigue should be investigated in order to determine the long term stability of the reacted surface.

APPENDIX 1

INFRARED SPECTRUM ANALYSIS

A.   Assignments

The assignments of the peaks of the spectrum of surface hydroxylated styrene-butadiene-styrene block copolymer shown in Figure V-3 are listed in Table A1-1. Those absorptions marked with an asterisk were not used for the quantitative analysis scheme.

Notes on Table A1-1

(a) Both the phenyl ether and vinyl ether absorptions refer to the half ether ($\geq$C-O) structures discussed in section IV-4-d(ii). The width of the peaks is discussed in section IV-4-c.

(b) The maximum of these peaks appeared sometimes near 1260 cm^{-1} and 1195 cm^{-1} due to interfering absorptions from hydroxyl and tetrahydrofuran groups. If these interfering absorptions were subtracted out, the maximum residual absorbance appeared at 1240 cm^{-1} and 1210 cm^{-1} respectively.

(c) The interfering C-O absorption of hydroxyl groups was relatively small.

(d) A number of model compounds was used to make this assignment; tetrahydrofuran, 1,5 bis (tetrahydro-2-furyl)-3-pentanol (Szymanski, 1964), linalool oxide (2-vinyl-2 methyl-5-(1'-hydroxy-1' methyl ethyl)-tetrahydrofuran) (Felix, 1963), and other terpenoid derivatives (Ohloff, 1964). This assignment was complicated by the multiplicity of tetrahydrofuran structures present, as discussed in Section IV-4-c. (See Figure A1-1)

Table A1-1

Peak Assignments; Spectrum of Surface Hydroxylated

Styrene-Butadiene-Styrene Block Copolymer   (Figure V-3)

frequency ν (cm^{-1})	major functional group	nature of absorption	model compound	reference	notes
3430	hydroxyl	O-H stretch	polyvinyl alcohol	(Krimm, et al., 1956)	see section III-5iii
3061	phenyl	C-H stretch	poly-styrene	(Liang and Krimm, 1958)	
3029	phenyl	C-H stretch	"	"	
3004*	cis alkene	C-H stretch	cis 1,4 polybuta-diene	(Binder, 1963)	
2950-* 2850	methylene, methine	C-H stretch	-	(Bellamy, 1958)	
1737	acetate	C=O stretch	polyvinyl acetate	(Stokr and Schneider, 1963)	
1710	ketone carbonyl	C=O stretch	-	(Bellamy, 1958)	
1657	cis alkene	C=C stretch	cis 1,4 polybuta-diene	(Binder, 1963)	
1637	vinyl alkene	C=C stretch	1,2 poly-butadiene	"	
1602	phenyl	ring vibra-tion	polystyrene	(Liang and Krimm, 1958)	
1493	phenyl	"	"	"	
1455*	methylene, methine	C-H bending	-	(Bellamy, 1958)	

Table A1-1 continued...

frequency ν (cm^{-1})	major functional group	nature of absorption	model compound	reference	notes
1378*	acetate	CH$_3$ deformation	polyvinyl acetate	(Stokr and Schneider, 1963)	e
1308	cis alkene	C-H binding	cis 1,4 polybutadiene	(Binder, 1963)	
1240	acetate &	ester skeleton	polyvinyl acetate	(Stokr and Schneider, 1963)	
"	phenyl ether	C-O stretch	diphenyl ether	(Szymanski, 1964, 1967)	a,b
1210	vinyl ether	C-O stretch	1-methoxy cyclohexene	(Sadtler, Szymanski, 1964, 1967)	a,b
1090	saturated acyclic ether	C-O stretch	dicyclohexyl ether	"	c
1067	tetrahydrofuran ring	ring stretch	see note d	see note d	d
1025	phenyl	C-H bending	polystyrene	(Liang and Krimm, 1958)	
995	vinyl alkene	C-H out of plane deformation	1,2 polybutadiene	(Binder, 1963)	
967	trans alkene	"	trans 1,4 polybutadiene	"	
910	vinyl alkene	CH$_2$ out of plane deformation	1,2 polybutadiene	"	e
882	epoxy	assymmetric ring stretch	2,3 epoxy butane	(Szymanski, 1964, Bomstein, 1958)	
807	epoxy	ring deformation	"	"	

Table A1-1 continued...

frequency ν (cm^{-1})	major functional group	nature of absorption	model compound	reference	notes
757	phenyl	C-H out of plane de-formation	polystyrene	(Liang and Krimm, 1958)	
737	cis alkene	"	cis 1,4 poly-butadiene	(Binder, 1963)	
699	phenyl	"	polystyrene	(Liang and Krimm, 1958)	

$1060 \ cm^{-1}$ (1) $1040 \ cm^{-1}$ (1)

$1090 \ cm^{-1}$ (1)

$1120 - 1020 \ cm^{-1}$
many bands (2)

$1060, \ 1040 \ cm^{-1}$ (2)

$1067 \ cm^{-1}$ (3) $1062 \ cm^{-1}$ (3)
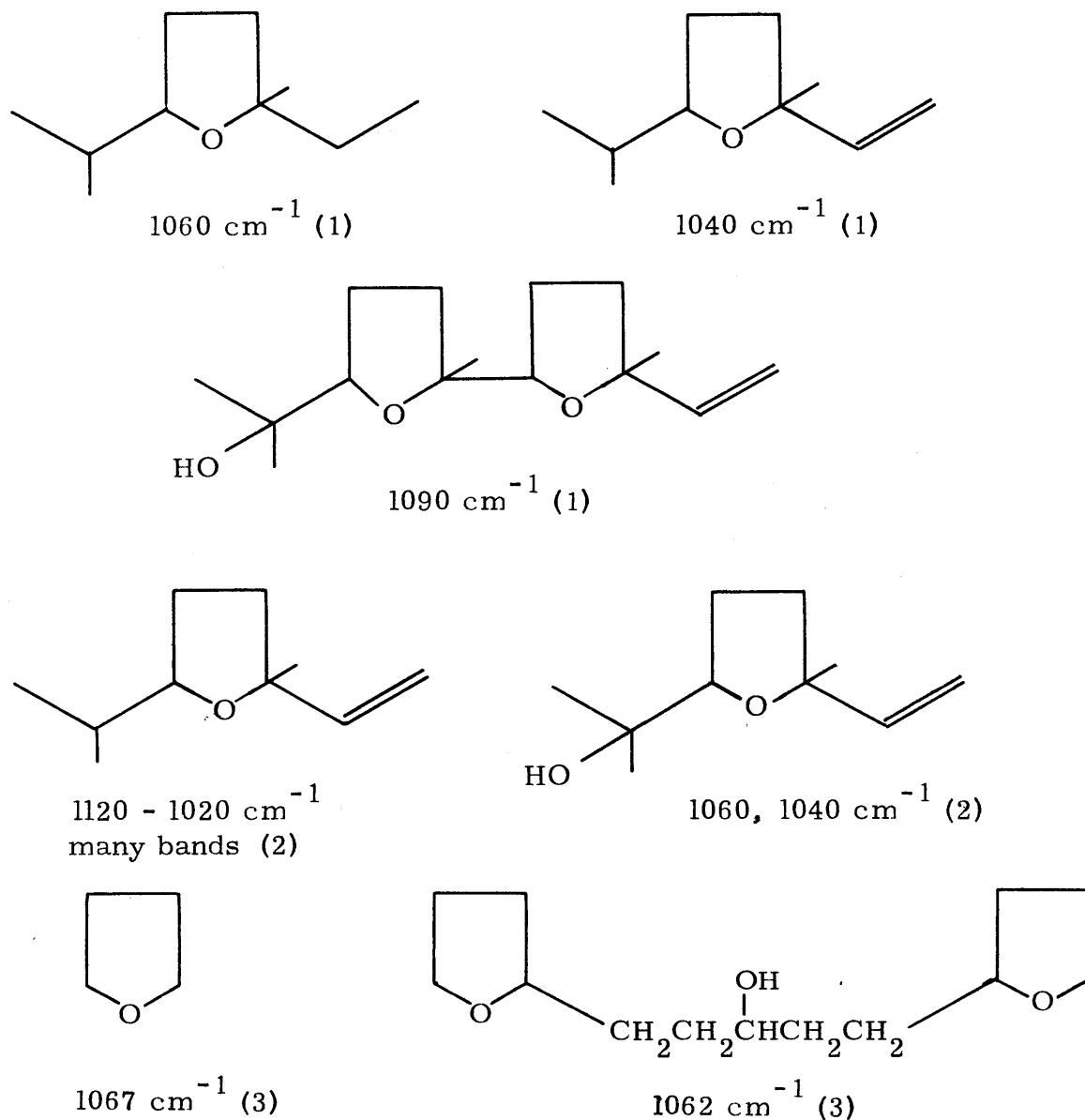
Figure A1-1. IR absorption frequencies of various tetrahydrofuran
structures ((1) Ohloff, et al., (1964), (2) Klein, et al.,
(1963), (3) Szymanski (1964)).

(e) The interfering absorptions of the assymmetric ring vibration at 908 cm^{-1} and the 1364 cm^{-1} CH_2 wagging vibration of tetrahydrofuran were relatively small.

The possibility of alternative assignments is discussed in section V-2a.

B. Calibration

The details of the calibration procedure are given in Table A1-2.

i) Solutions

Spectra were recorded for five concentrations of each calibration compound in each solvent. The solutions were prepared by dilution from a single solution of independently known concentration. The least squares linear correlation coefficient (and 95% confidence interval) of absorbance on concentration (grams/deciliter) was determined at each frequency of interest using an IBM 1130 computer. If the F-value was not high enough, the correlation coefficient was considered to be not significantly different from zero (95% confidence). The absorptivity was calculated from the following formula:

$$a_i^{\nu} = \frac{\beta^{\nu} \cdot Mw \cdot 100}{b' \cdot 2.303}$$

(A1-1)

where a_i^{ν} = molar absorptivity of component i at wavenumber ν

            $(cm^2/mole)$

    β^{ν} = correlation coefficient of absorbance at ν on concentration $(cm^3/mole)$

Table A1-2

Calibration of IR Quantitative Analysis

functional group	calibration compound	source	concentration range (gm/dl)		cell thick- ness (mm)	notes
			CS_2	$CHBr_3$		
phenyl	polystyrene	Dow Chemical Co.	.1-.6	.1-.6	.5/.05*	a,b
cis alkene	cis 1,4 polybutadiene	Polysciences, Inc.	0.5-3.	1.-6.	.5	a
vinyl alkene	dienite	Firestone Rubber Co.	0.1-1.0	0.7-3.	.5	a
trans alkene	Trans - 4	Phillips Petroleum Co.	0.1-3.0	0.2-1.2	.5/.05*	
acetate	polyvinyl acetate	T.R. Burke	-	-	-	films
hydroxyl	Gelvatol 20-60	Monsanto Co.	-	-	-	films
epoxy	2,3 epoxy butane	Pfaltz & Bauer	0.4-2.4	0.4-1.8	.5	
tetrahydro-furan	tetrahydro-furan	Mallinckrodt Chemical Works	0.1-0.7	-	.5	
vinyl ether	1-methoxy cyclohexane	Chemical Samples Co.	0.05-0.4	-	.5	
phenyl ether	diphenyl ether	Fisher Sci-entific Co.	0.05-0.3	-	.5	
saturated acyclic ether	dicyclo-hexyl ether	K + K Laboratories	0.2-0.9	-	.5	
carbonyl	methyl-n hexyl ketone	literature				(Cross & Rolfe, 1951)

Table Al-2, continued...

_____

*   .5/.05 indicates that cells of both thicknesses were used.

Notes:

        (a)   some of the absorptivities determined in solid films by comparison with known absorptivities (determined in solution)

        (b)   some of the polystyrene absorptivities determined using solutions in CS_2 as concentrated as 18 gm/dl.

Mw = molecular weight (of repeat unit)

b' = solution cell thickness (cm)

2.303 = conversion factor to get absorptivity in terms of

$\log_{10}$ when absorbances are computed in terms of (ln)

The thickness of the solution cell was determined by the method of interference fringes (Conley, 1966).

ii) Films

Spectra were recorded for a number of films (17 for polyvinyl acetate; 22 for Gelvatol 20-60) of varying thickness. The weights of 1.345 cm^2 samples of the film were determined using a Sartorius microbalance (see section IV-3). The least squares linear correlation coefficient (and 95% confidence interval) of absorbance on weight (milligrams) was determined at each frequency of interest using an IBM 1130 computer. If the F-value was not high enough, the correlation coefficient and the resulting absorptivity were considered to be not significantly different from zero (95% confidence). The 'mass' absorptivity (cm^2/gram) was calculated from the following formula:

$$\alpha_i^{\nu} = \frac{\beta^{\nu} \cdot 1.345 \cdot 1000}{2.303} \qquad \text{(A1-2)}$$

where α_i^{ν} = mass absorptivity of component i at wavenumber ν (cm^2/gram)

β^{ν} = correlation coefficient of absorbance on weight of 1.345 cm^2 of film (milligrams)$^{-1}$

For the acetate absorptivities, the mass absorptivity could be multiplied by the repeat unit molecular weight (Mw = 86) to get the molar

absorptivity. For the Gelvatol films 'effective' mass absorptivities were calculated from which the true mass absorptivities could be computed (section iv).

iii) Baselines

All absorbances were calculated as $\ln \frac{T_0}{T}$ where T_0 is the transmittance at the baseline while T is the transmittance at the peak maximum. (Because all absorptivities (Table A1-4) are reported on the basis of $\log_{10}$, a conversion factor of 2.303 is needed throughout the calculations). The baseline was drawn in all spectra to eliminate any interfering absorptions that could not be accounted for in the final analytical scheme. The baseline used was that logical baseline which gave the best fitting correlation of absorbance on concentration. The baselines are described in Table A1-3.

iv) Copolymer Calculations

Gelvatol 20-60 (partially acetylated polyvinyl alcohol):

It was assumed that the interfering absorption of hydroxyl at 1737 cm^{-1} was zero. Thus at 1737 cm^{-1}

$$\alpha_G^{1737} = \alpha_{Ac}^{1737} f_{ac} \qquad \qquad \text{(A1-3)}$$

where α_G^{1737} = effective mass absorptivity at $\nu = 1737$ cm^{-1} calculated using equation A1-2 from spectra of Gelvatol 20-60.

α_{Ac}^{1737} = mass absorptivity of acetate groups at $\nu = 1737$ cm^{-1} determined from spectra of polyvinyl acetate

f_{ac} = weight fraction acetate units

Table A1-3

Baselines for Calibration Spectra

calibration compound	solvent	baselines (wavenumber cm^{-1})
polystyrene	CS_2	3130-2970; 1400-H(E: 790-650)
	$CHBr_3$	1650-H(E: 1520-1470)
cis polybutadiene	CS_2	3080-3035; 3035-2975; H-1120; 1120-880; 850-625*
	$CHBr_3$	1850-1530; 1530-1360
trans 1,4 polybutadiene	CS_2	3050-3000Sh; H-1150; 1150-980; 800-650*
	$CHBr_3$	1730-1575; 1370-1240
1,2 polybutadiene	CS_2	3100-3015; H-1150; 1050-830; 750-H
	$CHBr_3$	1700-1200
polyvinyl acetate	film	3020-2870; 1800-1657*; 1470-1300; 1300-875
gelvatol 20-60	film	3650-3000; 1770-1657; 1610-875; 875-775; 775-480
2,3 epoxybutane	CS_2	H-1200-675
	$CHBr_3$	1650-1550
tetrahydrofuran	CS_2	1400-760

Table A1-3 continued...

calibration compound	solvent	baselines (wavenumber cm^{-1})
1-methoxy cyclohexene	CS_2	1320-1080
diphenyl ether	CS_2	1320-1120[†]; 930-840[†]
dicyclohexyl ether	CS_2	1210-970[†]

LEGEND to Table A1-3

$\nu_1 - \nu_2$:	baseline drawn from valley at ν_1 to valley at ν_2
$H - \nu_2$:	baseline drawn as a horizontal line from ν_2 towards higher frequencies
$\nu_1 - H$:	baseline drawn as a horizontal line from ν_1 towards lower frequencies
$(E: \nu_1 - \nu_2)$:	an exception to the preceeding baseline with the baseline drawn from ν_1 to ν_2
*	baselines not drawn from valley to valley but rather to intersect spectrum near 100% transmittance
†	tails of major peak estimated for background absorption
Sh:	Shoulder of peak

f_{ac} was thus calculated to be 0.799.

Using equation Al-4, the molar absorptivities for the hydroxyl group were calculated:

$$a_{OH}^{\nu} = \frac{(\alpha_G^{\nu} - \alpha_{Ac}^{\nu}) \cdot .201}{.799} \cdot 44 \qquad (A1-4)$$

where a_{OH}^{ν} = molar absorptivity of hydroxyl groups at wavenumber ν $cm^{-1}(cm^2/mole)$

Polybutadienes:

The method of Silas et al. (1959) was used to compute the absorptivities of the individual polybutadiene isomers. The absorptions at each of the three major analytical frequencies (967, 910 and 737 cm^{-1}) were divided into two parts: one corresponding to the isomer which absorbs the most strongly at that frequency and a second part reflecting the interfering absorption of the other two components. This interfering part was considered to be zero at the analytical frequency for the largest component of the polymer (e.g. at 967 cm^{-1} for the high trans content polymer). Using the effective molar absorptivities calculated according to equation AI-1, with the assumption of 100% unsaturation in the calibration polymers, the weight fractions of each isomer in each polymer and the true absorptivities of each functional group were calculated using the equations described by Silas (1959).

Since some of the absorptivities were not significantly different from zero, the equations of Silas had to be modified to yield a consistent set of weight fractions and absorptivities. The resulting weight fractions were:

	f_{trans}	f_{cis}	f_{vinyl}
TRANS - 4	.951	--	.049
cis 1,4 polybutadiene	.017	.954	.028
DIENITE	.020	.007	.973

v) Absorptivities

The absorptivities are listed in Table A1-4 on the basis of $\log_{10}$. The ether absorptivities are per mole of $\geq$C-O bonds as discussed in section IV-4d(ii).

C. Errors

Two sets of errors were distinguished in the calculation procedure. One set was due to the least squares solution of an overdetermined system (see section III-3), and one set due to the propagation of uncertainties in the value of each individual absorptivity. This latter set of errors was calculated using standard formulas for propagation of errors when multiplying or adding quantities to which there are associated errors. The geometric mean of the two sets of errors was considered to be the best estimate of the errors in the set of concentrations $<\underset{\sim}{X}>$. The errors from the least squares solution are given by equation III-8 (Clifford, 1973)

$$\underset{\sim}{E}' = \sigma\sqrt{(\underset{\sim}{a}^T\underset{\sim}{a})^{-1}}$$

where $\underset{\sim}{E}'$ = vector of length m of standard deviations of $<\underset{\sim}{X}>$ resulting from the least squares solution to the system

Table A1-4: Absorptivities $\left(\dfrac{cm^2}{mole} \times 10^{-3}\right)$ (log$_{10}$ units)

frequency (cm-1)	phenyl	cis	trans	vinyl	hydroxyl	epoxy	tetrahydro-furan	acetate	carbonyl	saturated ether	vinyl ether	phenyl ether
3340	-	-	-	-	22270.	-	-	-	-	-	-	-
3061	37.39	.495	-	18.39	2.765	-	-	-	-	-	-	-
3029	67.86	2.410	6.338	.428	-	-	-	2.471	-	-	-	-
1737	2.122	.956	-	-	-	-	-	259.8	68.80	-	-	-
1720	.672	1.503	-	-	-	-	-	102.3	175.	-	-	-
1657	-	0.954	1.622	1.022	-	-	-	-	-	-	-	-
1637	-	2.788	-	37.62	-	-	-	-	-	-	-	-
1602	23.28	-	-	-	-	2.026	-	-	-	-	-	-
1493	59.09	-	-	-	-	-	-	-	-	-	-	-
1308	5.659	8.376	7.642	3.250	13.72	2.577	4.437	5.881	-	-	-	7.399
1240	2.431	5.680	2.774	1.052	2.732	2.026	9.677	231.0	-	-	-	498.7
1210	2.785	2.771	-	-	6.441	-	11.69	18.80	-	-	433.3	23.43
1090	2.652	.835	3.611	-	30.60	-	21.86	29.84	-	148.5	-	-
1067	7.744	1.420	4.77	-	14.52	-	204.9	29.73	-	25.28	-	-

[continued]

Table A1-4, continued

frequency (cm^{-1})	phenyl	cis	trans	vinyl	hydroxyl	epoxy	tetrahydro-furan	acetate	carbonyl	saturated ether	vinyl ether	phenyl ether
995	3.174	7.323	11.48	54.33	3.846	-	5.172	7.464	-	3.490	-	-
967	4.120	3.584	139.8	3.008	2.556	-	5.888	9.196	-	-	-	-
910	3.554	1.376	.910	133.18	2.042	2.467	67.30	1.582	-	-	-	-
882	1.423	-	-	-	-	62.04	16.92	-	-	-	-	-
807	1.582	.871	-	-	1.278	34.04	3.262	-	-	-	-	-
757	55.20	11.30	.889	-	1.333	4.988	-	-	-	-	-	-
737	15.70	31.15	-	-	2.203	7.057	-	-	-	-	-	-
699	289.52	12.03	.443	6.193	4.197	1.089	-	-	-	-	-	-

of equations $\underset{\sim}{A} = \underset{\sim}{a} \underset{\sim}{X}$

σ = standard error of the estimate

$$= \sqrt{\frac{\underset{\sim}{r}^T \underset{\sim}{r}}{n-m}}$$

$\underset{\sim}{a}$ = absorptivity matrix of dimension n x m (cm^2/mole)

$\underset{\sim}{A}$ = vector of absorbances of length n

$\underset{\sim}{<X>}$ = vector of computed area-concentrations of length m

  (moles/cm^2)

$\underset{\sim}{r}$ = vector of residual absorbances of length n

  = $\underset{\sim}{A} - \underset{\sim}{a} \underset{\sim}{X}$

n = number of components

T : denotes transpose

$\sqrt{}$: denotes square root of each element in the matrix/vector

The errors propagated from the absorptivity matrix were calculated according to:

$$\underset{\sim}{E''} = (\underset{\sim}{a}^T\underset{\sim}{a})^{-1} \sqrt{\underset{\sim}{A}^T \underset{\sim}{E}\, \underset{\sim}{E}^T \underset{\sim}{A} + \underset{\sim}{<X>}^T\, \underset{\sim}{E'''}^T\underset{\sim}{E''}\, \underset{\sim}{<X>}} \qquad (A1-5)$$

where $\underset{\sim}{E''}$ = errors in $\underset{\sim}{<X>}$ propagated from the set of errors $\underset{\sim}{E}$ in $\underset{\sim}{a}$

  $\underset{\sim}{E}$ = matrix of errors in $\underset{\sim}{a}$

  $\underset{\sim}{E'''}$ = errors in $(\underset{\sim}{a}^T\underset{\sim}{a})$ propagated from $\underset{\sim}{E}$, calculated according to equation (A1-6); dimension (m x m)

Each element of $\underset{\sim}{E'''}$ was calculated according to:

$$E'''_{1,k} = \sqrt{\sum_{j=1}^{n} (E_{j,1}\, a_{j,k})^2 + (E_{j,k}\, a_{j,1})^2} \qquad (A1-6)$$

where $a_{j,k}$ = the element of the absorptivity matrix $\underset{\sim}{a}$ corresponding to frequency $\nu = j$ and component k

$E_{j,k}$ = the corresponding element of the error matrix $\underset{\sim}{E}$

The combined errors in $<X>$, E_X, was then given by:

$$E_{\underset{\sim}{X}} = \sqrt{\underset{\sim}{E''}^T \underset{\sim}{E''} + \underset{\sim}{E'}^T \underset{\sim}{E'}} \qquad\qquad \text{(A1-7)}$$

The elements of $\underset{\sim}{E}$ are computed directly from the correlations of absorbance on concentration or film weight. It should be noted that the two sets of errors were calculated at two different levels of confidence: the errors in the absorptivity matrix were at a 95% degree of confidence (approximately two standard deviations) while the errors from the least squares correlation were of only one standard deviation.

APPENDIX 2

MISCELLANEOUS EXPERIMENTS

A. ^{13}C NMR

^{13}C NMR spectra of two of our samples were recorded on a Varian 25.2 MHz XL - 100 NMR spectrometer[1] and on a Bruker WH - 90 spectrometer[2] using broad band (random noise) decoupling and Fourier transform techniques. The samples were swollen surface reacted films in deuterio-chloroform.

While excellent spectra of the gels were obtained, they were of little specific value to this thesis. The hydrocarbon peaks were easily assigned (Stother, 1972), but due to the lack of chemical shift correlations for ethers (cyclic or acyclic) and the limited accessibility to a ^{13}C NMR instrument it was impossible to assign the peaks in the ether region (60 - 70 ppm) to any definite structure. Additional complications arose because of the dissolution of the unreacted part in the solvent (chloroform - d_3). The spectrum of this dissolved part gave rise to narrow peaks and, in fact, was the major contribution to the spectrum of the whole sample. A complication also arose from the presence of chloroform in the sample, the Carbon atom of which gives rise to a triplet near 78 ppm.

This triplet may also hide other peaks due to ether structures present in our samples. These complications could be avoided by using the gel portion of an already delaminated sample (section IV-4) in a deuterated solvent which does not absorb near the ether region but does swell the gel layer.

B. Laser Raman

A laser Raman spectrum of one of our samples was obtained using a SPEX Ramalog 1401, with excitation of the Ar^+ ion at 488.0 nm[1].

Again, due to the absence of complete correlations, a limited access to the spectrometer and the fact that ethers do not generally absorb strongly in a Raman spectrum, the obtained spectrum was of little value.

C. Dyeing

A number of our samples were dyed with toluidine blue (5% solution) and attempts were made to section the films, after embedding in paraffin. The results were extremely inconsistent.

Films that had been in the dye solution for longer than a month were relatively easy to section with a LKB microtome with a glass knife. On the other hand, pieces of the same films which were in contact with dye for only one week could not be sectioned because they were too rubbery. Attempts to section at low temperatures or by embedding in epoxy rather than in paraffin were similarly unsuccessful.

Even with those samples that could be sectioned, the results were of little value. It had been supposed that the water soluble dye would only stain the hydroxylated region of the film, leaving the hydrophobic unreacted region free from color. By sectioning the film and looking at the film transversely (cross-section) in a microscope, the depth of penetration of the reaction could be determined visually. There were two problems, however: 1) some of the films appeared with a much smaller thickness than measured by other means (section III-2) and 2) when the thickness correlated reasonably well with other measurements, the depth of penetration of the dye was much less than the depth of penetration of the reaction as determined by delamination. (sections IV-3, V-5).

The low thickness was caused by the fact that the sections were not necessarily oriented normal to the microscope optical axis. Therefore, the thickness seen in the microscope was b cos α where b is the true thickness of the film and α is the angle made between the section and the horizontal. The thickness and the coloured/uncoloured sections were accordingly foreshortened when viewed in the microscope.

Because the sections were collected by floating them onto water the dye was able to diffuse out of the samples into this water before the sections could be viewed in the microscope. The measured depths of penetration would then be much less than those measured in other ways.

It might be possible to avoid all of these problems by embedding in a very viscous, concentrated, chloroform solution of polystyrene, sectioning with a glass knife and collecting the films over hexanol. The polystyrene would be firmly bound to the reacted SBS copolymer making sectioning easier while none of the dye would diffuse out of the film onto the

hexanol (a non-solvent for toluidine blue and the copolymer). However the problem of orientation of the films would remain making the whole procedure of doubtful value.

D.   Solution Reaction

In order to get information on the properties of hydroxylated styrene-butadiene-styrene block copolymers, many attempts were made to isolate hydroxylated block copolymer prepared in solution according to the procedure described in section IV-5c. Unlike the patented procedure (Winkler, 1971) for the hydroxylation of SBS copolymers, this method used an excess of acetic acid in order to prepare the hydroxy acetate addition product rather than the epoxide product. This modification presented a number of problems, which were not considered to be worth solving:

1)   Neutralization of large amounts of acid; the presence of residual acid in the product would result in a crosslinked and hence useless product. The use of sodium carbonate solutions with or without prior washing with water resulted in extremely stable slurries or emulsions, which were impossible to separate further.

2)   Finding solvent/nonsolvent systems for the hydroxylated product; the solubility of the hydroxylated product was very dependent on the degree of hydroxylation.

Although the hydroxylated SBS remained in solution in the peracetic acid (chloroform/acetic acid) reaction bath during the complete reaction process, at high extents of reaction the reaction solution showed evidence of Tyndall scattering, indicating that this mixture is not a good solvent

system. Once most of the acetic acid was removed, the polymer precipita-
ted, with crosslinking occuring, catalysed by the remaining acid. To
keep the product from becoming crosslinked it must be kept in solution
during the acid neutralization step and so another cosolvent must be
added before neutralization of the acid.

A cosolvent was needed because the hydroxylated block copolymer was
composed of two parts: the relatively non-polar polystyrene and the more
polar hydroxylated polybutadiene block. Hence a solvent of intermediate
polarity was required. As more and more cosolvent was added the bulk of
the system increased to the point where normal laboratory separations
became infeasible. This was especially true when the polymer had to be
removed from solution (precipitation) so that the base hydrolysis step
could be carried out under optimum conditions.

Similar problems arose with regards to the choice of a nonsolvent
for precipitation of the hydroxy acetate product, a solvent for the hy-
drolysis step (made even more complex here by the presence of KOH) and
then a nonsolvent for the final hydroxylated product. These problems were
all complicated by the fact that any set of solvents and nonsolvents that
were suitable at one degree of reaction were generally not suitable for
a product prepared at a different extent of reaction. Many, but not all,
of the possible solvent/nonsolvent combinations were attempted with little
overall success.

E.   Contact Angle

The contact angle of water on surfaces of polybutadiene ('DIENE',
Firestone Rubber Company; same microstructure as TR-41-2443), polystyrene

(Dow Chemical Company) and SBS TR-41-2443 was determined by standard techniques using a Unitron EPT Gonimeter Eyepiece (Tirrell, 1974).

The results were inconclusive because of the differences between the mercury and air surfaces of both polystyrene and SBS TR-41-2443. The measured contact angles were:

polystyrene / air	$90.5° \pm 0.6$
polystyrene / mercury	$65.7° \pm 4.3$
polybutadiene / air	$102.1° \pm 4.0$
SBS / air	$112.4° \pm 0.5$
SBS / mercury	$74.2° \pm 3.6$

It was expected that the contact angle for SBS TR-41-2443 / air interface would be between the values for polystyrene / air and for polybutadiene / air interfaces, but closer to the value of polybutadiene. It is not clear why it is so much higher than the value for polybutadiene. On the other hand the contact angles for polystyrene and SBS / mercury interfaces are, within experimental error, nearly identical so it can be concluded that the mercury surface of a cast film of SBS TR-41-2443 is mainly composed of polystyrene (as would be expected from the lower mercury interfacial tension of polystyrene--section III-16). However it is not at all clear why the contact angle for the polystyrene / mercury interface is so much less than that for the air interface. Perhaps a specific orientation occurs at the mercury / polystyrene interface which results in a low contact angle. Extending this to the SBS copolymer renders the conclusion made above suspect if a similar orientation

process occurs (especially considering the unavailability of a contact angle for the polybutadiene / mercury interface).

Further determinations of contact angle and especially the critical contact angle might help elucidate the structure of the SBS interfaces. However any unknown orientation / adsorption processes would make these contact angles subject to interpretation.

A better means to determine the surface structure, though, would be autoradiography using tritium labelled surfaces. The tritium could be added to the polymer surface by using tritiated water in the hydrolysis of the hydroxy acetate product of the surface hydroxylation reaction.

APPENDIX 3:   DELAMINATION CALCULATIONS

A. λ_x

The defining equation for λ_x is:

$$W_x = 2\rho_x A \lambda_x \qquad \text{(A3-1)}$$

where W_x = weight of gel fraction

ρ_x = density of crosslinked gel

A = area of sample = 1.345 cm^2

λ_x = depth of penetration, based on weight of gel fraction

ρ_x is calculated from the slope of the initial linear portion of curves of W_x versus b (initial thickness of film).

B. λ_s, λ_s'

Defining:

$$W_r = W_t - W_s \qquad \text{(3-2)}$$

where W_r = weight of reacted material

W_t = weight of sample before delamination

W_s = weight of soluble unreacted fraction

then:

$$\frac{W_r}{W_t} = \frac{V_r \rho_r}{W_t} = \frac{2\lambda_s A \rho_r}{W_t} \qquad \text{(A3-3)}$$

where V_r = volume of reacted material

ρ_r = average density of reacted material

A = area of sample = 1.345 cm^2

λ_s = depth of penetration, based on the weight of soluble unreacted material, and in the final reacted state.

λ_s is calculated from the slope of a plot of $\dfrac{W_r}{W_t} = \dfrac{W_t - W_s}{W_t}$ versus $\dfrac{1}{W_t}$

assuming $\rho_r \approx \rho_x$, the density of fully crosslinked gel.

A second type of depth of penetration λ_s', can be calculated using the same data. This depth of penetration is based on the initial thickness of polymer. The formula for its calculation is derived by initially assuming that the volume fraction of the reacted portion is unchanged during reaction:

$$\frac{V_r^o}{V_t^o} = \frac{V_r}{V_t} = \frac{V_r}{V_r + \dfrac{W_s}{\rho_s}} \qquad\qquad \text{(A3-4)}$$

where V_r^o = volume of the portion of sample that is to be reacted (before reaction)

V_r = volume of the portion of sample that has reacted (after reaction)

V_t^o, V_t = total volume of sample before and after reaction, respectively

ρ_s = density of unreacted fraction = density of pure SBS (= $.943 \text{ gm/cm}^3$)

Since $V_r = \dfrac{W_t - W_s}{\rho_r}$, Equation A3-4 can be rearranged:

$$\frac{V_r^\circ}{V_t^\circ} = \frac{W_t - W_s}{W_t + W_s\left(\dfrac{\rho_r}{\rho_s} - 1\right)} \tag{A3-5}$$

$\dfrac{V_r^\circ}{V_t^\circ}$ is then the volume fraction of prereacted polymer that is to be re-acted and the product of $\dfrac{V_r^\circ}{V_t^\circ}$ and the film thickness before reaction is then equal to $2\lambda_s'$ or:

$$\frac{W_t - W_s}{W_t + W_s\left(\dfrac{\rho_r}{\rho_s} - 1\right)} = \frac{1}{b} \cdot 2\lambda_s' \tag{A3-6}$$

where b = original thickness of the film

λ_s' = depth of penetration based on the original thickness

A plot of the left hand side versus $\dfrac{1}{b}$ yields a straight line with slope equal to $2\lambda_s'$ (assuming as before $\rho_s \simeq \rho_x$). This value of the depth of penetration is then used to test the assumptions used to calculate it: namely, the constancy of the volume fraction of the reacted portion during reaction.

APPENDIX 4

LOCATION OF ORIGINAL DATA

The data and calculations of this thesis are contained in laboratory notebooks, computer printouts and on spectra chart paper on file with Professor E. W. Merrill Room 12-108, Massachusetts Institute of Technology, Cambridge Massachusetts 02139.

APPENDIX 5

NOMENCLATURE

This appendix lists the more important variables in the body of this thesis. Additional variables which were used only in specific derivations are defined in the text.

$\underset{\sim}{A}$, A^{ν}	absorbance
A	area of sheet during swelling (Crank, 1953)
A	area of sample prior to delamination (cm^2)
A_c^{OH}	area concentration of hydroxyl groups (moles/cm^2)
A_m	area of sheet in the absence of stress and at equilibrium with penetrant (Crank, 1953)
A_0	initial area of dry sheet (Crank, 1953)
$\underset{\sim}{a}$, a_i^{ν}	absorptivity (cm^2/mole)
a'	integrated absorption intensity
a_i	activity of penetrant i in polymer
a_i^s	activity of penetrant i at surface
b	path length of radiation in sample, film thickness prior to reaction (cm)
b'	solution cell thickness (cm)
C_a	concentration of acetic acid (moles/cm^3)
C_e	concentration of epoxide groups (moles/cm^3)
c_i^0	initial concentration of component i (moles/cm^3)
c_i^s	concentration at surface of penetrant i (moles/cm^3)
C_p	concentration of peracetic acid (moles/cm^3)

C_r	concentration of reacted double bonds (moles/cm^3)
C_{OH}	local concentration of hydroxyl groups (moles/cm^3)
C_u	concentration of unreacted double bonds (moles/cm^3)
C_w	concentration of water (moles/cm^3)
c, c_i	concentration (moles/cm^3)
D	diffusivity (cm^2/sec)
D_i^1, D_i^2	diffusivities in swollen and unswollen regions respectively when area = A (Crank, 1953)
D_i^m, D_i^0	diffusivities in swollen and unswollen regions respectively in the absence of stress (Crank, 1973)
D_i^T	thermodynamic diffusivity of penetrant i
$\underset{\sim}{E}$	errors in absorptivities $\underset{\sim}{a}$
$\underset{\sim}{E}'$	errors in standard deviations of the area of concentration $<\underset{\sim}{X}>$ due solely to the regression
$\underset{\sim}{E}''$	errors in $<\underset{\sim}{X}>$ propagated from the set of errors in $\underset{\sim}{a}$
$\underset{\sim}{E}'''$	errors in ($\underset{\sim}{a}^T\underset{\sim}{a}$) propagated from $\underset{\sim}{E}$
E_0, E_m	Young's moduli of unswollen and swollen zones respectively (Crank, 1953)
$\underset{\sim}{E}_x$	errors in $<\underset{\sim}{X}>$ from all sources
F_i	number of moles of component i per 100 moles of unsaturation present in the original sample before reaction
f_i	fraction of oxygen-containing functional groups that are of one type
K_1, K_1	measures of time course of surface hydroxylation
K_2	measure of thickness dependence of surface hydroxylation
k_a	kinetic constant of acetic acid mediated epoxide cleavage (cm^3/mole-sec)
k_p	kinetic constant of epoxidation (cm^3/mole-sec)

k_w kinetic constant of water mediated epoxide cleavage (cm^3/mole-sec)

k_i/k_k ratio of kinetic constants of epoxidation of double bond isomer i and k respectively

Mw   molecular weight

m   number of components in sample

N   ratio of moles of phenyl groups to 100 moles of unsaturation in the copolymer

N_i moles of double bond isomer i remaining in sample after reaction

N_i^o moles of double bond isomer i in sample prior to reaction

n   number of frequencies used in overdetermined system

P_i^T thermodynamic permeability of penetrant i in polymer

R_i rate of disappearance of penetrant i due to reaction

r^ν residual from least squares solution to over determined system

S   solubility (moles/cm^3)

S_i quasi-thermodynamic solubility of penetrant i in polymer

S_i' Henry's law solubility

S_i^1, S_i^2 solubilities in swollen and unswollen regions respectively when area = A (Crank, 1953)

S_i^m, S_i^0 solubilities in swollen and unswollen regions respectively in the absence of stress

T   (apparent) intensity of transmitted radiation, transmittance at peak

T   absolute temperature

T_0 (apparent) intensity of incident radiation, transmittance at baseline

t   time

V_m	volume of swollen polymer (cm^3)
V_0	volume of dry unswollen polymer (cm^3)
V_r	volume of reacted material
V_r^0	volume of part of sample that is to be reacted (before reaction)
V_t	total volume of sample after reaction
V_t^0	total volume of sample before reaction
W_r	weight of reacted material
W_s	weight of soluble unreacted fraction
W_t	total weight of sample before delamination
W_x	weight of crosslinked gel fraction
X_i	area concentration of component i (moles/cm^2)
x	coordinate in diffusion direction

Greek Symbols

α^ν	mass absorptivity (cm^2/gram)
β^ν	correlation coefficient of absorbance on concentration (cm^3/mole) or on film weight (milligrams)$^{-1}$
δA_m	mean compression in swollen region (Crank, 1953)
δA_0	mean extension in unswollen region (Crank, 1953)
γ	interfacial tension (dynes/cm.)
γ_m, γ_0	coefficients relating the effect of compression or extension respectively on the relevant stress free solubilities
λ	true depth of penetration of reaction, depth of penetration of swelling agent (Crank, 1953)
λ_s	depth of penetration calculated from weight of soluble fraction of delaminated sample (microns)
λ_s'	depth of penetration based on original thickness (microns)

λ_x depth of penetration calculated from weight of gel fraction of delamination sample (microns)

μ_m, μ_0 coefficients relating the effect of compression or extension respectively on the relevant stress free diffusivities

ν frequency (wavenumber, cm^{-1})

ν_{max} frequency at peak maximum

$\Delta\nu_{1/2}$ half-absorbance peak width

ρ_r density of reacted layer near surface

ρ_s density of unreacted fraction, density of pure SBS

ρ_x density of fully crosslinked material

σ standard error of the estimate (least squares solution to the overdetermined system)

Miscellaneous

T   transpose

-1   inverse

$\sim$ matrix/vector

$\sqrt{}$ square root of each element in matrix/vector

$\langle \ \rangle$ average

BIBLIOGRAPHY

Adamson, A.W., "Physical Chemistry of Surfaces". 2nd ed., Wiley-Interscience, New York, p. 76 (1967)

Allport, D.C. and W.H. Janes, "Block Copolymers". Applied Science Publishers, London, England (1973)

ASTM, "Manual on Electron Metallography Techniques". ASTM STP #547 (1973)

Barker, R.E., "Diffusion in Polymers: Optical Techniques". J. Poly. Sci., 58, 553 (1962)

Barr, D., Personal Communication, July 12 (1973)

Barrer, R.M., "Diffusion and Permeation in Heterogeneous Media". p.165 in J. Crank, and B.S. Park, ed., Diffusion in Polymers, Academic Press, London, England (1968)

Bartlett, P.D., "Recent Work on the Mechanisms of Peroxide Reactions". Record. Chem. Progr. 11, 47 (1950)

Bauer, R.S., "Linear Polymers from Diepoxides". J. Poly.Sci., A-4,5 2192 (1967)

Bauman, R.P., "A Least Squares Method for Multicomponent Analyses". Applied Spectroscopy, 13, 156 (1959)

Beecher, J.F., L. Marker, R.D. Bradford and S.L. Aggarwal, "Morphology and Mechanical Behaviour of Block Polymers". J. Poly.Sci. C26, 117 (1969)

Bellamy, L.J., "Infrared Spectra of Complex Molecules". Wiley, New York (1958)

Binder, J.L., "The Infrared Spectra and Structures of Polybutadienes". J. Poly.Sci., A1, 47 (1963)

Bishop, E.T. and W.P. O'Neill, "Block Copolymers for Use in Blood Pumps and Oxygenators: Preparation and Characterization". Proc. Artificial Heart Program Conference, p. 133 (1969)

Bomstein, J., "Infrared Spectra of Oxirane Compounds; Correlations with Structure". Analytical Chemistry 30, 544 (1958)

Bradford, E.B. and L.D. McKeever, "Block Copolymers". Prog. Polym. Sci., 3, 109 (1971)

——————————., Personal Communication, Feb. 12 (1974)

Bruck, S.D., "Blood Compatible Synthetic Polymers: An Introduction". Charles C. Thomas, Springfield (1974)

Bruice, T.C. and T.H. Fife, "Hydroxyl Group Catalysis III. The Nature of Neighbouring Hydroxyl Group Assistance in the Alkaline Hydrolysis of the Ester Bond". J.A.C.S. 84, 1973 (1962)

Buchanan, J.G. and H.Z. Sable, "Stereoselective Epoxide Cleavages" p. 1 in B.S. Thyagarajan, ed., "Selective Organic Transformations". 2, Wiley-Interscience, New York (1972)

Burgess, A.R., "Photo-Oxidation and Stabilization of Polythene" in "Polymer Degradation Mechanisms". U.S. Nat. Bur. Standards, circ. 525, 149 (1953)

Clifford, A.A., "Multivariate Error Analysis". Wiley, New York (1973)

Conley, R.T.. "Infrared Spectroscopy". Allyn and Bacon, Boston (1966)

Coscarelli, W., "Biological Stability of Polymers", p. 377 in W.L. Hawkins, ed., "Polymer Stabilization". Wiley-Interscience, New York (1972)

Crank, J., "A Theoretical Investigation of the Influence of Molecular Relaxation and Internal Stress on Diffusion in Polymers". J. Poly. Sci., 11, 151 (1953)

——————., "The Mathematics of Diffusion". Oxford Press, Oxford (1956)

——————., and G.S. Park, editors, "Diffusion in Polymers". Academic Press, London, England, pp 75-106, 259-314 (1968)

Cross, L.H. and A.C. Rolfe, "Molar Extinction Coefficients of Certain Functional Groupings with Special Reference to Compounds Containing Carbonyl". Trans. Faraday Society, 47, 354 (1951)

Danckwerts, P.V., "Gas-Liquid Reactions". Mc-Graw Hill, New York, pp 30-70 (1970)

Daniels, F. and R.A. Alberty, "Physical Chemistry". 3rd edition, Wiley, New York, p. 330 (1966).

Dittman, W., and K. Hamann, "The Effect of Microstructure on the Epoxidation of Liquid Polybutadienes". Chemiker Zeitung, 95, 684 (1971)

——————., and ——————, " The Solvolysis of Polyepoxides of Unbranched Polybutadienes". ibid 96, 1 (1972)

Douy, A., and B.R. Gallot, "Studies of Liquid Crystalline Structures of Polystyrene-Polybutadiene Block Copolymers by Small Angle X-ray Scattering and Electron Microscopy". Molec. Cryst. Liq. Cryst., 14, 191 (1971)

Euranto, E.K., "Esterification and Ester Hydrolysis". p. 505 in
S. Patai, ed., "The Chemistry of Carboxylic Acids and Esters".
Wiley-Interscience, New York (1969)

Felix, D., A. Melera, J. Seible and E.S.Z. Kovats, "The Structure of
So-Called 'Linalool oxide'". Helv. Chim. Acta., 46, 1513 (1963)

Feughelman, M., "The Sortion of Water by Dry Keratin Fibers in
Atmospheres Above 90% R.H.". J. Appl. Poly. Sci. II, 189 (1959)

Fitzgerald, M.A., and D.F. Waugh, "Quantitative Aspects of Anti-
thrombin and Heparin in Plasma". Am. J. Physiol.,184, 627 (1956)

Flory, P.J., "Principles of Polymer Chemistry". Cornell University
Press, Ithaca, New York, p. 53 (1953a)

————————., ibid pp 541-563, 576-593 (1953b)

FMC Corporation, "Peracetic Acid 40%, Technical Information".

Frisch H.L., T.T. Wang, and T.K Kwei, "Diffusion in Glassy Polymers II".
J. Poly. Sci., A-2, 7, 879 (1969)

Goddard, J.D., J.S. Schultz, and R.J. Bassett, "On Membrane Diffusion
with Near Equilibrium Reaction". Chem. Eng. Sci., 25, 665 (1970)

Grauer, A.J., "Hydroxylation of Styrene-Butadiene-Styrene Block Co-
polymers in the Solid State". S.B. Thesis, Department of Chemical
Engineering, M.I.T., June (1973)

Greenspan, F.P., and D.G. MacKellar, "Analysis of Aliphatic Peracids".
Analytical Chemistry 20, 1061 (1948)

————————————, "Reactions of Unsaturated Polymeric Hydrocarbons: E.
Epoxidation". p. 152 in E.M. Fettes, ed.,"Chemical Reactions of
Polymers", Wiley Interscience, New York (1964)

Hartley, G.S., "Diffusion and Swelling of High Polymers. Part III:
Anisotropic Swelling in Oriented Polymer Films". Trans. Faraday Soc.,
45, 820 (1948)

Hawkins, W.L., "Polymer Stabilization". Wiley-Interscience, New York (1972)

Hendus, H., K.H. Illers and E. Ropte, "Investigation of the Structure of
Styrene-Butadiene-Styrene Block Copolymers". Kolloid Zeitschrift
216-217, 110 (1967)

Henniker, J.C., "Infrared Spectrometry of Industrial Polymers". Academic
Press, London (1967)

Hermans, J.J., "Diffusion with Discontinuous Boundary". J. Colloid. Sci.,
2, 387 (1947)

Herschberg, I.S., and F.L.J. Sixma, "Precision Spectrophotometry of Multicomponent Systems". Koninul Ned. Akad. Wetenschap, Proceedings Series B 65, 244 (1962)

Hoffman, M., G. Kampf, H. Kromer and G. Pampus, "Kinetics of Aggregation and Dimensions of Supramolecular Structures in Noncrystalline Block Copolymers". Advances in Chemistry, #99, 531 (1971)

Holden, G., E.T. Bishop, and N.R. Legge, "Thermoplastic Elastomers". J. Poly. Sci., C26, 37 (1969)

Inoue, T., T. Soen, T. Hashimoto, and H. Kawai, "Thermodynamic Interpretation of Domain Structure in Solvent Cast Films of A-B Type Block Copolymers of Styrene and Isoprene". J. Poly. Sci., A-Z, 7, 1283 (1969)

—————., —————, ——————, and ———— , "Studies in Domain Formation of A-B Type Block Copolymer from its Solution". p. 53, in S.L. Aggarwal, ed., "Block Copolymers", Plenum Press, New York (1970)

—————., M. Moritani, T. Hashimoto and H. Kawai, "Deformation Mechanism of Elastomeric Block Copolymers Having Spherical Domains of Hard Segments under Uniaxial Tensile Stress". Macromol., 4, 500 (1971)

Ishii, Y., and S. Sakai, "1,2 Epoxides", p. 13 in K.C. Frisch and S.L. Reegan, eds., "Ring Opening Polymerization". Marcel Dekker, New York (1969)

Katz, S.M., E.T. Keebu, and J.H. Wakelin, "The Chemical Attack on Polymeric Materials as Modified by Diffusion". Text. Res. J., 20, 754 (1950)

Keelen, T.L.,"Experimental Block Copolymers: Technical Information". Shell Chemical Co., (1972)

Keller, A., E. Pedemonte and F.M. Willmouth, "Macrolattice From Segregated Amorphous Phases of a Three Block Copolymer". Kolloid Zeitschrift, 238, 25 (1970)

Kemp, D.R., and D.R. Paul, "Gas Sorption in Polymer Membranes Containing Adsorptive Fillers". J. Poly. Sci., Polymer Physics, 12, 485 (1974)

Krigbaum, W.R., S. Yazgan, and W.R. Tolbert, "Some Comments on Domain Structure in Block Copolymers". ibid, 11, 511 (1973)

Krimm, S., C.Y. Liang, and G.B.B.M. Sutherland, "Infrared Spectra of High Polymers V. Polyvinyl Alcohol". J. Poly. Sci., 22, 227 (1956)

Leary, D.F., and M.C. Williams, "Statistical Thermodynamics of ABA Block Copolymers II". J. Poly. Sci., Polymer Physics, 11, 345 (1973)

—————., and ————— , "Statistical Thermodynamics of ABA Block Copolymers III. Microstructural Transitions and Model Verification". ibid, 12, 265 (1974)

Lebedev, N.N., and K.A. Gus'kov "Reactions of α-Oxides III Kinetics of the Secondary Reactions in the Interaction of Ethylene Oxide and Acetic Acid". Kinetika i Kataliz 4, 581 (1963)

Lebedev, Y.S., "Diffusion Kinetics of Bimolecular Reactions in the Solid Phase - Reactions of Immobile Centers with Mobile Components of a Heterophase". ibid, 6, 522 (english edition, p. 451) (1965)

Lewis, P.R., and C. Price, "The Morphology of $(Styrene)_x(Butadiene)_y$ $(Styrene)_x$ Block Copolymers". Polymer 12, 258 (1971)

—————., and ————, "Electron Microscopy of Sym-SBS Block Copolymers". ibid, 13, 20 (1972)

Liang, C.Y. and S. Krimm, "Infrared Spectra of High Polymers VI Polystyrene". J. Poly. Sci., 27, 241 (1958)

Mackenzie, K., "Alkene Rearrangements". p. 387 in S. Patai, ed., "The Chemistry of Alkenes, Vol. 1, Wiley-Interscience, London (1964)

Makowski, H.S., M. Lynn, and D.H. Rotenberg, "Epoxidation of Alkyllithium Polybutadienes". J. Macromol. Sci. Chem., A4, 1563 (1970)

McIntyre, D., and E. Compos-Lopez, "Small Angle X-ray Scattering Studies of Triblock Copolymers". p. 19 in S.L. Aggarwal, ed., "Block Polymers", Plenum Press, New York (1970)

Meier, D.J., "Theory of Block Copolymers I. Domain Formation in A-B Block Copolymers". J. Poly. Sci., C26, 81 (1969)

—————., "A Theory of the Morphology of Block Copolymers" A.C.S. Div. Polym. Chem., Polym Preprints, 11, 400 (1970)

—————., "A Theory of the Interface in Block Copolymers". Ibid, 15, 170 (1974)

Merrill, E.W., E.W. Salzman, P.S.L. Wong, T.P. Ashford, A.H. Brown and W.G. Austen, "Polyvinyl Alcohol-Heparin Hydrogel 'G'" J. Appl. Physiol. 29, 723 (1970)

—————., and P.S.L. Wong, "Acetalated Crosslinked Poly(vinyl alcohol) Hydrogels". U.S. Patent 3,658,745, Jan 14 (1970)

—————., "Progress Report: Thrombo-Resistant Biomaterials" DSR 80771, M.I.T., Han (1974)

Meyer, B.H., "Hydroxylation of Polydienes for Membrane Purposes".
    Ph.D. Thesis, University of Akron (1970)

Mochel, V.D., "NMR Composition Analysis of Copolymers". Rubber Chem.
    Tech. 40, 1200 (1967)

Morrison, R.T., and R.N. Boyd, "Organic Chemistry". 2nd ed., Allyn
    and Bacon, Boston p.895 (1966)

Morton, M. "Anionic Polymerisation and Block Copolymers". p. 1 in
    C.E.H. Bawn, ed., "Macromolecular Science". MTP International Review
    of Science, Physical Chemistry, Series 1, 8 (1972)

Mousseron-Canet, M. Mousseron, and C. Levallois, "The Oxide of Linalool".
    Compt. Rend., 253, 1386 (1961)

—————————., and C. Levallois, "The Oxides of Alcohols Similar to
    Linalool". Bull. Soc. Chim. France, 1339 (1965)

—————————., and C. Levallois, and H. Huerre, "The Oxides of Alco-
    hols Similar to Linalool: Epoxidation in Alkaline Medium of
    Dimethyl Heptanol". ibid., 658 (1966)

N.V. de Bataafsche Petroleum Maatschappij, "Can Coating Compositions
    by Polymerization of Olefins". British Patent 837,689 June 15
    (1960); reported in Chemical Abstracts 55, 2140b.

Nyilas, E., E.L. Kupski, P. Burnett, and R.M. Haag, "Surface Microstruc-
    ture Factors and the Blood Compatibility of a Silicone Rubber".
    J. Biomed. Mater. Res., 4, 371 (1970)

Odian, G., and R.L. Kruse, "Diffusional Effects in Radiation Induced
    Graft Polymerization". J. Poly.Sci., C22, 691 (1969)

Ohloff, G., K.H. Schulte-Elte and B. Wilhalm, "The Preparation of
    Tetrahydropyran and Tetrahydrofuran Derivatives from 1,7 or 1,6 diols
    Through Dehydration in the Allyl Position". Helv. Chim. Acta.,
    47, 602 (1964)

Park, G.S., "An Experimental Study of the Influence of Various Factors
    on the Time Dependent Nature of Diffusion in Polymers". J. Poly.
    Sci., 11, 97 (1953)

Peterlin, A., "Diffusion in a Network with Discontinuous Swelling".
    J. Poly. Sci., B3, 1083 (1965)

Peters, R.H., "Kinetics of Dyeing", p. 315 in J. Crank and G.S. Park,
    eds., "Diffusion in Polymers". Academic Press, London (1968)

Petropoulos, J.H., and P.P. Roussis, "Study of Non-Fickian Diffusion
    Anomalies Through Time Lags I. Some Time Dependent Anomalies".
    J. Chem Phys. 47, 1491 (1967a)

—————————————., and —————————., "II. Simpler Cases of Distance
    and Time-Distance Anomalies". ibid., 47, 1496 (1967b)

—————————————., and —————————., "III Simple Distant Dependent
    Anomalies in Microporous Media", ibid., 48, 4619 (1968)

—————————————., and —————————., "IV More Complex Cases of Axial
    Distance-Dependent Anomalies". ibid., 50, 3951 (1969a)

—————————————., and —————————., "V Simple Distance Dependent
    Anomalies in Laminated Media". ibid., 51, 1332 (1969b)

—————————————., and —————————., "Anomalous Diffusion of Good
    and Poor Solvents or Swelling Agents in Amorphous Polymers".
    J. Poly. Sci., C22, 917 (1969c)

—————————————., and —————————., "Diffusion of Penetrants in
    Organic Solids Accompanied by Other Rate Processes" p. 3430
    in G. Adler, ed., "Organic Solid State Chemistry". Gordon and
    Breach, New York (1969d)

Pinazzi, C., J.C. Sontif, and J.C. Brosse, "Modification Chemique par
    epoxydation de polyisoprenes et de polybutadienes de faible masse
    moleculaire". Bull. Soc. Chim. France, (5), 1652 (1973)

Pritchard, J.G., and F.A. Long, "Kinetics and Mechanism of the Acid
    Catalysed Hydrolysis of Substituted Ethylene Oxides".
    J.A.C.S., 78, 2667 (1956)

Ramsay, D.A., "Intensities and shapes of Infrared Absorption Bands
    of Substances in the Liquid Phase". ibid., 74, 72 (1952)

Reese, C.E., and H. Eyring, "Mechanical Properties and the Structure
    Of Hair". Textile Res. J., 20, 743 (1950)

Rogers, C.E.,S. Sternberg and R. Salovey, "Preparation and Analysis of
    Assymmetric Membranes". J. Poly.Sci., Al, 6, 1409 (1968)

Rosenberg, R.D., Personal Communication,May (1973)

Rosowsky, A., "Ethylene Oxides". p. 1 in A. Weissberger, ed., "Hetero-
    cyclic Compounds with Three and Four Membered Rings", Part 1,
    Wiley Interscience, New York (1964)

Sadtler Research Laboratories, "Standard Grating Infrared Spectra".
    Philadelphia, PA

Sakaguchi, Y., A. Omori, and Y. Omura, "Preparation of Head to Head Type Poly(vinyl alcohol) by Means of Epoxidation of Polybutadiene". Kobunshi Kàgaku [English Ed.] 1, 17 (1972)

Salzman, E.W., "Nonthrombogenic Surfaces: Critical Review", Blood, 38, 509 (1971)

Scott, H., P.L. Kronick, and E.E. Hillman, "Active Vapor Grafting of Hydrogels in Medical Prosthesis". August (1971), PB 206, 499, as discussed in S.D. Bruck, Blood Compatible Synthetic Polymers, 85 (1974)

Shelton, J.R., "Stabilization Against Thermal Oxidation". p. 29 in W.L. Hawkins, ed., "Polymer Stabilization". Wiley Interscience, New York (1972)

Silas, R.S., J. Yates, and V. Thornton, "Determination of Unsaturation Distribution in Polybutadienes by Infrared Spectrometry" Analytical Chemistry 31, 529 (1959)

Soen, T., T. Inoue, K. Miyoshi, and H. Kawai, "Domain Structures of Amorphous Block Copolymers Cast from Solution". J. Poly. Sci., A-2, 10, 1757 (1972)

Southern E., and A.G. Thomas, "Effect of Constraints on the Equilibrium Swelling of Rubber Vulcanizates". J. Poly. Sci., A3, 641 (1965)

Stokr, J., and B. Schneider, "Vibration Spectra of Polyvinyl Acetate and Some Model Substances". Collection Czech. Chem. Commun., 28, 1946 (1963)

Stother, J.B., "Carbon-13 NMR Spectroscopy". Academic Press, New York (1972)

Swern, D., G.N. Billen and J.T. Scanlon, "Hydroxylation and Epoxidation of Some 1-Olefins with Peracids". J.A.C.S., 68, 1504 (1946)

————., "Electronic Interpretation of the Reactions of Olefins with Organic Peracids". ibid., 69, 1692 (1947)

————., "Organic Peracids", Chem. Rev., 45, 1 (1949)

————., "Epoxidation and Hydroxylation of Ethylenic Compounds with Organic Peracids". Organic Reactions, 7, Wiley, New York, 378 (1953)

————., "Organic Peroxy Acids as Oxidixing Agents. Epoxidation", p. 355 in D. Swern, ed., "Organic Peroxides", Vol II., Wiley Interscience, New York (1971)

Szymanski, H.A., "Interpreted Infrared Spectra". Plenum Press,
    New York (1964)

——————————., "The C-O, O-O, and O-H Group Frequencies of Alco-
    hols, Esters, Phenol, Hydroperoxides, Peroxides and Ethers".
    p. 11 in H.A. Szymanski, ed., "Progress in Infrared Spectroscopy".
    3, Plenum Press, New York (1967)

Tirrell, D., Personal Communication, March (1974)

Traut, D.L., "Hydroxylation of Styrene Butadiene Block Copolymers
    in Solid Phase". S.M. Thesis, Department of Chemical Engineering,
    M.I.T., August (1973)

Turecek, J. "Supramolecular Structures of Ultrathin Films of Styrene-
    Butadiene-Styrene Block Copolymers". Chem. Vlakna, 21, 55 (1972);
    Chemical Abstracts 77, 48926y

Uchida, T., T. Soen, T. Inoue, and H. Kawai, "Domain Structure and
    Bulk Properties of A-B-A Block Copolymers of Styrene-Isoprene-
    Styrene". J. Poly. Sci., A-2, 10, 101 (1972)

Van Krevelen, D.W., "Properties of Polymers: Correlations with
    Chemical Structure". Elsevier, Amsterdam, pp 95-106 (1972)

Wang, T.T., T.K. Kwei, and H.L. Frisch, "Diffusion in Glassy Polymers
    III". J. Poly. Sci., A-2, 7, 2019 (1969)

Winkler, D.E., "Hydroxylated Styrene Butadiene Styrene Block Copolymers".
    U.S. Patent 3,555,112, Jan 12 (1971)

Winslow, F.H., W. Matreyak and A.M. Trozzolo, "Weathering of Poly-
    ethylene". A.C.S. Div. of Polym. Chem., 10, 1271 (1969)

Zimmerman, J., "Degradation and Crosslinking in Irradiated Polyamides
    and the Effect of Oxygen Diffusion". J. Poly. Sci., 46, 151
    (1960)

BIOGRAPHICAL NOTE

Michael Vivian Sefton, son of Mr. and Mrs. Wolf Sefton, was born in a suburb of London, England in 1949. After living near Liverpool for a little over a year, his family moved to Canada and eventually settled in Toronto in 1953. He has an older brother, David and a younger sister, Sara.

Since his father and brother were civil engineers, he entered the University of Toronto in September 1967 and graduated with honours in June 1971 with a Bachelor of Applied Science degree in Chemical Engineering. He passed the time in his fourth year by being President of the University of Toronto Engineering Society (the engineering student association) and by being an S.D. on the Faculty Council.

In order to study with Prof. E.W. Merrill, he entered M.I.T. in the fall of 1971 and passed the doctoral qualifying examinations in January 1972. While at M.I.T. he has held appointments as a research assistant to Professors K.A. Smith and E.W. Merrill. His minor field was biochemistry and medicine.

The author has accepted an appointment as an Assistant Professor in the Department of Chemical Engineering and Applied Chemistry at the University of Toronto, Toronto, Ontario.